# *CELLULAR AND MOLECULAR EVENTS DURING EARLY CHICK MYOGENESIS*

**Daniel A. Sieiro Mosti**

Submitted in fulfilment of the requirements for the degree of

**Doctor of Philosophy**

Australian Regenerative Medicine Institute
&
Faculty of Medicine, Nursing and Health Sciences

Monash University

February 2015

*Esta tesis se la dedico a mi papá, mi mamá y mi hermana. Esta la culminación de muchos años de trabajo y esfuerzo. Sin su ayuda y sobre todo su apoyo y paciencia, aunque fuera desde muy lejos, nunca lo habría logrado. Los quiero mucho mucho.*

# SUMMARY

In chick embryos, skeletal muscle formation is initiated in selected epithelial somite progenitor cells, which, upon receiving external molecular cues, translocate into the nascent muscle where they differentiate into multinucleated myofibres. Here, two highly regulated mechanisms involving complex gene networks and choreographed cellular movements ensure the correct formation of the future musculature. The first involves a crucial myogenic cell-fate choice on whether to remain in a proliferative state or to begin differentiation. While this choice is known to involve both WNT and NOTCH pathways, the exact mechanisms and relationships between these pathways remains unknown. During the course of my doctoral studies, I uncovered at the heart of this response a signalling module encompassing NOTCH, GSK-3β, SNAI1 and WNT. This module transduces the activation of NOTCH into i) an inhibition of GSK-3β activity by non-transcriptional NOTCH signalling; ii) a SNAI1-induced epithelial to mesenchymal transition (EMT) leading to iii) the recruitment of membranal β-catenin to trigger WNT/β-catenin signalling and myogenesis independently of WNT ligand. While these results intimately associate the initiation of myogenesis to a change in cell adhesion, they may have wider implications, as they may reveal a general principle for coupling cell-fate changes to EMT in many developmental and pathological processes.

The second process that is crucial for the correct formation of skeletal muscle, which I focused on extensively during my studies, is the fusion of myoblasts into multinucleated fibres. This event, which can occur up to tens of thousand of times within each muscle fibre, ensures not only the correct growth of muscle but also the proper functioning of repair mechanisms in adult muscles. During my PhD, I focused on investigating how early myoblasts initiate fusion and with which cellular partners. Here, I show that a complex fusion interaction takes place in the trunk, where primary myotome cells from the medial somite border rarely fuse to one another, but readily do so with other border cells. Conversely, resident muscle progenitors actively fuse with one another, but do so poorly with the primary myotome. I have also characterised fusion events in limb muscles, demonstrating key differences in the progression of this event. These studies revealed important physical interactions while suggesting complex molecular networks are in play. Based on this knowledge, by performing functional studies on potential novel fusion genes. I have gained further insight into the fusion process.

# TABLE OF CONTENTS

# PART A: DECLARATION

**Monash University**

**Declaration for thesis based or partially based on conjointly published or unpublished work**

**General Declaration**

**In accordance with Monash University Doctorate Regulation 17.2 Doctor of Philosophy and Research Master's regulations the following declarations are made:**

**I hereby declare that this thesis contains no material which has been accepted for the award of any other degree or diploma at any university or equivalent institution and that, to the best of my knowledge and belief, this thesis contains no material previously published or written by another person, except where due reference is made in the text of the thesis.**

This thesis includes **1 original paper** published in peer-reviewed journals and **1 unpublished publication**. The core theme of the thesis is the study of cellular and molecular interactions during early chick myogenesis. The ideas, development and writing up of all the papers in the thesis were the principal responsibility of myself, the candidate, working within the Australian Regenerative Medicine Institute under the supervision of **Prof. Christophe Marcelle**.

In the case of chapters 2 and 3 my contribution to the work involved the following:

During the course of this thesis I received training and assistance in electroporation techniques from **Anne C. Rios** and **Olivier Serralbo**. Assistance and training in cloning of constructs was provided by **Olivier Serralbo**, **Claire Hirst** and **Nadège Veron**. Training on confocal microscopy was provided by **Monash Micro Imaging** and **Anne C. Rios**, and assistance provided by **Nadège Veron**.

I also acknowledge the training and contribution of **Prof. Christophe Marcelle** in figure preparation, manuscript and thesis drafting.

| Thesis chapter | Publication title | Publication status* | Nature and extent of candidate's contribution |
|---|---|---|---|
| 2 | Myogenesis and epithelial-mesenchymal transition triggered by cytoplasmic NOTCH and membranal β-catenin. | Article submitted to *Nature* | Concept, planning of experiments, cloning of constructs, electroporation, immunohistochemistry, imaging, data analysis, statistics, figure preparation, manuscript drafting. |
| 3 | A dynamic analysis of muscle fusion in the chick embryo. | Article published in *Development* | Concept, planning of experiments, cloning of constructs, electroporation, immunohistochemistry, imaging, data analysis, statistics, figure preparation, manuscript drafting. |

I have / **have not** renumbered sections of submitted or published papers in order to generate a consistent presentation within the thesis.

Signed: ……

Date: ……

# ETHESIS COPYRIGHT

**Notice 1**

Under the Copyright Act 1968, this thesis must be used only under the normal conditions of scholarly fair dealing. In particular no results or conclusions should be extracted from it, nor should it be copied or closely paraphrased in whole or in part without the written consent of the author. Proper written acknowledgement should be made for any assistance obtained from this thesis.

**Notice 2**

I certify that I have made all reasonable efforts to secure copyright permissions for third-party content included in this thesis and have not knowingly added copyright content to my work without the owner's permission.

Signed ……

Date ……

# ACKNOWLEDGEMENTS

First of all, I would like to thank my supervisor Christophe for all the help and support. I really feel I've grown as a researcher and as person during these years and I owe a lot of that to you. Your faith and belief in me helped me to keep going and I am very grateful for that. What I have learned here will most likely define me as a researcher for the rest of my career and I feel lucky to have been in your lab. Thank you so much.

To Anne, learning from you has been a humbling experience. You taught me to never settle with anything less than the best, I learned to hold myself to a higher standard because you expected more from me than I believed I could, and in the end, the skills and ideas I have learned from you are priceless. Thank you.

Thank you Claire for teaching me how to clone and become more efficient in the lab. These are skills I will take with me. I wish you good luck in your next adventure.

I want to thank Nadège for all her help without expecting anything in return. You bring joy to everyone around you and working with you has been an absolute pleasure. Thank you so much.

Thank you to Olivier. I annoyed you with too many questions for a very long time, and I'm grateful you held on and taught me so many things. I really appreciate it.

I want to thank the rest of the lab, past and present. Manu, David, Cyril, Jeremy, Fred, Mitra and Phoebe. You have all taught me and helped in some or many ways throughout these years and I take all of that with me.

Last but not least, I want to thank Steve and the crew at MMI for all their support and expertise. Imaging is at the heart of what we do and nothing I did would have been possible without your excellent help. Thank you.

# PUBLICATIONS AND SUBMISSIONS

The following publications have been accepted, published or under submission during the course of this thesis:

- Rios AC*, **Sieiro-Mosti D***, Hirst C, Marcelle C. Myogenesis and epithelial-mesenchymal transition triggered by cytoplasmic NOTCH and membranal β-catenin. Submitted to *Nature*. February 2015.

  * : these authors contributed equally to the work.

- **Sieiro-Mosti D**, de la Celle M, Pelé M, Marcelle C. A dynamic analysis of muscle fusion in the chick embryo. *Development.* 2014, Sep;141(18):3605-11.

# PUBLISHED ABSTRACTS, CONFERENCE PRESENTATIONS, MEDIA STATEMENTS AND PATENTS

The following abstracts have been accepted, published and presented at domestic or international conferences over the course of this degree:

- **Sieiro-Mosti D**, de la Celle M, Pelé M, Marcelle C. A dynamic analysis of muscle fusion in the chick embryo. *The EMBO meeting 2013, European Molecular Biology Organization. Amsterdam, Netherlands.* (Poster Presentation).

- **Sieiro-Mosti D**, de la Celle M, Pelé M, Marcelle C. A dynamic analysis of muscle fusion in the chick embryo. *Avian Model Systems 2014. Cold Spring Harbor Meetings. Cold Spring Harbor, New York, USA.* (Oral Presentation).

# AWARDS

The author is the recipient of the following awards:

- Monash Graduate Research Scholarship (2010-2014)

- Faculty of Medicine International Postgraduate Scholarship (2010-2015)

- Australian Regenerative Medicine Institute (ARMI) Director's Award for Excellence in Doctoral Research (2014)

- Australian Regenerative Medicine Institute (ARMI) Graduate Student Travel Grant (2014)

- Monash Institute of Graduate Research Travel Grant (2013)

# LIST OF FIGURES AND TABLES



*Figures and tables from manuscript(s) and/or publication(s) not included.

# List of Abbreviations and Acronyms

A

ABI: abl interactor protein

ADAM: a disintegrin and metalloproteinase domain AL: anterior lip

AFF-1: anchor cell fusion failure 1

AJ: adherens junction

ANK: ankyrin

ANTS: antisocial

APC: adenomatosis polyposis coli

ARF6: ADP- ribosylation factor 6

ARP: actin-related protein

ATP: adenosine triphosphate

B

BAG3: Bcl-2 associated athanogene 3

BAI: brain-specific angiogenesis inhibitor

BLOW: blown fuse

BrdU: bromodeoxyuridine

BRK: breast tumour kinase

C

CA: constitutively active

CBP: CREB binding protein

CD: cluster of differentiation

CDC42: cell division cycle 42

CDK: cyclin-dependent kinase

cDNA: complementary DNA

cIAP: cellular inhibitor of apoptosis

CIP: cyclin-dependent kinase inhibitor

CK1$\alpha$: casein kinase 1$\alpha$

CKII: casein kinase 2, alpha 1 polypeptide

CNN3: calponin 3

CRK: CT10 regulator of kinase

CSL: see RBP-J

CXCR4: chemokine (C-X-C motif) receptor

**D**

DAAM1: dishevelled associated activator of morphogenesis 1

DAG: diaglycerol

DALLY: division abnormally delayed

DGO: diego

DKK: Dickkopf

DLL1: delta-like 1

DML: dorsomedial lip

DN: dominant negative

DNA: deoxyribonucleic acid

DOCK: dedicator of cytokinesis

DOS: daughter of sevenless

DSH: dishevelled

DSL: delta/serrate/lag-2

DUF: dumbfounded

E

EDTA: ethylenediaminetetraacetic acid

EFF-1: epithelial fusion failure 1

EGF: epithelial growth factor

EGFP: enhanced GFP

EHD: EH domain-containing protein

ELMO: engulfment and cell motility

EMT: epithelial to mesenchymal transition

ER: endoplasmic reticulum

ERV: endogenous retrovirus

F

FAK: focal adhesion kinase

FC: founder cell

FCM: fusion competent myoblast

FGF: fibroblast growth factor

FGFR: fibroblast growth factor receptor

FZD: frizzled

FMI: flamingo

FOXO1a: forkhead box protein O1

FuRMAS: fusion restricted myogenic-adhesive structure

G

GEF: guanine nucleotide exchange factor

GFP: green fluorescent protein

GO: gene ontology

GSK-3β: glycogen synthase kinase 3β

GPC4: glypican 4

GPCR: G-protein coupled receptor

H

HA: haemagglutinin

HBS: hibris

HD: heterodimerization domain

HES: hairy and enhancer of split

HGF: hepatocyte growth factor

I

IGF: insulin growth factor

IgSF: immunoglobulin superfamily

IL-4: interleukin 4

IP3: inositol-1,4,5-triphosphate

IRES: internal ribosome entry site

IRREC: irregular of chiasm

ISH: in situ hybridisation

J

JAM: junctional adhesion molecule

K

KIRRE: kin of irreC

KIRREL: kirre-like

L

LACZ: lactose operon Z

LBX1: ladybird homeobox 1

LEF: lymphoid enhancer-binding factor

LNR: lin12-Notch repeats

LPC: lysophosphatidylcholine

LRP: low density lipoprotein

M

MAML: mastermind-like MRF: myogenic regulatory factor

MBC: myoblast city

MDX: muscular dystrophy mice

MEF2: myocyte enhancer factor 2

MET: mesenchymal to epithelial transition

MFR: macrophage Fusion Receptor

MR: mannose receptor

MRF4: myogenic regulatory factor 4

MYF5: myogenic factor 5

MYHC: myosin heavy chain

MYOD: myogenic differentiation 1

N

NCAM: neural cell adhesion molecule

NCC: neural crest cell

NED: notch extracellular domain

NFATc: nuclear factor of activated T cell

NF-κβ: nuclear factor κβ

NICD: notch intracellular domain

NLS: nuclear localisation sequence

NRR: negative regulatory region

NSF: *N*-ethylmaleimide sensitive fusion protein

P

PA: phosphatidylserine

PAR-1: Prader-Willi/Angelman region-1

PAX: paired box

PCP: planar cell polarity

PEST: peptide sequence rich in proline (P), glutamic acid (E), serine (S), and threonine (T)

PK: prickle
PKC: protein kinase C
PL: posterior lip
PP2A: protein phosphatase 2a
PRB: retinoblastoma protein
PSM: pre-somitic mesoderm

R
RAB39: ras-related protein 39
RAC1: ras-related C3 botulinum toxin substrate 1
RBFOX1: RNA binding protein, fox-1 homolog
RBP-J: recombination signal binding protein for immunoglobulin kappa J region
REEP1: receptor expression-enhancing 1
RFP: red fluorescent protein
RHOA: ras homolog family member A
RNA: ribonucleic acid
RNA-seq: RNA sequencing
ROCK: rho-associated, coiled-coil containing protein kinase 1
ROLS: rolling pebbles
RSPO: r-spondin
RST: roughest
RT-PCR: reverse transcription polymerase chain reaction

S
SDF1: stromal cell-derived factor 1
SF: scatter factor
sFRP: secreted frizzled-related protein
SGCD: sarcoglycan delta
shRNA: short hairpin RNA
SING: singles-bar
siRNA: small interfering RNA
SNARE: soluble N-ethylmaleimide-sensitive factor attachment protein receptor
SNS: stick and stones
SOST: sclerostin
SRA: specifically Rac1-associated protein
STAT6: signal transducer and activator of transcription 6

STBM: strabismus

T

TCF: transcription factor

TGFβ: transforming growth factor β

TLE: transducin-like enhancer of split

TMD: transmembrane domain

TMEM: transmembrane protein

t-SNARE: target SNARE

TWEAK: TNF-like weak inducer of apoptosis

V

VANG: van gogh

VCA: very common antigen

VLL: ventrolateral lip

VRP1: verprolin 1

v-SNARE: vesicle SNARE

W

WASp: Wiskott–Aldrich Syndrome protein

WG: wingless

WIF: Wnt inhibitory protein

WNT: wingless-type MMTV integration site family

# 1 INTRODUCTION

During early morphogenesis, the amniotic myotome forms from the activation and translocation of muscle progenitors located at different areas of the dermomyotome. A complex gene network and choreographed cellular movements drive these cells from muscle progenitors to committed myoblasts and differentiated multinucleated myofibres. During the course of my thesis, I have attempted to resolve two questions related to this process: i) how do epithelial muscle progenitors decide to commit to a myogenic fate and ii) how do committed myoblasts initiate fusion and with which cellular partners.

## 1.1 Principles of Myogenesis

### 1.1.1 Somitogenesis

With the exception of head muscles, which form from cranial and splanchnic mesoderm (Meier 1981), all other vertebrate muscle groups derive from somites. Somite formation, or somitogenesis, is a process that occurs in a cranial to caudal fashion. At regular intervals, a pair of somites “bud off” from the unsegmented pre-somitic mesoderm (PSM) located in the caudal region of the embryo. The clock and wavefront model is used to describe the periodic formation of somites in vertebrates (Cooke & Zeeman 1976). This model predicts that negative and positive feedback loops involving Wnt, Notch, FGF and retinoic acid create a rhythmic wave of gene expression (the "clock") throughout the PSM, while the "front" triggers the position where somite formation occurs (Dequéant & Pourquié 2008). The speed of this process varies in different species: in chickens one somite forms every 90 minutes while in mice it happens every 120 minutes. Also, the final number of somites is species-specific (50 in chicks, 65 in mice, many hundreds in snakes) (Cooke 1975). The maturation of somites follows this pattern, with cranial-most somites being further differentiated than caudal ones.

The epithelial cells that compose a newly formed somite are initially multipotent, and adopt different fates depending on their location within this structure (Aoyama & Asamoto 1988; Dockter & Ordahl 2000). This fate decision is influenced by external cues coming from neighbouring tissues such as the

notochord, neural tube, overlying ectoderm and intermediate mesoderm. These signals induce epithelial somitic cells to initially form two main structures: cells located ventrally undergo an epithelial-mesenchymal transition (EMT) to give rise to the bone and cartilage-forming sclerotome, while dorsal somite cells form an epithelial structure called the dermomyotome (Figure 1.1A).

### 1.1.2 The dermomyotome and its borders

The formation of the dermomyotomal compartment of the somites in mice and chickens is characterised by the expression of members of the paired homeodomain (Pax) family *PAX3* and *PAX7* (Goulding et al 1991; Jostes et al 1990). Both genes are also expressed in the dorsal neural tube (Tremblay et al 1998), neural crest cells (Kalcheim & Burstyn-Cohen 2005), the developing eye and in the brain (Dahl et al 1997). In the early somites, *PAX3* and *PAX7* expression occurs together throughout the dermomyotome (Otto et al 2006), and their expression is regulated by various cues from the neural tube and the overlying ectoderm. The expression of *WNT1*, *WNT3a* and *WNT4* in the neural tube is necessary for correct *PAX7* expression, while signals from the lateral plate mesoderm regulate the expression of *PAX3* (Fan et al 1997; Bryson-Richardson & Currie 2008). Furthermore, removal of the overlying ectoderm leads to ablated expression of both these proteins, and this process is mediated by expression of *WNT6* (Otto et al 2006).

As its name indicates, the dermomyotome gives rise to the dorsal dermis as well as the musculature. In addition, it also gives rise to aortic smooth muscles, lymphatic and endothelial cells (Mauger 1972; Christ et al 1983; Yamashita et al 2000). From a dorsal view, the newly formed dermomyotome has a roughly square shape (see Figure 1.1B), and can be divided into 5 separate domains. These are the four epithelial borders: dorsomedial lip (DML), ventrolateral lip (VLL), anterior lip (AL), posterior lip (PL) and the dorsal dermomyotome located at the centre. While early studies focusing on serial sections of chicken embryos suggested the entire trunk musculature forms exclusively from cells located at the DML and the VLL (Boyd 1960; Hamilton 1952) (Remak 1855; Bardeen 1900), it has recently been shown

that all 5 regions of the dermomyotome contribute to muscle formation (Gros et al 2004; Scaal et al 2004). However, as most studies have mainly focused on the DML as the model for myogenic induction, I will therefore use this region of the somite as an example of how the myogenic program initiates.

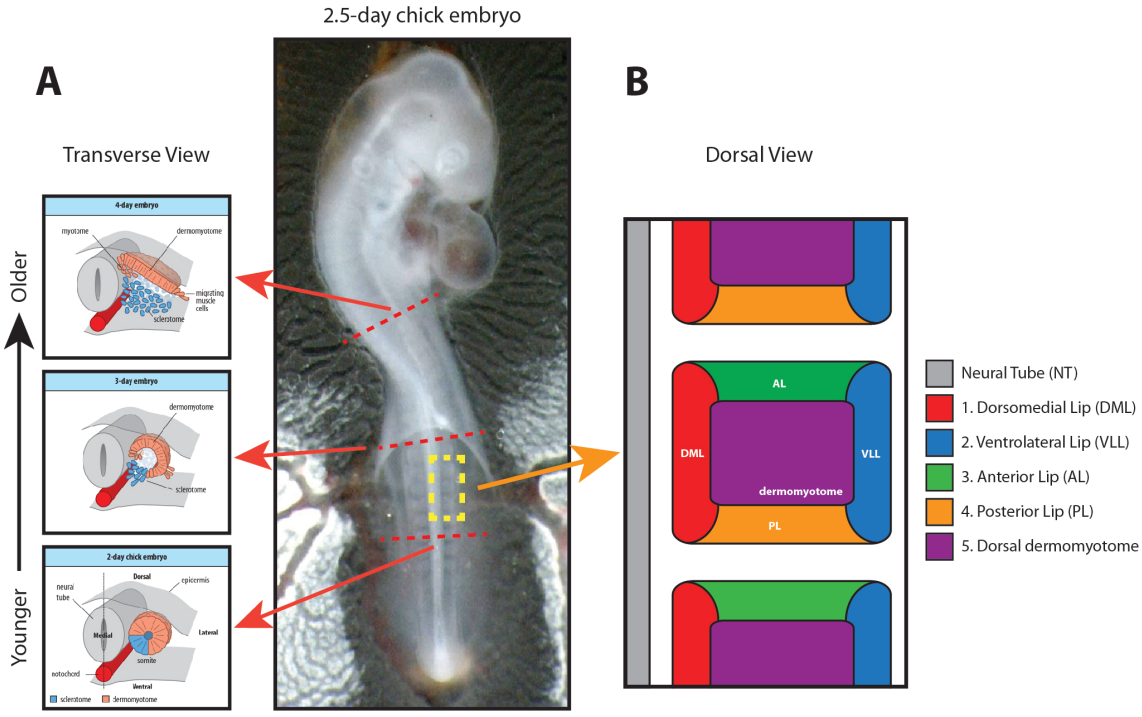


**Figure 1.1 Early amniote somite development and its derivatives**

**A.** Diagrams depicting transverse views of chick embryos at different stages of development. Somite development begins cranially and moves dorsally, resulting in older somites located anterior to younger somites within the same embryo. Somites initially form an epithelial structure (bottom panel) that further divides into two domains (top panel): ventrally located sclerotome (blue) and dorsally located dermomyotome (orange). **B.** Diagram depicting a dorsal view of somites following development of the dermomyotome. The dermomyotome is divided into 5 separate domains: dorsomedial lip (DML, red), ventrolateral lip (VLL, blue), anterior lip (AL, green) and posterior lip (PL, orange), and the dorsal dermomyotome located at the centre (purple). Dashed lines show approximate area of focus. A. adapted from http://www.mun.ca/biology/desmid/brian/

The DML (and other dermomyotome borders) is composed of *Pax3*$^{+}$/*Pax7*$^{+}$ epithelial progenitor cells, and expression of these proteins is crucial for future muscle formation. *Pax3*$^{-/-}$ mutant mice are only able to form certain muscles, but

these appear disorganised, while most ventral musculature fails to form altogether (Tremblay et al 1998). While *Pax7*$^{-/-}$ mice have no observable defects aside from a lower survival of adult muscle stem cells (Seale et al 2000), in double *Pax3*$^{-/-}$/*Pax7*$^{-/-}$knockout mice, formation of most muscle masses is highly disrupted. Furthermore, the similarity between both proteins is such that insertion of the *Pax7* sequence into the *Pax3* native locus rescues the observed phenotype of the *Pax3*$^{-/-}$ mutant mice (Relaix et al 2004). This redundancy indicates that while interchangeable to a degree, either Pax protein is essential for correct myogenesis.

The function of the DML progenitor cell pool is to provide a constant stream of cells that enter the myogenic program while also maintaining its own population for a period of time. The efficiency of the self-renewing mechanisms not only ensures an overall correct muscle formation, but can also affect the final muscle size by creating more or less total cells over the course of development. Although its exact function has not been determined, as studies report it promotes proliferation (von Scheven et al 2006) or differentiation (Hammond et al 2007; Buckingham 2006), Fibroblast Growth Factor (FGF) signalling plays a potential role in this process. Indeed, the negative regulator of FGF signalling, Sprouty1, stimulates the self-renewal of the *Pax3*$^{+}$/*Pax7*$^{+}$ progenitor population (Lagha et al 2008), while FGF receptor 4 (*FGFR4*) is potentially involved in promoting differentiation, as its expression pattern strongly correlates with the initiation of myogenesis (Marcelle et al 1995). However, *FGFR4*-null mice display no muscle phenotype (Weinstein et al 1998), possibly due to overlapping functions with other unknown FGF receptors.

Two additional signalling pathways have been identified as direct regulators of muscle size in embryonic muscle growth by controlling proliferation, Insulin Growth Factor (IGF) and Transforming Growth Factor β (TGFβ) pathways. *IGF-1* overexpression within muscle cells causes significant fibre hypertrophy (excess size) due to increased muscle progenitor proliferation (Coleman et al 1995). In contrast, a secreted factor of the TGFβ pathway, *myostatin*, has been shown to act as a promoter of differentiation. Cattle that carry a *myostatin*-null mutation are known as “double-muscled” due to uncontrolled muscle growth that leads to

enormous size (Grobet et al 1997; McPherron & Lee 1997), and similar phenotypes have been observed in mice, dogs and humans (Schuelke et al 2004; Mosher et al 2007). Therefore, *myostatin* acts as a regulator of the balance between proliferation and differentiation; overexpression leads to progenitor pool depletion while inhibition results in expansion of the progenitor population (Manceau et al 2008), and this occurs by increasing the expression of myogenic factors and cell-cycle related genes (mentioned below).

### 1.1.3 Wnt, Notch and the induction of differentiation

While maintenance of a proliferative versus a differentiating state in the dermomyotome is crucial for correct muscle formation, and as mentioned above various factors play roles in this process, the first true sign of commitment to a myogenic fate is the expression of the Myogenic Regulatory Factors (MRFs). This cell-fate choice to whether or not enter the myogenic program is absolutely essential, and is one of the main topics of my research. Numerous studies spanning decades have suggested Wnts arising from the neural tube and ectoderm (*WNT1*, *WNT3a* from the neural tube (Marcelle et al 1997) and *WNT6* from the ectoderm (Tajbakhsh et al 1998) direct the expression of early MRFs (Münsterberg et al 1995; Dietrich et al 1997; Tajbakhsh et al 1998; Borello et al 2006). Furthermore, this Wnt-mediated activation has been shown to act through the β-catenin Canonical Wnt pathway (Borello et al 2006; Gros et al 2009). However, a recent study performed by Rios et al (2011) demonstrated that it is instead Notch signalling which directs DML progenitor cells to initiate myogenesis through the activation of MRFs. This activation is directed by neural crest cells (NCCs) expressing the Notch ligand Delta-like 1 (*DLL1*). As the migrating NCCs pass in close proximity to the somites, ligand-receptor interactions occur and induction of MRFs is induced (Rios et al 2011). This study not only revealed a novel function of neural crest cells as inducers of myogenesis, it further showed that Notch is necessary for activation of the myogenic program. Initially, this data contrasts with studies showing that *DLL1* expression in the DML, and its subsequent Notch response, inhibits differentiation of muscle progenitors instead of promoting it

(Schuster-Gossler et al 2007). This Notch-dependent maintenance of the progenitor pool is mediated by the transcriptional activity of Notch factor *RBP-J* (Vasyutina et al 2007). *RBP-J* activity is also necessary to maintain a progenitor pool in adult muscles, as evidenced by the spontaneous activation and subsequent depletion of muscle stem cells in *RBP-J* deficient muscle cells (Bjornson et al 2012). Conversely, activation of *Notch-1* in these cells leads to increased proliferation (Conboy & Rando 2002). This effect is also observed during aging, as a reduced regenerative capacity in old muscles is associated with a failed maintenance of the progenitor muscle stem cell population due to reduced Notch activity (Conboy et al 2003).

However, the Notch-mediated induction of differentiation reported by Rios et al was dependent on a transient activation of Notch signalling. In contrast, artificially maintaining Notch signalling reverts their entry into myogenesis, consistent with the aforementioned reports. Differing effects dependent on levels of activation suggest a permissive role of Notch signalling that may be context- and timing-dependent; for example, within cells already expressing Wnts. Indeed, during the course of my thesis, I aimed to understand the relationship between Notch and Wnt signalling in the context of this crucial myogenic cell-fate choice between proliferating and differentiating, while reconciling differing views on the effect of Notch within this population. Therefore, a detailed analysis of both Wnt and Notch pathways is provided ahead, while the results obtained in this study are presented in chapter 2.

### 1.1.4 The roles of *MYF5* and *MYOD*

As mentioned above, a commitment to a myogenic fate begins with the expression of the Myogenic Regulatory Factors (MRFs). There are four MRFs, themselves part of an extended family of basic helix-loop-helix transcription factors: *MyoD* (Davis et al 1987), *Myf5* (Braun et al 1989), *MyoG/myogenin* (Edmondson & Olson 1989) and *Myf6/MRF4* (Braun et al 1990; Miner & Wold 1990). These genes are expressed exclusively in skeletal muscles and are so potent in their induction of myogenesis that ectopic expression of any of these genes can convert many cell

types into fully differentiated myoblasts (Davis et al 1987; Braun et al 1989, 1990). All four proteins heterodimerize with E-proteins which bind specifically at highly conserved CANNTG sites (called E-boxes), found within the promoters of many muscle-specific genes (Buckingham 1996).

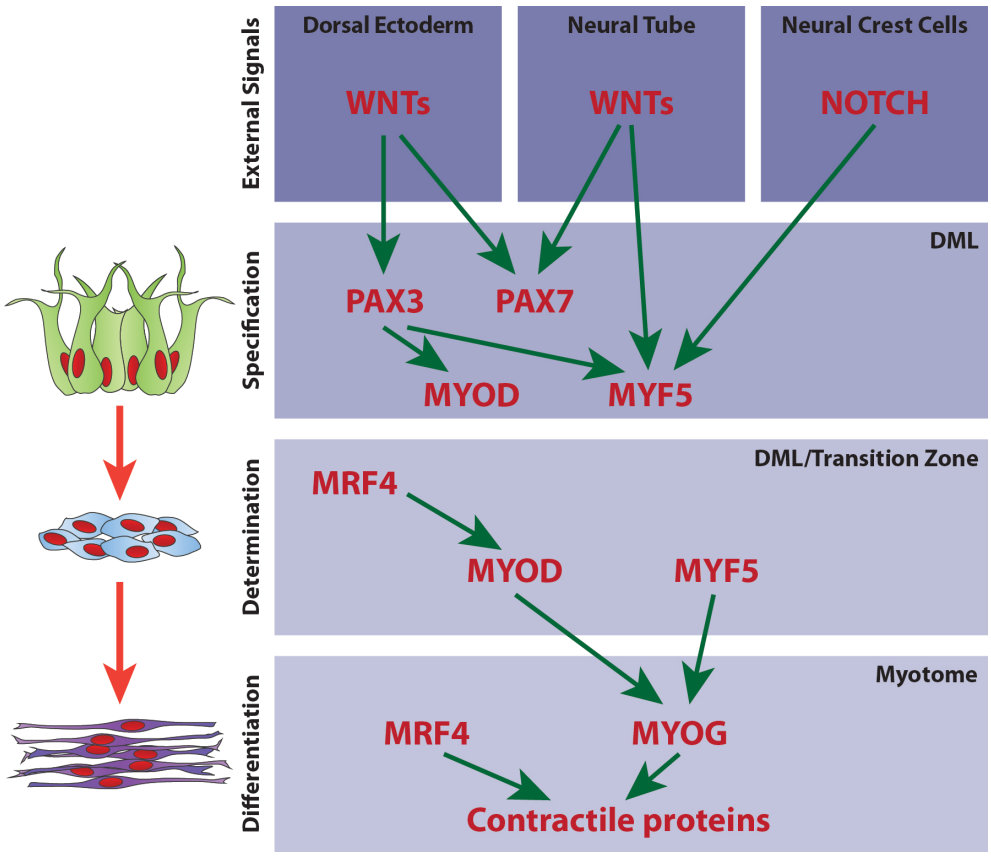


**Figure 1.2 Simplified model of induction of Pax3/7 and MRFs during trunk myogenesis**

Wnt signalling arising from the dorsal ectoderm as well as the neural tube induce expression of PAX3 and PAX7 within the dorsomedial lip (DML). Wnt signalling from the neural tube and/or Notch signalling from neural crest cells induces expression of MYF5. Pax3 also induces expression of MYOD. Myogenin (MYOG) is located downstream of MYF5 and MYOD and directly induces the expression of contractile genes. MRF4 can act upstream of MYOD prior to differentiation or downstream of myogenin. DML: Dorsomedial lip.

Activation of myogenesis is marked by the expression of *Myf5* and *MyoD*. In chickens and mice, *MyoD* and *Myf5* are expressed at the earliest stages of dermomyotome formation *in vivo* (Emerson 1990). In chickens, however, *MYOD*

appears at an earlier stage, marking cells in the median wall of the newly formed somite (Kiefer & Hauschka 2001). While neither *MyoD* nor *Myf5* alone are absolutely necessary for myogenesis, as shown by the presence of muscles in single *MyoD* or *Myf5* knockout mice (Braun et al 1992; Kablar et al 1997), they each compensate for the other's absence (Rudnicki et al 1992), as seen in the double *MyoD*$^{-/-}$/*Myf5*$^{-/-}$ mouse, which lacks all skeletal muscles (Rudnicki et al 1993). These defects in muscle development are due to a failure of progenitors to progress through differentiation, further demonstrating MYOD and MYF5 regulate the cell-fate choice that directs undifferentiated progenitors towards a mature muscle fate. However, this choice occurs within the context of *Pax3/7* expression, and while single *Myf5*$^{-/-}$ or *Pax3*$^{-/-}$ mutant mice do not display any gross muscle defects (Franz et al 1993; Tajbakhsh et al 1997), the double-knockout mice for *Myf5*/*Pax3* have a complete absence of muscle in both the trunk and the limbs (Tajbakhsh et al 1997). In this mouse, MYOD is unable to compensate for the absence of MYF5, suggesting PAX3 acts upstream of both these genes. Conversely, overexpression of PAX3 in the neural tube or presomitic mesoderm results in the ectopic activation of *MYOD* (Maroto et al 1997). These results establish a model where progenitor cells are dependent on *Myf5* and/or *MyoD* to initiate myogenesis, but only in a context where *PAX3* or *7* are present (Figure 1.2). However, it must be mentioned that initial experiments on *Myf5* knockout mice did not account for the close proximity between the *Myf5* and *MRF4* loci. This meant that *Myf5*/*Pax3* double knockout mice where in fact triple knockout for *MRF4* as well. Exclusive *MyoD*$^{-/-}$/*Myf5*$^{-/-}$ knockouts have since been created but have not re-addressed this question (Kassar-Duchossoy et al 2004).

### 1.1.5 Cell-cycle regulation

The switch from a proliferative to a differentiated state also requires cells to exit the cell cycle in order to become postmitotic. In culture, myoblasts will remain in a proliferative state until they either reach confluence or are starved by removal of nutrients, at which point they move to G0 and begin expressing differentiation markers. *In vitro* studies have revealed key molecules involved in myogenic cell

cycle progression. Some of the known regulators of cell cycle cyclins (*cyclin A* and *cyclin D*) and cyclin-dependent kinases (CDKs), play a role in progression from G1 to S phase and are known to be downregulated specifically during myogenic differentiation. Furthermore, the members of the cyclin inhibitor family type CIP/KIP; *p21*, *p27* and *p57* are strongly expressed in muscle masses during formation of the primary myotome (Matsuoka et al 1995; Zabludoff et al 1998) and are essential in allowing the switch from a proliferative to a terminally differentiated state (Zhang et al 1999; Manceau et al 2008). Another molecule involved in arresting cells at G0 is the tumour repressor retinoblastoma protein (*pRb*). Transgenic mice that express low levels of *pRb* die at birth with skeletal muscle defects and extensive cell death. Muscle fibres from these mutant mice display hyper-polyploidy, suggesting this protein plays a vital role in the control of the proliferation, differentiation and cell death during muscle formation (Zacksenhaus et al 1996).

In cycling cells, MYOD also controls the expression of *p21*, therefore regulating the cells' transition from G2 to M phase (Charrier-Savournin et al 2004). Furthermore, the downregulation of *Myf5* and *MyoD* in proliferating myoblasts can cause cells to enter G0 phase. Expression levels of MRFs are intimately linked to cell cycle progression. Undifferentiated, quiescent G1 cells *in vitro* will strongly express *Myf5* but not *MyoD*. In contrast, cells moving towards G0 will decrease *Myf5* expression levels while increasing *MyoD* (Lindon et al 1998; Kitzmann et al 1998).

### 1.1.6 Formation of the primary myotome

As epithelial progenitor cells within the dorsomedial lip initiate myogenesis, they undergo a crucial epithelial to mesenchymal transition (EMT, Rios et al, 2011) and move towards the forming myotome through a region termed the transition zone (Gros et al, 2009). The movement potentially marks the beginning of the formation of the primary myotome. This structure is located ventral to the dermomyotome and dorsal to the sclerotome (Figure 1.3A) and is populated by myocytes that go on to form postmitotic, differentiated early fibres spanning the width of the myotome, and are believed to serve as a basic organising structure prior to the

secondary growth phase. However, the initial steps of primary myotome formation and what structure initiates it have been a matter of contention within the field. Lineage tracing experiments performed by the groups of C. Ordahl and C. Kalcheim have come to opposite conclusions regarding which cells initiate formation of the primary myotome in vertebrates. By using the lipophilic dye DiI to label cells within the borders, Ordahl's group concluded that the very first muscle precursors originate from the DML and translocate to initiate epaxial (medial) myotome formation. One day later, cells from the VLL undergo a similar process, moving into the myotome to form new hypaxial (lateral) fibres. Furthermore, they reported cells originating from the anterior and posterior lips do contribute to hypaxial muscles, but do so at negligible levels (Denetclaw & Ordahl 2000; Denetclaw et al 1997) (Figure 1.3B).

The alternate model proposed by Kalcheim and colleagues states that three consecutive waves of cell migration establish the primary myotome. Initially cells located at the median wall of the somite (prior to dermomyotome border formation) form the very first fibres (Kahane et al 1998). DiI tracing of these "pioneer cells" showed that they first migrate towards the anterior border of each somite, before elongating until reaching the posterior border of the somite (Kahane et al 2007). Furthermore, pioneer progenitors were shown to colonize both the epaxial and hypaxial myotome. Kalcheim's model states that following pioneer cell migration, all four borders of the dermomyotome produce cells that generate fibres (after an anterior-ward migration similar to pioneer cells) that intercalate with the first wave (Cinnamon et al 2001). The third wave is composed of mitotically active AL and PL cells that enter the myotome, divide to increase muscle mass and differentiate into fibres, all within the primary myotome (Kahane et al 2001) (Figure 1.3C).

In order to settle the debate between these two models, lineage tracing of these different populations using GFP was performed in our lab (Gros et al 2004). While the use of DiI as a lipophilic cell membrane marker allows precise targeting of specific cell groups, the fast turnover of cell membrane leads to its rapid re-distribution throughout it, therefore impairing the correct visualization of the

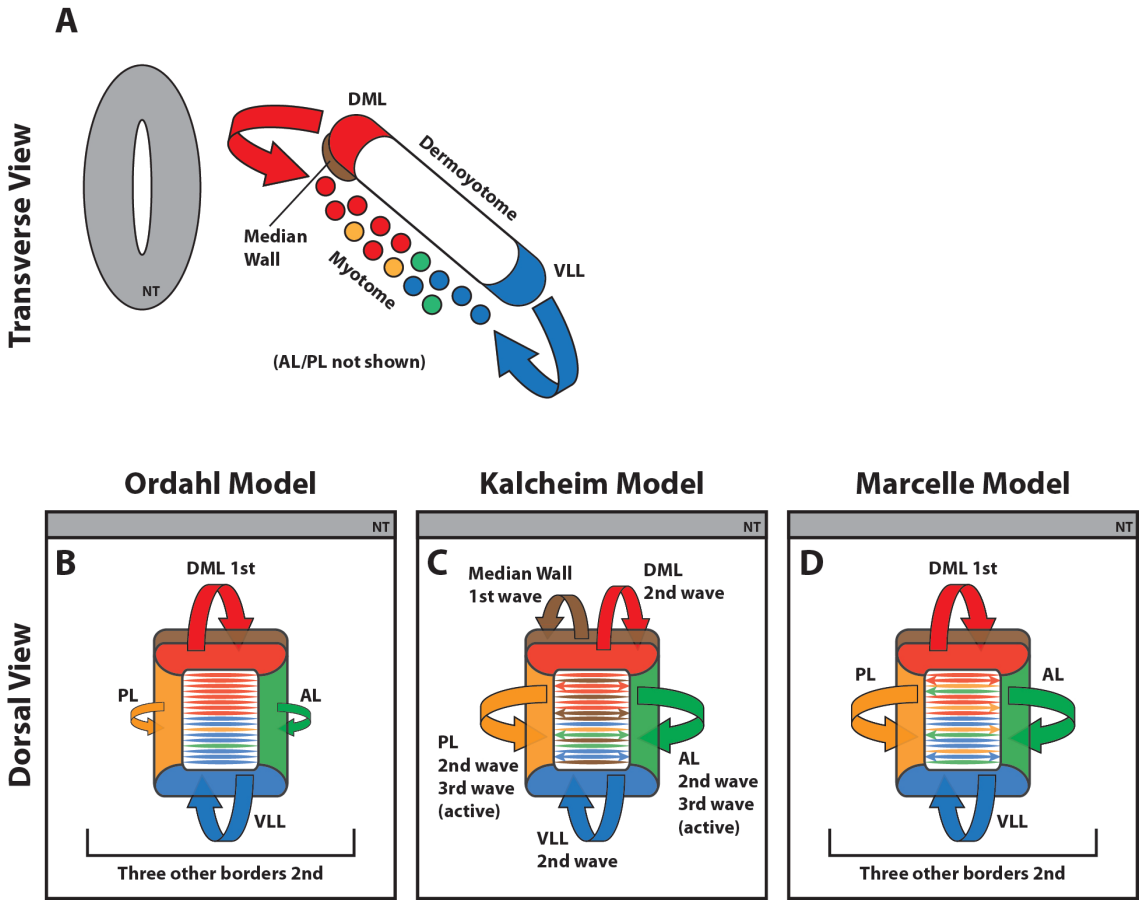


**Figure 1.3 Mechanisms of formation of the chick primary myotome**

**A.** Diagram showing a transverse view of a chick dermomyotome and myotome. Progenitors from all borders (DML in red, VLL in blue, AL and PL not shown) translocate into the myotome (shown as circles), located ventral to the dermomyotome, as they differentiate. The median wall is located ventral to the DML (brown). **B-D.** Diagrams showing a dorsal view of a chick dermomyotome borders and myotome (no central dermomyotome showed). **B.** Ordahl's model of primary myotome formation. **C.** Kalcheim's model of primary myotome formation. **D.** Marcelle's model of primary myotome formation. NT: neural tube, DML: dorsomedial lip, VLL: ventrolateral lip, AL: anterior lip, PL: posterior lip. Arrows depict fibre elongation patterns.

entire cell structure. In Gros et al (2004), progenitors from all four borders of the dermomyotome were electroporated with a GFP construct driven by a ubiquitous promoter. Lineage tracing of these cells revealed all four borders contribute to myotome formation in similar amounts. In an initial wave, cells from the DML form the first fibres. In a second wave, PL-, AL- and VLL-derived cells elongate from the borders to contribute to muscle formation. In contrast to Kalcheim's model, i) the anterior-ward migration prior to elongation was not observed and ii) the epaxial

and hypaxial domains remain markedly segregated. In contrast to Ordahl's model, Gros et al reported progenitors from the AL and PL contribute a large amount of fibres to the primary myotome (Figure 1.3D).

### 1.1.7 The roles of *myogenin* and *MRF4* in the myotome

Just as initial expression of *Myf5* marks a transition from a progenitor to a committed myogenic state, the regulatory factor *myogenin* is a marker of fully differentiated muscle cells. Chick embryos express *myogenin* at two days of development, shortly after *MYOD* is detected (Hacker & Guthrie 1998), while in mice *myogenin* appears slightly prior to *MyoD* expression (Sassoon et al 1989). In both models expression increases during fibre differentiation and is maintained in adult fibres. Soon after myogenin is detected, cells elongate and begin a process of fusion to other muscle cells that allows them to elongate further. This crucial process will continue well after birth and until puberty, as mature fibres elongate by undergoing extensive fusion. The dynamics and mechanisms underlying this process are poorly understood and are also the focus of my doctoral studies. Therefore a detailed review of fusion in muscles and other mechanisms is presented ahead.

*Myogenin*$^{-/-}$ mice display a striking phenotype, where the muscle masses are populated by unfused myoblasts with only occasional fibres (Hasty et al 1993; Nabeshima et al 1993). These results suggest *myogenin* is placed immediately upstream of the fusion cascade. However, as will be discussed later, further evidence from other knockout models suggests this is not the case. However, results from double knockout *MyoD*$^{-/-}$/*myogenin*$^{-/-}$ or *Myf5*$^{-/-}$/*myogenin*$^{-/-}$ mice exhibit the same phenotype as single *myogenin*-null mice (Valdez et al 2000), demonstrating that, irrespective of fusion, myogenin does acts downstream of either MRF (Figure 1.2). Meanwhile, the last remaining factor, *MRF4*, displays a complex behaviour within the myogenic signalling cascade. This gene has a transient muscle expression between embryonic days 9 and 11.5 of mouse development after which it is re-expressed at day 16, then maintained in fibres up to adulthood (Bober et al 1991). Interestingly, *MRF4*-null mice develop normal

musculature but have a four-fold increase in *myogenin* expression (Braun & Arnold 1995; Patapoutian et al 1995; Zhang & McLennan 1995), suggesting myogenin could be compensating for the lack of this protein. However the relationships among the MRFs are not as simple, as analysis of various mutant lines show that in some *MyoD*$^{-/-}$/*Myf5*$^{-/-}$ mutant mice *MRF4* expression remains unchanged (Rudnicki et al 1993). Furthermore, these mice fail to display any of the muscle defects originally described in the original double knockouts, instead appearing normal (Zhang et al 1995). These results suggest MRF4 can act upstream of *MyoD*. However, evidence that both myogenin and MRF4 are able to directly activate transcription of differentiated muscle-specific proteins such as troponin I (Yutzey et al 1990), together with the downregulation of *MRF4* in the *myogenin* mutant (Venuti et al 1995), provide evidence for two conclusions: first, myogenin is located downstream of MYOD/MYF5 and is actively involved in directing terminal differentiation, and secondly, MRF4 can act both upstream of MYOD and downstream of myogenin in a combined role (Figure 1.2).

In contrast to the initial myogenic steps described before, the genetic mechanisms regulating terminal fibre maturation are not as well studied. The vast number of genes upregulated upon muscle differentiation compared to the small number of targets described so far suggests much remains to be understood (Blais et al 2005). It is known that MRFs, along with Myocyte Enhancer Factor 2 (*MEF2*) (Molkentin et al 1996) act upstream of many of these genes. A large number of promoters of structural and contractile proteins, such as the anchoring molecule utrophin, contain E-boxes to which MRFs bind (Dennis et al 1996). In addition, forced expression of *MyoD* in mesenchymal stem cells results in expression of Myosin Heavy Chain, a key component of the contractile apparatus, as well as dystrophin, an important protein that anchors to the cell membrane (Akizawa et al 2013). Recently, research combining genome-wide transcription factor binding and expression profiling have attempted to decipher how and who induces markers of terminal differentiation (Li et al 2011; Blais et al 2005). Evidence shows MRFs are not only involved in the expression of structural and contractile proteins, but also

in the formation of the crucial neuromuscular junction and its related components (Blais et al 2005).

Aside from the potential role of Wnt ligands in directing muscle differentiation, Wnts secreted from the neural tube have a function in the establishment of the polarity axis of elongating muscle fibres. Gros et al (2009) showed that neural tube-secreted WNT1 and WNT3a induces *WNT11* expression in the DML, which in turn functions as a directional cue, inducing primary fibres to correctly elongate along the anterior-posterior axis of the somite (Gros et al 2009). This behaviour is mediated by the non-canonical planar cell polarity Wnt pathway. Interestingly, neural crest cells seem to have a role in this process, as heparan sulfate proteoglycan glypican 4 (GPC4) expressed on neural crest cells acts as a "trap" on the cell surface, where secreted Wnts are caught and transported to the dermomyotome as NCCs migrate by (Serralbo & Marcelle 2014).

### 1.1.8 Second step of myogenesis

The first step of myogenesis described above results in a thin layer of muscle fibres constituting the primary myotome. Following this, a second step is necessary to increase the size of the myotome, which arise from cells originating in the central dermomyotome. In the chick and mice models, the second step of myogenesis begins at around E3.5/E10.5 respectively, and is initiated by an EMT of the central dermomyotome cells (Figure 1.4). It is characterised by changes in polarity, cytoskeletal re-organisations and loss of cell junctions, as shown by loss of epithelial markers β-catenin and N-cadherin (Gros et al 2005). Unlike the cells emanating from the borders, which readily differentiate, those that delaminate from the dermomyotome are true progenitors, as they maintain the capacity to proliferate and differentiate within the myotome (Relaix et al 2005), thereby contributing to the formation of new muscle fibres, and massively increasing the size of the myotome (Kassar-Duchossoy et al 2005).

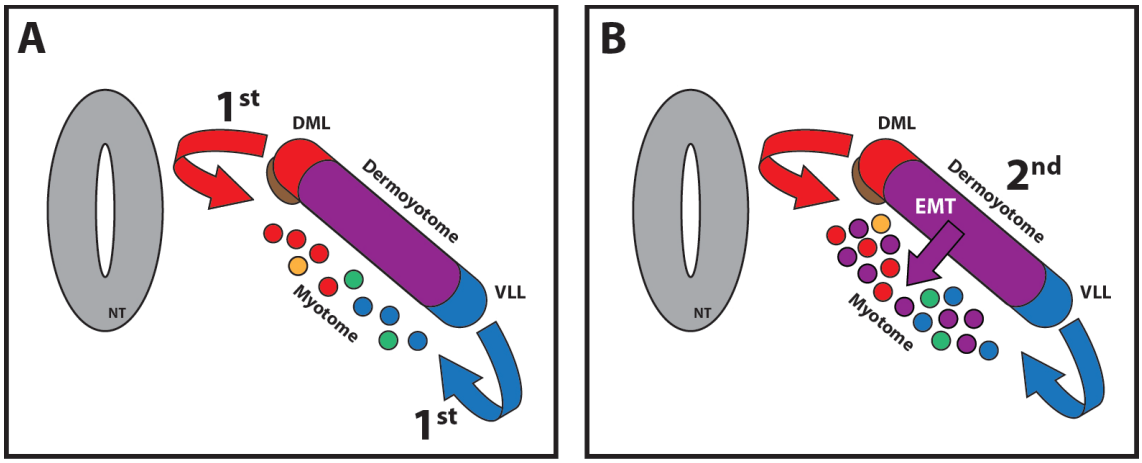


**Figure 1.4 Second step of myogenesis**

**A.** The first step of myogenesis involves translocation of muscle progenitors from the four borders of the dermomyotome towards the myotome. **B.** In the second step of myogenesis, muscle progenitors undergo EMT and "parachute" down to the myotome, where they begin forming fibres that will constitute the bulk of the muscle. NT: neural tube, DML: dorsomedial lip, VLL: ventrolateral lip.

### 1.1.9 Limb musculature

In amniotes, all limb muscles are formed by somite-derived cells, originating from the ventrolateral lips (VLL) of limb-level somites. In the chicken, this occurs only from somites 16-21 and 26-33, corresponding to the location where the future fore- and hindlimbs form (Chevallier et al 1977; Christ et al 1977; Christ & Ordahl 1995). Here, PAX3 present in the VLL epithelial progenitors induces expression of the tyrosine kinase receptor c-*Met* (Epstein et al 1996). *Pax3* is essential for limb muscle specification, as *Pax3*$^{-/-}$ mice have a complete absence of limb musculature (Franz et al 1993). Meanwhile, FGF signalling by the forming limb bud induces the mesenchymal cells neighbouring the somites to express scatter factor/hepatocyte growth factor (*SF/HGF*) (Heymann et al 1996). The two proteins interact in a paracrine manner, with SF/HGF guiding the *c-Met* expressing cells through the limb bud mesenchyme (Dietrich et al 1999). These interactions induce a large portion of the *Pax3*$^{+}$ VLL progenitors to undergo an EMT and begin migrating outwards, toward the developing limb bud (Chevallier et al 1977; Hayashi & Ozawa 1995). *Pax3* expression is transient, being lost by E12.5, while PAX7 is not present as these cells undergo EMT, instead appearing by E11.5 and remaining

active throughout muscle formation. Chicken expression patterns differ slightly to mice. Here, *PAX3* expression is lost before *PAX7* becomes active, as cells move away from the VLL (Galli et al 2008). While c-Met and SF/HGF are absolutely essential for progenitor migration, as shown by the complete absence of limb musculature in knockout mice models (Bladt et al 1995; Dietrich et al 1999), migratory muscle progenitors also require expression of the homeobox gene *Lbx1* (Jagla et al 1995) for their correct migration. VLL-derived progenitors in *Lbx1*$^{-/-}$ mice delaminate from the border correctly, but either fail to migrate or do so aberrantly (Gross et al 2000; Brohmann et al 2000). It is likely that LBX1 controls expression of genes required for recognition or interpretation of signalling cues during migration. As muscle progenitors migrate, they express the chemokine receptor *CXCR4*. The corresponding ligand SDF1 is expressed within the limb and serves to guide the *CXCR4*$^{+}$ cells; ectopic expression of SDF1 acts as a chemo-attractant to migrating myoblasts (Vasyutina et al 2005). As expected, migration of limb progenitors in *CXCR4*-knockout mice is defective (Vasyutina et al 2005). The migrating cells are highly proliferative; therefore, the muscle progenitor mass increases in size as it moves further into the limb (Duprez 2002). Initially, these cells migrate as a single unit, but begin separating into dorsal and ventral masses, divided by the prechondrogenic core, prior to reaching the end of their migration (Chevallier et al 1977; Schramm & Solursh 1990) (See Figure 1.5).

Once these cells reach their destination, they organize into pre-muscular masses consisting of two parts: a superficial layer of proliferating cells and a deeper differentiating core that will eventually form fibres (Patel et al 2002; Füchtbauer 1995). At this point, in both chicken and mice, PAX3 directly activates expression of *Myf5* and *MyoD* (Kassar-Duchossoy et al 2005; Bajard et al 2006). While *Myf5* remains active in fetal and adult myoblasts, *MyoD* is only required during embryonic differentiation. In mice, *myogenin* begins expression at E11.5 and maintains its level of expression throughout muscle growth (Yablonka-Reuveni & Rivera 1994). The last regulatory factor to appear is *MRF4*, initially expressed at E13.5 and remaining as the highest expressed MRF in adult musculature (Bober et al 1991). Here, in contrast to what occurs in the trunk, MRF4 does not act both

upstream of *MyoD* and downstream of myogenin. Instead, expression patterns and double knockout models have shown it is exclusively required only at later stages of myogenesis (Kassar-Duchossoy et al 2004; Rawls et al 1998).

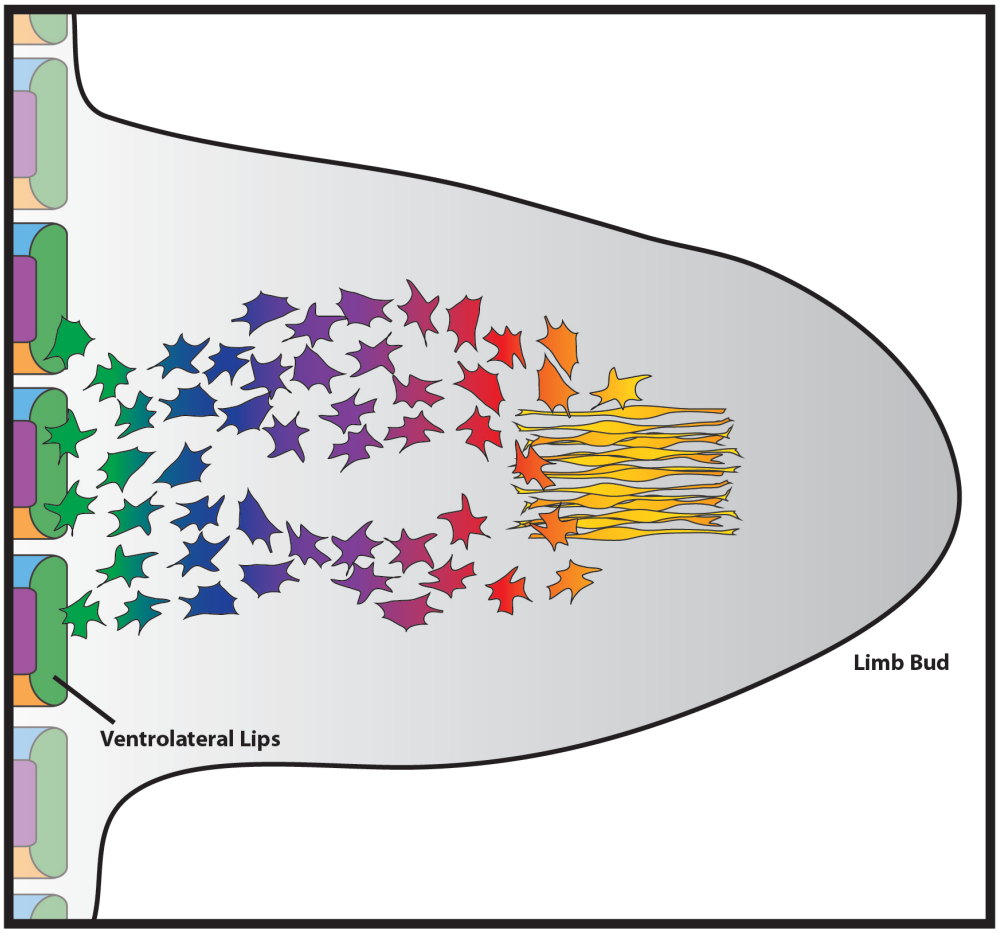


**Figure 1.5 Limb myogenesis**

Schematic showing skeletal muscle formation and main genes involved in the limb. LM: Limb Mesenchyme. Single arrows: direct induction. Double arrows: paracrine interactions. Dorsal view. Adapted from (Buckingham et al 2003).

### 1.1.10 Satellite cells and the repair of adult muscle

While fully differentiated, functional muscle fibres are postmitotic and unable to further proliferate, the ability to repair damaged muscle and increase muscle mass after stimulus remains. This post-natal skeletal muscle growth and repair is due to a population of remnant muscle stem cells termed satellite cells. These cells were first identified through electron microscopy images looking at amphibian muscle tissues, and termed satellite cells due to their localisation outside of the plasma membrane, but within the basal lamina of mature muscle fibres (MAURO & ADAMS 1961). Considered now as the *de facto* muscle stem cells (Chargé & Rudnicki 2004), they display a very high nucleus-cytoplasm ratio, few organelles and condensed chromatin, all hallmarks of quiescent cells (Schultz & McCormick 1994; Bischoff & Heintz 1994; MAURO & ADAMS 1961; Ontell & Kozeka 1984). Most quiescent satellite cells express *Pax7*, *CD34* and *M-cadherin* (Beauchamp et al 2000; Seale et al 2000). Upon fibre injury (due to damage, exercise, disease, etc.), satellite cells exit the G0 state and become highly proliferative, initiating expression of MRFs. Concordant with their role as resident stem cells, division is asymmetrical, with some cells continuing down the myogenic pathway and fusing to the existing fibres in order to repair them, while a fraction of them return to the quiescent state, thus maintaining the resident pool (Zammit et al 2004).

## 1.2 A cell-fate choice in the DML

As mentioned before, during primary myogenesis, the dorsomedial lip (DML) of the dermomyotome provides cells that will undergo EMT, differentiate and create fibres, or alternatively self-renew to maintain their own progenitor pool and avoid premature depletion (Ordahl et al 2001). This transition from unique expression of markers *Pax3* and *Pax7* to activation of MRFs (namely *Myf5*) is seen as a hallmark of commitment to a myogenic fate (Rios et al 2011). Therefore, it can be argued that the control of this Pax to MRF switch decides the cell's fate. During my studies I focused in part on investigating the control of this switch, namely the relationship between the pathways involved in directing it as well as the relationship between this fate change and the morphogenetic movements that accompany it, specifically the epithelial to mesenchymal transition. Here I will review the two main pathways involved, Wnt and Notch signalling, as well as the regulation of epithelial to mesenchymal transition.

### 1.2.1 Wnt signalling

Wnt signalling pathway was initially discovered through *Drosophila melanogaster* mutagenesis experiments, where they found that *wingless* (*wg*, (Sharma 1973)) and its subsequent mammalian homologue *Int1* (now *Wnt*, (Rijsewijk et al 1987)) were involved in directing formation of mammary carcinomas (Cabrera et al 1987; Rijsewijk et al 1987). Since then, Wnt signalling has been found to be involved in developmental processes such as cell proliferation, cell fate specification and cell polarity in a variety of tissues.

#### 1.2.1.1 Wnt pathway components

##### *1.2.1.1.1 Wnt ligands*

WNTs are a family of highly conserved secreted glycoproteins found in all studied metazoans so far (Willert et al 2003). They are all characterised by the presence of a conserved cysteine-rich sequence at the N-terminal which functions as an important signal peptide for secretion. The C-terminal end is also vital; truncation of this region leads to the formation of a dominant-negative form that inhibits

correct signalling (Hoppler et al 1996). Upon secretion, WNT ligands associate with glycosaminoglycans located at the extracellular matrix and can act as morphogens capable of short and long range signalling. Their relationship with extracellular matrix lipids is crucial, as these can regulate the degradation and diffusion of WNT molecules, as well as act like low-affinity co-receptors (Yan & Lin 2009). Proteoglycans such as DALLY and DALLY-like are able to transport WNT ligands by moving them from cell to cell, effectively creating a gradient of Wnt signalling (Lin & Perrimon 1999).

*1.2.1.1.2 WNT receptors*

Two families of receptor proteins are involved in Wnt signalling, the seven-pass membrane receptors Frizzled (FZD) and the Low density lipoprotein Receptor-related Proteins (LRP, (Logan & Nusse 2004)). The mammalian Fzd family consists of 10 members with a variable capacity to activate Wnt signalling. In contrast, there are only two LRP proteins, LRP 5 and 6. Between them, LRP6 plays a dominant role and is essential during development, while LRP5 is dispensable during embryogenesis; however, it is required for correct adult homeostasis (He et al 2004). Although *in vivo* evidence has not been reported, *in vitro* ligand binding assays and fusion proteins have demonstrated that binding of WNT ligand induces the formation of a FZD-LRP complex (He et al 2004), likely a necessary step to induce downstream signalling.

*1.2.1.1.3 Wnt extracellular agonists and antagonists*

Extracellular modulation of Wnt signalling occurs through the presence of secreted molecules. NORRIS and R-spondin (RSPO) can act as agonists of the Wnt pathway. Norris binds FZD4 (Xu et al 2004), while RSPO can interact with WNT, FZD and LRP6 (Kazanskaya et al 2004; Carmon et al 2011). Their mechanisms of action have not been described, but it is likely that the binding of these molecules to the ligand and receptors creates a positive feedback that reinforces Wnt signalling and stabilises the system (Kazanskaya et al 2004).

Wnt Inhibitory Proteins (WIFs) and secreted Frizzled-related proteins (sFRPs) can bind WNT ligands and function as inhibitors of the pathway (Hoang et al 1996;

Hsieh et al 1999). However, evidence suggests interactions between these inhibitors and the ligands can also work to regulate their stability and modify diffusion and distribution patterns (Bovolenta et al 2008). A separate group of inhibitors involves the Dickkopf (DKK) (Glinka et al 1998) and Wise/SOST families. DKK are LRP ligands, thus potently inhibiting Wnt signalling by competition with WNT ligands (Semënov et al 2001; Mao et al 2001), while SOST acts by potentially disrupting the FZD-LRP complex (Semënov et al 2005).

#### 1.2.1.2 Wnt pathways

Following ligand-receptor interactions, Wnt signalling can mainly occur through 3 separate pathways, these are the Canonical, Non-canonical Planar Cell Polarity (PCP) and Non-canonical Wnt/Calcium pathways.

##### *1.2.1.2.1 Canonical pathway: Wnt/β-catenin signalling*

The Wnt canonical pathway functions through the constant production and degradation of the protein β-catenin. At its essence, accumulation of β-catenin leads to activation of Wnt downstream targets while inhibition of this protein results in an "off" state.

Cytoplasmic β-catenin is constantly being degraded by a destruction complex consisting of the proteins AXIN, adenomatosis polyposis coli (APC), protein phosphatase 2a (PP2A), casein kinase 1α (CK1α) and glycogen synthase kinase 3 (GSK-3). Sequential phosphorylation of β-catenin by GSK-3 creates binding sites for E3 ubiquitin ligase β-TCRP, which results in its constant ubiquitination and degradation (Kimelman & Xu 2006). Upon activation of Wnt signalling by WNT-FZD-LRP binding, the cytosolic phosphoprotein Dishevelled (DSH) is recruited (Wong et al 2003). The exact mechanisms by which FZD interacts with and activates DSH are not well known, but phosphorylation of the protein either directly or through kinases PAR-1 and CKII are possible options (Chen et al 2003; Wong et al 2003; Sun et al 2001). Meanwhile, a crucial component of the destruction complex, AXIN, is recruited to the membrane by binding to the

phosphorylated cytoplasmic tail of LRP. Thus, proteasomal degradation no longer occurs, allowing cytoplasmic β-catenin to accumulate and enter the nucleus. Once

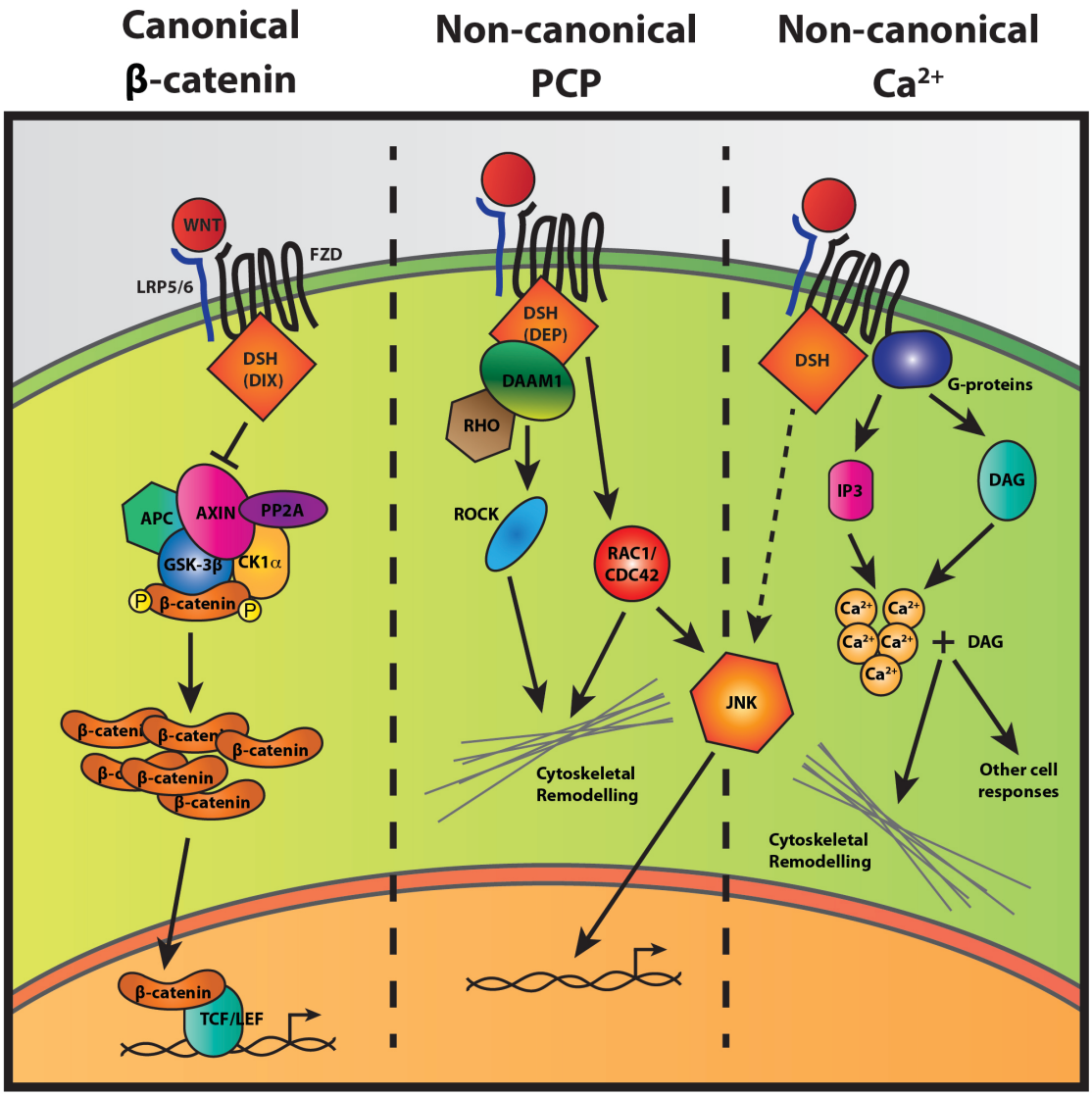


**Figure 1.6 Wnt pathways**

Schematic representing the 3 main Wnt pathway responses following binding of Wnt ligand to the FZD receptor (On state). Pathways depicted are: Canonical β-catenin-dependent pathway, Non-canonical Planar cell Polarity (PCP) pathway and Non-canonical $Ca^{2+}$ dependent pathway. See main text for abbreviations.

there, β-catenin binds to the N-terminus of the TCF/LEF protein, displacing the bound co-repressors TLE and Groucho (Daniels & Weis 2005) and converting it into a strong transcriptional activator (Behrens et al 1996; Molenaar et al 1996; van de Wetering et al 1997). Co-activator proteins such as CBP, BRG-1, Hyrax and

many others will then effect changes in local chromatin structure in order to allow transcription of Wnt target genes (Städeli et al 2006) The large number of possible co-activators of β-catenin allows the single pathway a great plasticity across tissues and developmental stages. See figure 1.6 for a simplified view of canonical Wnt signalling.

*1.2.1.2.2 Non canonical: planar cell polarity pathway*

As their name denotes (Frizzled, Dishevelled, Prickle), many of the proteins involved in Wnt signalling were initially found as causing defects in the organisation of the hairs and bristles covering the cuticle of *Drosophila* flies (Gubb & García-Bellido 1982; Vinson & Adler 1987; Vinson et al 1989). The observed phenotypes were due to a disruption in planar cell polarity (PCP), the signalling cascade that senses a cells' directionality and helps establish polarity in developing tissues (Strutt 2003), such as the convergence and extension movements observed during gastrulation (Mlodzik 2002).

Wnt/PCP signalling requires FZD and DSH for its activation. However, mutations to the DSH protein have revealed that different domains are required for canonical versus PCP signalling. For example, changes to the DSH DEP domain are absolutely required for PCP but dispensable for β-catenin-dependent signalling (Heisenberg et al 2000). Upon activation of FZD and the subsequent phosphorylation and binding of DSH, other core PCP proteins such as Flamingo (FMI), Van Gogh/Strabismus (VANG/STBM), Prickle (PK) and Diego (DGO) are recruited to form a transmembranal multiprotein complex (Strutt 2003). DSH then forms a complex with DAAM1 that activates the small G-protein RHOA through a guanine exchange factor. RHO then activates ROCK (Rho-associated kinase), a major player in cytoskeletal regulation. DSH also interacts with the GTPase RAC1, thus allowing the cell to establish a polarity along a specific axis (Figure 1.6).

*1.2.1.2.3 Non canonical: Wnt/$Ca^{2+}$ pathway*

Gain of function experiments in zebrafish revealed that expression of *wnt5a* and the receptor *fzd* led to an increase in the levels of intracellular calcium (Slusarski et al 1997). Further research has shown that FZD signals through heterotrimeric G-

proteins to activate diacylglycerol (DAG) and Inositol-1,4,5-triphosphate (IP3, (Li et al 2009)). IP3 then binds to its receptor at the endoplasmic reticulum, causing intracellular $Ca^{2+}$ levels to increase (Figure 1.6). Increased concentrations of DAG and calcium can activate the regulator of cytoskeleton remodelling Cdc42 through Protein Kinase C (PKC, (Choi & Han 2002)). In vertebrates, Wnt/$Ca^{2+}$ signalling is activated by the same ligands as PCP, which along with activation of actin-related proteins suggests both pathways may partially overlap (Strutt 2003).

## 1.2.2 Notch signalling

In contrast to Wnt signalling where short-range and long-range diffusion gradients direct developmental, homeostatic and disease processes, Notch signalling requires direct cell-cell contact, thus mediating signalling between neighbouring cells. Notch signalling is widespread during embryonic development, playing critical roles in pattern formation, cell-fate decisions and delineating borders within tissues.

### 1.2.2.1 Notch pathway components

#### *1.2.2.1.1 NOTCH ligands*

NOTCH ligands are mostly Type I transmembrane proteins consisting of an N-terminal DSL motif, specialised EGF repeats called a DOS domain and EGF-like calcium and non-calcium binding repeats. Both the DSL and DOS domains are involved in binding to the receptors, with the DSL domain acting through both *trans* and *cis* interactions. NOTCH ligands are classified based by the presence (Jagged/Serrate) or absence (Delta) of a cysteine-rich domain (Komatsu et al 2008).

#### *1.2.2.1.2 Notch receptors*

In mammals, four paralogous Type I transmembrane proteins constitute the NOTCH receptor family (Krebs et al 2003). Similar to the NOTCH ligands, the extracellular domain of the receptors is composed of tandem EGF-like repeats that mediate interactions with the ligands (Cordle et al 2008). Some of these repeats are calcium-binding, which play a role in determining the structure and affinity of

the receptor to its ligand (Cordle, Johnson, et al 2008). Following the EGF repeats is a unique negative regulatory region (NRR) consisting of three cysteine-rich Lin12-Notch repeats (LNR) and a heterodimerization domain (HD). Given the similarities between receptors and ligands, the NRR is necessary to prevent activation in the absence of the ligand (Gordon et al 2009). Following the extracellular domain (NED) is the single transmembrane domain (TMD), which is terminated by a stop translocation signal involving Arginine/Lysine residues. At the Notch intracellular domain (NICD), a RAM domain is followed by a long linker containing a nuclear localisation sequence (NLS) and seven ankyrin repeats (ANK domain). Further NLS sequences and a C-terminus PEST domain, involved in regulating NICD stability, complete the protein (Lubman et al 2007) (Figure 1.7A).

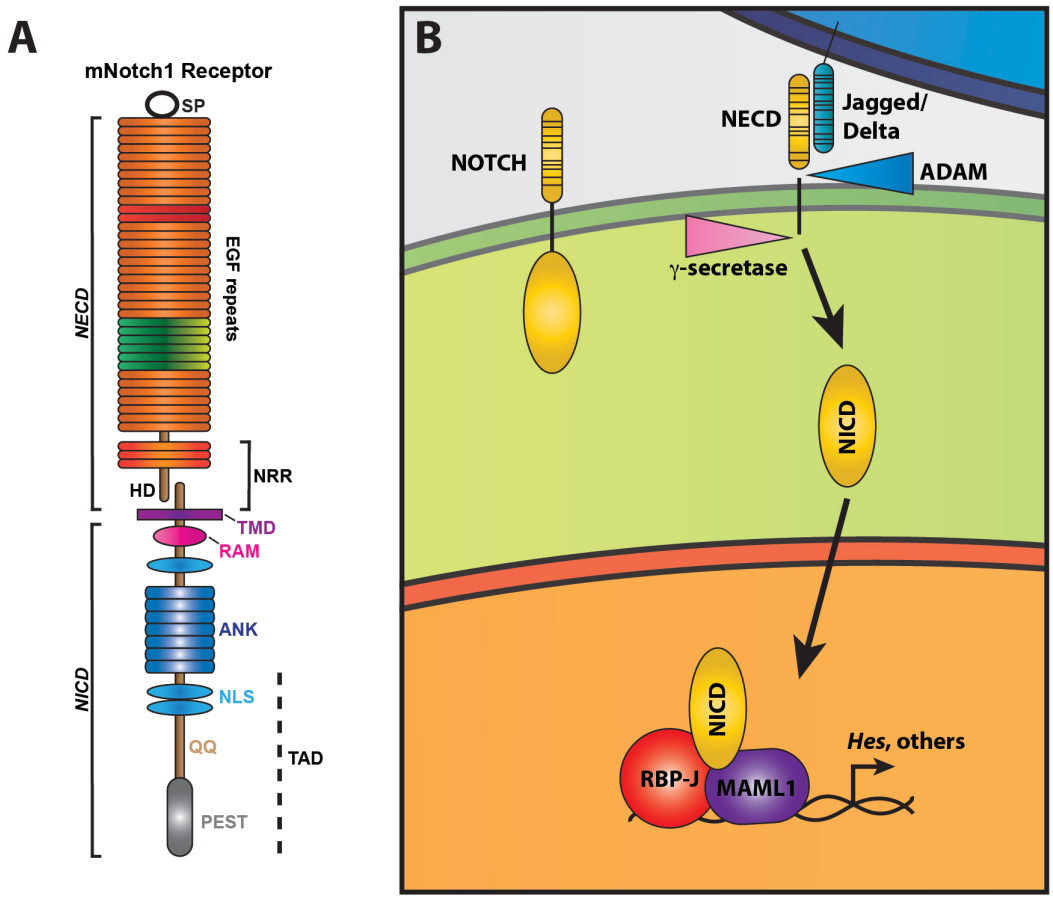


**Figure 1.7. Notch Pathway**

**A.** Diagram showing the individual protein domains constituting the mouse NOTCH1 receptor. Adapted from (Kopan & Ilagan 2009). **B.** Schematic of Notch canonical signalling. See main text for abbreviations.

#### 1.2.2.2 Notch downstream activation

NOTCH ligand-receptor binding causes a series of proteolytic events that lead to the cleavage and subsequent activation of the intracellular domain NICD as a transcription factor. Two cleavage events occur, one mediated by ADAM metalloproteases at site 2 (12 amino acids upstream of the TMD) (Sotillos et al 1997; Hartmann et al 2002) and a second one that involves progressive cleaving of the TMD by γ-secretase (Wolfe & Kopan 2004; Hartmann et al 2002). These actions results in a free NICD that contains numerous NLS domains, and thus is able to translocate to the nucleus where is forms a trimeric complex with the DNA-binding protein CSL (CBF1/RBP-Jκ/Su(H)/LAG-1) via its RAM domain. The ANK domain then mediates CSL binding to the co-activator Mastermind/LAG-3b (MAML). This action results in the recruitment of the MED8 mediator complex, eventually leading to the activation of downstream targets (Lubman et al 2004) (Figure 1.7B). Although many genes have been identified as directly controlled by Notch-mediated signalling (*p21*, *Myc*, etc.), the *Hes* (hairy and enhancer of split) family of transcription co-repressors is intimately related to NICD activity (Jarriault et al 1995). *Hes* genes are cyclical: NICD/CSL binding causes co-repressors including HES to dissociate and allow transcription. However, NICD then induces *Hes* expression causing again a transcriptional repression (Kobayashi et al 2009). This dynamic interaction allows *Hes* genes to regulate events such as the biological clock that determines somite segmentation (Pourquié 2011).

### 1.2.3 Regulation of epithelial to mesenchymal transition (EMT)

The transition of DML cells from a progenitor to a committed fate is not only marked by activation of the Wnt and Notch pathways, but also an epithelial to mesenchymal transition that allows them to move towards the myotome. As will be argued later, we believe both these pathways and EMT are linked and work together in directing this behaviour.

EMT involves the conversion of a cell from an epithelial phenotype to a mesenchymal migratory one. The process is transient in nature; cells can reverse the process numerous times through the activation of a mesenchymal to epithelial

transition (MET). EMT is a stereotypical process that follows certain hallmarks regardless of what cell type is performing it. These include dissolution of the cell-cell junctions, loss of apical-basal polarity, cytoskeletal remodelling and change of shape, while at a transcriptional level core epithelial genes are downregulated while mesenchymal ones become active (Lamouille et al 2014).

Vertebrate epithelial cells contact their neighbours through tight, adherens and gap junctions, among others (Huang et al 2012). Adherens junctions (AJ) are composed of a group of anchoring proteins that include E-cadherin and importantly, the regulator of Wnt canonical activity β-catenin. This dual-function protein can act not only to regulate transcription in the nucleus as was described before, but are also a key structural component of cell adhesion complexes. Cadherins and other structural molecules such as claudins and occludins are constantly being turned over, and upon EMT induction, their downregulation immediately causes their depletion at the junctions (Beco et al 2009). During AJ disassembly, E-cadherin is internalised through endocytosis (Palacios et al 2001). What occurs to the rest of the anchoring proteins, including β-catenin is a matter of debate. They could either internalise along with cadherins and disassemble (Ivanov et al 2004; Le et al 1999), or return back to the cytoplasm, where β-catenin could incorporate into the canonical Wnt signalling pool, move to the nucleus and transcriptionally activate downstream targets (Morali et al 2001; Lu et al 2003).

The SNAIL proteins are main players in the induction of EMT (Barrallo-Gimeno & Nieto 2005). They do so by down-regulating expression of anchoring proteins such as E-cadherins (Batlle et al 2000; Lin et al 2010; Peinado et al 2004), while activating genes needed for acquisition of a mesenchymal phenotype (Lamouille et al 2014). Initiation and progression of EMT not only involves the transcriptional induction of *Snail*. Similar to β-catenin, cytoplasmic SNAIL is constantly being phosphorylated and targeted for degradation by GSK-3β, the same protein involved in the Wnt canonical destruction complex (Figure 1.6). Several signalling pathways have been related to the activation and regulation of *Snail* and therefore EMT, including NFκβ, TGFβ, and as discussed below, both Wnt and Notch.

## 1.2.4 Interactions between Wnt, Notch and EMT

### 1.2.4.1 Wnt and Notch

Throughout development, many morphogenetic and patterning processes involve the activation of both the Wnt and Notch pathways, suggesting a possible link between the two. Initial evidence of this interaction came from wing patterning studies in *Drosophila*, where both pathways drive expression of each other during wing growth. Here, Notch signalling promotes the expression of *wingless* (the fly *Wnt* orthologue) at the forming wing margin. *Wingless* then returns the favour by promoting expression of the Notch ligands *Delta* and *Serrate*, creating a positive feedback loop during wing patterning. In higher organisms, this morphogenetic interplay has also been shown, with Notch and Wnt signalling playing opposite roles during mammary tissue elongation and branching morphogenesis. Here, WNT induces branching while NOTCH limits its expression pattern (Uyttendaele et al 1998). Similar interactions have also been reported in sea urchin germ layer specification (Angerer & Angerer 2003), vertebrate skin development (Estrach et al 2006) and segmentation clock formation in somites (Dale et al 2006).

While pattern formation involves Wnt/Notch crosstalk across tissues, both signalling cascades can interact at a molecular level within a single cell. Wnt signalling can block Notch by inhibition of the Wnt-related protein DSH towards the Notch transcriptional co-activator CSL (Collu et al 2012). Furthermore, the key mediator of Wnt/β-catenin dependent signalling GSK-3β is able to bind and phosphorylate NICD. The effect of this interaction is matter of debate, as GSK-3β either increases NICD half-life, therefore acting as a potential enhancer of Notch-induced signalling (Foltz et al 2002) or GSK-3β kinase is acting as an inhibitor of Notch signalling, instead of an enhancer (Espinosa et al 2003). Furthermore, ablation of *Notch* in *Drosophila* epithelial cells leads to β-catenin-induced tissue overgrowth (Sanders et al 2009). This function does not require CSL ligands, and is suggested to occur through sequestration of β-catenin at the cell surface by the NOTCH receptor (Brennan et al 2005). A similar effect is observed in mice, where

removal of *Notch-1* results in high levels of activated β-catenin, which leads to an increase in tumour formation (Nicolas et al 2003).

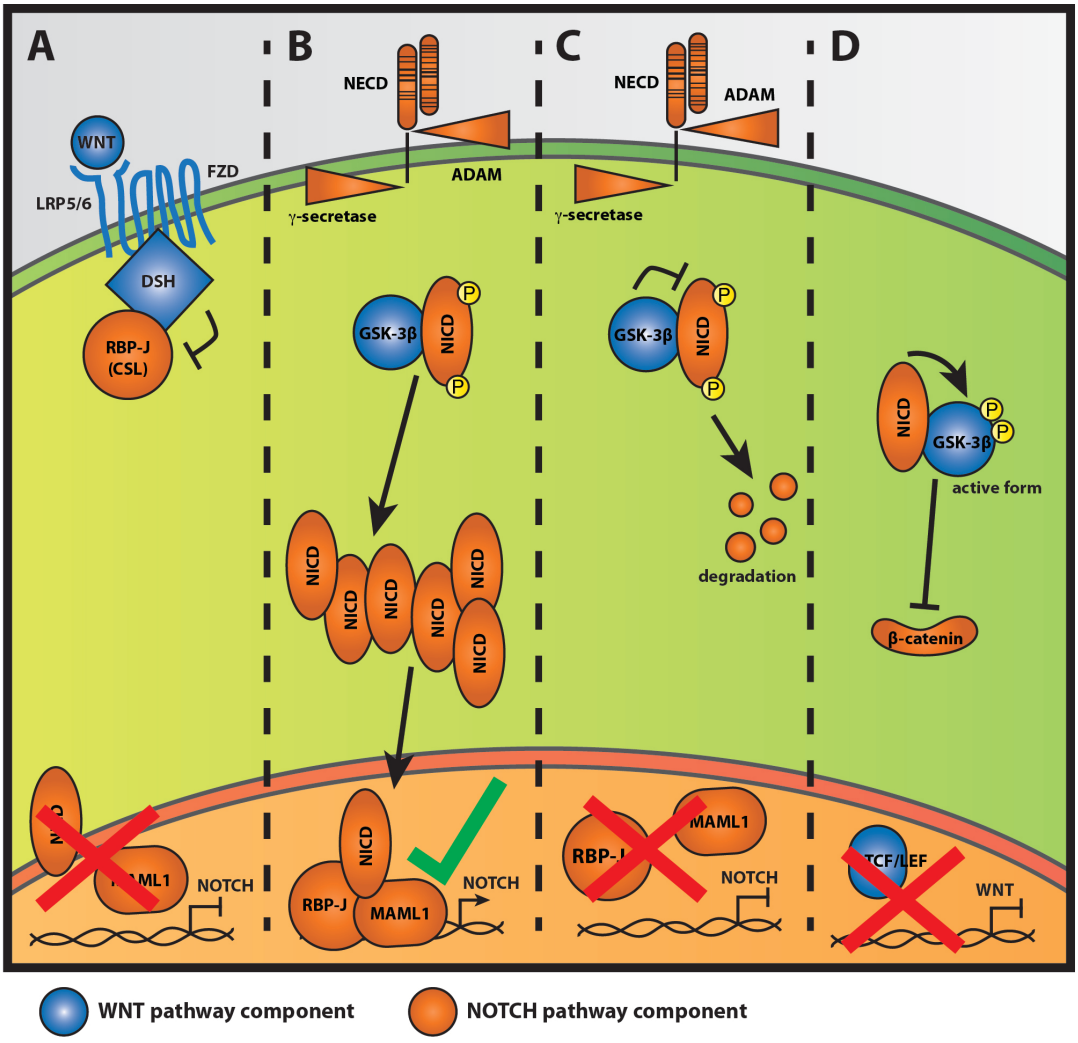


**Figure 1.8 Examples of reported intracellular interactions between Wnt and Notch pathways**

**A.** Dishevelled (DSH) binds and inhibits CSL, blocking Notch transcriptional activity (Collu et al 2013). **B.** Phosphorylation of NICD by GSK-3β increases its half-life, resulting in Notch up-regulation (Foltz et al 2002). **C.** Phosphorylation of NICD by GSK-3β leads to its degradation and Notch down-regulation (Espinosa et al 2003). **D.** NICD interacts with GSK-3β, leading to its phosphorylation into the active form. This leads to downregulation of canonical Wnt activity (Brack et al 2008). Conversely, Notch downregulation leads to inactive GSK-3β and subsequent Wnt target activation (not shown).

A crucial example of the complex interactions observed between Notch and Wnt pathways, made more relevant to this review by their effects on muscle cells are provided by Brack et al (2008). Here, a model is presented where a cell-fate choice within adult satellite cells on whether to proliferate or differentiate is dependent upon a balance between Notch and Wnt activation. An initial high Notch activity maintains cells in a progenitor state, while various factors including repression by Notch keep Wnt levels low. Once proliferation levels reach adequate numbers, the balance changes and Wnt activity increases while Notch decreases. Importantly, this interaction is again mediated by GSK-3β, where high Notch activity induces activation of GSK-3β, thus keeping canonical Wnt activity suppressed (Brack et al 2008). As has just been described, while Wnt and Notch pathways seem to be intimately related, the nature and directionality of their interactions appear tissue and timing dependent. Examples of suggested Wnt/Notch interactions are shown in Figure 1.8, however as will be shown in Chapter 2, new kinds of interactions remain to be found.

#### 1.2.4.2 An additional player: EMT

The numerous interactions reported between Wnt and Notch (for a detailed review see Hayward et al 2008) become even more intriguing when considering their possible roles during EMT. GSK-3β is not only a crucial component of the Wnt/β-catenin pathway and a potential regulator of NICD-mediated transcription (Zhou et al 2004), but is also essential in regulating SNAIL stability and thus its activity. Therefore, regulating GSK-3β activity could potentially regulate all 3 systems. AXIN could be acting as a chaperone to its fellow β-catenin destruction complex protein GSK-3β, transferring it to the nucleus and allowing SNAIL to stabilise and downregulate epithelial genes, thus driving EMT (Yook et al 2006). This is direct evidence of Canonical Wnt/β-catenin signalling triggering EMT. However, other interactions have been reported. For example, induction of *Snail* by EGF treatment results in downregulation of E-cadherin and increase in β-catenin-dependent TCF/LEF transcriptional activity, indicating SNAIL-mediated EMT is able to drive Wnt activation (Lu et al 2003). Similarly, IGF-induced EMT allows a

redistribution of β-catenin from the membrane to the nucleus, where it drives activation of TCF/LEF mediated genes (Morali et al 2001). EMT mediating Wnt is also shown with *Snail* overexpression leading to an increase in β-catenin-dependent transcription. SNAIL is suggested to directly bind to β-catenin, and although the mechanism by which transcriptional activation occurs is not explained, it is argued that competition with co-repressors for binding sites may allow β-catenin to more efficiently activate its targets (Stemmer et al 2008).

Similar to Wnt, the Notch pathway has been directly linked to EMT activation. In the embryonic heart, Notch induces TGFβ-mediated EMT. *Notch* inhibition in zebrafish embryos results in inhibited expression of *Snail*, while overexpression *in vitro* causes a strong EMT phenotype accompanied by elevated *Snail* expression (Timmerman et al 2004). Similarly, presence of the Notch ligand JAGGED1 is necessary for TGFβ-mediated EMT in the mouse mammary gland, kidney tubules and epidermis (Zavadil et al 2004). While these studies reported Notch directing EMT through the TGFβ pathway, a direct connection has also been shown. Notch can induce EMT on *Xenopus* embryos by directly upregulating *snail* expression through recruitment of NICD to the *snail* promoter (Sahlgren et al 2008).

## 1.3 A crucial stage in myogenesis: muscle fusion

During formation of the primary myotome, following the previously described cell-fate choice and the progenitors' eventual translocation from the dermomyotomal borders and differentiation, cells elongate and undergo fusion. This fusion process is not exclusive to early muscle formation. Adult fibres elongate by undergoing tens of thousands of rounds of fusion in order to attain the size needed to span from one joint to another. Fusion is also crucial for muscle satellite cells to repair the muscle. During my doctoral studies, I have attempted to understand the dynamics and mechanisms underlying this process. As membrane fusion is not exclusive to muscle cells and parallels can be drawn among different systems, here I will briefly describe other fusion models before reviewing the current knowledge on invertebrate and vertebrate muscle fusion.

### 1.3.1 Principles of membrane fusion

The lipid bilayer surrounding every cell forms a protective, mostly impermeable layer that keeps it functioning as a single unit. However, there are situations in which two membranes need to fuse to one another. Because lipid membranes will not spontaneously fuse without any energy input, as their physical properties mean they are naturally kept apart by a collection of physical forces (Rand et al 1988; Chernomordik et al 2006), specialised molecules are required for this fusion to occur. The function of these transmembrane proteins is to bring both membranes closer together than the distance at which they are at equilibrium, effectively creating an area between them devoid of any polar water molecules. At this point, the energy accumulated by bringing the membranes so close together is greater than that at normal conditions, and the lipid bilayers effectively join, creating what is termed a fusion stalk through hemifusion (Figure 1.9). The formation of this structure occurs because it is energetically favourable to its previous state (Yang et al 2003) and thus what was once two membranes becomes one.

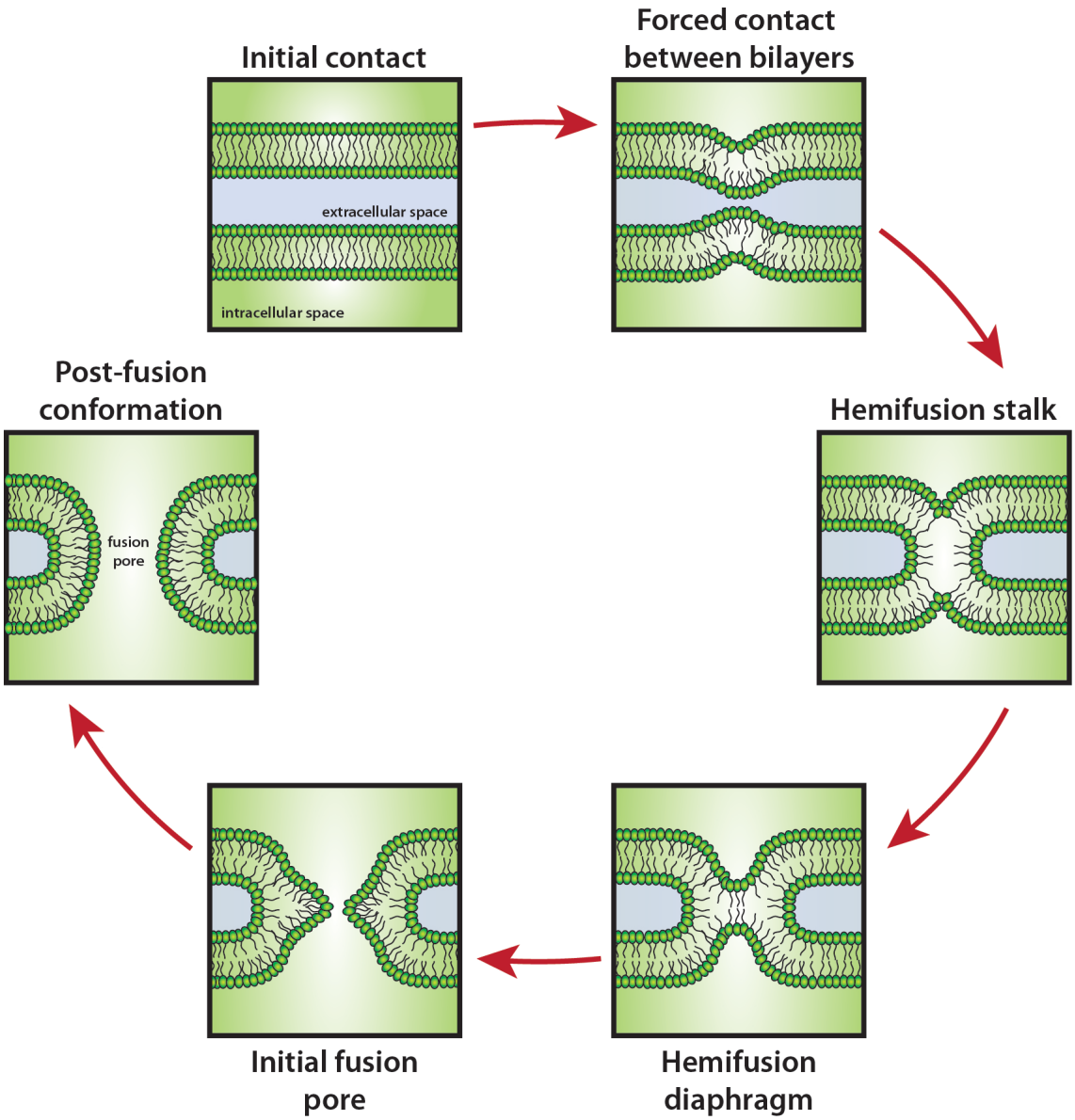


**Figure 1.9 Process of fusion by hemifusion stalk formation**

Schematics showing the conformational changes that lipid bilayers go through during membranal fusion by stalk formation. Based on (Chernomordik et al 2006).

### 1.3.2 Vesicle fusion

Vesicular fusion events are mediated by a family of transmembranal proteins called the SNAREs (soluble N-ethylmaleimide-sensitive factor attachment protein receptor) (Trimble et al 1988; Zeng et al 1998; Jahn & Scheller 2006). These proteins are present in organisms ranging from yeast to humans and are characterised by a "SNARE motif" consisting of 60-70 amino acids arranged in heptad repeats (Fasshauer 2003). SNARE proteins are classically identified as

either v-SNAREs or t-SNAREs (Söllner et al 1993), terms related to the concept of an asymmetry in the fusion partners (v- for vesicle and t- for target). During a fusion event, SNARE proteins present at both the vesicular and target membranes interact and form a *trans*-complex. The assembly begins at the N-terminal of the motif and proceeds down towards the C-terminus. As these proteins coil around each other they bring the membranes closer together up to the point of contact (Jahn & Scheller 2006). The resulting *cis*-SNARE complex is very stable, and it is possible that the energy produced by this coiling is sufficient to force the formation of a hemifusion stalk (Figure 1.10A). However, the ubiquitous presence of $Ca^{2+}$ sensing transmembrane proteins, synaptotagmins, suggests that calcium transport may be essential for this process (Tang et al 2006; Rickman & Davletov 2003).

Disassembly of the fusion complex is just as important, allowing the same molecules to undergo multiple fusion events. Performing this function is the yeast SEC18-homologue NSF (*N*-ethylmaleimide sensitive fusion protein) (Wilson et al 1989). This protein, along with its partner NSF-attachment protein (SNAP), recruits energy to dissociate the SNARE complex, allowing its recycling (Söllner, Bennett, et al 1993). The exact mechanisms by which this disassembly is achieved are unknown, but it occurs most likely through catalytic events involving ATP-hydrolysis (Hanson et al 1995).

### 1.3.3 Virus-cell fusion

In order to propagate, viruses need access to the cells they are infecting. Some classes of these infectious agents are surrounded by a lipid bilayer (obtained by the budding of new viral capsules from infected cells) and need to undergo membrane fusion between the virus and the new host cell for infection to occur (Kielian & Rey 2006). Fusion of viruses to cell membranes can happen either at the outer cell surface or within the cell following endocytosis (Smith & Helenius 2004). Fusion on the outer surface occurs through protein interactions at a neutral-pH (Feng et al 1996), while intracellular fusion requires the presence of an acidic pH within specific organelles (Helenius et al 1980).

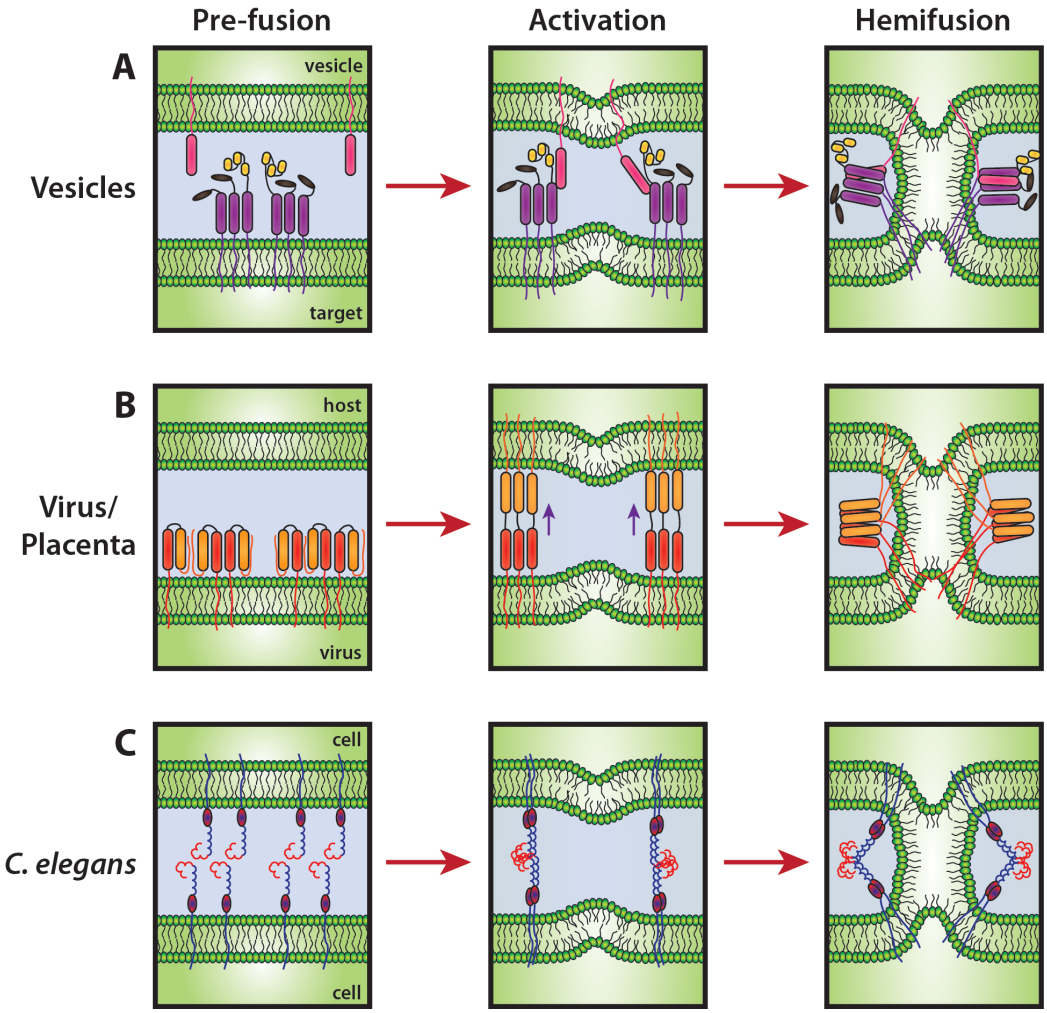


**Figure 1.10 Mechanisms of membrane fusion**

**A.** Fusion between vesicle and target membranes is asymmetrical, mediated by v-SNARE and t-SNARE proteins respectively. **B.** Viral fusion mechanisms require fusion proteins present only at the virus membrane. Placental fusion genes (syncytins) are of viral origin, therefore the mechanisms are the same. **C.** Fusion in *C. elegans* cells requires the same fusion protein present at both membranes. Based on (Sapir et al 2008).

Class I proteins such as the influenza-virus haemagglutinin (HA) work by undergoing a loop to helix transformation, triggered by low pH, that projects the fusion protein directly towards the host membrane, becoming irreversibly buried within the target's lipid bilayer (Bullough et al 1994) (Figure 1.10B). Further conformational changes bring both membranes closely together, and the energy released from these structural changes drives the fusion of both membranes (Carr et al 1997; Melikyan et al 2000). While class II proteins display a very different

structure when inactive, they also require conformational changes and membrane insertion for fusion to occur (Gibbons et al 2003). All viral fusion genes described so far induce fusion by hemifusion stalk formation, as shown by the ability of the hemifusion-blocking lipid lysophosphatidylcholine (LPC), (Chernomordik et al 1993) to arrest the process in viral fusogen-expressing cells (Podbilewicz et al 2006). This demonstrates that, while the molecules involved in fusion may differ (Wickner & Schekman 2008), the physical processes by which fusion occurs must follow the same steps. An interesting aspect of virus-cell fusion is that all fusion-specific proteins are only present at just one of the membranes, as the other membrane happens to belong to a naïve cell where these fusion proteins are not present. This contrasts with other fusion mechanisms, where both cells contain mechanisms required for membranal fusion.

### 1.3.4 Cell-cell fusion

#### 1.3.4.1 C. elegans fusion

In the nematode *Caenorhabditis elegans* cell fusion is used for the formation of major organ complexes, with around one third of all somatic cells undergoing fusion in order to create 44 distinct syncytia (Podbilewicz & White 1994). In 2002 a mutagenic screen on worms led to the identification of the EFF-1 (Epithelial Fusion Failure 1) gene (Mohler et al 2002; Podbilewicz et al 2006). This gene has no existing homology to any vertebrate genes (Mohler et al 2002), and while the protein is structurally similar to viral fusion molecules, the mechanism by which it brings membranes together is slightly different (Pérez-Vargas et al 2014) (Figure 1.10C). However, once membranes are close, fusion by hemifusion stalk still occurs (Podbilewicz et al 2006). While all epithelial fusion in *C. elegans* requires EFF-1, the so-called anchor cells that form the vulva and hymen of the worm still undergo fusion in EFF-1 mutants; here, AFF-1 (Anchor cell Fusion Failure 1) is essential for fusion (Sapir et al 2007). Interestingly, ectopic expression of both EFF-1 and AFF-1 is sufficient to drive fusion in non-fusing tissues in *C. elegans* (Shemer et al 2004), and even in *Drosophila* cultured cells (Podbilewicz et al 2006). However, unlike viral fusion proteins, expression of either molecule at only one of the two cell

membranes is insufficient for fusion to occur (Podbilewicz et al 2006; Sapir et al 2007).

The fact that both EFF-1 and AFF-1 can be enough to drive fusion in other tissues is a pivotal concept. The "fusogen" protein which in theory is able to drive the entire fusion process by itself must meet three conditions: it must be necessary for membrane fusion, it must localise exclusively at the fusion sites and most importantly, it must be able to induce fusion events in cells whose normal fate is never to fuse. Prior to the discovery of the nematode fusion genes, only genes involved in cell-vesicle or cell-virus fusion had exhibited some of these characteristics (Hu et al 2003; Earp et al 2005; Top et al 2005). Now, studies have shown that the *C. elegans* fusogens are able to drive the entire process by themselves, going from hemifusion, pore formation, expansion and fusion, with the proteins present at both membranes as the only requirements (Sapir et al 2008).

#### 1.3.4.2 Gamete fusion

So far, only a few molecules have been identified as involved in mammalian sperm-egg fusion. The tetraspanin CD9 was found simultaneously as a cause of infertility due to a failure of sperm and egg to undergo fusion (Miyado et al 2000; Naour et al 2000; Kaji et al 2000). CD9 is located at the egg surface, perhaps participating in the formation of microvilli that could be needed for fusion (Runge et al 2007). Injection of the sperm into the *CD9*$^{-/-}$ egg results in normal development, indicating that fusion is the only cause of infertility in this model. IZUMO1, an immunoglobulin superfamily protein, is located within the acrosome, and is exported to the surface membrane prior to fusion (Inoue et al 2005). Blocking of IZUMO by antibodies results in morphologically normal spermatozoa that fail to fuse to the egg after penetrating the Zona Pellucida (Inoue et al 2005). However, recombinant IZUMO is still able to bind *CD9*-null eggs, suggesting they are not working together (Inoue et al 2013). Instead, Juno, a GPI-anchored protein located at the egg surface is the only receptor binding IZUMO (Bianchi et al 2014). It was further shown that not only is Juno required for gamete fusion, but also it is rapidly

shed from the egg surface after fusion, effectively blocking potential polyspermy by depleting the receptor.

#### 1.3.4.3 Placental tissue fusion

The syncytiotrophoblast works as the placental interface between maternal and fetal blood supply, allowing the transport of oxygen, nutrients and waste (Huppertz et al 2006) and is continuously formed throughout pregnancy by the fusion of mononucleated cytotrophoblasts to form a large syncytium. The fusion of placental endothelium is partially mediated by two cell-surface proteins, Syncytin 1 and 2 (Mi et al 2000; Blond et al 2000) (Figure 1.10B). Interestingly, these proteins originated through the integration of enveloped-virus genetic material onto mammalian genomes (de Parseval et al 2003). In fact, the integration and use of syncytins as fusion proteins has occurred more than once: in rodents, syncytins are only present within the *Muridae* family. In primates, the presence of both proteins in certain lineages indicates that integration events occurred independently of rodents (Dupressoir & Marceau 2005). All mammalian placentas undergo fusion events in order to form a functional syncytiotrophoblast, suggesting that syncytins are not the only proteins involved in this process. However, in those species where these integration events have occurred, the complexity of the placental barrier is much higher, with various layers of fused cells that are otherwise not present in other mammals (Sapir et al 2008). It is worth noting that the forced expression of both syncytins on other non-placental cells induces fusion and syncytium formation, suggesting these endogenous retrovirus (ERVs) can act as possible fusogens (Blond et al 2000).

#### 1.3.4.4 Macrophage fusion

Osteoclasts, the highly specialised multinucleated cells in charge of bone resorption originate from the fusion of macrophages in order to form one large, functional cell. Another specialised cell type, giant cells, also form through the fusion of macrophages (Mariano & Spector 1974). Here, IL-4 has been shown to specifically induce fusion competence in macrophages through the STAT6 transcription factor (Moreno & Mikhailenko 2007; Helming & Gordon 2007).

However, IL-4 is not enough to induce expression of all known genes required for fusion, suggesting other signalling pathways are also at work (Helming et al 2009). In contrast, the IL-4-dependent fusion gene *DC-STAMP* is actually required during membrane fusion. *DC-STAMP* was identified in fusion-prone dendritic cells (Yagi et al 2005) and does not seem to be involved in the chemotaxis of macrophages prior to fusion, as shown by the lack of fusion in *DC-STAMP*-deficient cells when cultured even at high confluence (Yagi et al 2005). Mice null for *DC-STAMP* have a complete absence of macrophage fusion, while all other markers exhibit normal expression (Han et al 2000; Saginario et al 1995, 1998).

MFR (Macrophage Fusion Receptor), along with its ligand CD47 are both immunoglobulin superfamily proteins essential for macrophage fusion (Cui et al 2007). Expression of *CD47* is constant throughout osteoclast formation, while *MFR* is strongly but transiently expressed at the onset of fusion. Another example of a receptor-ligand interaction where expression patterns differ is CD200. While its receptor *CD200R* is expressed in osteoclasts and other myeloid lineage cells at consistent levels, *CD200* is only transiently expressed in macrophages at the onset of fusion (Lee et al 2006). The ATPase Atp6v0d2 is also required for efficient osteoclast fusion. Atp6v0d2 deficiency led to an increase in bone mass likely due to a lack of functional osteoclasts; researchers suggested that an inhibition of osteoclast fusion could even be used as a therapeutic way to increase bone mass and density (Cui et al 2007). *CD200*-null mice displayed the same bone-growth effect (Bate 1990).

### 1.3.5 Myoblast fusion

Most of the current knowledge of muscle fusion has been obtained through the use of the fruit fly, *Drosophila melanogaster*, as a model. In contrast to vertebrate musculature where each muscle is made up of large numbers of fibres, the *Drosophila* larval musculature is composed of 30 segmentally repeated abdominal muscles and they each consist of a single multinucleated muscle fibre (Baylies & Bate 1996). In vertebrates, the basic steps of muscle fusion described in *Drosophila* are present; however, what seems to diverge most, and where a uniform model is

lacking, is regarding the molecular pathways involved in vertebrate myoblast fusion. Most of this knowledge has come from *in vitro* studies because unlike *Drosophila*, mammalian development occurs *in utero*, making it virtually impossible to visualise processes such as fusion *in vivo*. However, in recent years studies using mainly zebrafish and mice models have begun to address these issues. Here, I will describe the current literature on myoblast fusion, focusing on vertebrate fusion mechanisms and the similarities and differences with invertebrate systems.

### 1.3.5.1 Where does fusion fit within the vertebrate myogenic program?

Myogenesis follows an ordered set of steps, each defined by the location and structure of cells, but more importantly, by a set of myogenic factors that follow a predetermined order. These steps lead to the eventual formation of muscle cells, which will fuse to form myotubes. Therefore, the question arises: where exactly does fusion fit within the tightly controlled myogenic program?

#### *1.3.5.1.1 Myogenin, cell cycle arrest and the initiation of fusion*

In order for muscle cells to become functional contractile units, three main processes need to have occurred by the end of differentiation: cells need to have expressed the necessary contractile proteins, have become postmitotic and fused to create myotubes. In cell culture, mononucleated myoblasts begin expressing myogenin while still capable of undergoing DNA replication, as shown by BrdU pulse experiments (Andrés & Walsh 1996; Bayne & Simpson 1977). Conversely, expression of the cell cycle regulator p21, which occurs after myogenin appears, leads to cell cycle arrest. Therefore, expression of *p21* and not *myogenin* correlates with the establishment of the postmitotic state in differentiating muscle cells.

Once mononucleated cells express *myogenin* and *p21* they begin production of contractile proteins, as shown by *MyHC* expression (Adamo et al 1976). Only then do they begin the fusion process, as shown by a reverse experiment where inhibition of fusion *in vitro* through a low $Ca^{2+}$ environment shows that differentiation and contractile-protein formation remains unchanged (Hasty et al 1993; Nabeshima et al 1993). These data initially suggest a cascade where

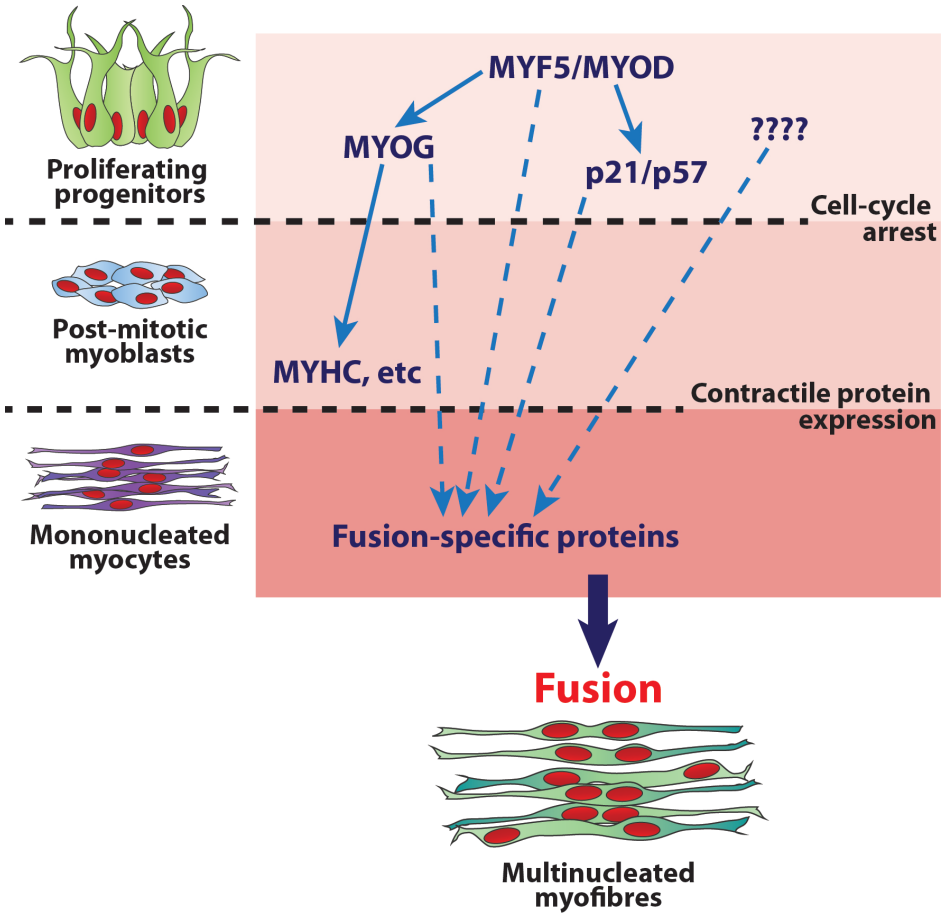


**Figure 1.11 Fusion within the vertebrate myogenic program**

MYF5/MYOD induce expression of p21/p57as well as myogenin (MYOG). The former are required for cell-cycle arrest while the latter is necessary for contractile protein expression. Cells only become fusion competent once these hallmarks have been achieved. Solid arrows indicate known interactions. Dashed arrows indicate unknown interactions.

myogenin induces expression of cell-cycle arrest markers, contractile protein formation and finally fusion. Indeed, *myogenin*-knockout mice display formation of muscle fields but an almost complete lack of fusion (Zhang et al 1999). However, double knockout mice for *p21* and *p57* (another cell-cycle arrest molecule found in muscles) display the same muscle fusion defects as *myogenin*-null mice, while *myogenin* expression remains unchanged from wild type levels (Shainberg et al 1969; Yaffe 1971). While this fits the model of cell cycle arrest being downstream of myogenin, data showing that expression of *p21* and *p57* remains unchanged in *myogenin*$^{-/-}$ mice suggests otherwise. It is thus possible that while *myogenin*

expression drives further differentiation, the expression of *p21* and *p57* is a concomitant but separable event that arrests the cell cycle and allows myogenin to act on downstream genes, including contractile proteins.

Based on information from cell culture and knockout mice, a model where upstream myogenic factors such as MYF5 and MYOD induce expression of *myogenin* and *p21/p57* in parallel is likely. The former will promote further differentiation and contractile protein expression, while the latter will induce cell cycle arrest. Fusion will only occur once these milestones have been achieved (Figure 1.11).

### 1.3.5.2 Dissecting the molecular components of muscle fusion

#### *1.3.5.2.1 Calcium dependence*

While basal extracellular and intracellular levels of calcium ($Ca^{2+}$) are required for any muscle differentiation to occur (Shainberg et al 1969; Yaffe 1971), higher extracellular $Ca^{2+}$ levels are absolutely essential for fusion. Depletion by either lower overall concentration (Knudsen & Horwitz 1977) or EDTA treatment (Knudsen & Horwitz 1977; Gibralter & Turner 1985) leads to a fusion failure without perturbing differentiation. These cells appear to not aggregate properly (David et al 1981; Horsley & Pavlath 2004), suggesting calcium is required for proper cell adhesion, although it likely plays a more extensive role throughout several stages of fusion (Cifuentes-Diaz et al 1995; Schwander et al 2003), as is also seen during cell vesicle fusion where the calcium-binding protein synaptotagmin is required.

#### *1.3.5.2.2 Membrane-bound proteins*

##### *1.3.5.2.2.1 Cell-cell adhesion*

Asymmetry of the fusion partners is a concept found throughout membrane fusion models, as evidenced by vesicular or gamete fusion. While in vertebrates such asymmetry has not been conclusively described so far, it is a crucial feature of invertebrate myogenesis. In *Drosophila*, two distinct myoblast populations partner together in order to produce fused myotubes. These are the founder cells (FCs) and

the fusion competent myoblasts (FCMs). Both cell types arise from the same progenitor population located within the somatic mesoderm and express the transcription factor *Twist* (Tixier et al 2010), but are further differentiated by a complex molecular network that involves Notch mediated inhibition and asymmetric cell division (Bataillé et al 2010; Knirr et al 1999; Abmayr & Keller 1998; Duan et al 2001). A founder cell essentially works as a "seed" for an individual muscle (Haralalka & Abmayr 2010), as well as providing each one with its own identity. Importantly, founder cells are not able to fuse with each other; instead they increase muscle size (and number of nuclei) by addition of FCMs (Bate 1990). These fusion competent cells are also unable to fuse to each other. As FCs are the ones to determine cell fate, FCMs acquire this fate upon fusing to the forming myofibre

*1.3.5.2.2.1.1 Immunoglobulin superfamily members*

In *Drosophila* myoblasts, the step of cell-cell recognition and adhesion is mediated by members of the immunoglobulin superfamily (IgSF), and these are expressed differentially in FCs and FCMs (Figure 1.12). Dumbfounded/Kin of irreC (*Duf/Kirre*) is exclusively expressed in founder cells (FCs) prior and during fusion but not after (Strünkelnberg et al 2001), while Roughest/Irregular of chiasm (*Rst/IrreC*) (Bour et al 2000) is more extended as it is also expressed in FCMs (Strünkelnberg et al 2001). When both *Kirre* and *Rst* are deleted from the genome, it results in embryonic lethality and fusion defects, which can be partially rescued by reintroduction of *Rst*, showing that both proteins act redundantly during myoblast fusion (Bour et al 2000). Studies in zebrafish have provided evidence that at least some of the fusion adhesion machinery might have been conserved through evolution. Kirre family members have been identified in fish and one, designated *kirrel* (kirre-like), is expressed in all fusogenic fast-muscle progenitor cells (Srinivas et al 2007), while muscle precursor cells depleted of this protein fail to fuse and develop into mononucleated myocytes (Sohn et al 2009).

Conversely, Sticks and stones (*Sns*) (Artero et al 2001) and Hibris (*Hbs*) (Ruiz-Gómez et al 2000) are IgSF members exclusively expressed in *Drosophila* FCMs.

The earliest expression of *Sns* occurs prior to the onset of myoblast fusion, and persists at high levels throughout the entire process (Artero et al 2001), while *Hbs*' expression, though marginally different, also involves the somitic mesoderm during myoblast fusion, and disappears shortly after completion of this process (Bour et al 2000). Mutant embryos for *Sns* show a complete absence of muscle fibres; instead, a large number of mononucleated myoblasts can be observed at the sites where muscles should form. These cells also fail to migrate to the site where FCs are located and lack filopodia, suggesting *Sns* functions both as an attractant and a cell-surface receptor for FCMs (Artero et al 2001). The vertebrate homolog of *Sns*, nephrin, is only required in myoblasts but not in myotubes, and in the absence of nephrin, zebrafish myotubes form normally but myoblasts fail to fuse to them (Moore et al 2007). The function of nephrin in vertebrate fusion is currently unknown but based on its structure it likely has a similar function to Sns, in which a large protein complex located downstream would signal intracellularly.

Hibris (*Hbs*) shares a high similarity with *Sns*, but in contrast to mutations in *Sns*, fly *Hbs* mutants have only a mild muscle phenotype, consisting of few missing fibres and a slight increase in mononucleated myoblasts. Intriguingly, overexpression leads to a more pronounced fusion defect when compared to mutants (Kim et al 2007). Similar to *Kirre* and *Rst*, both proteins act redundantly during muscle fusion, although only *Sns* is able to drive the entire process and it is now established that initial cell-cell contact between FCs and FCMs is likely mediated by *Kirre/Rst* in FCs and *Sns/Hbs* in FCMs (Figure 1.12).

Further demonstrating the evolutionary conserved role of the immunoglobulin superfamily in adhesion prior to fusion are two IgSF members, *jamb* and *jamc*, which are essential for muscle fusion in zebrafish embryos (Sakaguchi et al 2006; Praetor et al 2008; Imhof et al 2007). MyHC-positive muscle fibres elongate and span entire somites, but remain mononucleated in null-mutants, indicating that fusion is the only step of the process being affected. Although the phenotypes observed in the fish are striking, numerous knockout mice models for either gene have never reported any obvious muscle defects (Doherty et al 2005).

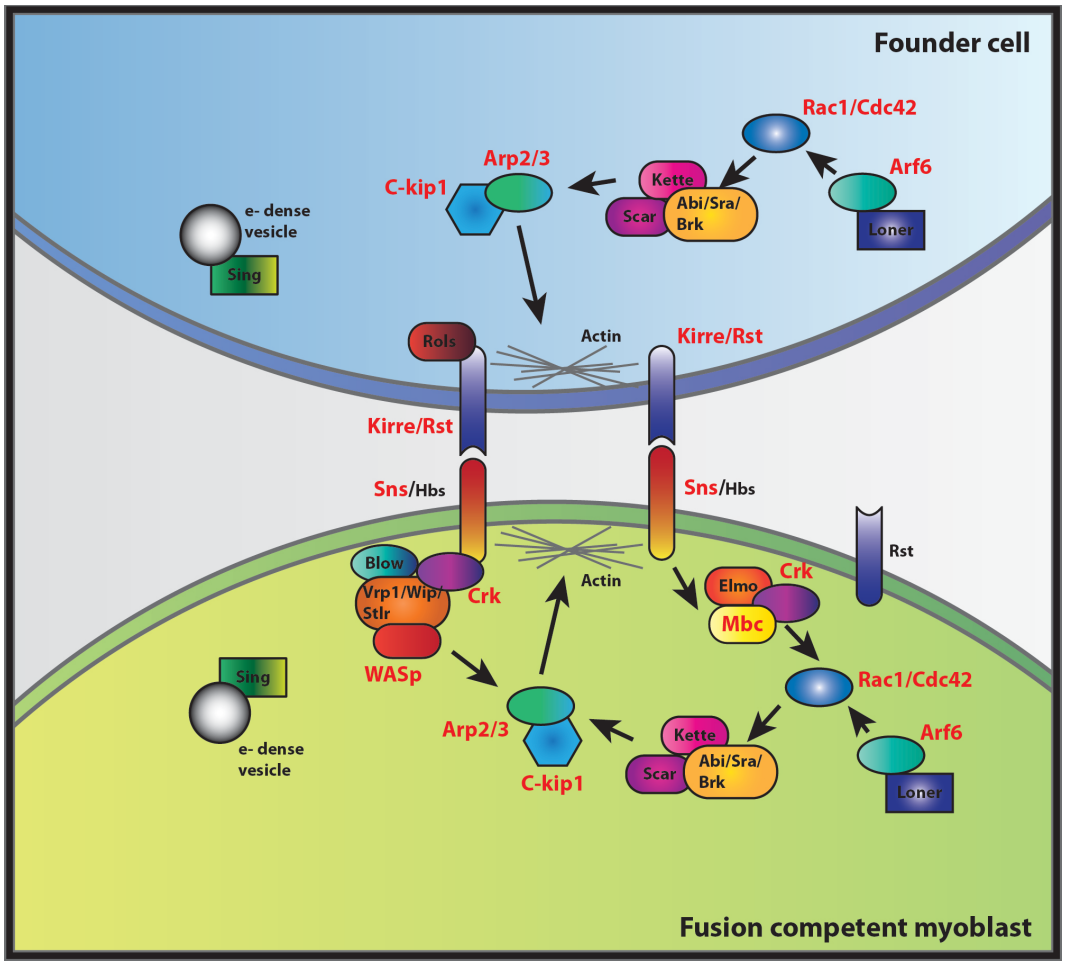


**Figure 1.12 Molecular control of fusion in *Drosophila* muscles**

Schematic showing the molecular pathways controlling myocyte fusion in fruit flies, from adhesion to actin remodelling. Proteins with homologues known to control vertebrate fusion are labelled in red.

*1.3.5.2.2.1.2 Cadherins and integrins*

In vertebrate models, adhesion molecules such as cadherins and integrins are commonly found at the points of cell-cell contact *in vitro* (Charrasse et al 2006, 2007). While M-cadherin is required for myotube formation in culture (Hollnagel et al 2002), mutant mice have no defects in skeletal muscle (Knudsen et al 1990). This suggests that other cell-surface molecules such as neural cell adhesion molecule (*NCAM*) may compensate for the lack of this protein. Inhibition of *NCAM* blocks chick myoblast fusion *in vitro*, while ectopic expression promotes fusion in mouse muscle cells (Charlton et al 2000). However, null myoblasts isolated from

mutant mice fuse in the same manner as wild-type ones (Charrasse et al 2013). Recently, the small GTPase RAB35 has been proposed as a regulator of cadherins at the membrane. This protein accumulates at the points of cell-cell contact, and when ablated, N- and M-cadherin fail to be recruited to the membrane where fusion is occurring. However, this does not seem to be a fusion specific behaviour, as the same effect was observed in non-fusing human HeLa cells (Srinivas et al 2007).

The absence of β1, α3 and α9 integrins impair myoblast fusion *in vitro* (Schwander et al 2003). Similarly, knockout mice for *β1 integrin* present muscle defects and when mutant myoblasts are cultured, they fail to fuse (Lafuste et al 2005). This regulation of fusion through *β1 integrin* expression (as well as *caveolin 3*) is controlled by the focal adhesion kinase (*FAK*) (Quach et al 2009). Mutant mice lacking *FAK* in muscle stem cells display impaired regeneration potential, and *in vitro* studies show this is due to an impaired fusing ability. ADAM12 (disintegrin and metalloproteinase 12), a transmembrane protein capable of binding α9β1 integrin in muscle, produces a fusion defect *in vitro* when inhibited by antisense oligonucleotides (Reporter & Raveed 1973).

*1.3.5.2.2.1.3 Other potential cell-adhesion molecules*

Ectopic expression of sperm-egg fusion protein CD9 in C2C12 myoblasts results in increased fusion and large syncytia. Conversely, blocking CD9, as well as another tetraspanin CD81 results in less fusion *in vitro* with no delay in differentiation (Tachibana & Hemler 1999). However, *CD9* and *CD81* mutant mice have not been shown to have muscle or fusion defects (Powell & Wright 2011). Another protein likely involved in adhesion prior to fusion is myoferlin, a muscle-specific homologue of dysferlin. This protein is strongly expressed during myotube formation and myoblasts isolated from null mice form smaller myotubes, while myofibres fail to achieve full size during regeneration (Posey et al 2011). Interestingly, dysferlins are related to synaptotagmin, a crucial protein of the SNARE complex that promotes vesicle fusion by binding of calcium. Characterisation of the novel ferlin family member FER1L5 has provided further

evidence for the involvement of ferlins during fusion (Posey et al 2011). This protein interacts with the EHD1 and 2 molecules, whose function is to recycle plasma membranes after internalisation. The authors propose that FER1L5, and perhaps also dysferlin and myoferlin act to also mediate the membrane trafficking events taking place during fusion.

*1.3.5.2.2.1.4 Myomaker, a possible muscle fusogen?*

The search for the "fusogen" protein that is alone able to drive fusion in myoblasts had perhaps its greatest development with the discovery of the transmembranal protein TMEM8c, also called "myomaker" (Millay et al 2013). Full knockout mice for *Tmem8c* die prior to postnatal day seven likely from respiratory failure and their muscles display normal levels of expression for *MyoD*, myogenin and MyHC, indicating any defects are not due to lack of differentiation. All muscle groups are present, but composed entirely of mononucleated cells. *In vitro* loss of function experiments confirmed that TMEM8c is indeed required for fusion; conversely, overexpression of the protein leads to a hyperfusion phenotype. Furthermore, a 1.7kb region upstream of the *Tmem8c* coding sequence (the putative promoter) driving LacZ shows upregulation following muscle injury, either from an external source (cardiotoxin) or within the muscle (using dystrophic MDX mice), while tamoxifen-inducible site-specific loss of *Tmem8c* leads to impaired regeneration (Millay et al 2014). *Tmem8c*'s requirement for fusion is also demonstrated in zebrafish, suggesting this molecule could potentially be conserved amongst all vertebrates. Morpholino knockdown of the gene leads to morphologically normal embryonic fish that are unable to swim because fast-fibres fail to undergo fusion and elongation (Landemaine et al 2014).

While fibroblasts transfected with *Tmem8c* alone do not fuse to each other, when plated alongside C2C12 cells, fusion between fibroblasts and myoblasts readily occurs. This and other evidence suggest a model were tmem8c is sufficient to drive fusion in a non-fusogenic cell, but only when the opposing cell contains a yet-unidentified complementing molecule (Millay et al 2013). Therefore, it is likely that vertebrate myoblast fusion follows an asymmetric pattern similar to that

described in *Drosophila*, where TMEM8c is required at one cell surface and a complementary unknown protein at the other (Figure 1.13).

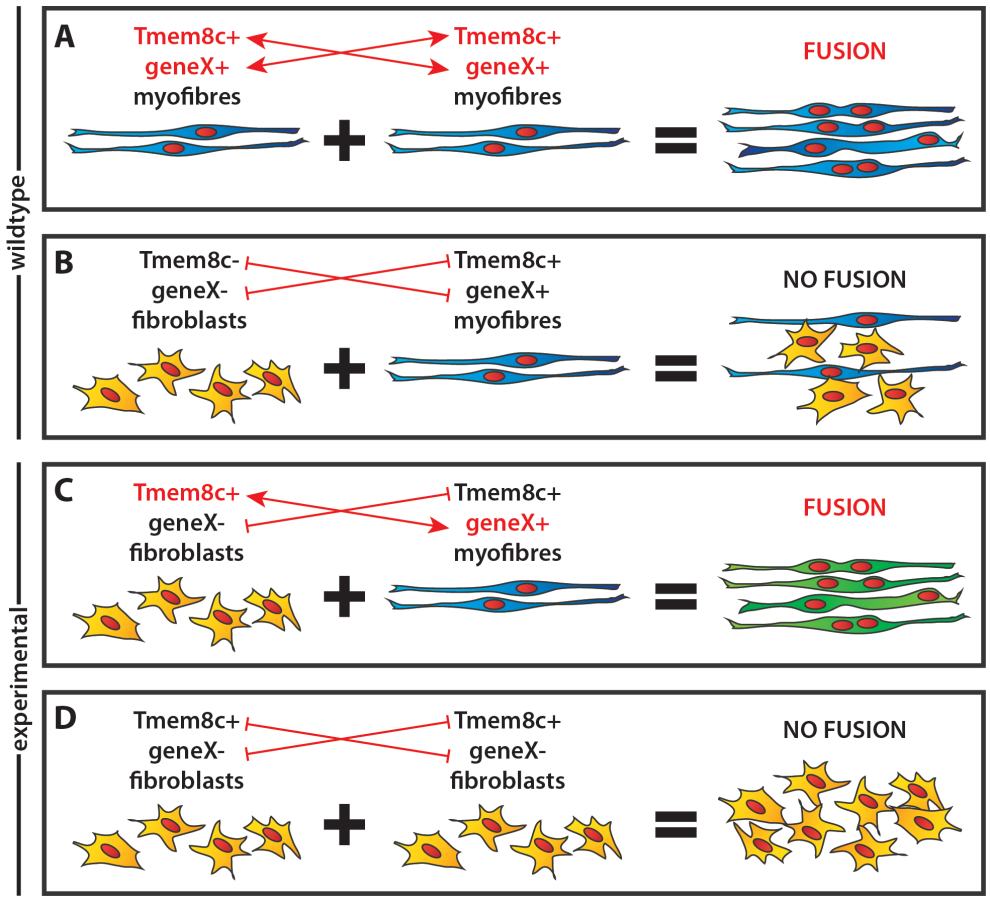


**Figure 1.13 Role of tmem8c in fusion**

**A.** In a wild-type setting, tmem8c$^+$ muscle fibres fuse to other tmem8c$^+$ muscle fibres. **B.** Meanwhile, tmem8c$^-$ fibroblasts are unable to fuse to tmem8c$^+$ muscle fibres. **C.** Forced expression of tmem8c in fibroblasts confers them fusion competence when mixed with tmem8c$^+$ muscle fibres. **D.** However, tmem8c$^+$ fibroblasts are unable to fuse to other tmem8c$^+$ fibroblasts, suggesting a second gene (geneX) is required to partner with tmem8c to induce fusion.

*1.3.5.2.3 Actin cytoskeleton remodelling is necessary for fusion*

Following cell-cell recognition, electron-dense vesicles of around 40nm are observed at the points of myoblast contact over an area of around 1µm$^2$. These vesicles originate at the Golgi apparatus and become coated with F-actin (Shimada

1971). Current hypotheses suggest that these vesicles give rise to membrane plaques, consisting of electron dense material covering an area of 500nm along the plasma membrane (Shimada 1971). These plaques give way to pores, where they appear to eventually vesiculate "inside-out", surrounding extracellular space and allowing the cytoplasms to mix. This process has been described mainly in vertebrate cells (Estrada et al 2007), but appears to occur in all organisms studied, including flies. Interestingly, mutants for the MARVEL-domain containing protein Singles-bar (*Sing*) have an increased number of vesicles present, although the protein's exact function is not known (Chen & Olson 2001). All these extensive membrane rearrangements, as well as formation of invasive filopodia that facilitate fusion require extensive cytoskeletal remodelling. This process is mainly mediated by changes in the actin filaments, and the main players involved in its regulation, both in vertebrate and invertebrate fusion are *Rac1* and *Cdc42*.

*1.3.5.2.3.1 Rac1 and Cdc42 mediate actin remodelling*

RAC1, and the related G-protein CDC42 are small Rho GTPases commonly found directing actin-mediated processes such as cell adhesion, motility and others in a wide variety of tissues (reviewed in (Duquette & Lamarche-Vane 2014)). They are both necessary for fusion in mice embryos (Bach et al 2010). Those lacking either RAC1 or CDC42 in limb myoblasts produce differentiated limb musculature that remains largely mononucleated, while cells isolated *in vitro* reveal the same results. Conversely, *Drosophila* Rac1 (*Drac1*) or Cdc42 (*Dcdc42*) are also essential for fusion in that model (Luo et al 1994).

Consistent with the role of asymmetry in invertebrate fusion, the recruitment of *Rac1* follows a different pathway in FCs than in FCMs. Sns present at the FCMs surface links to adaptor proteins including the CT10 regulator of kinase (Crk). Crk, along with myoblast city (Mbc) appear to induce Rac1 recruitment to the membrane (Geisbrecht et al 2008). Also, Mbc along with Elmo/Ced-12 activate *Rac1*, as overexpression of both genes leads to a similar phenotype to that of active Rac1. Similarly, loss of *Rac1* suppresses the Elmo overexpression phenotype (Kaipa et al 2013), suggesting a positive feedback loop between Rac1 and its

effector proteins (Figure 1.12). This system is conserved, as the Mbc homologs Dock1 and Dock5 and its adaptor protein Crk are required for fast-twitch muscle cell fusion in zebrafish embryos (Schwander et al 2003; Lafuste et al 2005).

Similarly, another player of *Drosophila* fusion, the GTPase ARF6 (ADP- ribosylation factor 6), associates with M-cadherin and RAC1 at the sites of vertebrate myoblast fusion (Bach et al 2010). This action is mediated by the production of phosphoinositide PI(4,5)P2 (Baas et al 2012) meaning ARF6 is potentially both triggering phospholipid production as well as directing cytoskeletal reorganisation. This is also reported in fruit flies, where phosphoinositide PI(4,5)P2 localises at the sites of actin accumulation and potentially functions as a link between receptor-mediated signalling and the actin cytoskeleton remodelling required for pore formation (Richardson et al 2007).

In FCs, immediately downstream of Kirre/Rst is Antisocial/Rolling pebbles (Ants/Rols) (Menon & Chia 2001). This protein is recruited to the contact sites when Kirre/Rst is engaged with Sns and acts in a positive feedback loop to stabilise the receptor, ensuring its continued availability at the points of cell contact (Chen et al 2003) (Figure 1.12). Interacting with the cytoplasmic domain of Kirre is Schizo/Loner, a guanine nucleotide exchange factor (GEF) (Chen et al 2003) that potentially mediates Rac1 recruitment to the membrane also through Arf6. Although *Schizo* mutants show strong fusion defects, *Arf6* mutants do not, suggesting Rac1 recruitment is controlled by another mechanism as well (Bulchand et al 2010). Furthermore, it is shown that the cytoplasmic domain of Kirre is not essential for fusion (Dottermusch-Heidel et al 2012), indicating that Schizo is likely controlled by a more complex mechanism than has been revealed so far. Schizo has also been described to act as a negative regulator of N-cadherin during fusion events. In larvae, the loss of N-cadherin leads to a partial rescue of the *Schizo/Loner*-null fusion defect phenotype. It is proposed that N-cadherin must be removed from the membrane in order to provide a protein-free area at the point of cell-cell contacts (Erickson et al 1997), but this contradicts evidence pointing at M- and N-cadherin as necessary for vertebrate fusion to occur (Charrasse et al 2007, 2006, 2002; Knudsen, Myers, et al 1990).

*1.3.5.2.3.2 The SCAR and WASp complexes*

Rac1-mediated actin polymerization and remodelling is directed downstream by two related pathways: the Scar and WASp complexes (Figure 1.12). At the points of cell-cell contact, actin-rich foci form in FCMs (Sens et al 2010), while thin sheaths of F-actin form below the membrane of founder cells (Schröter et al 2004; Richardson et al 2007). In both cell types these processes are mediated by the Scar and Kette subunit of the pentameric Scar complex (Eden et al 2002; Derivery & Gautreau 2010; Kurisu & Takenawa 2010). The complex is initially inactive when conformed by Scar, Kette, Abi (Abl interactor protein), Sra (Specifically Rac1-associated protein) and Brk (Breast tumour kinase) proteins (Kim et al 2000), but upon binding of Rac1, the domain is released and is free to interact with actin-related protein 2/3 (Arp2/3) (Kim et al 2007), whose function is to control the formation of branched actin networks to pre-existing filaments, as well as promoting formation of new ones. Importantly, evidence in vertebrates shows these mechanisms remain conserved; depletion of the Arp2/3 binding partner C-kip1 shows a drastic reduction in fusion *in vitro* as well as in zebrafish muscles (Gruenbaum-Cohen et al 2012).

*1.3.5.2.3.3 WASp/WIP signalling directs actin remodelling*

In *Drosophila* FCMs, the actin nucleation-promoting factor WASp (Wiscott-Aldrich syndrome protein) and its associated Vrp1/D-wip/Sltr (Verprolin 1) also promote actin polymerisation along with the Scar complex (Figure 1.12). Here, Vrp1 is recruited to Sns by interaction with Crk (Jin et al 2011). Crk also binds to blown fuse (Blow), which functions to modulate the stability of the Vrp1/WASp complex (Martinez-Quiles et al 2001; de la Fuente et al 2007). Similar to Scar, WASp usually exists in an inactive form but in the presence of the stabilising Vrp1, the VCA domain is liberated, allowing it to bind to Arp2/3 and promote actin polymerisation (Kim et al 2007; Richardson et al 2007). However, actin foci are still present in mutants for *WASp*, *Vrp1*, *Kette* or *Scar* (Gildor et al 2009) meaning other actin polymerisation proteins must be present. In embryos lacking *Kette*, fusion pores fail to form suggesting the Scar complex has a role in their formation (Massarwa et al 2007; Sens et al 2010).

In mice, knockdown of the main regulator of actin polymerisation *N-WASp* leads to a massive decrease in muscle size due to small, thin, mononucleated fibres (Gruenbaum-Cohen et al 2012). Therefore, evidence for fusion defects in vertebrates carrying mutations for *Rac1*, *Cdc42*, *Arp2/3* and *WASp* among others, propose a very strong case for the conservation of the actin-remodelling machinery during fusion, as well as its exclusive role in fusion separate from the rest of myogenesis, as evidenced from the normal myogenic differentiation observed in these mutants.

*1.3.5.2.3.4 Actin-dependent podosome formation*

While the cytoskeletal remodelling process seems to be conserved between invertebrates and vertebrates, it is also likely that the invading podosomes that occur in fruit flies and mammalian cells are mediated by the same mechanisms. In mammals, dynamin is known to regulate cellular vesicle fission (Ochoa et al 2000) as well as the formation of actin-dependent podosomes (Abramovici & Gee 2007). Primary myoblasts cultured from conditional-knockout mice for dynamin show a 60% reduction in fusion with abnormal formation of actin-rich membrane protrusions, suggesting dynamin is indeed involved in the proper formation of actin-dependent podosomes.

In *Drosophila*, the F-actin foci observed at the points of cell-cell contact form in the centre of a ring composed of Sns (Kesper et al 2007). These areas are proposed to be the core of the adhesive podosome-like structure here termed FuRMAS (Fusion Restricted Myogenic-Adhesive Structure) (Haralalka & Abmayr 2010; Rochlin et al 2010). At first they were thought to be present in both cell types (Sens et al 2010), but are almost exclusively seen in FCMs (Haralalka et al 2011; Sens et al 2010). These FuRMAS are part of an invasive structure that pushes into the founder cell/myotube (Sens et al 2010) and includes finger-like projections that are devoid of cytoplasm, instead being composed entirely of filaments, probably WASp dependent, as these invadopodia collapse in *WASp* mutants (Shimada 1971a). Also accumulating at the ends of myoblast pseudopodia prior to myotube contact is diacylglycerol kinase ζ, a phosphatic acid-generating enzyme, which along with its

binding scaffold protein syntrophin interacts with Rac1 and N-cadherin (Enwere et al 2012).

*1.3.5.2.4 Phosphatidylserine-dependent fusion*

Differences in the organisation of aminophospholipids within fusion sites, especially phosphatidylserine (PA), precede myoblast fusion (van den Eijnde et al 2001). PA, usually found in the inner leaflet of cell membranes, shifts to the outer leaflet of the bilayer at the cell-contact sites prior to fusion. Indeed, PA is required at the points of cell contact in order for C2C12 cells to fuse, and this process potentially involves the presence of annexins (Mukai & Hashimoto 2008). Annexins are a large family or proteins whose common property is $Ca^{2+}$ dependent binding of phospholipids. They serve several functions, including patching membrane damage, bending membranes and anchoring proteins to them; importantly, the bind phosphatidylserine. Leikina and colleagues (2013) used an *in vitro* system in which they cultured C2C12 cells and primary myoblasts in the presence of LPC, which blocks hemifusion stalk formation. Upon removal of LPC, cells fuse in a single synchronised event. These experiments found that indeed annexins A1 and A5 are required for fusion of myoblast membranes. PA is possibly required at the fusion sites in order to change the bilayer's physical properties. It is known that the rigidity of the membrane prior to fusion appears to be vital, as cholesterol-containing lipid rafts accumulate at the cell contact sites and are required for localisation of adhesion molecules (Fadok et al 1992).

*1.3.5.2.4.1 BAI1 and apoptotic cells*

PA translocation to the outer leaflet of the membrane is also one of the hallmarks of programmed cell death, apoptosis (Park et al 2007). The seven-pass G-coupled receptor BAI1 (Brain-specific Angiogenesis Inhibitor 1) acts as an engulfment receptor for apoptotic cells working upstream of the DOCK/Rac1 pathway. Importantly, PA acts as a ligand for BAI1 activation (Hochreiter-Hufford et al 2013). BAI1's connection with both DOCK/Rac1 and PA suggested a potential involvement in myoblast fusion, and *in vitro* culture of C2C12 cells revealed *Bai1* upregulation during fusion events. Overexpression of the wild-type form leads to

increased fusion in these cells, while overexpression of a mutant form unable to engage the DOCK/Rac1 module no longer has an effect, showing that BAI1 acts upstream of the actin machinery in muscle cells (Park et al 2007).

It is proposed that not only is BAI1 acting on myoblasts during fusion, but it actually mediates the apoptosis of myoblasts, and that these apoptotic cells are required for the healthy myoblasts to fuse. Blocking of apoptosis by several methods decreases fusion, but interestingly, the addition of apoptotic cells to the myoblast culture restores their fusion capability. Importantly, myogenin levels (and therefore the myogenic program) are not affected. The theory proposed is interesting, but poses several problems. The cells on which this study is based (C2C12) originated from adult muscle satellite cells, used in muscle repair (Vasyutina et al 2009). Therefore, it is likely that these cells contain an extra program not present during development by which they interact with apoptotic cells present at the site of injury. The study also includes *in vivo* evidence that actually supports this possibility. *Bai1*$^{-/-}$ mice have only very slight differences in fibre size at birth, but display a markedly reduced regeneration ability following cardiotoxin injury (Park et al 2007). Further studies based on developing myoblasts will determine how relevant BAI1 is during all aspects of muscle fusion.

*1.3.5.2.4.2 Bai3 is also involved in myoblast fusion*

Researchers searching for ELMO1 (a DOCK/Rac1 partner) interactions in muscle cells identified another GPCR protein, BAI3, as a potential mediator of fusion (Hamoud et al 2014). This protein is expressed in C2C12 cells during fusion, and knockdown by shRNA results in impaired myotube formation. Expression levels of *myogenin*, Myosin Heavy Chain (*MyHC*) and Troponin-T do not change. Interestingly, BAI1 expression is not able to rescue the phenotype of *Bai3*-mutants and it is suggested there is no redundancy between these two proteins. However, the binding of BAI3 to ELMO is essential for fusion. This may indicate that, while both BAI proteins are mediating signals to the actin-cytoskeleton machinery, they do so through different partners.

*1.3.5.2.5 Potential pathways and transcriptional regulators of vertebrate fusion*

A possible transcriptional mediator of muscle fusion is the non-canonical nuclear factor κβ (NF-κβ) pathway, well known as a regulator of apoptosis as well as a number of developmental processes. Constitutive activation of NF-κβ by knockdown of its inhibitors such as cellular inhibitor of apoptosis (*cIAP1*) and TNF-like weak inducer of apoptosis (*TWEAK*) leads to an increased number of fusion events and large syncytia in cell culture. Conversely, expression of key NF-κβ components like *p52* and *RelB* also increases fusion (Horsley et al 2001; Pavlath & Horsley 2003). These results fit into the context of apoptotic pathways being involved in fusion, as was shown with BAI1 and related proteins. However, as mentioned previously, these experiments being performed on adult satellite cell-derived cell lines could mean that apoptosis is only needed for fusion in a regeneration context, and not during embryonic development.

The nuclear factor of activated T cell (NFATc2) appears to play a role in myotube-myoblast fusion. In the absence of this protein, nascent myotubes form normally but fail to add new myoblasts (Horsley et al 2003). Furthermore, experiments showed that NFATc2 regulates the production of intereukin-4. IL-4 promotes fusion by regulating the expression of mannose receptor (MR), a cell-surface lectin (Jansen & Pavlath 2006). MR null myoblasts show a reduction on motility and impaired directed migration towards fusing cells (Bois & Grosveld 2003).

Intracellularly, the transcription factor FOXO1a appears to mediate the rate of fusion. This molecule is expressed in skeletal muscle and translocates to the nucleus at the onset of differentiation. Expression of a mutated form of the protein inhibits fusion in C2C12 cells, without affecting expression of differentiation markers (Nishiyama et al 2004). Similarly expression of a non-phosphorylatable form enhances fusion (Kamei et al 2004). Mutant mice are embryonic lethal, while mice overexpressing FOXO1a show decreased muscle mass (Bois et al 2005). The studies suggest that the presence of FOXO1a induces fusion. As FOXO1a likely acts downstream of the Rho/ROCK pathway, and can be phosphorylated by both ROCK and GMP-dependent kinase 1 (Singh et al 2014), these proteins could produce a negative feedback loop by which the rate of fusion is controlled.

Very recently, a role for the alternative splicing of two proteins during myoblast fusion was reported (Gallagher et al 2011; Kuroyanagi et al 2007). RBFOX2 is an RNA binding protein that regulates up to 30% of the splicing events occurring during myogenesis (Shibukawa et al 2013). When ablated in C2C12, fusion failure occurs without any changes to differentiation, suggesting this protein is involved exclusively in fusion. RNA-seq and RT-PCR analyses reveal a series of genes affected by *Rbfox2* knockdown, mainly *Mef2d* transcription factor and *Rock2* Rho-associated kinase. Further experiments show both these genes are spliced by RBFOX2 and required for correct myoblast fusion. While both genes are under the control of a single molecule and are both necessary for fusion, their function within the cell is likely different. MEFD2 modulates transcription of a yet unknown fusion target while ROCK2 along with ROCK1 acts to phosphorylate the inhibitor myosin expression and fusion calponin 3 (CNN3), therefore allowing fusion to occur (Shibukawa et al 2013).

# 2 MYOGENESIS AND EPITHELIAL-MESENCHYMAL TRANSITION TRIGGERED BY CYTOPLASMIC NOTCH AND MEMBRANAL β-CATENIN

# PART B: SUGGESTED DECLARATION FOR THESIS CHAPTER

**Monash University**

**Declaration for Thesis Chapter 2**

**Declaration by candidate**

In the case of Chapter 2, the nature and extent of my contribution to the work was the following:

| Nature of contribution | Extent of contribution (%) |
|---|---|
| Concept, planning of experiments, cloning of constructs, electroporation, immunohistochemistry, imaging, data analysis, statistics, figure preparation, manuscript drafting. | 40% |

The following co-authors contributed to the work.

| Name | Nature of contribution |
|---|---|
| Anne C. Rios | Concept, planning of experiments, cloning of constructs, electroporation, immunohistochemistry, imaging, data analysis, statistics, figure preparation, manuscript drafting. |
| Claire E. Hirst | Planning of experiments, cloning of constructs, manuscript drafting. |
| Christophe Marcelle | Concept, planning of experiments, manuscript drafting. |

The undersigned hereby certify that the above declaration correctly reflects the nature and extent of the candidate's and co-authors' contributions to this work*.

| | | |
|---|---|---|
| Candidate's Signature | | Date |
| Main Supervisor's Signature | | Date |

# Myogenesis and epithelial-mesenchymal transition triggered by cytoplasmic NOTCH and membranal β-catenin

Anne C. Rios*, **Daniel Sieiro-Mosti***, Claire Hirst and Christophe Marcelle

EMBL Australia; Australian Regenerative Medicine Institute (ARMI), Monash University, Building 75, Clayton, VIC 3800, Australia

* : these authors contributed equally to the work.

Corresponding author:

Prof. Christophe Marcelle

Australian Regenerative Medicine Institute (ARMI) / EMBL Australia

Monash University, Building 75,

Clayton, VIC 3800, Australia

[redacted]

SUMMARY

How cells in the embryo display complex behaviours while being exposed to an ever-changing cellular environment is largely unknown. In chick embryos, skeletal muscle formation is initiated by migrating neural crest cells that, in passing, trigger myogenesis in selected epithelial somite progenitor cells, which translocate into the nascent muscle to differentiate. Here, we uncovered at the heart of this response a signalling module encompassing NOTCH, GSK-3β, SNAI1 and WNT. This module transduces the activation of NOTCH by neural crest cells into i) an inhibition of GSK-3β activity by non-transcriptional NOTCH signalling; ii) a SNAI1-induced epithelial to mesenchymal transition (EMT) leading to iii) the recruitment of membranal β-catenin to trigger WNT/β-catenin signalling and myogenesis independently of WNT ligand. Our results intimately associate the initiation of myogenesis to a change in cell adhesion and may reveal a general principle for coupling cell fate changes to EMT in many developmental and pathological processes.

## INTRODUCTION

During early embryogenesis, a succession of extensive tissue rearrangements and cell migration events, intimately associated with rapid cell fate changes, establish the tissues and organs of the future adult. A model where such complex issues are amenable to experimentation is the early formation of skeletal muscles in the chick embryo.

Over many days of development, the medial border of the dermomyotome (DML) generates the first skeletal muscle cells that assemble into a primary myotome. This arises from a crucial cell fate decision: epithelial cells in the DML either self-renew or undergo myogenic differentiation and this is accompanied by an EMT that allows their translocation into the primary myotome[1-4].

Signalling cues from tissues surrounding somites act as inducers of muscle formation. WNT1 and WNT3a from the dorsal neural tube are candidates for the *in vivo* activation of myogenic regulatory factors (MRFs)[5-7]. Since the downstream effectors of WNT "canonical" signalling, T cell factor/lymphoid enhancer factor (TCF/LEF1) and β–catenin, control MYF5 and MYOD expression in somites and TCF/LEF binding sites are required for the expression of MYF5 in the DML[3,8,9], this has led to the largely accepted theory that myogenesis in somites is under the control of WNTs from the dorsal neural tube acting through a WNT/β-catenin-dependent pathway.

This raises a paradox: although presumably all cells in the DML are equally exposed to WNTs emanating from axial structures and are fully competent to initiate myogenesis[1], only a small proportion of DML cells do so at any given time, suggesting that other mechanisms affect the cell fate decision to either differentiate or self-renew.

We recently demonstrated that the activation of MYF5 and MYOD in the DML is dependent upon the transient activation of NOTCH signalling, itself triggered by Delta1-positive neural crest cells migrating from the dorsal neural tube[1]. This finding is attractive, as it is compatible with the well-documented role of the dorsal

neural tube in myogenesis. Importantly, the mosaic expression of Delta1 in the migrating neural crest cell population ensures that NOTCH signalling is regularly triggered in selected DML cells, thus explaining the binary cell fate choice necessary to generate myotomal cells over an extended period of time while self-renewing the progenitor population. However, this finding was not in accordance with the established role of WNT/β–catenin signalling in myogenesis, nor did it explain why the initiation of the myogenic program in selected progenitors within the DML is associated with their translocation into the primary myotome *via* an EMT.

Here, we propose a model integrating the respective roles of NOTCH and WNT in the formation of the primitive skeletal muscle, and explaining why the decision to undergo myogenesis is intimately associated with an EMT. In DML cells, the selective triggering of NOTCH signalling by Delta1-positive neural crest cells dramatically decreases GSK-3β activity and therefore the ubiquitination of the zinc finger transcription factor SNAI1, a major activator of EMT. This results in the mobilization of β–catenin from the cell membrane pool, which combined with the inhibition of GSK-3β activity, allows entry of β–catenin into the nucleus where it activates MYF5 expression in a WNT ligand-independent manner.

## RESULTS

### Co-activation of NOTCH and WNT signalling in early myogenesis

Since canonical WNT and NOTCH signalling are required to initiate myogenesis[1,3,8,9] and are both active in DML cells[1,10], it was important to determine whether both pathways are operating within the same cells. To address this, we co-electroporated the DML of trunk-level somites (Supplementary Figure 1a-d) with a NOTCH reporter[1,11] upstream of a destabilized RFP, together with a "TOPflash" WNT reporter[10,12] upstream of a destabilized EGFP. The destabilized fluorescent reporter proteins allow the visualization of cells that are actively engaged in NOTCH and WNT signalling. We found that, within the DML, 38.3 % of the epithelial cells that activated canonical WNT signalling were also positive for NOTCH signalling (Figure 1a,c,e). Remarkably, nearly all (98.5 %) epithelial cells that co-activated NOTCH and WNT signalling were MYF5-positive (Figure 1a-c,f). This suggests a strong link between the co-activation of both signalling pathways and the initiation of myogenesis in the DML.

### NOTCH acts upstream of WNT signalling to activate myogenesis.

NOTCH and WNT signalling could act either in parallel or hierarchically during myogenesis. To determine this, we first co-electroporated a constitutively active form of β-catenin[10] together with the NOTCH reporter. This did not lead to any change in NOTCH response (17.7%), compared to controls (15.6%, Supplementary Figure 2a-g). In sharp contrast, the co-expression of a constitutively active form of NOTCH1 (chicken NOTCH Intra-Cellular Domain, NICD[13]) led to robust increase in WNT response compared to controls (75.4%; controls: 35.5%, Figure 1g-m). If NOTCH were to act upstream of WNT signalling to activate MYF5, a blockage of the NOTCH pathway should be rescued by constitutive activation of the WNT pathway. We have previously shown that a dominant-negative form of the NOTCH co-activator Mastermind (DN-MAML1[14]) strongly inhibits MYF5 expression in the DML (6.7% MYF5-positive cells, versus controls: 23%, see Figure 2i-l,s in[1]). A

constitutively active form of the most downstream effector or the WNT pathway, LEF1 (CA-LEF1[8]), co-electroporated with DN-MAML1 not only rescued the inhibition of MYF5 expression by DN-MAML1, but in fact led to a strong activation of MYF5 expression (87.2%, Figure 1p-r) that was indistinguishable from that observed after electroporation of CA-LEF1 alone (87.8%, Figure 1n,o,r). Altogether, these results strongly suggest that NOTCH signalling acts upstream of WNT signalling to activate MYF5 expression in the early somite.

The activation of WNT signalling and myogenesis by NOTCH is WNT ligand-independent.

While extraneous WNT can promote the activation of MYF5 expression in experimental settings[5-7], this does not prove that it does so *in vivo*. We challenged the hypothesis that WNT ligands are important for MYF5 expression in the DML. *Dickkopf* (*Dkk*) genes comprise an evolutionarily conserved family of genes that encode secreted proteins that antagonize Wnt/β-catenin signalling, by inhibiting in the extracellular space the Wnt co-receptors Lrp5 and 6[15]. We tested whether DKK1 efficiently inhibits Wnt/*β*-catenin signalling by co-electroporating DKK1 into one half of the neural tube of developing embryos, together with the WNT reporter described above. As control, the WNT reporter was electroporated alone. Without DKK1, we observed a robust WNT activity in the neural tube (Supplementary Figure 3b-d). The co-electroporation of DKK1 abrogated WNT response (Supplementary Figure 3e-h), underlining the efficiency of this molecule to block Wnt/β-catenin signalling in the extracellular domain.

We then performed a similar experiment in somites. A striking difference from the control experiment in the neural tube was that the Wnt/β-catenin reporter was still active, even after DKK1 expression Figure 2d,e). A quantification of this showed that despite a decrease in overall TOPflash activity compared to controls (Ctrl: 35.7%, Figure 2b,g; with DKK1: 13.4%, Figure 2e,g), virtually all (i.e. 100%) cells that remained TOPflash-positive expressed MYF5 (controls: 54.2%; Figure

2h). As a consequence, the proportion of electroporated DML cells that activated MYF5 expression was not significantly different with or without DKK1 (47.3% or 44.9% respectively; Figure 2i).

To verify that the remaining TOPflash activity was due to NOTCH pathway activation, we electroporated DKK1 together with a NOTCH1-specific siRNA (NOTCH1 is the likely NOTCH receptor implicated in myogenesis at the DML[1]). In these conditions, we observed that the activity of the TOPflash reporter was significantly decreased (34.2%; Figure 2n,p) when compared to controls co-electroporated with DKK1 and a control siRNA (49.3%, Figure 2j,p). Altogether, this supports the premise that the Wnt/β-catenin response in the DML is regulated by NOTCH, triggered by DLL1-positive neural crest cells, and not by a WNT ligand.

To directly test that migrating neural crest cells can elicit a WNT/β-catenin response the DML independent of the WNT ligand, we over-expressed the NOTCH ligand Delta1 (DLL1, the likely ligand of NOTCH in neural crest that triggers MYF5 expression in the DML[1]) in neural crest cells, while inhibiting the WNT ligand in somites. We performed a double electroporation (illustrated in Figure 2q): firstly, we electroporated the dorsal portion of one half of neural tube with a plasmid coding for DLL1[16] under the control of a neural crest-specific promoter, U3[1,17]. The second electroporation targeted the DML of somites facing the electroporated neural tube with the TOPflash reporter described above, together with two plasmids coding for DKK1 and H2B-RFP (as an electroporation marker). The over-expression of DLL1 in neural crest cells resulted in a remarkable 96.2% of electroporated cells within the DML that activated the TOPflash reporter (Figure 2r-v), compared to the control DML only electroporated with the TOPflash reporter (39.8%, see Figure 1a,e).

Altogether, our data strongly suggests that DLL1-expressing neural crest cells trigger the activation of WNT/β-catenin signalling in the DML in a WNT ligand-independent manner. This provocative conclusion prompted a search for a mechanism that could explain how this can be accomplished, starting from the end-point (i.e. the activation of MYF5 by the WNT downstream effectors TCF/LEF

and β-catenin) and unravelling the molecular steps upstream until the initial event (the activation of NOTCH by neural crest cells).

Membranal β-catenin is required for the NOTCH-mediated activation of MYF5

In the DML, the WNT/β-catenin dependent initiation of myogenesis is accompanied by an EMT[1,3]. Because it integrates two distinct functions i) as a transcription co-factor together with TCF/LEF and ii) as a structural adaptor protein linking cadherins to the actin cytoskeleton in cell-cell adhesion, β-catenin is a prime candidate to play a central role in these two processes. However, despite experimental evidence that the dissociation of adherens junction (AJ) can induce the release of β-catenin into the cytoplasm, a functional connection between the nuclear and membranal pools of β-catenin *in vivo* is still a matter of debate[18-20]. Strong β-catenin immunostaining was observed at the AJ of DML cells, and along the plasma membrane, as expected in epithelial cells (Supplementary Figure 4a-d). We tested the hypothesis that membranal β-catenin in DML cells is required for the activation of MYF5, using a mutant Y489F β-catenin that cannot be mobilized from the junctional complex[21] together with an inducible form of NICD (see Methods). Y489F β-catenin was first over-expressed for 10 hours in the DML. Using a Tet-on inducible system, NICD expression was then induced for 6 hours (Figure 3a). As a control, the same experiment was performed using a wild-type (WT) β-catenin. In these control embryos, the expression of NICD induced a robust translocation of WT β-catenin into the nucleus (arrowheads in Figure 3d). As a direct consequence, most (88%) NICD+/WT β-catenin+ cells expressed MYF5 (Figure 3e,l), in accordance with the level of MYF5 that we previously reported after NOTCH activation[1]. In sharp contrast, after electroporation of the mutant form of β-catenin, we observed only few (8.1%) MYF5 positive DML electroporated cells and we could not detect the Y489F β-catenin in the nucleus, despite a strong expression of NICD in electroporated cells (Figure 3f-i,l). MYF5 expression was in fact similarly decreased whether NICD was co-electroporated or not with Y489F β-catenin (6.4%

Figure 3j-l), indicating that the phosphorylation of Y489 is necessary for the activation of MYF5 expression. Altogether, our data strongly suggests that the phosphorylation of tyrosine 489 of β-catenin is a key event required for its mobilization from the cell membrane and/or AJ of DML cells and is necessary for the NOTCH-dependent activation of myogenesis in this structure.

SNAI1 is a necessary and sufficient step of the NOTCH-dependent activation of MYF5.

The results described above provide a mechanistic link between the activation of NOTCH in DML cells and the combined changes in cell adhesion and cell fate. However, they do not reveal how this process is mediated. Major players in cell adhesion are the zinc finger transcriptional repressors *Snail* (or SNAI) family members. An essential function of SNAI is to repress epithelial gene expression and thereby promote epithelial-mesenchymal transitions (EMT) during vertebrate and invertebrate development and metastatic progression of cancers[22]. In early chick embryos, SNAI1 is expressed in the epithelial dermomyotome, including the DML. Its activation leads to the down-regulation of N-cadherin expression present at the adherens junction of epithelial cells from the central dermomyotome and to their subsequent EMT[23]. Coherent with this, the over-expression of SNAI1 in the DML induced a significant increase in the translocation of DML cells into the myotome (89%; Ctrl: 46.7%; Supplementary Figure 5a-c), while the inhibition of its function by a SNAI1-specific siRNA[23] inhibited their translocation (9.3%; Ctrl: 41.6%; Supplementary Figure 5d,f,h). This data supports the hypothesis that SNAI1 plays a role during EMT that allows DML cells to translocate into the nascent myotome. Since we showed above that the EMT is a key event in the activation of MYF5, we tested whether SNAI1 would regulate the activation of MYF5 expression in the DML. The electroporation of SNAI1 in the DML induced a strong activation of MYF5 expression, compared to controls (Figure 4a,b,g; 73%, Ctrl 23.1%, Figure 4c,d,g). Conversely, the electroporation of a dominant-negative form of SNAIL-1[23,24] or a siRNA directed against SNAI1[23] resulted in a significant decrease in MYF5

expression (DN-SNAI1: 7.7%; Ctrl 23.1%, Figure 4c,d,g and siRNA SNAI1: 6.3%, Ctrl: 26.2%, Supplementary Figure 5e,g,i). While this suggests that SNAI1 can modulate MYF5 expression in the DML, it does not prove that SNAI1 plays this role in the signalling process initiated by NOTCH activation. To address this, we co-electroporated NICD together with the dominant-negative form of SNAIL-1. We observed that the massive increase in MYF5 expression that is observed after NICD over-expression (80-89%[1]; see also Figure 3e,j) was profoundly reduced by DN-SNAI1 (6% Figure 4e-g). This result demonstrates that SNAI1 is a necessary step, downstream of NOTCH, in the chain of events that leads to the activation of MYF5 in DML cells. This data also provides a mechanistic link between the activation of MYF5 and the EMT.

NOTCH regulates SNAI1 degradation through inhibition of GSK-3β activity.

We then determined whether NOTCH regulates SNAI1. NICD regulates the transcription of many target genes[25,26], including SNAIL[27]. Therefore, we wondered whether this would be the case in the DML. However, the over-expression of NICD did not result in any significant increase in SNAI1 transcription (as judged by in situ hybridization, data not shown). These results led us to explore alternative mechanisms. SNAI1 mRNA is widely expressed, however its activity is tightly regulated post-translationally through phosphorylation by GSK-3β, which leads to its β-Trcp-mediated ubiquitination and degradation. Due to this continuous degradation, SNAI1 protein displays has a short half-life, estimated to be about 25 min[28]. We first determined whether NOTCH signalling can modify the stability of SNAI1 in DML cells by electroporating SNAI1 fused to GFP (SNAI1-GFP) in the DML, either alone, or in combination with NICD. As control, SNAI1-GFP was electroporated at a low concentration (that does not lead to any visible phenotype, e.g. EMT or activation of MYF5, data not shown). GFP immunostaining was undetectable under UV examination, but visible after immunostaining and confocal examination in a small proportion of electroporated cells (Figure 4h,i). In sharp contrast, the co-electroporation of NICD with the same concentration of SNAI1-GFP

led to a massive increase in GFP staining in most electroporated cells (Figure 4j,k), suggesting that the activation of NOTCH signalling prevents the degradation of SNAI1 that normally occurs in DML cells.

Since GSK-3β is the main regulator of SNAI1 stability[22], we tested whether NOTCH regulates the activity of GSK-3β. Taelman and colleagues cleverly designed a GSK-3β fluorescent "biosensor" (see Methods[29]). When GSK-3β is active, the biosensor fluorescence is reduced; in contrast, when GSK-3β is inactive, its fluorescence is increased. We first determined whether the GSK-3β biosensor is active in DML cells, and observed that fluorescence of the biosensor was only detected in a small proportion of electroporated DML cells (Figure 4l,m). This observation indicates that in the majority of DML cells under normal, unperturbed conditions, GSK-3β is active (i.e. low or no biosensor detectable). However, in a minority of cells GSK-3β is inhibited (i.e. high level of biosensor). To find out what these "high biosensor" cells are, we performed a series of co-electroporations followed by immuno-stainings. This showed that the vast majority of cells in which the fluorescence of the biosensor is observed are those that i) activate the NOTCH reporter (86.9% Supplementary Figure 6a,b,d,e), ii) in which SNAI1 is active (89.4%, Supplementary Figure 6g-k) and iii) are MYF5-positive (88.2%, Supplementary Figure 6a,c,f). This reinforces the hypothesis of a mechanistic link between the initiation of myogenesis in DML cells, NOTCH activation, the stability of SNAIL and the inhibition of GSK-3β activity.

We then tested whether NOTCH regulates GSK-3β by co-electroporating the biosensor together with NICD. This resulted in a massive increase in the fluorescence of the GSK-3β biosensor (Figure 4n,o), suggesting that NICD inhibits GSK-3β kinase activity. To eliminate the possibility that the increase in fluorescence of the biosensor was due to a non-physiological effect of NICD over-expression in DML cells, we induced the activation of NOTCH signalling in the DML by electroporating DLL1 in the neural crest cell population (as described above in Figure 2q), with the GSK-3β biosensor electroporated in the adjacent somites. We

observed a strong increase in the fluorescence of the biosensor in somites (64.6 %, Figure 4r,s,t) compared to controls (26.4%, Figure 4p,q,t).

Since GSK-3β also has a central role in the degradation of cytoplasmic β-catenin by the APC/Axin destruction complex[30], the inhibition of its kinase activity may therefore allow the β-catenin mobilized from the cell membrane and AJ of DML cells to play its transcriptional role. Indeed, the electroporation of a dominant-negative form of GSK-3β (DN-GSK-3β [29]) mimicked the effects of NOTCH activation on SNAI1 and MYF5, resulting in a significant increase in the proportion of DML cells undergoing EMT and translocating into the myotome when compared to controls (61.2%; Ctrl: 45.8%: Supplementary Figure 7d,e,g) and in a robust increase in MYF5 expression in DML cells (57.2%), compared to controls embryos (23.1%; Supplementary Figure 7c,f,h). Altogether our data strongly suggests that a direct consequence of the activation of NOTCH signalling by migrating DLL1-positive neural crest cells in an inhibition of GSK-3β activity that leads to a stabilization of the SNAI1 protein and to an EMT of DML cells.

NOTCH controls myogenesis independently of its transcriptional role in the nucleus.

The decrease of GSK-3β activity in DML cells could be a transcriptional response to the activation of NOTCH signalling. However, NOTCH can also act in a RBPJ/CSL-independent manner[31,32]. To discern between the two possibilities, we electroporated a constitutively active and a dominant negative form of RBPJ[33] in DML cells. As expected, the DN-RBPJ and CA-RBPJ significantly inhibited or activated the NOTCH reporter, respectively, compared to controls (DN-RBPJ: 8%; CA-RBPJ: 77.6%; Ctrl: 15.8%; Supplementary Figure 8a-l,m). However, both constructs failed to modify the expression of MYF5 in this structure, compared to controls (DN-RBPJ: 17.3%; CA-RBPJ: 17.1%; Ctrl: 15.9%; Supplementary Figure 8a-l,n). These results indicate that NICD regulates myogenesis in the DML

independently of its transcriptional activity with RBPJ, suggesting that NICD could mediate this activity in the cytosol.

To address this, we constructed an artificial, membrane-tethered, HA-tagged NICD (see Methods). Unlike wild-type NICD, which upon electroporation readily enters the nucleus and activates the NOTCH reporter, immuno-staining for the CD4-NICD was not observed in the nucleus and, coherent with this, it did not activate the NOTCH reporter (6.4%; Figure 5a-e). Despite this, CD4-NICD over-expression resulted in a massive stabilization of the GSK-3β biosensor (88.6%; Figure 5f-j) that was indistinguishable from that obtained after electroporation of NICD (91.6%, Figure 4n-o). This suggests that the regulation of GSK-3β activity by CD4-NICD is not a transcriptional response to NOTCH signalling.

These results prompted us to test whether CD4-NICD over-expression would mimic the effects of NICD on SNAI1 and MYF5. Indeed, we observed that the electroporation of CD4-NICD led to i) a massive stabilization of SNAI1 protein (90%; Figure 5k-o) comparable to NICD alone (96.7%, Figure 4j,k) and ii) to a robust increase of MYF5 expression in DML cells (71.1%; Figure 5p-t), not significantly different from the NICD alone (83.7%, Figure 1j-l and Figure 3h-o in[1]). This data shows that the activation of MYF5 in DML cells is the result of a cytoplasmic function of NICD that can be uncoupled from its role as a transcriptional co-activator in the nucleus.

## DISCUSSION

The findings presented here uncovers a simple signalling module that is triggered by a signal presented by migrating neural crest cells to selected progenitors in the somites. This signal is transduced into two distinct, but inter-related outcomes i) a cell fate decision in the receiving cells that leads to their entry into the myogenic program and ii) an EMT that allows their translocation into the myotome (illustrated in Supplementary Figure 9).

EMT is intimately associated with essential changes in cell specification in many other developmental processes (e.g. gastrulation, neural crest formation, etc.), but also during metastatic progression of carcinomas and cell reprogramming[34-36]. The EMT master regulators SNAI genes play crucial roles in these processes. A large spectrum of secreted factors belonging to most signalling pathways can activate EMT by stimulating SNAI transcription. This mechanism i) likely requires a robust activation of SNAI transcription to counteract its continual ubiquitination and degradation and ii) is unlikely to trigger at the same time the cell changes associated with the EMT[22,37]. Remarkable of the signalling module described here is that it targets the heart of the degradation mechanism, GSK-3β. This seems to be a very efficient approach, judging the dramatic effects on the GSK-3β biosensor and on the stabilisation of SNAI1. In addition, aiming at GSK-3β likely insures that the β-catenin released during the EMT process is not degraded and can accumulate sufficiently to act as a transcriptional co-factor, thereby resulting in a quasi-automatic coupling of EMT and a WNT/β-catenin-dependent cell fate change. Given the large distribution of the key players we described in this paper, it is plausible that the same signalling circuitry could couple EMT to WNT/β-catenin-dependent cell fate decision in a wide variety of epithelia in normal and pathological conditions.

At both ends of this signalling module, NICD and β-catenin display unexpected functions. The "canonical" role of NICD is to act as a co-transcriptional activator together with RBPJ. However, cytosolic interactions of NICD with various

molecular partners that result in cellular responses independent of RBPJ, have been described in a few *in vitro* experimental settings (reviewed in[31,32]), but also in *Drosophila*[38]. Our data uncovers a novel function of NOTCH1 that takes place in the cytosol and leads to GSK-3β inhibition. It is known that the transcriptional activity of NICD is modified by its phosphorylation *in vitro*, probably by GSK-3β[39-41]. It is therefore not totally surprising that the same would happen in the DML. What is remarkable is that this leads to a decrease in the overall activity of GSK-3β that has important consequences for the cell. It is probable that the dramatic response we observed results from a titration of GSK-3β kinase activity by NICD that is amplified by the stabilization of SNAI, itself a substrate for this kinase.

While textbooks state that β-catenin participates in adhesion and signalling functions in a mutually exclusive manner. However, experimental evidence suggests that the pools of β-catenin located at the plasma membrane and AJ of epithelial cells can regulate WNT/β-catenin signalling *in vitro*[18-20]. The results we obtained here provide direct support that this is also the case *in vivo* and demonstrate that the pool of β-catenin accumulated at the membrane and/or at the AJ has additional functions to it's established role in cell-cell adhesion.

Our study provides a model that reconciles apparently divergent observations on the respective role of NOTCH and WNT signalling in the initial phases of myogenesis. The necessary function of NOTCH in this process[1] is confirmed, but the present work demonstrates that the NOTCH signal is a permissive one, while the instructive role is executed by the downstream effectors of WNT/β-catenin signalling, β-catenin and TCF/LEF. This is in accordance with the role assigned to WNT signalling in somite myogenesis decades ago[5-7], however the results presented here shed an entirely novel light on the origin of the signal and the pathway that mediates it.

Finally, the coupling of an activation of NOTCH with EMT is of particular importance for the activation of MYF5 at the DML: we had previously shown that it is crucial that NOTCH is transiently activated in receiving DML cells, since

artificially sustaining its activity in those cells results in aberrant behaviour and a reversal of myogenesis[1]. It is remarkable that the migration of DML cells away from the signalling source is a hard-wired feature of this signalling module that likely ensures that NOTCH is indeed transiently activated. The complexity of the cellular responses triggered by migrating neural crest cells in somites is puzzling as is raises the question of how two distinct tissues have become so perfectly coordinated during evolution to generate such sophisticated interactions.

## METHODS

### Electroporation

The somite electroporation technique that was used throughout this study has been described elsewhere[1,3,10,42]. Briefly, we targeted the expression of various constructs to the dorsomedial portion of newly formed interlimb somites of Hamburger–Hamilton (HH[43]) stage 15–16 chick embryos (24–28 somite). We have previously shown that this technique allows the specific expression of cDNA constructs in the DML of the dermomyotome. To target the neural crest population, we electroporated the dorsal neural tube of HH stage 13–14 chick embryos at the level of the presomitic mesoderm[1].

### Expression constructs

The following constructs have been previously published:

The WNT reporter 12Tf-d2EGFP contains 12 TCF/LEF1 binding sites[12] upstream of a TK minimal promoter driving a destabilized GFP (d2EGFP, 2 hours half-life, Clontech[10]).

The CAGGS-H2B–RFP (provided by Dr. S. Tajbakhsh[1]) contains a fusion of Histone 2B with RFP, downstream of the CAGGS strong ubiquitous promoter (CMV/chick β-actin promoter/enhancer).

The CAGGS–EGFP[1] contains the CAGGS promoter followed by the EGFP reporter gene.

The constitutively active form of LEF1, CA-LEF1 (provided by Dr. A. Münsterberg) is described in[8].

The CAGGS-DN-MAML1–EGFP contains a truncated, dominant-negative form of the human Mastermind (DN-MAML1), fused with EGFP[14], downstream of the CAGGS promoter.

pCS2+ DKK1-flag (Addgene #16690) contains a human *DKK1* fused to a flag tag downstream of a CMV promoter[44].

U3-DLL1[1] was made by inserting the U3 evolutionarily conserved Sox10 enhancer sequences[17] in the TK-EGFP plasmid[45].

A Tet-on (Clontech) inducible system was used to activate NICD expression[1]. The doxycyclin inducible system is composed of two plasmids that are co-electroporated: first, the pCIRX-rtTA (provided by O. Pourquié) contains a Tet-On Advanced transactivator (rtTA, Clontech) downstream of the CAGGS promoter. Second, the pBI-HA-NICD-EGFP is the response plasmid (Clontech) in which the HA-tagged constitutively active form of the NOTCH1 receptor from chick, NICD[13] (provided by Dr. N. Daudet), was cloned. The bidirectional tetracyclin-response element drives the expressions of EGFP (which serves as an internal control of the induced response) and HA-NICD.

CAGGS-cSNAI1 contains the wild type chicken Snail1 gene downstream of the CAAGS promoter upstream of an IRES EGFP[23].

The dominant negative form of SNAI1 consists of the chicken SNAI1 in which the repressor domain was replaced by the VP16 activator domain of the Herpes simplex virus[23].

SNAI1-GFP (Addgene #16225) contains a CMV promoter upstream of a human wild type Snail1 fused to EGFP[28].

CAGGS NICD contains the chicken NICD downstream of the CAGGS promoter[1].

The GSK3 biosensor (pCS2 GFP-GSK3-MAPK, Addgene #29689) contains a CMV promoter upstream of a GFP molecule followed by a polypeptide tail that contains 3 GSK-3β phosphorylation sites, a priming site for MAPK/Erk and a site for the binding of E3 polyubiquitin ligases[29].

HES1–d2EGFP (provided by Dr. R. Kageyama) contains the HES1 mouse promoter followed by a destabilized d2EGFP[11].

The constitutively active form of β-catenin was described in[3]

A constitutively active form of RBPJ (pCMX-N/VP16-RBPJ, obtained from Dr. T. Honjo) comprises the CMV promoter driving a VP16 activation domain fused to the mouse RBPJ gene[33].

The dominant-negative GSK-3β (Addgene #29681) is a kinase dead variant of the Xenopus GSK-3β gene fused to an EGFP protein[29].

The SNAI1 siRNA (as well as the Luciferase control) were described and tested in[23]. It leads to an efficient down-regulation of SNAI1 transcript level in chick tissues.

The NOTCH1 siRNA was described in[1]. It leads to an efficient down-regulation of NOTCH1 transcript level in chick tissues.

The following plasmids were constructed for this study:

HES1-DSRed-Express-DR was created by replacing the d2EGFP from HES1–d2EGFP (provided by Dr. R. Kageyama[11]) with a fast-folding, unstable variant of DSRed (Clontech).

The wild-type human β-catenin was amplified from pFG8 (provided by Dr. N. Plachta), then cloned into pCX-Myc (pCAGGS with 6xMyc tag, obtained from Dr. X. Morin).

Human β-catenin containing the Y489F (Tyr to Phe[21]) mutation was amplified from Addgene #24197, then cloned into pCX-Myc.

The membrane tagged NICD was constructed using Gibson assembly (NEB) with the signal peptide FGFR2 (from Danio rerio), the extracellular and transmembrane domain of human CD4 (both obtained from Dr. J. Kaslin) followed by the HA tagged NICD previously described, cloned either into the bidirectional vector tetracycline responsive vector or into the pCX-Myc described above.

The H2B-BFP has been made by replacing the RFP from the CAGGS-H2B–RFP described above by a TagBFP (Evrogen).

The SNAI1-RFP has been made by replacing the GFP from SNAI1-GFP (Addgene #16225) by RFP (Clontech).

CAGGS-BFP has been made by cloning the TagBFP (Evrogen) into the pCAGGS vector.

Immunohistochemistry

Whole-mount antibody stainings were performed as described[3]. The following antibodies were used: rabbit polyclonals directed against chick myogenic regulatory factor MYF5 (obtained from Dr. B. Paterson[46]; 1/200); and anti-RFP (Abcam #62341, 1/1000). Chicken polyclonal antibody against EGFP (Abcam #13970, 1/1000). The neural-crest-specific monoclonal antibody HNK1 was provided by Dr. A. Eichmann. Mouse monoclonal antibodies against c-myc-tag (Abcam #32072, 1/200), HA-tag (CST, #2367S, 1/100) and β-catenin (BD biosciences, #610154) were also used.

Doxycyclin-mediated induction of NOTCH signalling

We have tested the role of β-catenin from the membrane and AJ using a mutant (Y489F) form of β-catenin and a doxycyclin inducible (Tet-On system) NICD. The association of β-catenin with proteins partners (α-catenin and cadherin) at the membrane is regulated by its phosphorylation at highly conserved tyrosine residues 142, 489 and 654[21,47,48]. In the neural tissue, the phosphorylation of β-catenin on tyrosine 489 reduces its affinity for N-cadherin and a mutant form of the β-catenin where this tyrosine is mutated to a phenylalanine (Y489F) cannot be mobilized from the junctional complex[21]. In DML cells, where β-catenin is also associated with N-cadherin[49], we hypothesized that cells in which endogenous wild-type β-catenin was replaced by Y489F mutant β-catenin would not be able to activate myogenesis. Due to the fast turnover of the junctional complex[50], and the rapid degradation of cytoplasmic β-catenin by the APC/Axin destruction complex[30],

we speculated that the forced expression of the Y489F mutant β-catenin would rapidly replace the endogenous wild type (WT) β-catenin with its mutant counterpart, thereby allowing us to test the role of this variant in the induction of myogenesis. We tested whether the massive upregulation of MYF5 expression resulting from the constitutive activation of NOTCH signalling[1] could be inhibited in presence of the mutant Y489F β-catenin.

Ten hours after electroporation of pCIRX-rtTA and pBI-HA-NICD-EGFP, doxycyclin (300 µl of a 0.75 µg/ml solution) was added onto the embryos. We have shown that the response plasmid is completely silent before doxycyclin addition, while it is strongly and rapidly activated 6 h after doxycyclin addition[1].

Confocal analyses

Dorsal views of somites shown in all figures are projections of stacks of confocal images taken using a 4-channel Leica SP5 confocal microscope (Leica). Confocal stacks of images were visualized and analyzed with the Imaris software suite (Bitplane). Cell counting was performed using the cell counter plugin (Kurt De Vos, University of Sheffield) within the ImageJ software[51].

Quantifications and statistical analyses

Electroporation results in the transfection of a portion of the targeted cell population, which is variable from embryo to embryo. To precisely evaluate the phenotypes obtained after electroporation of cell-autonomously acting cDNA constructs, the number of positive cells was compared to the total number of electroporated cells, recognized by an internal fluorescent reporter construct. On average, more than 700 cells were counted per point and the corresponding quantifications are shown in Figs 1–6 and Supplementary Figs 2,4.

To analyze the fluorescence intensity of electroporated cells (Figure 2j-p), embryos where fixed and imaged. Laser and gain parameters during confocal acquisition

were set and unchanged for all samples. Minimum and maximum pixel intensity values for confocal stacks were established using TOPflash controls (Figure 2j-k) and used across all samples. Using ImageJ software, the entire DML area was selected and the average pixel intensity for both green (12TF-d2EGFP) and red (CAGGS-RFP) channels were obtained. Average RFP intensity values within each sample were normalized to 100 and average GFP intensity were given as the percentage of this value.

Statistical analyses were performed using the GraphPad Prism software. Mann–Whitney non-parametric two-tail testing was applied to populations to determine the P values indicated in the figures. In each graph, columns correspond to the mean and error bars correspond to the standard deviation. ***P value < 0.001, extremely significant; **P value 0.001 to 0.01, very significant.

ACKNOWLEDGEMENTS

We thank Monash Micro Imaging (MMI) for imaging support; and Drs N. Rosenthal and J-L Bessereau for critical reading of the manuscript.

AUTHOR CONTRIBUTIONS

AR, DSM, CH, CM designed the experiments, AR, DSM, CH performed the experiments. The manuscript was prepared by CM, with the help and feedback from all authors.

REFERENCES

1. Rios, A. C., Serralbo, O., Salgado, D. & Marcelle, C. Neural crest regulates myogenesis through the transient activation of NOTCH. *Nature* 473, 532–535 (2011).

2. Ordahl, C. P., Berdougo, E., Venters, S. J. & Denetclaw, W. F. J. The dermomyotome dorsomedial lip drives growth and morphogenesis of both the primary myotome and dermomyotome epithelium. *Development* 128, 1731–1744 (2001).

3. Gros, J., Serralbo, O. & Marcelle, C. WNT11 acts as a directional cue to organize the elongation of early muscle fibres. *Nature* 457, 589–593 (2009).

4. Denetclaw, W. F., Christ, B. & Ordahl, C. P. Location and growth of epaxial myotome precursor cells. *Development* 124, 1601–1610 (1997).

5. Munsterberg, A. E., Kitajewski, J., Bumcrot, D. A., McMahon, A. P. & Lassar, A. B. Combinatorial signaling by Sonic hedgehog and Wnt family members induces myogenic bHLH gene expression in the somite. *Genes Dev.* 9, 2911–2922 (1995).

6. Tajbakhsh, S. *et al.* Differential activation of Myf5 and MyoD by different Wnts in explants of mouse paraxial mesoderm and the later activation of myogenesis in the absence of Myf5. *Development* 125, 4155–4162 (1998).

7. Stern, H. M., Brown, A. M. & Hauschka, S. D. Myogenesis in paraxial mesoderm: preferential induction by dorsal neural tube and by cells expressing Wnt-1. *Development* 121, 3675–3686 (1995).

8. Abu-Elmagd, M. *et al.* Wnt/Lef1 signaling acts via Pitx2 to regulate somite myogenesis. *Dev. Biol.* 337, 211–219 (2010).

9. Borello, U. *et al.* The Wnt/beta-catenin pathway regulates Gli-mediated Myf5 expression during somitogenesis. *Development* 133, 3723–3732 (2006).

10. Rios, A. C., Denans, N. & Marcelle, C. Real-time observation of Wnt beta-catenin signaling in the chick embryo. *Dev. Dyn.* 239, 346–353 (2010).

11. Ohtsuka, T. *et al.* Visualization of embryonic neural stem cells using Hes promoters in transgenic mice. *Mol Cell Neurosci* 31, 109–122 (2006).

12. Korinek, V. *et al.* Constitutive Transcriptional Activation by a β-Catenin-Tcf Complex in APC−/− Colon Carcinoma. *Science* 275, 1784–1787 (1997).

13. Daudet, N. & Lewis, J. Two contrasting roles for Notch activity in chick inner ear development: specification of prosensory patches and lateral inhibition of hair-cell differentiation. *Development* 132, 541–551 (2005).

14. Weng, A. P. *et al.* Growth suppression of pre-T acute lymphoblastic leukemia cells by inhibition of notch signaling. *Molecular and cellular biology* 23, 655–664 (2003).

15. Niehrs, C. Function and biological roles of the Dickkopf family of Wnt modulators. *Oncogene* 25, 7469–7481 (2006).

16. Henrique, D. *et al.* cash4, a novel achaete-scute homolog induced by Hensen's node during generation of the posterior nervous system. *Genes Dev.* 11, 603–615 (1997).

17. Werner, T., Hammer, A., Wahlbuhl, M., Bosl, M. R. & Wegner, M. Multiple conserved regulatory elements with overlapping functions determine Sox10 expression in mouse embryogenesis. *Nucleic Acids Research* 35, 6526–6538 (2007).

18. Nelson, W. J. & Nusse, R. Convergence of Wnt, ß-Catenin, and Cadherin Pathways. *Science* 303, 1483–1487 (2004).

19. Gavard, J. & Mège, R.-M. Once upon a time there was β-catenin in cadherin-mediated signalling. *Biology of the Cell* 97, 921–926 (2012).

20. Brembeck, F. H., Rosário, M. & Birchmeier, W. Balancing cell adhesion and Wnt signaling, the key role of β-catenin. *Current Opinion in Genetics & Development* 16, 51–59 (2006).

21. Rhee, J., Buchan, T., Zukerberg, L., Lilien, J. & Balsamo, J. Cables links Robo-bound Abl kinase to N-cadherin-bound beta-catenin to mediate Slit-induced modulation of adhesion and transcription. *Nature cell biology* 9, 883–892 (2007).

22. Barrallo-Gimeno, A. & Nieto, M. A. The Snail genes as inducers of cell movement and survival: implications in development and cancer. *Development* 132, 3151–3161 (2005).

23. Delfini, M.-C. *et al.* The timing of emergence of muscle progenitors is controlled by an FGF/ERK/SNAIL1 pathway. *Dev. Biol.* 333, 229–237 (2009).

24. Mayor, R., Guerrero, N., Young, R. M., Gomez-Skarmeta, J. L. & Cuellar, C. A novel function for the Xslug gene: control of dorsal mesendoderm development by repressing BMP-4. *Mechanisms of development* 97, 47–56 (2000).

25. Fortini, M. E. Notch Signaling: The Core Pathway and Its Posttranslational Regulation. *Dev. Cell* 16, 633–647 (2009).

26. Guruharsha, K. G., Kankel, M. W. & Artavanis-Tsakonas, S. The Notch signalling system: recent insights into the complexity of a conserved pathway. *Nature reviews* 13, 654–666 (2012).

27. Grego-Bessa, J., Díez, J. & Pompa, J. L. de L. Notch and Epithelial-Mesenchyme Transition in Development and Tumor Progression: Another Turn of the Screw. *cc* 3, 716–719 (2004).

28. Zhou, B. P. *et al.* Dual regulation of Snail by GSK-3β-mediated phosphorylation in control of epithelial–mesenchymal transition. *Nature cell biology* 6, 931–940 (2004).

29. Taelman, V. F. *et al.* Wnt Signaling Requires Sequestration of Glycogen Synthase Kinase 3 inside Multivesicular Endosomes. *Cell* 143, 1136–1148 (2010).

30. Clevers, H. & Nusse, R. Wnt/β-Catenin Signaling and Disease. *Cell* 149, 1192–1205 (2012).

31. Ayaz, F. & Osborne, B. A. Non-Canonical Notch Signaling in Cancer and Immunity. *Front. Oncol.* 4, (2014).

32. Andersen, P., Uosaki, H., Shenje, L. T. & Kwon, C. Non-canonical Notch signaling: emerging role and mechanism. *Trends Cell Biol* 22, 257–265 (2014).

33. Kuroda, K. *et al.* Delta-induced Notch Signaling Mediated by RBP-J Inhibits MyoD Expression and Myogenesis. *Journal of Biological Chemistry* 274, 7238–7244 (1999).

34. Thiery, J. P., Acloque, H., Huang, R. Y. J. & Nieto, M. A. Epithelial-Mesenchymal Transitions in Development and Disease. *Cell* 139, 871–890 (2009).

35. Mani, S. A. *et al.* The Epithelial-Mesenchymal Transition Generates Cells with Properties of Stem Cells. *Cell* 133, 704–715 (2008).

36. Shu, X. & Pei, D. The function and regulation of mesenchymal-to-epithelial transition in somatic cell reprogramming. *Curr Opin Genet Dev* 28, 32–37 (2014).

37. Lamouille, S., Xu, J. & Derynck, R. Molecular mechanisms of epithelial–mesenchymal transition. *Nature reviews* 15, 178–196 (2014).

38. Le Gall, M., De Mattei, C. & Giniger, E. Molecular separation of two signaling pathways for the receptor, Notch. *Dev. Biol.* 313, 556–567 (2008).

39. Schweisguth, F. Regulation of Notch Signaling Activity. *Curr Biol* 14, R129–R138 (2004).

40. Foltz, D. R., Santiago, M. C., Berechid, B. E. & Nye, J. S. Glycogen Synthase Kinase-3β Modulates Notch Signaling and Stability. *Curr Biol* 12, 1006–1011 (2002).

41. Espinosa, L., Inglés-Esteve, J., Aguilera, C. & Bigas, A. Phosphorylation by Glycogen Synthase Kinase-3 Down-regulates Notch Activity, a Link for Notch and Wnt Pathways. *Journal of Biological Chemistry* 278, 32227–32235 (2003).

42. Gros, J., Scaal, M. & Marcelle, C. A two-step mechanism for myotome formation in chick. *Dev. Cell* 6, 875–882 (2004).

43. Hamburger, V. & Hamilton, H. L. A series of normal stages in the development of the chick embryo. 1951. *Dev. Dyn.* 195, 231–272 (1992).

44. Semënov, M. V. *et al.* Head inducer Dickkopf-1 is a ligand for Wnt coreceptor LRP6. *Curr Biol* 11, 951–961 (2001).

45. Uchikawa, M., Ishida, Y., Takemoto, T., Kamachi, Y. & Kondoh, H. Functional analysis of chicken Sox2 enhancers highlights an array of diverse regulatory elements that are conserved in mammals. *Dev. Cell* 4, 509–519 (2003).

46. Manceau, M. *et al.* Myostatin promotes the terminal differentiation of embryonic muscle progenitors. *Genes Dev.* 22, 668–681 (2008).

47. Lilien, J. & Balsamo, J. The regulation of cadherin-mediated adhesion by tyrosine phosphorylation/dephosphorylation of β-catenin. *Curr. Opin. Cell Biol.* 17, 459–465 (2005).

48. Palka-Hamblin, H. L. *et al.* Identification of -catenin as a target of the intracellular tyrosine kinase PTK6. *Journal of Cell Biology* 123, 236–245 (2010).

49. Gros, J., Manceau, M., Thomé, V. & Marcelle, C. A common somitic origin for embryonic muscle progenitors and satellite cells. *Nature* 435, 954–958 (2005).

50. Baum, B. & Georgiou, M. Dynamics of adherens junctions in epithelial establishment, maintenance, and remodeling. *Journal of Cell Biology* 192, 907–917 (2011).

51. Schneider, C. A., Rasband, W. S. & Eliceiri, K. W. NIH Image to ImageJ: 25 years of image analysis. *Nat Meth* 9, 671–675 (2012).

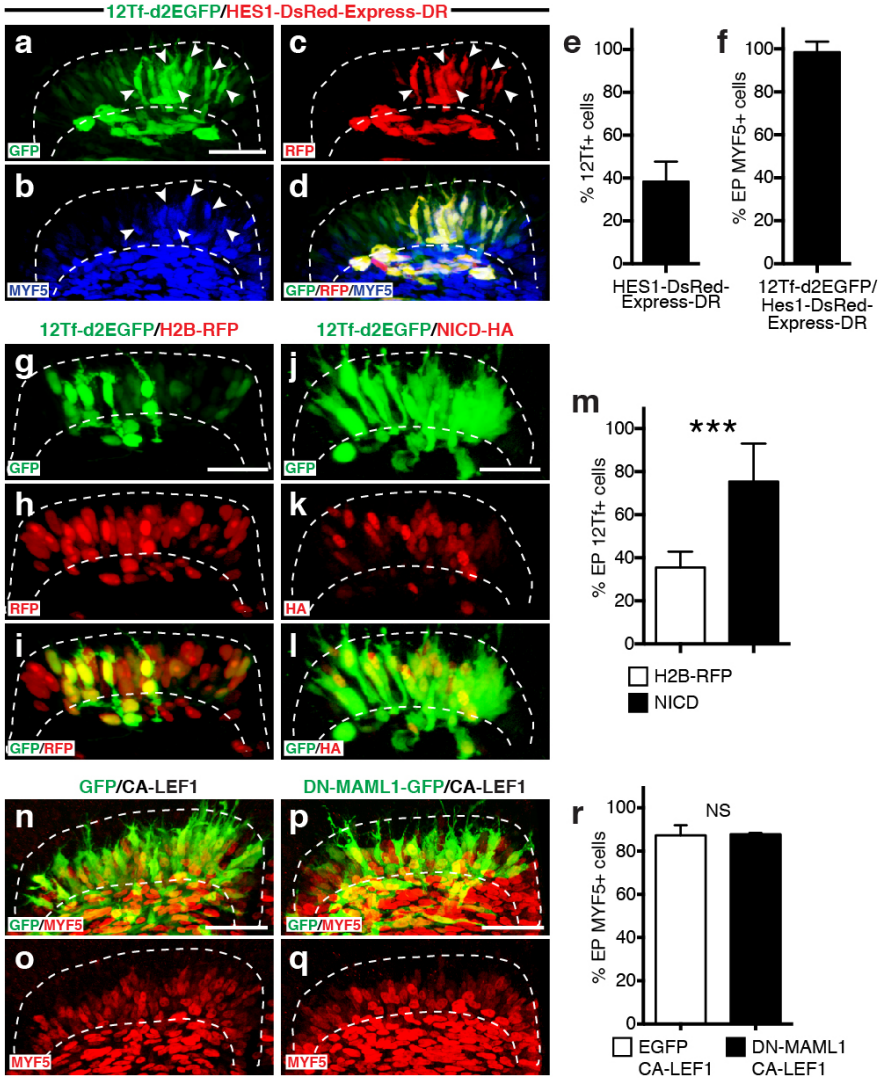


**Figure 1: NOTCH acts upstream of WNT signalling to activate MYF5 expression**
a-d, Confocal stacks of somites, in dorsal view, 12h after electroporation of 12Tf-d2EGFP (WNT reporter, in green), Hes1-DsRedExpress-DR (NOTCH reporter, in red) and immunostained for MYF5 expression (in blue). Arrowheads indicate cells that activate NOTCH and WNT signalling and are MYF5-positive. e,f, Bar charts showing (e) the percentage (%) of cells activating the NOTCH reporter within the WNT reporter-positive population and (f) the % of cells expressing MYF5 that co-activate the WNT and the NOTCH reporters. g-l, Confocal stacks of somites 6h after co-electroporation of a 12Tfd2EGFP reporter construct (in green), and an ubiquitously expressed H2B-RFP (red in h,i) or with a constitutive active form of Notch1 NICD (red in k,l). m. Bar charts showing the % of cells expressing the WNT reporter in the controls (in white) or with NICD (in black) . n-q, Confocal stacks of somites 6h after co-electroporation of (n-o) a constitutive active form of LEF1 and GFP (in green) or (p-q) a dominant negative form of MAML1 fused to GFP (in green) and a constitutive active form of LEF1; in n-q MYF5 expression is shown in red. r, Quantification of n-q in % of MYF5-positive cells. In each panel are indicated the antigens that were detected by immunostaining. Abbreviation: EP: electroporation. Scale bars: 50 μm

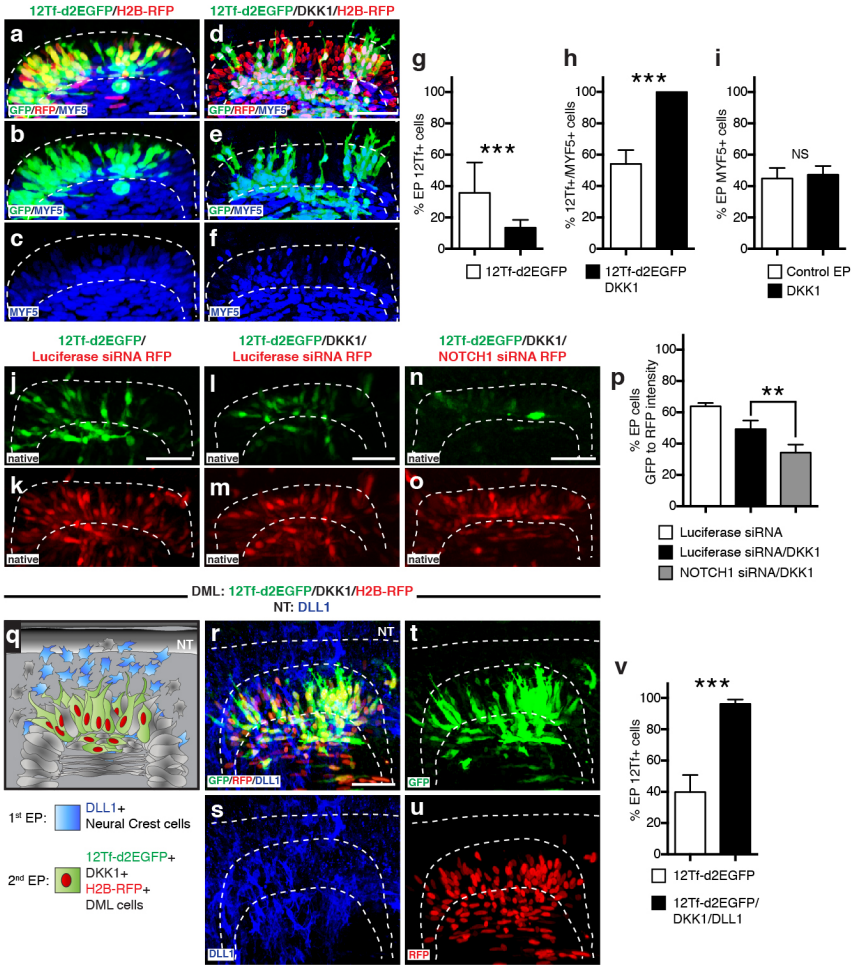


**Figure 2: Activation of WNT signalling and myogenesis by NOTCH is WNT-ligand independent.**

a-f, Confocal stacks of somites, 6h after co-electroporation of the 12Tf-d2EGFP WNT reporter (in green) with H2B-RFP (in red) with (d-f) or without (a-c) Dkk-1, immunostained for MYF5 (in blue) . g-i, Bar charts showing, (in g) the % of 12Tf-positive cells in the controls (in white) or with Dkk-1 (in black); (in h) the % of MYF5-positive cells in the electroporated population; (in i) the % of MYF5-positive cells that are positive for the WNT reporter. j-o, Confocal stacks of somites, 12h after co-electroporation of the 12Tf-d2EGFP WNT reporter (in green) Luciferase-specific siRNA (j-m, in red) or NOTCH1-specific siRNA (n,o, in red) with (l-o) or without (j,k) DKK-1. p, Bar charts showing the % of pixel intensity of the green channel (GFP) relative the the red channel (RFP) in the DML. q, Schematic representing the design of the double electroporation experiment, with the first electroporation in the neural tube (NT) to target the expression of DLL1 in the migrating neural crest (in blue) and the electroporation in the DML with the indicated plasmids. r-u, Confocal stacks of somites after a double electroporation experiments of DLL1 (in blue) in the dorsal neural tube and 12 hours later, 12Tf-d2EGFP (in green), H2B-RFP (in red) and DKK-1 in the DML. v, Bar charts showing the % of 12Tf-d2EGFP-positive cells in the control (in white) or with DLL1 in the NCC (in black). Abbreviations: NT: neural tube; DML: Dorso-Medial Lip; NCC: Neural Crest Cells; EP: electroporation. In each panel are indicated the antigens that were detected by immunostaining. Scale bars: 50 μm

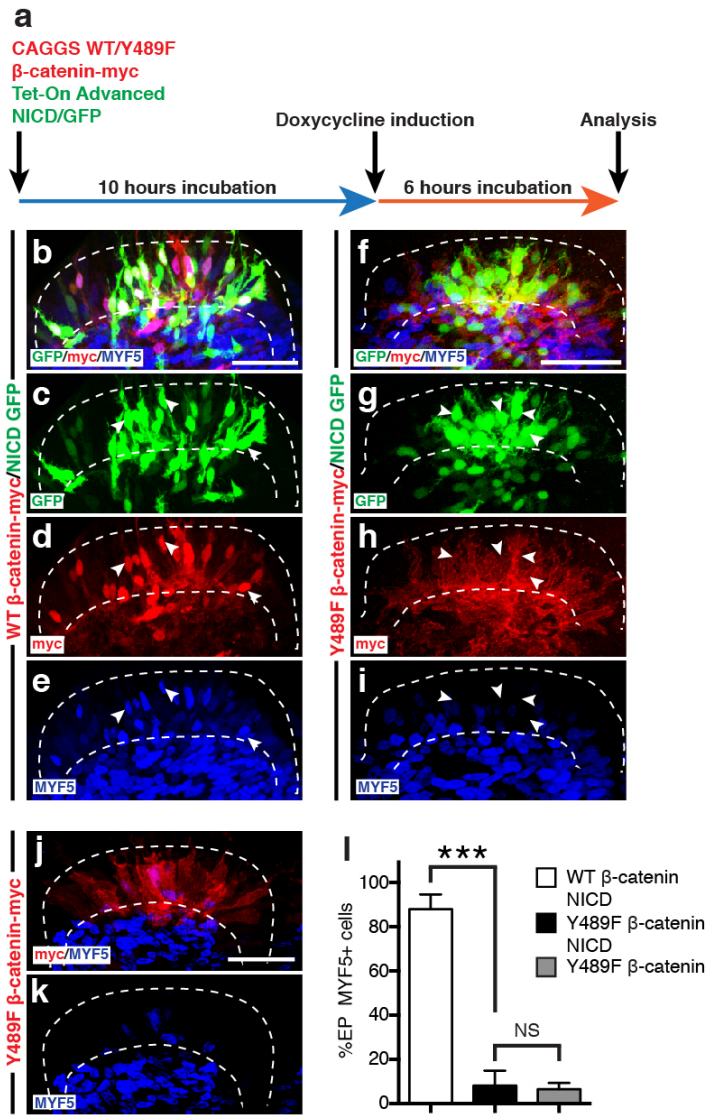


**Figure 3: β-catenin from the cell membrane and AJ is required for the NOTCH-mediated activation of MYF5 expression**

a, Schematic of the experimental design that was followed: (Myc-tagged) WT or a mutant Y489F β-catenin under a CAGGS ubiquitous promoter was electroporated in the DML together with the Tet-On Advanced transactivator (rtTA) and NICD inserted in the response vector. The bidirectional tetracyclin-response element drives the expression of NICD as well as EGFP upon induction with doxycyclin. The β-catenin was expressed from the start of the experiment; NICD was induced 10 hours later. b-i, Confocal stacks of somites after electroporation of (b-e) NICD (in green) and WT β-catenin (in red) or (f-i) NICD (in green) and Y489F β-catenin (in red). MYF5 expression is shown (in blue). j-k, Confocal stacks of somites after electroporation of Y489F β-catenin (in red). MYF5 expression is shown (in blue). l, Bar charts showing the % of MYF5-positive cells after elctroporation of WT β-catenin (in white) or with Y489F β-catenin (in black) together with NICD or only with Y489F β-catenin (in grey). In each panel are indicated the antigens that were detected by immunostaining. Scale bars: 50 μm

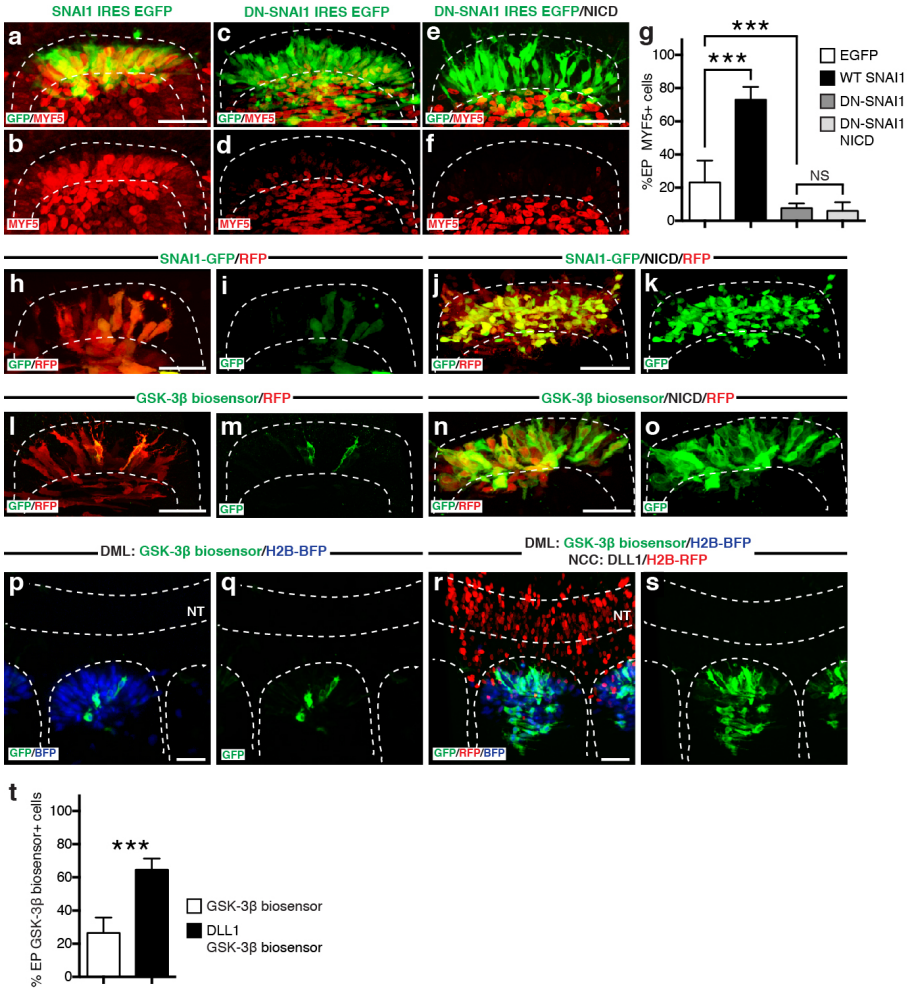


**Figure 4: NOTCH stabilizes the EMT master regulator SNAI1 via inhibition of GSK-3β.** a-f, Confocal stacks of somites, 6h after electroporation of (a,b) a WT chicken SNAI1 (in green); (c,d) a dominant negative (DN) form of SNAI1 (in green) alone or (e,f) together with NICD. MYF5 expression is indicated (in red). g, Bar charts showing the % of MYF5-positive cells after GFP electroporation (in white), with chicken SNAI1 (in black), with DN SNAI1 alone (in dark grey) or together with NICD (in light grey). h-k, Confocal stacks of somites, 6h after electroporation of RFP (in red) and SNAI1-GFP (fusion of SNAI1 and GFP, in green) alone (h,i) or together with NICD (j,k). l-o, Confocal stacks of somites, 6h after electroporation of (l,m) GSK-3β biosensor (in green) and RFP (in red) alone, or of (n-o) GSK-3β biosensor (in green) and RFP (in red) together with NICD. p-s, Confocal stacks of somites and adjacent neural tube electroporated as described in Figure 2q-u, (p,q) electroporated only in the DML with the GSK-3β biosensor (in green) and H2B-BFP (in blue) or (r,s) double-electroporated in the DML with the GSK-3β biosensor (in green) and H2B BFP (in blue) and in the neural tube with DLL1 under the control of a neural crest-specific promoter. t, Bar charts showing the % of GSK-3β biosensor-positive cells in the control (in white) or with DLL1 over-expressed in the neural crest (in black). In each panel are indicated the antigens that were detected by immunostaining, with the exception of p,r: native BFP blue fluorescence. Abbreviation: EP: electroporation; NT: neural tube. Scale bars: 50 μm.

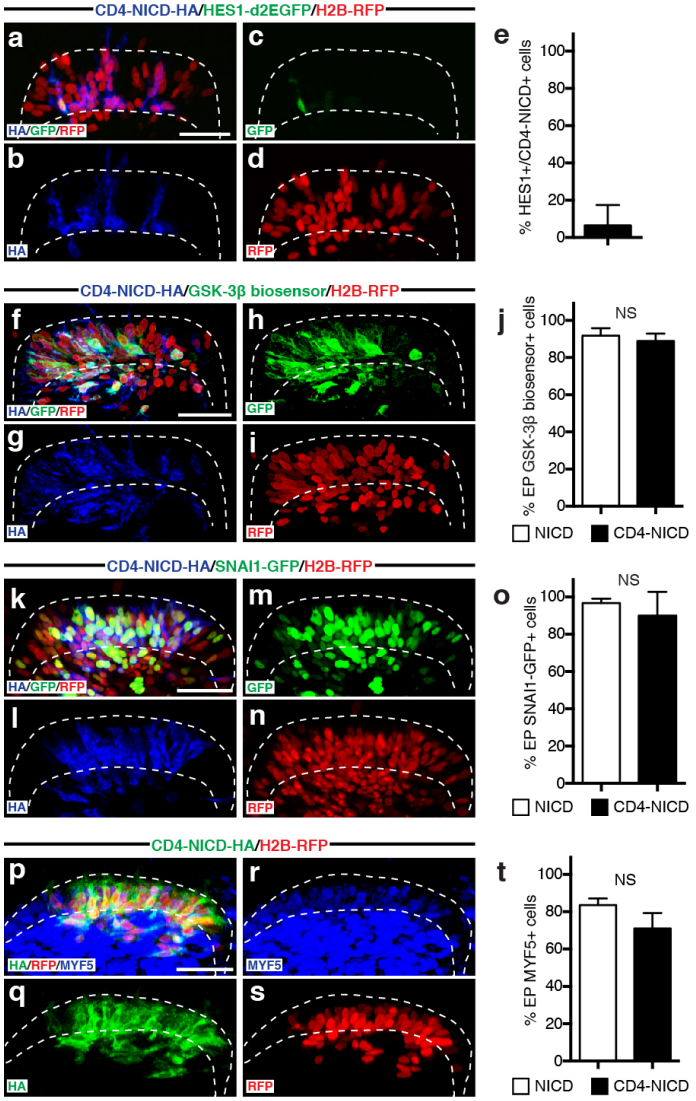


**Figure 5: NOTCH1 controls myogenesis independently of its transcriptional role in the nucleus.**

a-d, Confocal stacks of a somite, 6 hours after co-electroporation of a HA-tagged, membrane-tethered NICD, CD4-NICD (in blue), a NOTCH reporter (in green) and H2B-RFP (in red). e, Bar charts showing the percentage of NOTCH reporter-positive cells electroporated with CD4-NICD. f-i, Confocal stacks, 6h after electroporation of CD4-NICD (in blue), GSK-3β biosensor (in green) and H2B-RFP (in red). j, Bar charts showing the percentage of GSK-3β biosensor-positive cells after electroporation with NICD (in white) or with CD4-NICD (in black). k-n, Confocal stacks, 6h after co-electroporation of CD4-NICD (in blue), SNA1-GFP (in green) and H2B-RFP (in red). o, Bar charts showing the percentage of SNAI1-GFP-positive cells after electroporation with NICD (in white) or with CD4-NICD (in black). p-s, Confocal stacks, 6h after co-electroporation of CD4-NICD (in green), H2B-RFP (in red) and immunostained for MYF5 (in blue) . t, Bar charts showing the percentage of MYF5-positive cells after electroporation with NICD (in white) or with CD4-NICD (in black). In each panel are indicated the antigens that were detected by immunostaining. Abbreviation: EP: electroporation. Scale bars: 50 μm

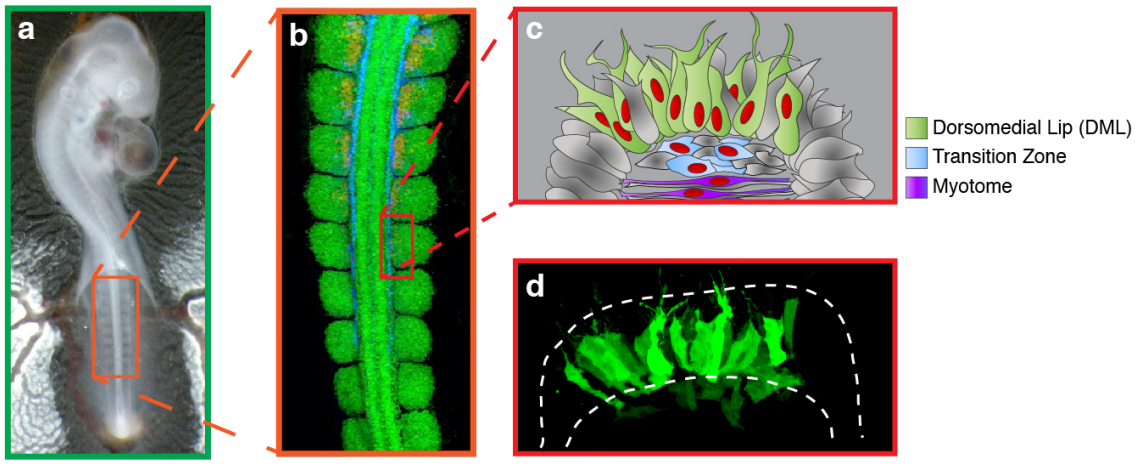


**Supplementary Figure 1: Summary of the experiments performed in this study.**
a, Chick embryos at HH stage 15–16 (24–28 somite) were electroporated in the medial part of the (4-5) newly formed somites (boxed region). b, Immunostaining of a HH 15 chick embryo with PAX7 (in green), HNK1 (in blue) and MYF5 (in red) to label the dermomyotome, the neural crest and the myotome, respectively. c, schematic illustrating regions of the somite which are represented in the confocal stacks of images shown throughout the study. It shows the medial portion of a somite 6-24 hrs after its DML was electroporated. Typically, it leads to the mosaic expression (in green) of the electroporated construct(s) in the DML, the transition zone (in blue) and the nascent primary myotome (in purple). d is a maximum intensity projection of a confocal stack of a somite electroporated with GFP.

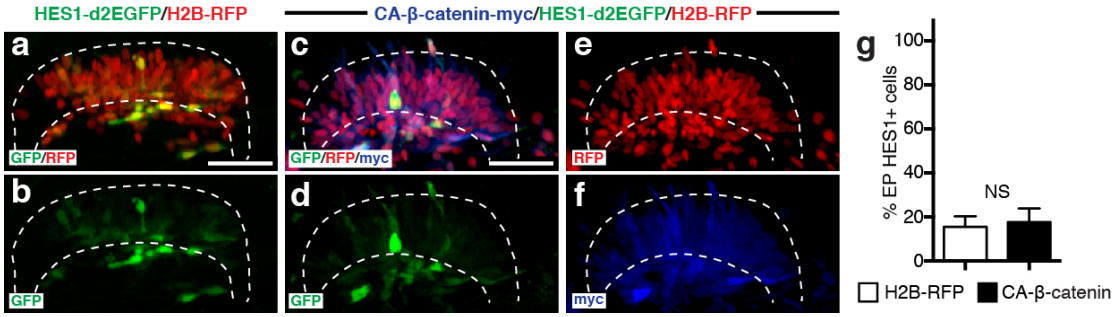


**Supplementary Figure 2: Notch signalling is not regulated by the Wnt/β-catenin pathway.**
a-f, Confocal stacks, 12h after electroporation of (a, f) the NOTCH reporter HES1-d2EGFP in green, H2B-RFP (in red) and (c-f) with a constitutively active form of β-catenin (in blue) . g, Bar charts showing the percentage of HES1-d2EGFP-positive cells in the control (in white) or with CA β-catenin (in black). In each panel are indicated the antigens that were detected by immunostaining. Abbreviation: EP: electroporation. Scale bars: 50 μm.

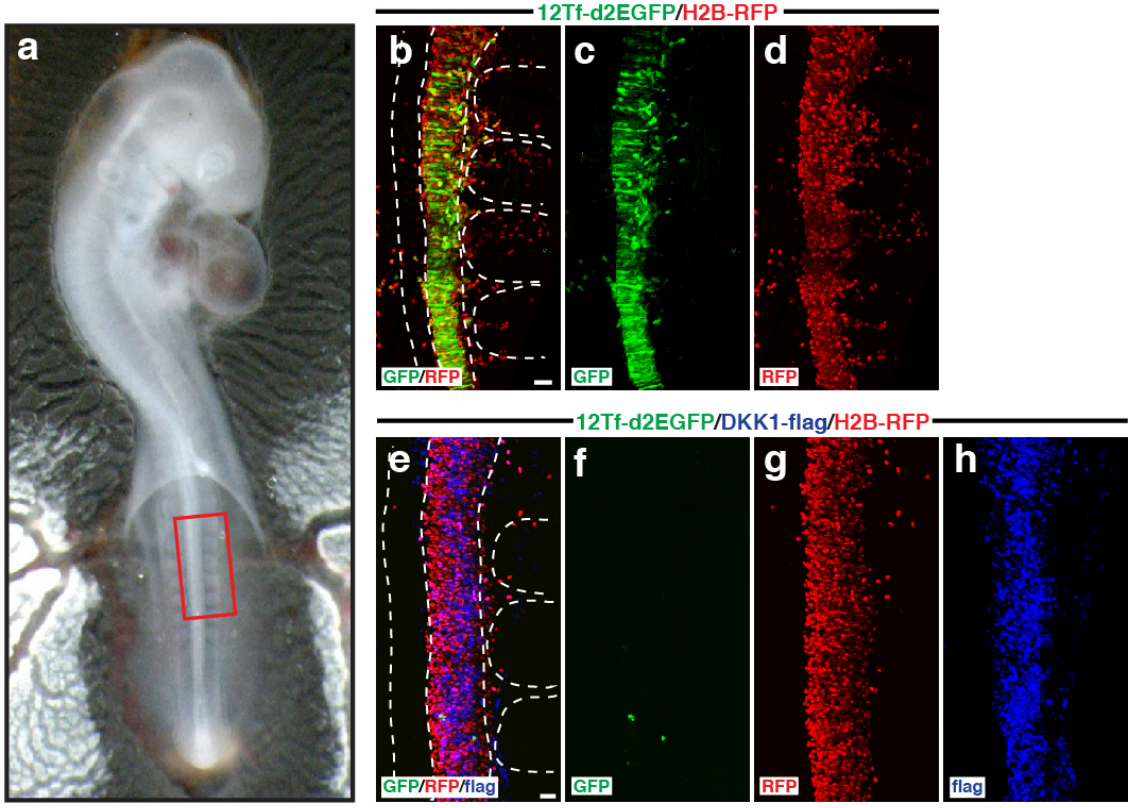


**Supplementary Figure 3: Over-expression of DKK1 in the neural tube abrogates WNT/β-catenin response.**
a, shows a E2.5 chick embryo at the end of the experiment. The box in (a) indicates the region that is analyzed in b-h. b-d, Confocal stacks of a control embryo showing the WNT reporter 12Tf-d2EGFP (b,c, in green). In red (b,d), RFP immunostaining, identifying all electroporated cells. e-h, Neural tube of an embryo in which DKK1 (e,h, in blue) was co-electroporated with the WNT reporter (e,f, in green) and the electroporation marker H2B-RFP (e,g, in red). Dotted lines indicate the borders of the neural tube and somites. In each panel are indicated the antigens that were detected by immunostaining. Scale bars: 50 μm.

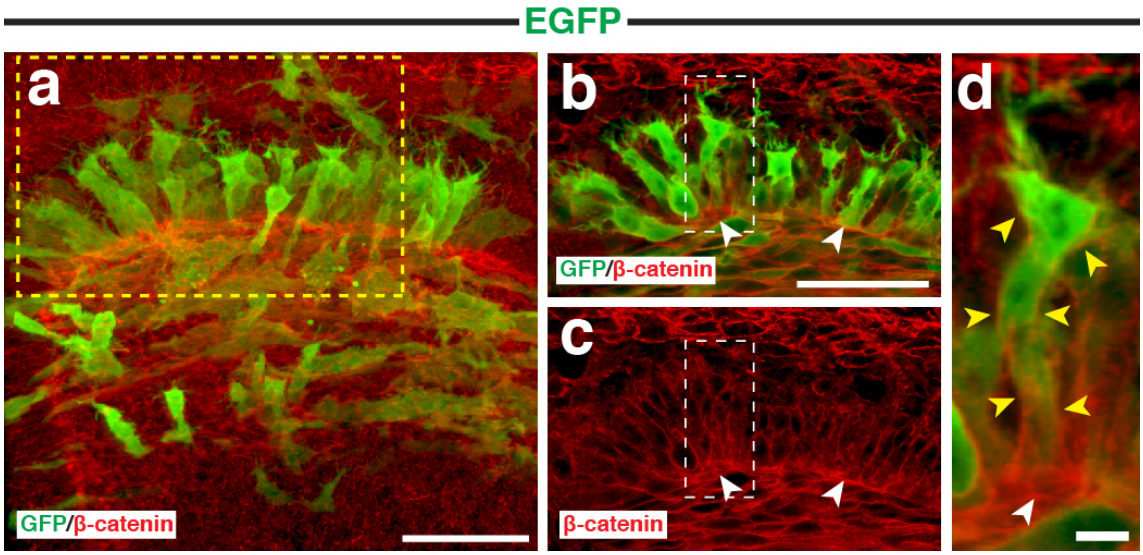


**Supplementary Figure 4: The phosphorylation of tyrosine 489 of β-catenin is necessary for the activation of myogenesis in the DML.**
a-d, Confocal optical slices of somites, 12 hours after electroporation of a DML with CAGGS_GFP and stained for endogenous β-catenin. The box in a indicates the region enlarged in b,c; the boxes in b,c indicate the region enlarged in d. White arrowheads in b-d indicate β-catenin at the AJ, yellow arrowheads in d indicate β-catenin along the plasma membrane. In each panel are indicated the antigens that were detected by immunostaining. Scale bars: a-c, 50 μm; d, 20 μm.

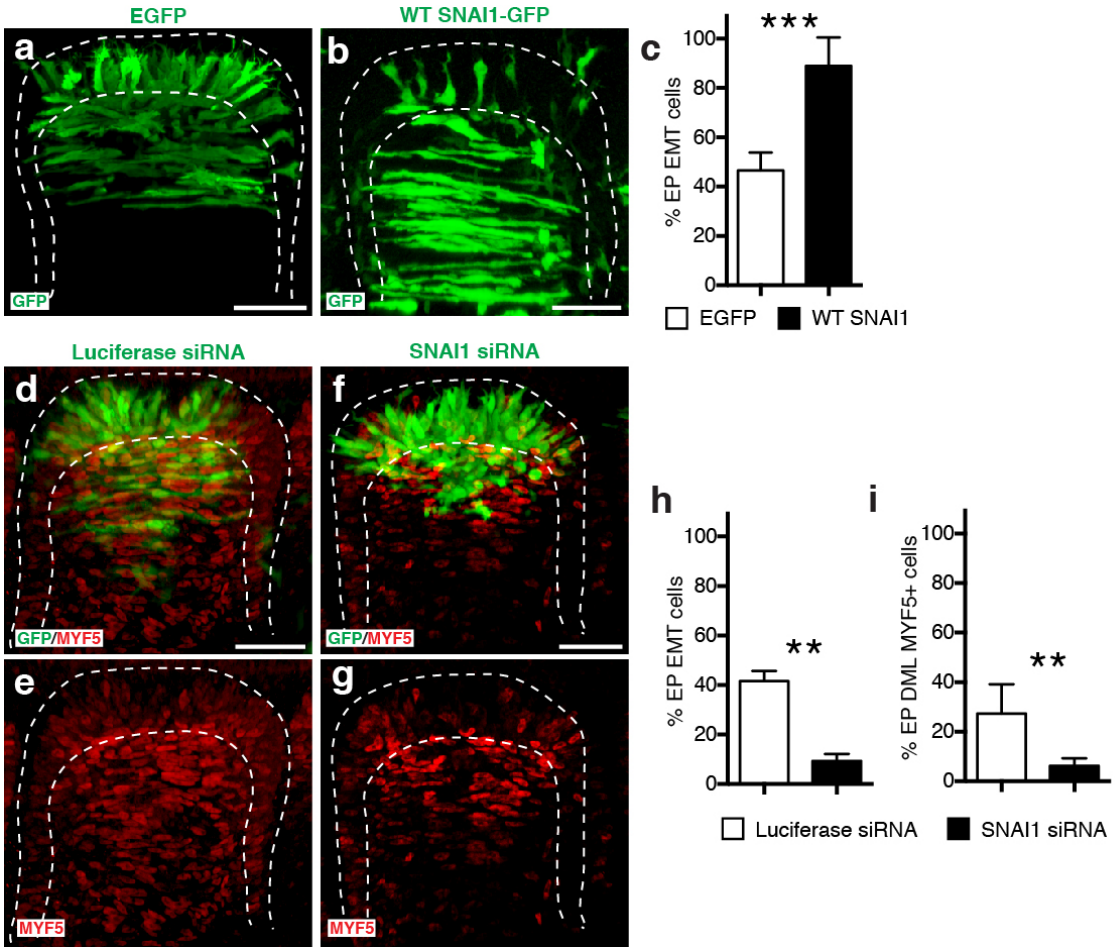


**Supplementary Figure 5: SNAI1 regulates EMT and myogenesis at the DML**
a-b, Confocal stacks of somites, 17 hours after electroporation of EGFP as control (a) or with SNAI1 (b). c, Bar charts showing the % of cells that have entered the primary myotome in the control (in white) of with the SNAI1 (in black). d-g, Confocal stacks of somites, 17 hours after electroporation of a Luciferase-specific siRNA as control (in green, d,e) or a SNAI1-specific siRNA (in green, f,g), immunostained for MYF5 (in red). h,i, Bar charts showing the % of electroporated cells that have entered the primary myotome (h) in the control (in white) of with the siRNA SNAI1 (in black) and the % of electroporated cells that are MYF5-positive (i) in the control (in white) of with the siRNA SNAI1 (in black). In each panel are indicated the antigens that were detected by immunostaining. Abbreviation: EP: electroporation. Scale bars: 50 μm.

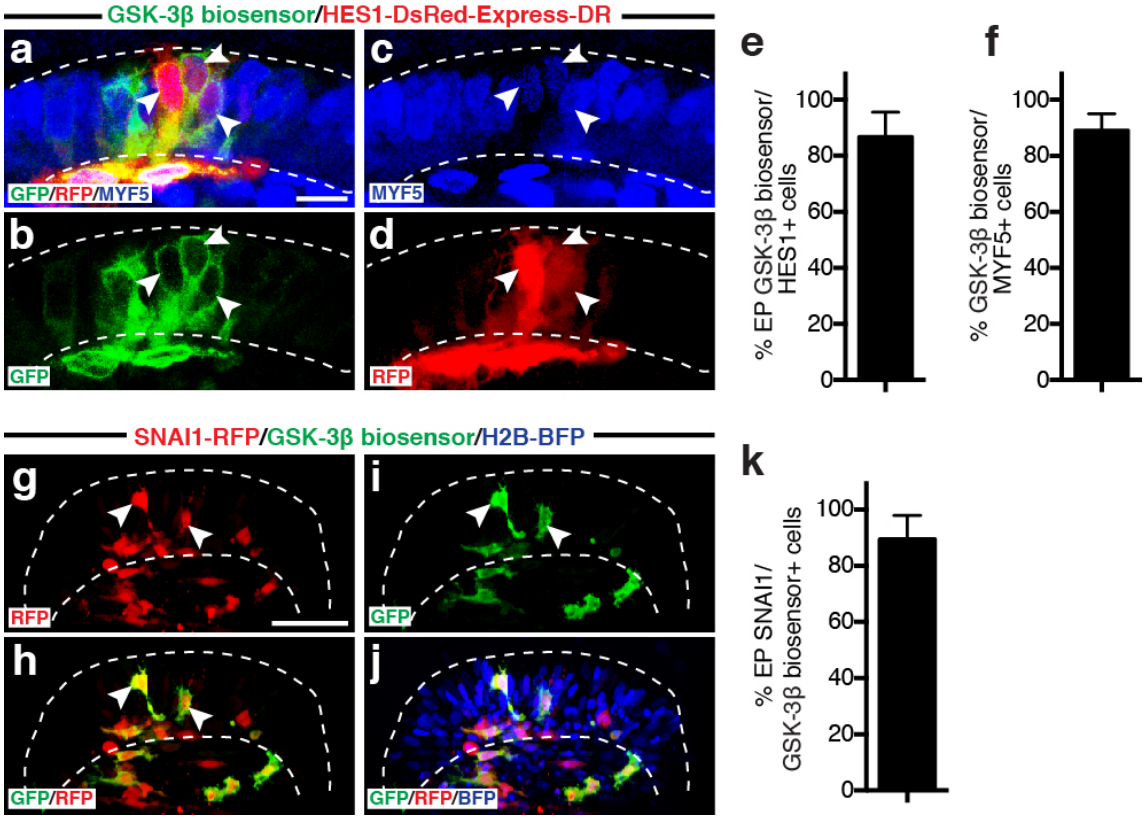


**Supplementary Figure 6: GSK-3β biosensor-positive DML cells stabilize SNAI1, activate NOTCH and myogenesis.**
a-d, Confocal stacks of a somite 6 hours after co-electroporation of the GSK-3β biosensor (green) and the NOTCH reporter (red) and immunostained for MYF5 (blue). e,f, Bar charts showing the % of GSK-3β biosensor-positive cells that activate NOTCH signalling (e) and that are MYF5-positive (f). g-j, Confocal stacks of a somite 6 hours after co-electroporation of a SNAI fused to RFP (in red), the GSK-3β biosensor (in green). In blue (j) the electroporated cells, identified by H2B-BFP. k, Bar charts showing the % of electroporated cells that are GSK-3β biosensor-positive and stabilize SNAI1. In each panel are indicated the antigens that were detected by immunostaining, with the exception of j: native BFP blue fluorescence. Abbreviation: EP: electroporation. Scale bars: a-d: 20 μm; g-j: 50 μm.

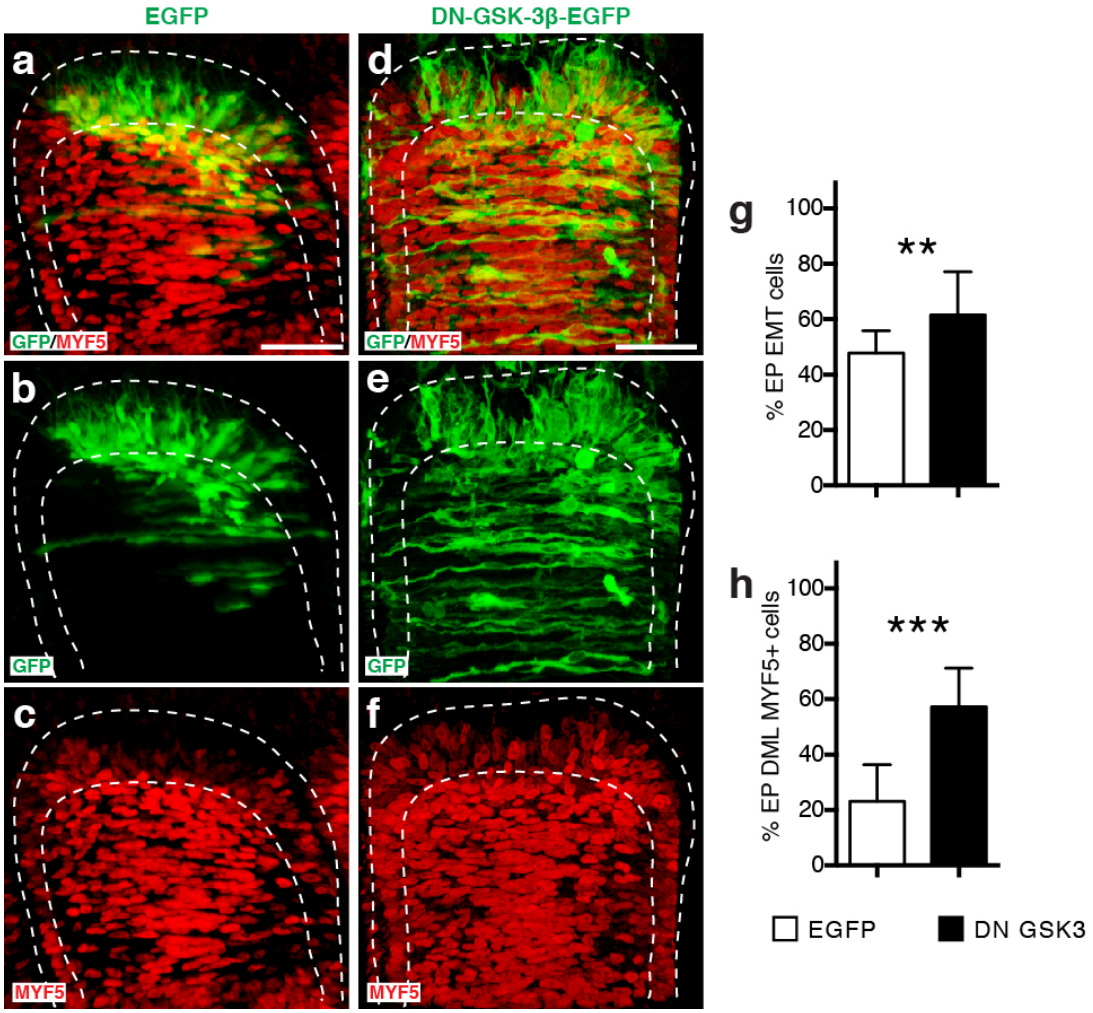


**Supplementary Figure 7: GSK-3β regulates EMT and myogenesis in the DML.**
a-f, Confocal stacks of somites 17 hours after electroporation of EGFP as control (a-c) or DN-GSK-3β (d-f) and immunostained for MYF5 (red). g, Bar charts showing the % of electroporated cells that have entered the primary myotome in the control (in white) of with the DN-GSK-3β (in black). h, Bar charts showing the % of electroporated cells that are MYF5-positive in the control (in white) of with the DN-GSK-3β (in black). In each panel are indicated the antigens that were detected by immunostaining. Abbreviation: EP: electroporation. Scale bars: 50 μm.

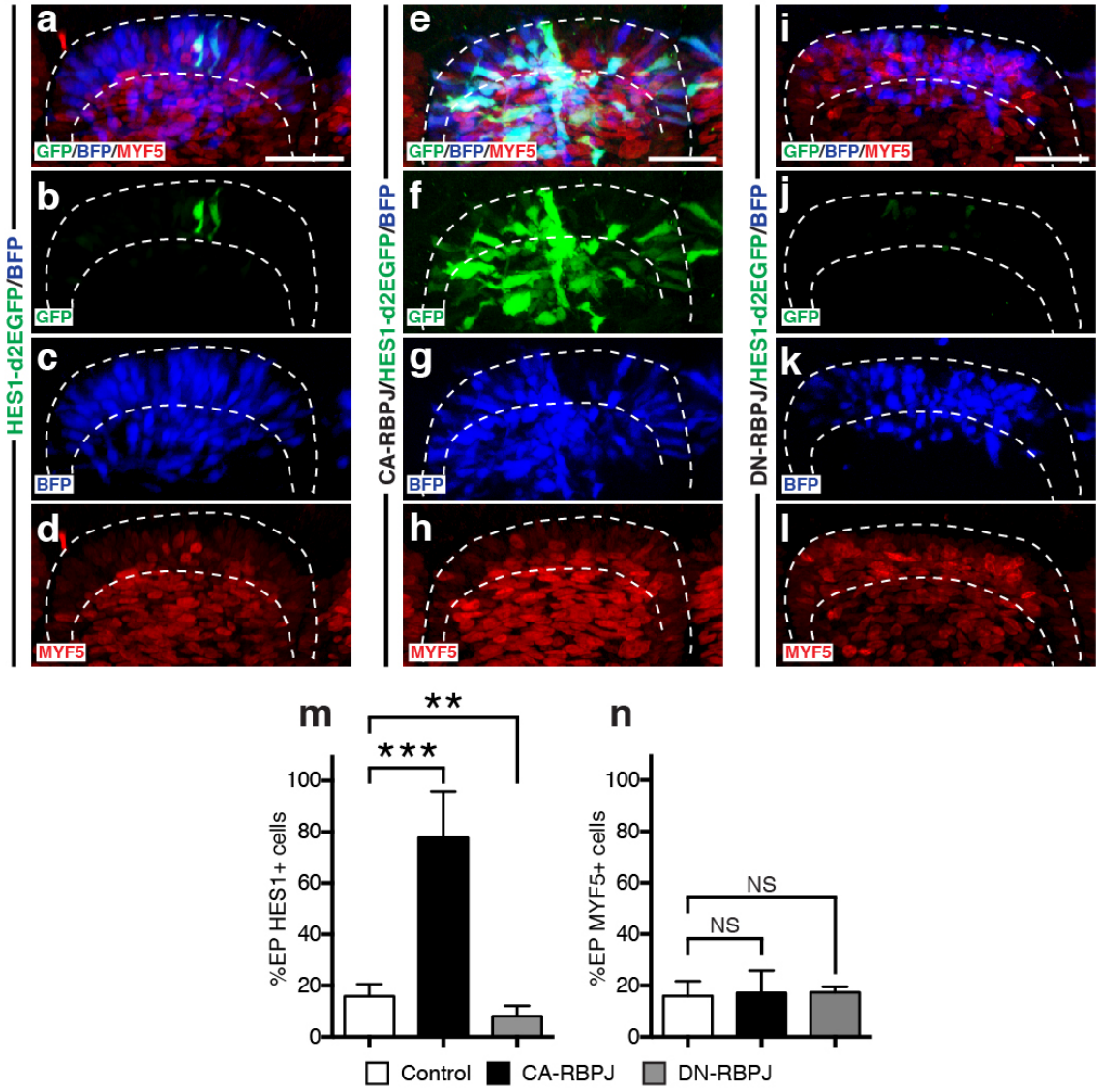


**Supplementary Figure 8: RBPJ does not regulate myogenesis in the DML.**
a-l, Confocal stacks of somites 6 hours after co-electroporation of H2B-BFP (blue) and the NOTCH reporter HES1-d2EGFP (green) alone (a-d) or together with CA-RBPJ (e-h) or DN-RBPJ (i-l) and immunostained for MYF5 (red). m, Bar charts showing the percentage of electroporated cells positive for the NOTCH reporter in the controls (in white), with CA-RBPJ (in black) or DN-RBPJ (in grey). n, Bar charts showing the percentage of electroporated cells positive for MYF5 in the controls (in white), with CA-RBPJ (in black) or DN-RBPJ (in grey). In each panel are indicated the antigens that were detected by immunostaining, with the exception of c,g,k: native BFP blue fluorescence. Abbreviation: EP: electroporation. Scale bars: 50 μm.

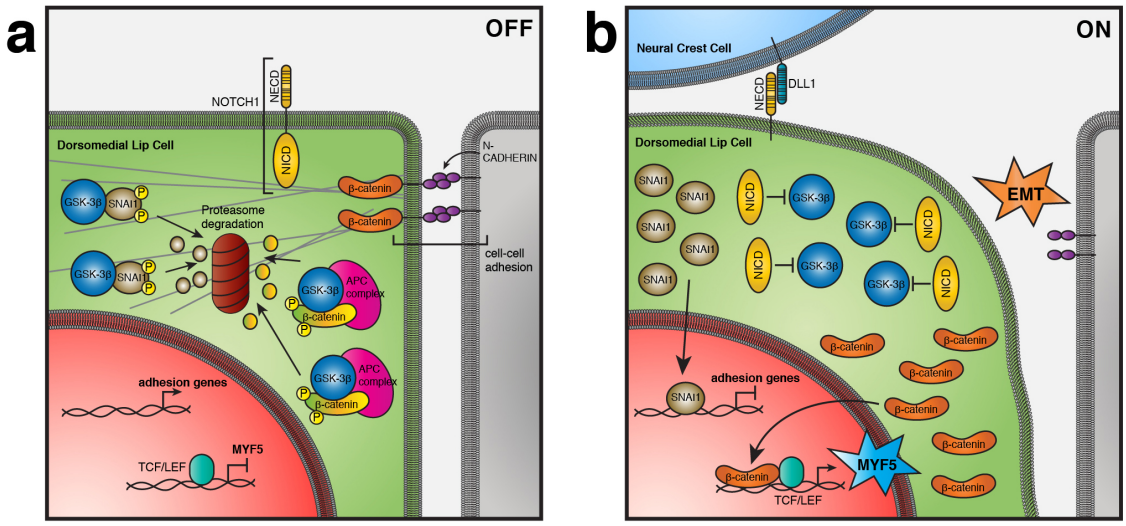


**Supplementary Figure 9: A signalling module in the DML that combines EMT and cell fate change.**
a, In the Off state, DML cells are epithelial. SNAI1 and β-catenin levels in the cytoplasm are maintained at low levels via GSK-3β-mediated degradation, while β-catenin levels are high at the AJ and cell membrane. b, The physical contact with DLL1-positive neural crest cells triggers the cleavage of NOTCH receptor and the release of NICD. NICD represses the activity of GSK-3β. The accumulation of SNAI1 allows its translocation in the nucleus where it activates EMT. This releases β-catenin from the membrane, which accumulates and enters into the nucleus where it activates MYF5 expression.

# 3 A DYNAMIC ANALYSIS OF MUSCLE FUSION IN THE CHICK EMBRYO

# PART B: SUGGESTED DECLARATION FOR THESIS CHAPTER

**Monash University**

**Declaration for Thesis Chapter 3**

**Declaration by candidate**

In the case of Chapter 3, the nature and extent of my contribution to the work was the following:

| Nature of contribution | Extent of contribution (%) |
|---|---|
| Concept, planning of experiments, cloning of constructs, electroporation, immunohistochemistry, imaging, data analysis, statistics, figure preparation, manuscript drafting. | 55% |

The following co-authors contributed to the work.

| Name | Nature of contribution |
|---|---|
| Marie de la Celle | Concept, planning of experiments, data analysis |
| Manuel Pelé | Concept, planning of experiments, data analysis |
| Christophe Marcelle | Concept, planning of experiments, manuscript drafting. |

The undersigned hereby certify that the above declaration correctly reflects the nature and extent of the candidate's and co-authors' contributions to this work*.

| | | |
|---|---|---|
| Candidate's Signature | | Date |
| Main Supervisor's Signature | | Date |

© 2014. Published by The Company of Biologists Ltd | Development (2014) 141, 3605-3611 doi:10.1242/dev.114546

RESEARCH ARTICLE

# A dynamic analysis of muscle fusion in the chick embryo

**Daniel Sieiro-Mosti, Marie De La Celle, Manuel Pelé and Christophe Marcelle***

## ABSTRACT

Skeletal muscle development, growth and regeneration depend upon the ability of muscle cells to fuse into multinucleated fibers. Surprisingly little is known about the cellular events that underlie fusion during amniote development. Here, we have developed novel molecular tools to characterize muscle cell fusion during chick embryo development. We show that all cell populations arising from somites fuse, but each with unique characteristics. Fusion in the trunk is slow and independent of fiber length. By contrast, the addition of nuclei in limb muscles is three times more rapid than in trunk and is tightly associated with fiber growth. A complex interaction takes place in the trunk, where primary myotome cells from the medial somite border rarely fuse to one another, but readily do so with anterior and posterior border cells. Conversely, resident muscle progenitors actively fuse with one another, but poorly with the primary myotome. In summary, this study unveils an unexpected variety of fusion behaviors in distinct embryonic domains that is likely to reflect a tight molecular control of muscle fusion in vertebrates.

**KEY WORDS: Electroporation, Chick embryo, Limb, Muscle fusion, Myotome**

## INTRODUCTION

During embryogenesis and early adult life, skeletal muscle fibers grow through the addition of new myonuclei, which are supplied by resident muscle progenitors during embryogenesis and by satellite cells after birth. Fusion can be extensive: the longest muscle fibers of the human thigh contain tens of thousands of nuclei. Although the number of muscle fibers does not change after birth, the number of nuclei per fiber continues to increase until puberty (Shavlakadze and Grounds, 2006; White et al., 2010). Myoblast fusion is not only crucial for fiber growth, but also for muscle repair in adults after injury or in pathological conditions such as myopathies (Rochlin et al., 2010; Simionescu and Pavlath, 2011; White et al., 2010).

Very little is known about the dynamics of muscle fusion in mammalian development. This is due to the poor accessibility of mouse to observation, the high complexity of the muscle tissue and the lack of specific tools to characterize myoblast fusion in this organism. By contrast, the fruit fly *Drosophila melanogaster* has been a major source of knowledge on muscle fusion, both at the cellular and molecular levels. In fly, two types of myoblasts contribute to muscle formation: muscle founder cells (FCs) and fusion-competent myoblasts (FCMs); FCs function as 'attractants' for the surrounding FCMs. Muscle fusion in the *Drosophila* embryo occurs over a 5.5 h period during late embryogenesis and results in the formation of multinucleated myotubes that can contain as few as two to as many as 24 nuclei per muscle fiber (Bate, 1990). Electron microscopy studies in the fly revealed that muscle fusion follows an ordered set of cellular events: recognition, adhesion, alignment, and membrane union resulting in the formation of a single multinucleated cell. Significantly, this process bears much resemblance at the cellular and ultrastructural levels with observations made *in vitro* using various murine and human muscle cell lines (Doberstein et al., 1997; Knudsen and Horwitz, 1977; Rash and Fambrough, 1973; Wakelam, 1985), suggesting that similar basic mechanisms underlie muscle fusion in vertebrates and invertebrates. In support of this hypothesis, recent studies on the molecular mechanisms regulating fusion in vertebrates (fish and rodents) have shown conservation with *Drosophila* (Horsley et al., 2001, 2003; Moore et al., 2007; Richardson et al., 2008; Srinivas et al., 2007). How much of the cellular and molecular strategies observed in the fly are conserved in vertebrates is unknown.

Amniote muscle derives from two main muscle progenitor populations that emerge sequentially in early embryos: the myocytes of the primary myotome and the resident muscle progenitors. Myocytes are generated in a first stage of myogenesis by cells arising from the four epithelial borders of the dorsal compartment of somites termed the dermomyotome. They organize into a primitive skeletal muscle called the 'primary' myotome (Denetclaw and Ordahl, 2000; Gros et al., 2004; Kahane et al., 2002). Resident muscle progenitors appear during a second stage of muscle morphogenesis. They originate from the central portion of the dermomyotome and invade the primary myotome after an epithelial-to-mesenchyme transition (EMT). In the trunk of the chick embryo, the EMT is observed at 4 days of development, whereas in the trunk of mouse embryos it is observed at embryonic day 10.5 (E10.5). Resident progenitors massively contribute to the formation of all muscles of the body and they later generate the adult muscle stem cells, termed satellite cells (Ben-Yair and Kalcheim, 2005; Delfini et al., 2009; Gros et al., 2005; Kassar-Duchossoy et al., 2005; Manceau et al., 2008; Relaix et al., 2005). In limbs, muscles derive from one wave of progenitors that migrate from the lateral portion of somites into the lateral plate-derived limb mesenchyme, where they differentiate (Chevallier et al., 1976; Christ et al., 1974; Schienda et al., 2006). Whether different muscle progenitor populations fuse and at what rate is unknown.

The amenability of the chick embryo to observation and imaging, combined with the electroporation technique that allows lineage and cell fate analyses, provide a unique environment to characterize the cellular and molecular mechanisms regulating fusion in amniotes. In this study we have analyzed the routes that myocytes and resident muscle progenitors follow to become multinucleated, from the time of the first fusion events to the first days of muscle development. We developed genome-integrated vectors and double electroporation protocols that allow the labeling of cells within the same or distinct populations with different fluorescent proteins. Using these techniques, we determined that the rate and partners of fusion, as well as nuclei occupancy, vary significantly in distinct embryonic domains.

EMBL Australia; Australian Regenerative Medicine Institute (ARMI), Monash University, Building 75, Clayton, VIC 3800, Australia.

*Author for correspondence [redacted]

**Received 19 June 2014; Accepted 30 July 2014**

RESEARCH ARTICLE Development (2014) 141, 3605-3611 doi:10.1242/dev.114546

## RESULTS

### Varying rate and mode of fusion during trunk and limb muscle morphogenesis

We determined whether the muscle populations that have been identified in chick embryos undergo fusion and at what rate.

#### Construction of a vector to evaluate fusion

Muscle fibers within growing muscle masses (in limb or somites) are tightly intertwined and it is practically impossible to distinguish single fibers from end-to-end and count nuclei with classic immunostaining techniques, even with confocal imaging. By contrast, the electroporation technique results in the mosaic expression of transgenes and we hypothesized that this property, together with the use of appropriate fluorescent reporters and confocal imaging, would allow the identification of individual fibers and the evaluation of the number of nuclei per fiber within this complex tissue. We constructed a vector that contains a nuclear RFP variant, NLSmCherry and a membrane EGFP (see Materials and Methods). Cis-sequences from the Tol2 transposable element were inserted on both sides of the fluorochromes, allowing their permanent integration into the genome of host cells. This eliminates the gradual dilution of the transfected episomal plasmid with cell divisions.

#### Fusion of myocytes derived from the DML

We electroporated the medial portion of newly formed epithelial somites in the interlimb region as previously described (Scaal et al., 2004). This leads to the specific labeling of the medial border of the dermomyotome (the DML; Fig. 1A), from which emerge the first myocytes of the primary myotome (Gros et al., 2004; Ordahl et al., 2001). We counted the number of nuclei in electroporated ($GFP^+/RFP^+$) myosin heavy chain (MyHC)-positive cells at successive developmental stages. Twenty-four hours after electroporation (at E3.5), nearly all electroporated myocytes contained only one nucleus. A small proportion of them contained two or three nuclei (Fig. 1B,C,L; mean nuclei number at E3.5, 1.1; see supplementary material Table S1). The number of nuclei per myofiber increased slightly, but significantly, at the next time point (Fig. 1D,E,L; mean nuclei number, 1.3; $P<0.001$). The rate of fusion increased strongly thereafter, and at E5.5 we observed myocytes containing up to seven nuclei (Fig. 1F,G,L; mean nuclei number, 2.7; $P<0.0001$). The mean fusion rate, expressed as the number of hours needed to add one nucleus to the entire population of electroporated myocytes, reached 16.4 h at the peak of fusion, occurring between E4.5 and E5.5 (see Fig. 3A). However, individual myocytes may fuse much more quickly, since some contained up to seven nuclei at E5.5 (whereas one day earlier, most were mononucleated), suggesting a maximal rate of fusion in individual fibers of one nucleus added every 4 h (about six nuclei per 24 h) between E4.5 and E5.5.

We observed that all myocytes, regardless of the number of nuclei, spanned the entire width of somites, indicating that nuclei number is independent of fiber length. To confirm this, we tested the correlation between fiber length and nuclei number and found that, during the time of our experiments, the two variables were not significantly linked (Fig. 3D).

#### Fusion of resident muscle progenitors

We then electroporated the dorsal portion of newly formed somites in the interlimb region as previously described (Gros et al., 2005). This leads to the specific labeling of the population of resident progenitors in the central dermomyotome that enter the primary myotome 36 h after somite formation (Gros et al., 2005). At E4.5,

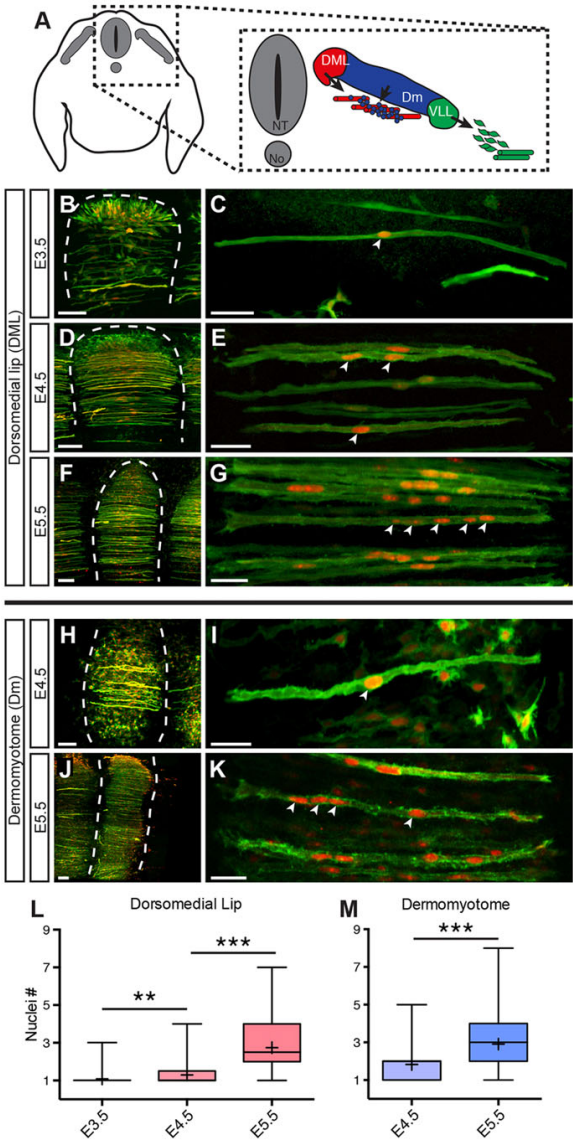


**Fig. 1. Analysis of fusion in the trunk.** (A) Diagram showing a transverse view of the E5 chick embryo. At the interlimb level, the medial border of the dermomyotome (DML), the lateral (VLL), as well as the anterior and posterior borders (not shown) contribute to the formation of the primary myotome, which is composed of myocytes (red), while the central dermomyotome (Dm) generates resident muscle progenitors (blue). At the limb level, muscle progenitors from the VLL (green) migrate into the limb mesenchyme, where they differentiate. NT, neural tube; No, notochord (B-G) Cells from the DML were electroporated at E2.5 and nuclei number per fiber was counted at E3.5 (B,C), E4.5 (D,E) and E5.5 (F,G). (H-K) Cells from the central dermomyotome were electroporated at E2.5 and analyzed at E4.5 (H,I) and E5.5 (J,K). All images are whole-mount confocal stacks of fixed embryos, immunostained for EGFP (green) and RFP (red). Dashed lines delineate somites at the end of experiments. Arrowheads (C,E,G,I,K) indicate cell nuclei within selected fibers. (L,M) Quantification of nuclei number per fiber at the time points in B-G (L) and H-K (M). Whiskers indicate minimal and maximal values; the bottom and top of the box indicate the first and third quartile; the horizontal line indicates the median; and '+' indicates the mean for each set of values. $^{**}P<0.001$; $^{***}P<0.0001$. Scale bars: 100 µm in B,D,F,H,J; 50 µm in C,E,G,I,K.

RESEARCH ARTICLE Development (2014) 141, 3605-3611 doi:10.1242/dev.114546

48 h after somite formation, 90% of the cells derived from the central dermomyotome are proliferating Pax7-positive resident progenitors (Gros et al., 2005), which display a mesenchyme-like morphology. However, a small proportion of electroporated cells spanned the entire width of somites. These were morphologically similar to the myocytes derived from the DML, expressed the terminal differentiation marker MyHC (not shown; Gros et al., 2005) and contained an average of 1.8 nuclei (Fig. 1H,I,M; supplementary material Table S1). At E5.5, the number of nuclei significantly increased and myofibers containing up to eight nuclei were observed (Fig. 1J,K,M; mean nuclei number, 2.9; $P<0.0001$). The mean rate of fusion of muscle progenitors from E4.5 to E5.5 is therefore one nucleus every 22 h, with a maximal rate very close to that observed in the DML-derived population (one nucleus per 4.5 h; Fig. 3B).

We also observed that resident progenitors in the trunk somites first elongate until they reach the somite borders, and then accumulate nuclei with no significant fiber growth. Thus, similar to DML-derived myocytes, during the time frame of our analysis there is no significant link between fiber length and nuclei number in myocytes derived from the population of trunk-resident progenitors (Fig. 3D).

### Fusion of limb muscle progenitors

In order to study muscle fusion in the limb, we electroporated the lateral portion of newly formed somites in the forelimb region (somites 16-21). This leads to the specific labeling of the lateral border of the dermomyotome (the VLL) from which all limb muscle progenitors emanate (Fig. 1A). We analyzed electroporated embryos at E4, E4.5, E5, E5.5 and E6, focusing our study on the dorsal muscle masses of the limb. We counted the number of nuclei in MyHC/GFP-positive cells. At E4, very little MyHC staining was observed (Fig. 2A). Of those cells, nearly all were mononucleated (89%; Fig. 2A-C,P; mean nuclei number, 1.1; supplementary material Table S1). Between E4 and E4.5, the number of nuclei did not change significantly (Fig. 2D-F,P; mean nuclei number, 1.2). From E4.5 onward (Fig. 2G-O), the number of nuclei per MyHC$^{+}$ myofiber dramatically increased, and fibers with up to 16 nuclei were observed at E5.5 (arrowheads in Fig. 2L), which is only 1 day after the initiation of fusion at E4.5. The mean number of nuclei also sharply increased during this period, from 1.2 (E4.5) to 4.3 (E5) to 5.6 (E5.5) and finally 7.2 (E6) (Fig. 3C; supplementary material Table S1). The sharpest increase in the mean fusion rate was observed between E4.5 and E5.5, when one nucleus was added every 5 h. Again, in individual myogenic cells, this rate may be much faster, with a maximum rate of around one nucleus added every 1.5 h (15 nuclei added in 24 h). We did not quantify the fusion rate of the ventral muscle masses of the forelimb, but the overall fusion pattern was similar to that of the dorsal ventral mass (supplementary material Fig. S1).

In sharp contrast to the situation observed in the trunk, it was apparent that, as the embryos developed, limb muscle fibers

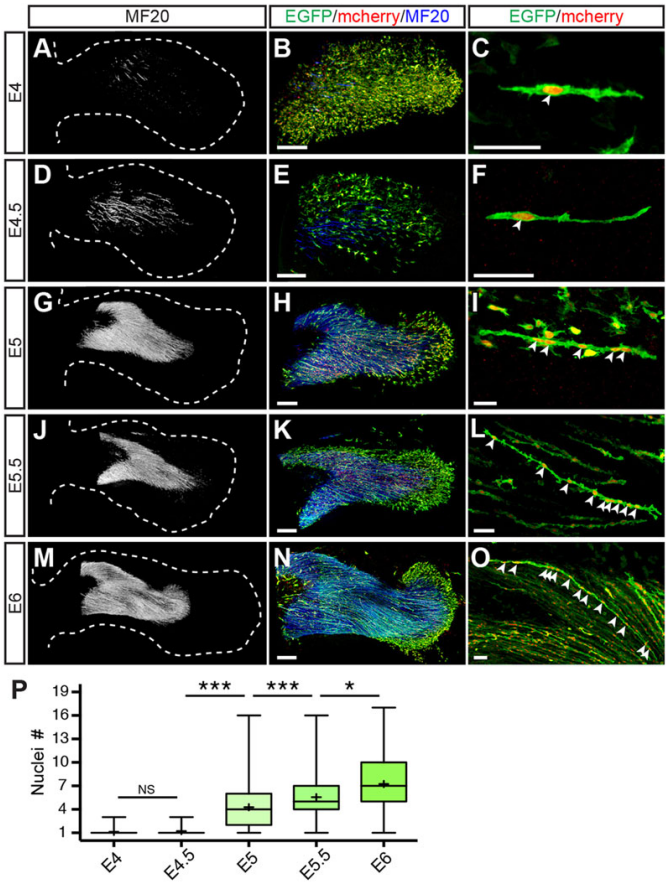


**Fig. 2. Analysis of fusion in the dorsal muscle masses of chick forelimbs.** (A-O) Cells from the VLL at forelimb level (somites 16-21) were electroporated at E2.5. The nuclei count per fiber was performed at E4 (A-C), E4.5 (D-F), E5 (G-I), E5.5 (J-L) and E6 (M-O). All images are whole-mount confocal stacks of fixed embryos. (A,D,G,J,M) Forelimbs (delineated by dashed lines) are immunostained for MyHC (white) to show the muscle masses; in all other images, blue is MyHC, green is EGFP and red is mCherry. Arrowheads (C,F,I,L,O) indicate cell nuclei within selected fibers. (P) Quantification of nuclei number per fiber at the time points in A-O (see Fig. 1 legend). *$P<0.05$; ***$P<0.0001$. Scale bars: 200 µm in B, E,H,K,N; 50 µm in C,F,I,L,O.

RESEARCH ARTICLE Development (2014) 141, 3605-3611 doi:10.1242/dev.114546

became longer and contained an increasing number of nuclei (Fig. 2C,F,I,L,O). To confirm this, we tested the correlation between fiber length and nuclei number and found that the addition of nuclei was very significantly linked to fiber growth, and each additional nucleus was accompanied by an increase in fiber length of ~40 µm (Fig. 3E).

### A complex matchmaking underlies trunk muscle fusion

Since myocytes of the primary myotome and resident progenitors initiate fusion after E4, i.e. immediately after the EMT of the dermomyotome is initiated (Gros et al., 2005), we hypothesized that both populations might fuse to one another. To address this, we devised protocols that allow the labeling of cells within a population with different fluorescent proteins. If these populations fused, both fluorescent proteins would be observed within one multinucleated fiber.

#### Construction of vectors to label a single population with two fluorochromes

It was reported that the efficiency of electroporation may be cell cycle-dependent (Brunner et al., 2002; Goldstein et al., 1989). Epithelial cells in the chick DML cycle asynchronously, with an estimated cell cycle length of 9-11 h (Primmett et al., 1988; Venters et al., 2008). We hypothesized that by electroporating the DML with two plasmids coding for GFP or for mCherry (a variant of RFP) 5 h apart, we would transfect distinct populations of cells, if indeed electroporation were cell cycle dependent. We found that a reasonable percentage (41.4%) of epithelial cells in the DML expressed only one fluorochrome when electroporated 5 h apart with mCherry or GFP, although a majority expressed both (58.6%; Fig. 4A,C; supplementary material Table S2).

Since this technique was not suitable for our purpose, we designed a new set of vectors that, combined with double electroporation, would result in the exclusive expression of either cytoplasmic EGFP or mCherry, but not both (see Materials and Methods; supplementary material Fig. S2A-D). We verified the efficiency of this approach by electroporating the DML consecutively with the two sets of vectors. Ten hours later, mononucleated myocytes were examined for GFP or mCherry expression and only 3.4% expressed both fluorochromes (Fig. 4A,D; supplementary material Table S2). This number thus represents the 'leakiness' of the labeling system that we devised and it was used to modulate the percentage of fusion observed in the following experiments [mean percentage (adjusted) in supplementary material Table S2].

#### Primary myocytes and resident progenitor fusion

Using these plasmids, we first electroporated the DML. Three days later, we analyzed the color of bi-nucleated myocytes (i.e. resulting from one fusion event). We observed that 49.7% of bi-nucleated myocytes expressed GFP, while 42.2% were mCherry positive and 8.2% expressed both (Fig. 4A,E,F; supplementary material Table S2). This indicates that the vast majority of cells generated at the DML do not fuse with one another. The small increase in yellow cells is not significantly different to the control, although it might indicate that a small percentage of DML cells nevertheless fuse.

We then electroporated this combination of plasmids into the dorsal dermomyotome, from which resident progenitors arise. Three days later 36.7%, 30.2% and 33.1% of bi-nucleated myocytes were green, red and yellow, respectively (Fig. 4A,G,H; supplementary material Table S2). This is significantly different to the control values and indicates that resident progenitors readily fuse to one another.

#### Primary myocytes do not fuse to resident progenitors

Using the same combination of vectors as above, we labeled the DML with GFP and the dorsal dermomyotome with mCherry. Three days later, we analyzed bi-nucleated cells in regions of the myotome, where $GFP^+$ cells were adjacent to $mCherry^+$ cells. Surprisingly, we observed that 48%, 42.7% and 9.3% expressed GFP, mCherry and both, respectively (Fig. 4A,I,J; supplementary material Table S2). The proportion of yellow cells is not significantly different to the control, indicating that DML myocytes do not fuse to progenitors. The slight increase in fusion might, however, indicate that they marginally fuse. $GFP^+$ and $mCherry^+$ cells were mostly intimately intertwined (Fig. 4J), suggesting that the low numbers of bi-labeled cells observed are unlikely to be due to a lack of proximity of the analyzed cells. This puzzling result prompted us to identify the cells that fuse with the DML-derived cells.

The anterior and posterior borders of the dermomyotome also generate myocytes, which intermingle with DML-derived cells (Gros et al., 2004). We determined whether these two cell populations fuse to DML-derived cells. We labeled the DML with GFP and either the anterior or the posterior border with mCherry. Importantly, the exclusive labeling vector system we used ensures that cells at the medio-anterior or medio-posterior corner of the dermomyotome are labeled with only one fluorescent protein in the event that they are electroporated twice in the procedure. When the

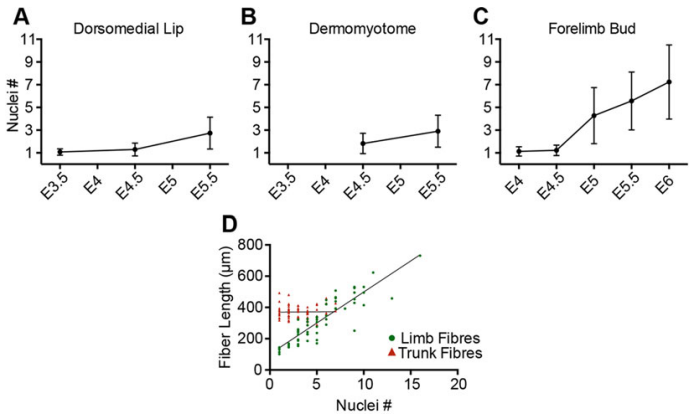


**Fig. 3. Fusion rates of muscle cells and ratio of fiber length to nuclei number for different regions.** (A-C) Fusion rates of muscle cells derived from the DML (A) or from the central dermomyotome (B) and in the forelimb muscle masses (C) were determined in chick embryos electroporated at E2.5 and tested at the indicated incubation times. Each point represents the mean nuclei per fiber in all electroporated cells; bars represent s.d. (D) Ratio of fiber length to nuclei number in the trunk (red) and limb (green). The best-fitting lines for the observed data indicate that in the trunk (D) there is no significant correlation between fiber length and nuclei number [Pearson's product-moment correlation $r(77)=0.19$, $P=0.09$]. By contrast, there is a strong correlation between fiber length and nuclei number in the limb [$r(58)=0.89$, $P<2.2^{-16}$; $y=39.7x+102.1$ (equation of the line of best fit)].

RESEARCH ARTICLE Development (2014) 141, 3605-3611 doi:10.1242/dev.114546

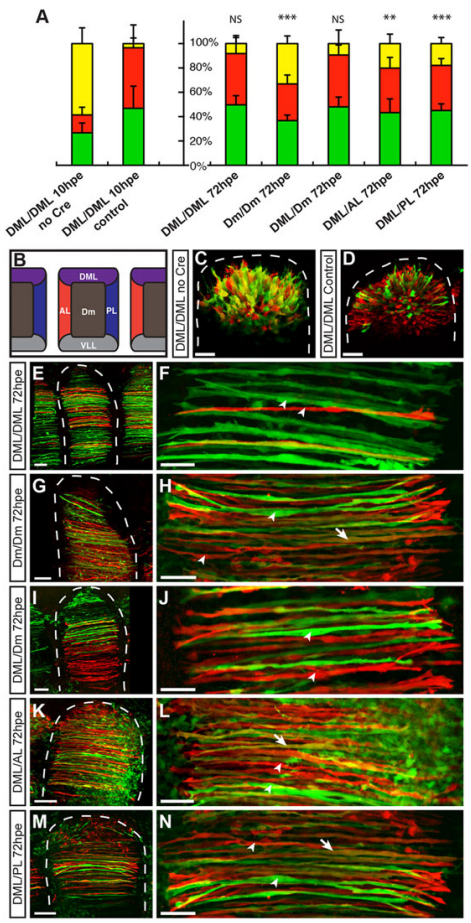


**Fig. 4. Primary myotome cells do not fuse to resident muscle progenitors.** (A) The percentage of fusion within cell populations electroporated with EGFP and mCherry at E2.5 and tested 10 (C,D) or 72 (E-N) hours post electroporation (hpe). Error bars indicate s.d. ***P*<0.001; ****P*<0.0001; NS, not significant. (B) Diagram showing a dorsal view of trunk somites in an E2.5 chick embryo. The regions of the somite that were electroporated in C-N are indicated: central dermomyotome (Dm) and medial (DML), lateral (VLL), anterior (AL) and posterior (PL) borders. (C,D) DML cells were double electroporated with EGFP-expressing and mCherry-expressing vectors 4-5 h apart (C), or with Cre-mediated EGFP-excluding and mCherry-excluding vectors (see Material and Methods), the latter resulting in a minor proportion of yellow cells (containing both fluorophores) 10 h post electroporation, i.e. before fusion is initiated (A, second bar). (E-N) Bi-nucleated fibers expressing EGFP (green), mCherry (red) or both (yellow) were counted 72 h post electroporation (see A). All images are whole-mount confocal stacks of fixed embryos immunostained for EGFP and mCherry. Arrowheads (F,H,J,L,N) indicate selected single-labeled fibers; arrows (H,L,N) indicate selected double-labeled fibers. Dashed lines delineate somites at the end of experiments. Scale bars: 100 µm in E,G,I, K,M; 50 µm in C,D,F,H,J,L,N.

DML was electroporated together with the anterior border of the dermomyotome, we observed after 72 h of incubation that 43.3%, 36.6% and 20.1% expressed GFP, mCherry and both, respectively. Likewise, when the DML was electroporated together with the posterior border, we observed after 72 h of incubation that 45.1%, 37.1% and 17.8% expressed GFP, mCherry and both, respectively. In each case, the percentage of yellow bi-nucleated myocytes was significantly higher than in the controls. These data indicate that DML cells fuse equally to cells emanating from the anterior or posterior borders of the dermomyotome.

## DISCUSSION

Altogether, our findings demonstrate that electroporation and confocal imaging allow a precise quantification of nuclei number in muscle fibers *in vivo* despite the increasing complexity of muscle masses as the embryo grows. Since electroporation targets seemingly random cells within somites, their progeny are evenly distributed within muscle masses, such that this allows a representative sampling of the entire population with no positional bias. Although this might not be crucial in somites, where fibers containing one or more nuclei are evenly distributed as fusion proceeds, it is important in limbs, where fibers containing the most nuclei are preferentially localized in the center of the muscle masses. Our analysis showed that the three muscle cell populations that we tested fuse. Although this was expected for resident progenitors in the trunk and the limb, which constitute the main reservoir of all muscles, it was however unknown whether myocytes of the primary myotome fuse as well. We had previously shown that myocytes become progressively diluted by fibers derived from the resident progenitor population, and that they constitute a negligible portion of the fetal muscle masses (Gros et al., 2005). Our current data indicate that, despite this, the primary myocytes generate bona fide multinucleated fibers that participate to the formation of embryonic muscles.

Our results show that, during early embryogenesis, muscle fusion in limb and trunk display distinct features. In trunk muscles, nuclei fused while the length of myofibers hardly changed. Since the diameter of myofibers was not significantly modified during the time frame of the experiment (Fig. 1), this implies that the volume of cytoplasm supported by each nucleus (the nuclear domain) decreased during that period. This differs from the widely accepted ‘karyoplasmic ratio hypothesis’, which postulates that cell and nuclear volumes are linked (Bruusgaard et al., 2003; Cavalier-Smith, 1978). By contrast, each additional nucleus in limb myofibers was accompanied by an increase in fiber length, indicating that, in limb muscles, the nuclear domain was constant during the period of the experiment.

A second feature that distinguishes trunk and limb muscle fusion is that the fusion rate is nearly identical in both populations of trunk progenitors, regardless of their origin, fate or cellular characteristics (e.g. resident progenitors are proliferative, display stem cell-like attributes, contribute to a variety of hypaxial and epaxial muscles; DML-derived primary myocytes readily differentiate, are postmitotic and contribute exclusively to epaxial muscle masses). By contrast, muscle fusion in early limb differentiation was much faster than in the trunk, with a maximal rate of one nucleus added every 1.5 h. This suggests that, at least during the time frame of this study, the fusion rate is defined at the level of the body region. The maximal rate of muscle fusion that we observed in the limb (1.5 nuclei/h) is remarkably similar to that observed in isolated fibers from mouse extensor digitorum longus muscle during a period of intense growth in the first two postnatal weeks (1.8 nuclei/h; White et al., 2010), and this number might in fact correspond to the maximal rate of muscle fusion in amniotes.

Following the characterization of chick myoblast fusion, we had aimed to determine whether some of the stereotyped patterns of fusion uncovered in flies are conserved in amniotes. In particular, it was interesting to determine whether myoblasts of the primary myotome act similarly to *Drosophila* myoblasts, the defining

RESEARCH ARTICLE Development (2014) 141, 3605-3611 doi:10.1242/dev.114546

characteristic of which is their complete inability to fuse with their own type. Our data suggest that this is not the case in chick, since resident progenitors mainly fuse with each other, and cells of the primary myotome fuse among themselves, but following a complex interaction with the neighboring lips. It is however possible that, within each population that fuses, cells with founder-like and fusion competence-like characteristics co-exist.

It was previously shown that the morphogenetic processes leading to the emergence of the resident progenitor and the primary myotome cell populations are clearly distinct (Gros et al., 2004, 2005). The gene networks regulating their differentiation are also different, since primary myotome formation is independent of Pax3 and Pax7 function, whereas resident muscle progenitors are absent when Pax3 and Pax7 function is abrogated (Kassar-Duchossoy et al., 2005; Relaix et al., 2005). That they do not readily fuse to each other further distinguishes these two cell populations.

In conclusion, this study of muscle fusion in the chicken embryo has uncovered the dynamics that orchestrate early myoblast fusion in amniotes. It will serve as a conceptual framework upon which future studies can rely to uncover the molecular mechanisms regulating this fascinating process. How this is controlled at the molecular level is unknown, but it is likely that a tightly knit network of inhibitors and activators of muscle fusion underlies the complex cell behaviors that we have revealed in this study.

## MATERIALS AND METHODS

### *In ovo* electroporation

Fertilized chick eggs were incubated at 38°C in a humidified incubator. Embryos were staged according to days of incubation. Newly formed somites were electroporated as previously described (Gros et al., 2004, 2005; Rios et al., 2011). Briefly, interlimb somites were electroporated so that only the borders of the dermomyotome (medial, lateral, anterior and posterior) or the central region of the dermomyotome would be electroporated. To follow limb muscle progenitor fusion, the lateral border of somites in the wing region (somites 16-21) was electroporated. One day after electroporation, the embryos were examined under UV light and those that were not adequately electroporated were discarded. We and others have shown previously that the electroporation process itself is harmless to the normal differentiation of electroporated cells. Electroporated embryos were analyzed after the indicated incubation times by fixing and processing for whole-mount immunostaining against GFP and RFP.

### Plasmids used for electroporation

#### Construction of vectors to count the number of nuclei per fiber

To easily count the number of nuclei of electroporated cells, we constructed a plasmid (Tol2-CAGGS-NLSmCherry-IRES-mEGFP) that leads to the co-expression of membrane GFP and nuclear mCherry fluorochromes under the control of the ubiquitous CAGGS promoter (supplementary material Fig. S2A). This plasmid was constructed by a triple Gateway reaction using the following donor plasmids: (1) p5E-CAGGS, containing the strong, ubiquitous CAGGS promoter (CMV/chick β-actin promoter/enhancer; kindly provided by Dr James Godwin, ARMI, Australia); (2) NLSmCherry, containing the monomeric form of Cherry linked to a nuclear localization signal; and (3) IRES-mEGFP, containing EGFP with a C-terminal fusion of 21 amino acids of human Harvey Ras (HRAS) that encodes a prenylation signal that directs the GFP protein to the membrane. The destination plasmid was pDEST-Tol2pA2 (kindly provided by Dr Thomas Hall, ARMI, Australia). Tol2 integration sites at both ends of the constructs allow long-term integration into the genome of transfected cells in the presence of exogenously provided transposase protein.

Staining with DAPI and immunostaining for RFP showed that the nuclear mCherry marker was present in all nuclei within fluorescent multinucleated fibers. Since only a portion of cells within the muscle progenitor population are electroporated, this indicates that the nuclear mCherry marker is readily transferred to all nuclei within multi-nucleated fibers, regardless of whether they originated from electroporated cells. The number of nuclei in fibers at specific developmental stages was also calculated as follows: mean=$\Sigma x/n$, i.e. the sum of the number of nuclei in all fibers analyzed at that stage ($x$) divided by the number of fibers ($n$).

#### Vectors to determine whether progenitors within cell subpopulations fuse

To determine whether cells from the same somitic population can fuse to one another, we constructed three plasmids that were designed for two sequential electroporations 3-4 h apart.

In the first electroporation, two plasmids were co-electroporated (see supplementary material Fig. S2B). One contains (cytoplasmic) EGFP driven by the CAGGS promoter. However, the GFP is silent, due to a loxP-flanked (floxed) polyadenylation (polyA) site upstream of its initiation methionine. The second plasmid has a floxed *Cre* downstream of the CAGGS promoter. When the two plasmids are present in the same cell, the Cre removes the polyA site, GFP is translated and the cell is green under UV light. The Cre protein also excises itself, such that Cre protein is active only during a short period of time. If the two plasmids are not present in the same cell, GFP is silent.

Three to four hours later, a plasmid containing a floxed mCherry (i.e. a cytoplasmic monomeric Cherry variant of RFP) driven by CAGGS is electroporated into the same cell population (supplementary material Fig. S2C). Cells transfected with only this construct are red. If a cell already contains the plasmids electroporated in the first round (or the Cre plasmid only), the Cre inactivates the mCherry. In each round of electroporation, an additional plasmid coding for the transposase is added to allow Tol2-mediated genomic integration. We verified the efficiency of this approach and found that only 3.4% of (mononucleated) cells sequentially electroporated with these plasmids express both fluorochromes. This number thus represents the 'leakiness' of the labeling system that we devised. To estimate the true percentage of fusion, we therefore subtracted 3.4 from the percentage of $GFP^+/RFP^+$ and added half of this (i.e. 1.7) to each of the percentages of $GFP^+$ and $RFP^+$ that we obtained (these are referred to as 'adjusted' percentages of fusion; supplementary material Table S2).

### Immunohistochemistry and confocal analysis

Embryos of the desired stages were dissected in PBS and fixed in 4% formaldehyde for 1 h.

For immunohistochemistry on whole-mount embryos, the following antibodies were used: chicken polyclonal antibody against GFP (1:1000; Abcam, AB13970); mouse monoclonal antibody against the embryonic form of myosin heavy chain MF20 (1:10; Developmental Studies Hybridoma Bank); and rabbit polyclonal antibody against RFP (1:1000; Abcam, AB62341). Species/isotype-specific secondary antibodies coupled with Alexa Fluor 488, 555 or 647 (Interchim) were used at 1:500 dilution.

Whole-mount embryos were examined using a Leica SP5 confocal microscope. Images were analyzed using Imaris (Bitplane) and ImageJ (NIH). All quantifications were performed by evaluating each fiber within optical sections of three-dimensional confocal stacks.

### Statistics

Statistical analyses were performed using GraphPad Prism software. Each quantification is the result of analyses on a minimum of six embryos. To test whether the numbers of nuclei per fiber in each embryo of a given experimental series were statistically different, an analysis of variance (ANOVA) non-parametric testing was applied. We tested embryos against each other in the study of fusion during normal embryonic development. This analysis showed that there was no significant difference among embryos within an experimental series ($P>0.05$; not shown). This demonstrates that the results we obtained are highly reproducible despite the variability in electroporation efficiency that is inherent to the technique. It also indicates that each fiber of a given experimental series can be considered as a separate measurement for statistical purposes.

Mann–Whitney non-parametric two-tail testing was applied to populations of fibers to determine $P$-values. Numbers of examined fibers for each time point are indicated in supplementary material Tables S1

RESEARCH ARTICLE Development (2014) 141, 3605-3611 doi:10.1242/dev.114546

and S2. To evaluate the dependence of fiber length on nuclei number (Fig. 3D), the Pearson product-moment correlation coefficient was calculated using R software (http://www.r-project.org/) to determine the linear correlation ($r$) between the two variables: a value at or near 0 indicates that there is no association, whereas a value between 0.5 (−0.5) and 1 (or −1) indicates an increasingly strong positive (or negative) correlation; the $P$-value indicates the strength of this association. In Fig. 3D, $r$ and the $P$-value were calculated separately for DML and dorsal dermomyotome; since they were nearly identical, they were averaged to determine the combined $r$ and $P$-value in the trunk.

**Acknowledgements**
We thank Monash Micro Imaging (MMI) for imaging support; and Drs C. Hirst, N. Rosenthal and P. Currie for critical reading of the manuscript.

**Competing interests**
The authors declare no competing financial interests.

**Author contributions**
D.S.-M., M.D.L.C., M.P. and C.M. planned the experiments. D.S.-M., M.D.L.C and M.P. performed and analyzed the experiments. D.S.-M. and C.M. wrote the manuscript.

**Funding**
This work was supported by a grant from the National Health and Medical Research Council (NHMRC) of Australia, and by the EU 6th Framework Programme Network of Excellence MYORES to C.M.

**Supplementary material**
Supplementary material available online at
http://dev.biologists.org/lookup/suppl/doi:10.1242/dev.114546/-/DC1

**References**

**Bate, M.** (1990). The embryonic development of larval muscles in Drosophila. *Development* **110**, 791-804.
**Ben-Yair, R. and Kalcheim, C.** (2005). Lineage analysis of the avian dermomyotome sheet reveals the existence of single cells with both dermal and muscle progenitor fates. *Development* **132**, 689-701.
**Brunner, S., Furtbauer, E., Sauer, T., Kursa, M. and Wagner, E.** (2002). Overcoming the nuclear barrier: cell cycle independent nonviral gene transfer with linear polyethylenimine or electroporation. *Mol. Ther.* **5**, 80-86.
**Bruusgaard, J. C., Liestøl, K. and Gundersen, K.** (2003). Number and spatial distribution of nuclei in the muscle fibers of normal mice studied in vivo. *J. Physiol.* **551**, 467-478.
**Cavalier-Smith, T.** (1978). Nuclear volume control by nucleoskeletal DNA, selection for cell volume and cell growth rate, and the solution of the DNA C-value paradox. *J. Cell Biol.* **34**, 247-278.
**Chevallier, A., Kieny, M. and Mauger, A.** (1976). The origin of the wing musculature of birds. *C R. Acad. Sci. Hebd. Seances Acad. Sci. D* **282**, 309-311.
**Christ, B., Jacob, H. J. and Jacob, M.** (1974). Über den Ursprung der Flügelmuskulatur. Experimentelle Untersuchungen mit Wachtel- und Hühnerembryonen. *Experientia* **30**, 1446-1449.
**Delfini, M.-C., De La Celle, M., Gros, J., Serralbo, O., Marics, I., Seux, M., Scaal, M. and Marcelle, C.** (2009). The timing of emergence of muscle progenitors is controlled by an FGF/ERK/SNAIL1 pathway. *Dev. Biol.* **333**, 229-237.
**Denetclaw, W. F. and Ordahl, C. P.** (2000). The growth of the dermomyotome and formation of early myotome lineages in thoracolumbar somites of chicken embryos. *Development* **127**, 893-905.
**Doberstein, S. K., Fetter, R. D., Mehta, A. Y. and Goodman, C. S.** (1997). Genetic analysis of myoblast fusion: blown fuse is required for progression beyond the prefusion complex. *J. Cell Biol.* **136**, 1249-1261.
**Goldstein, S., Fordis, C. M. and Howard, B. H.** (1989). Enhanced transfection efficiency and improved cell survival after electroporation of G2/M-synchronized cells and treatment with sodium butyrate. *Nucleic Acids Res.* **17**, 3959-3971.
**Gros, J., Scaal, M. and Marcelle, C.** (2004). A two-step mechanism for myotome formation in chick. *Dev. Cell* **6**, 875-882.
**Gros, J., Manceau, M., Thomé, V. and Marcelle, C.** (2005). A common somitic origin for embryonic muscle progenitors and satellite cells. *Nature* **435**, 954-958.
**Horsley, V., Friday, B. B., Matteson, S., Kegley, K. M., Gephart, J. and Pavlath, G. K.** (2001). Regulation of the growth of multinucleated muscle cells by an NFATC2-dependent pathway. *J. Cell Biol.* **153**, 329-338.
**Horsley, V., Jansen, K. M., Mills, S. T. and Pavlath, G. K.** (2003). IL-4 acts as a myoblast recruitment factor during mammalian muscle growth. *Cell* **113**, 483-494.
**Kahane, N., Cinnamon, Y. and Kalcheim, C.** (2002). The roles of cell migration and myofiber intercalation in patterning formation of the postmitotic myotome. *Development* **129**, 2675-2687.
**Kassar-Duchossoy, L., Giacone, E., Gayraud-Morel, B., Jory, A., Gomès, D. and Tajbakhsh, S.** (2005). Pax3/Pax7 mark a novel population of primitive myogenic cells during development. *Genes Dev.* **19**, 1426-1431.
**Knudsen, K. A. and Horwitz, A. F.** (1977). Tandem events in myoblast fusion. *Dev. Biol.* **58**, 328-338.
**Manceau, M., Gros, J., Savage, K., Thomé, V., McPherron, A., Paterson, B. and Marcelle, C.** (2008). Myostatin promotes the terminal differentiation of embryonic muscle progenitors. *Genes Dev.* **22**, 668-681.
**Moore, C. A., Parkin, C. A., Bidet, Y. and Ingham, P. W.** (2007). A role for the Myoblast city homologues Dock1 and Dock5 and the adaptor proteins Crk and Crk-like in zebrafish myoblast fusion. *Development* **134**, 3145-3153.
**Ordahl, C. P., Berdougo, E., Venters, S. J. and Denetclaw, W. F. J.** (2001). The dermomyotome dorsomedial lip drives growth and morphogenesis of both the primary myotome and dermomyotome epithelium. *Development* **128**, 1731-1744.
**Primmett, D. R., Stern, C. D. and Keynes, R. J.** (1988). Heat shock causes repeated segmental anomalies in the chick embryo. *Development* **104**, 331-339.
**Rash, J. E. and Fambrough, D.** (1973). Ultrastructural and electrophysiological correlates of cell coupling and cytoplasmic fusion during myogenesis in vitro. *Dev. Biol.* **30**, 166-186.
**Relaix, F., Rocancourt, D., Mansouri, A. and Buckingham, M.** (2005). A Pax3/Pax7-dependent population of skeletal muscle progenitor cells. *Nature* **435**, 948-953.
**Richardson, B. E., Nowak, S. J. and Baylies, M. K.** (2008). Myoblast fusion in fly and vertebrates: new genes, new processes and new perspectives. *Traffic* **9**, 1050-1059.
**Rios, A. C., Serralbo, O., Salgado, D. and Marcelle, C.** (2011). Neural crest regulates myogenesis through the transient activation of NOTCH. *Nature* **473**, 532-535.
**Rochlin, K., Yu, S., Roy, S. and Baylies, M. K.** (2010). Myoblast fusion: when it takes more to make one. *Dev. Biol.* **341**, 66-83.
**Scaal, M., Gros, J., Lesbros, C. and Marcelle, C.** (2004). In ovo electroporation of avian somites. *Dev. Dyn.* **229**, 643-650.
**Schienda, J., Engleka, K. A., Jun, S., Hansen, M. S., Epstein, J. A., Tabin, C. J., Kunkel, L. M. and Kardon, G.** (2006). Somitic origin of limb muscle satellite and side population cells. *Proc. Natl. Acad. Sci. USA* **103**, 945-950.
**Shavlakadze, T. and Grounds, M.** (2006). Of bears, frogs, meat, mice and men: complexity of factors affecting skeletal muscle mass and fat. *Bioessays* **28**, 994-1009.
**Simionescu, A. and Pavlath, G. K.** (2011). Molecular mechanisms of myoblast fusion across species. *Adv. Exp. Med. Biol.* **713**, 113-135.
**Srinivas, B. P., Woo, J., Leong, W. Y. and Roy, S.** (2007). A conserved molecular pathway mediates myoblast fusion in insects and vertebrates. *Nat. Genet.* **39**, 781-786.
**Venters, S. J., Hultner, M. L. and Ordahl, C. P.** (2008). Somite cell cycle analysis using somite-staging to measure intrinsic developmental time. *Dev. Dyn.* **237**, 377-392.
**Wakelam, M. J.** (1985). The fusion of myoblasts. *Biochem. J.* **228**, 1-12.
**White, R., Biérinx, A.-S., Gnocchi, V. and Zammit, P.** (2010). Dynamics of muscle fibre growth during postnatal mouse development. *BMC Dev. Biol.* **10**, 21.

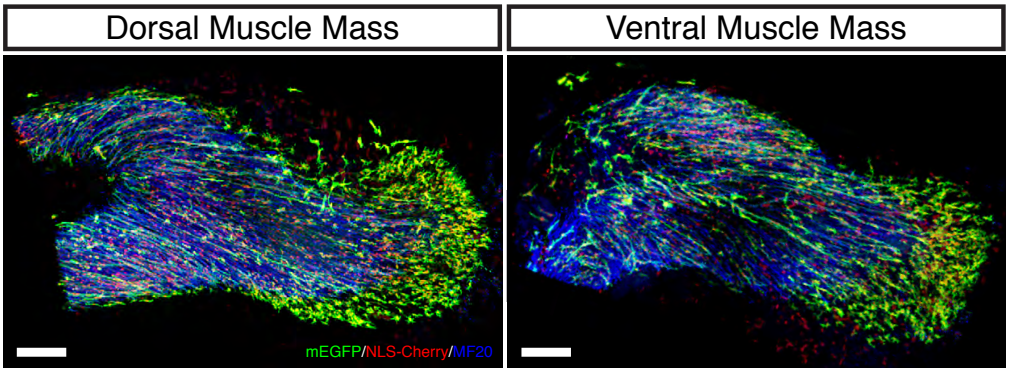


**Supplementary Figure 1.**

Dorsal and ventral muscle masses of a single E5.5 chick embryo forelimb co-electroporated at E2.5 in the VLL of somites in the fore-limb region with EGFP (in green) and a nuclear form of mCherry (in red). In blue, immuno-staining against MyHC. This shows that the distribution of plurinucleated myofibers is similar in both muscle masses (longest fibers in the central domain, shortest at the periphery), while a cloud of mononucleated progenitors is present at the distal leading edge of both muscle masses.

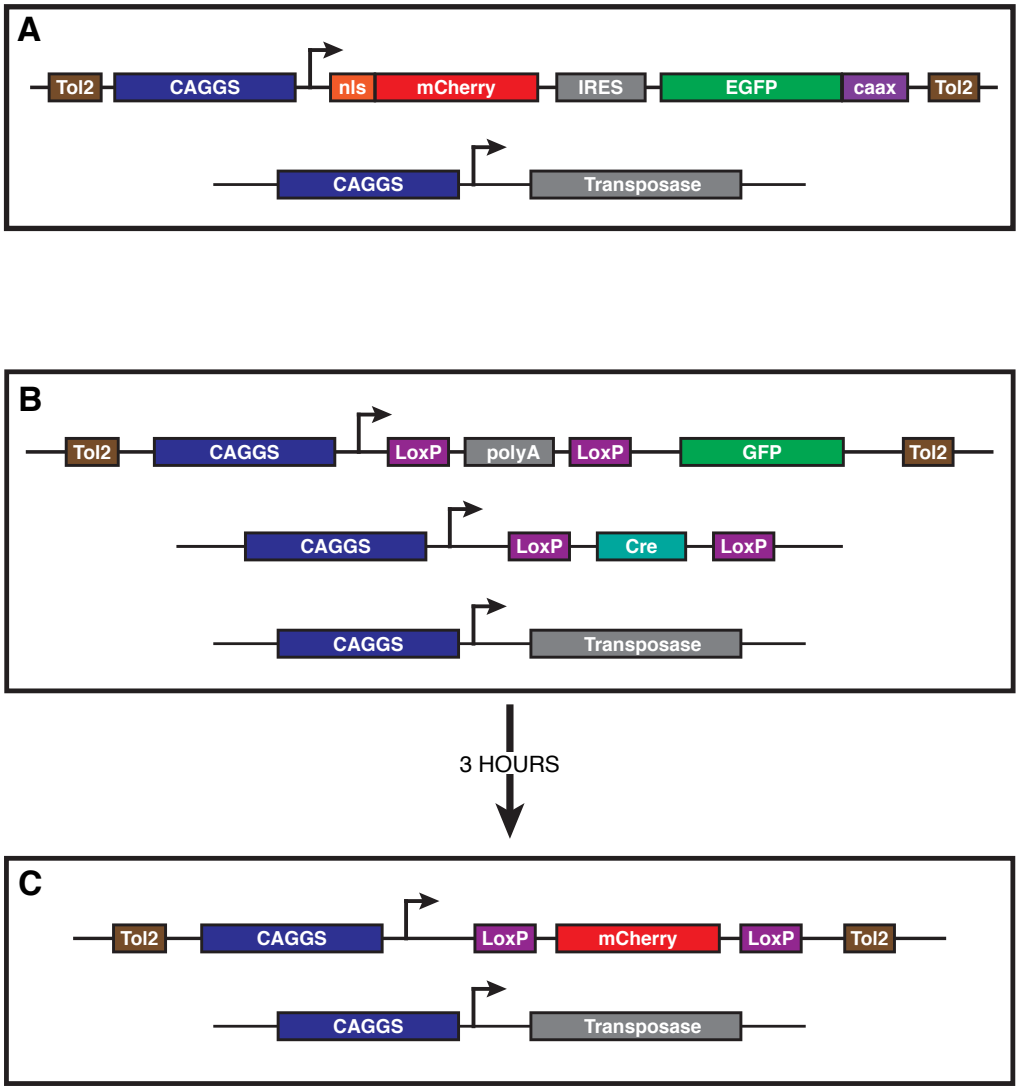


**Supplementary Figure 2.**

(A): Vectors utilized to count the number of nuclei per fiber. (B,C): Description of the double-electroporation protocol aimed at mosaically labelling a cell population with two fluorochromes. B: First co-electroporation with two plasmids, that encode a self-excising Cre and GFP, downstream of a floxed poly(A) signal. When both plasmids are co-expressed, epithelial cells are GFP-positive. If only one plasmid is expressed, cells are not fluorescent. (C): 4 hours later, the DML is electroporated once more with a plasmid encoding a floxed mCherry. DML cells express the mCherry fluorochrome, unless they were previously electroporated with Cre, which inactivates mCherry. The self-excising Cre ensures that the Cre protein is only temporarily present; if mosaically-labeled cells do not fuse, myocytes will be either red or green, if they fuse, a proportion of them will be yellow.

**Supplementary Table 1.**
Count of nuclei per fiber observed at the indicated times after DML, dorsal dermomyotome and limb electroporation.

| | E3.5 | E4 | E4.5 | E5 | E5.5 | E6 |
|---|---|---|---|---|---|---|
| **DML EP** | | | | | | |
| | n=189 | | n=353 | | n=336 | |
| **1N** | 176 | | 265 | | 68 | |
| **2N** | 12 | | 75 | | 98 | |
| **3N** | 1 | | 10 | | 80 | |
| **4N** | | | 3 | | 44 | |
| **5N** | | | | | 33 | |
| **6N** | | | | | 11 | |
| **7N** | | | | | 2 | |
| **Mean** | 1.1 | | 1.3 | | 2.8 | |
| **Dm EP** | | | | | | |
| | | | n=186 | | n=223 | |
| **1N** | | | 80 | | 40 | |
| **2N** | | | 71 | | 54 | |
| **3N** | | | 24 | | 58 | |
| **4N** | | | 10 | | 41 | |
| **5N** | | | 1 | | 21 | |
| **6N** | | | | | 7 | |
| **7N** | | | | | 1 | |
| **8N** | | | | | 1 | |
| **Mean** | | | 1.8 | | 2.9 | |
| **LIMB EP** | | | | | | |
| | | n=115 | n=59 | n=207 | n=238 | n=128 |
| **1N** | | 103 | 47 | 37 | 4 | 6 |
| **2N** | | 9 | 11 | 50 | 21 | 7 |
| **3N** | | 3 | 1 | 30 | 24 | 9 |
| **4N** | | | | 32 | 31 | 15 |
| **5N** | | | | 15 | 25 | 15 |
| **6N** | | | | 15 | 36 | 14 |
| **7N** | | | | 11 | 25 | 12 |
| **8N** | | | | 4 | 18 | 9 |
| **9N** | | | | 5 | 21 | 7 |
| **10N** | | | | 3 | 12 | 7 |
| **11N** | | | | 1 | 8 | 12 |
| **12N** | | | | | 2 | 12 |
| **13N** | | | | | 1 | 2 |
| **14N** | | | | | | 1 |
| **15N** | | | | | 1 | 1 |
| **16N** | | | | 1 | 1 | |
| **17N** | | | | | | 1 |
| **Mean** | | 1.1 | 1.2 | 3.6 | 6.1 | 6.7 |

**Supplementary Table 2.**
GFP (green), mCherry (red) and mixed (yellow) fibers after electroporation of the indicated somite sub-populations.

| | | | | |
|---|---|---|---|---|
| **DML/DML 10hpe no Cre** | | | | |
| | | **Green** | **Red** | **Yellow** |
| | **Fibers Counted** | 48 | 26 | 101 |
| | **Percentage Mean** | 26.7 | 14.7 | 58.6 |
| | **Standard Deviation** | 8.1 | 6.3 | 13.0 |
| **DML/DML 10hpe control** | | | | |
| | | **Green** | **Red** | **Yellow** |
| | **Fibers Counted** | 226 | 215 | 24 |
| | **Percentage Mean** | 46.9 | 49.7 | 3.4 |
| | **Standard Deviation** | 18.2 | 18.8 | 4.7 |
| **DML/DML 72hpe** | | | | |
| | | **Green** | **Red** | **Yellow** |
| | **Fibers Counted** | 193 | 150 | 49 |
| | **Percentage Mean (Adj.)** | 49.7 | 42.2 | 8.2 |
| | **Standard Deviation** | 7.6 | 13.2 | 6.6 |
| **Dm/Dm 72hpe** | | | | |
| | | **Green** | **Red** | **Yellow** |
| | **Fibers Counted** | 83 | 69 | 88 |
| | **Percentage Mean (Adj.)** | 36.7 | 30.2 | 33.1 |
| | **Standard Deviation** | 4.6 | 7.3 | 6.4 |
| **DML/Dm 72hpe** | | | | |
| | | **Green** | **Red** | **Yellow** |
| | **Fibers Counted** | 91 | 77 | 28 |
| | **Percentage Mean (Adj.)** | 48.0 | 42.7 | 9.3 |
| | **Standard Deviation** | 8.1 | 8.2 | 11.2 |
| **DML/AL 72hpe** | | | | |
| | | **Green** | **Red** | **Yellow** |
| | **Fibers Counted** | 78 | 66 | 42 |
| | **Percentage Mean (Adj.)** | 43.3 | 36.6 | 20.1 |
| | **Standard Deviation** | 11.3 | 8.8 | 7.8 |
| **DML/PL 72hpe** | | | | |
| | | **Green** | **Red** | **Yellow** |
| | **Fibers Counted** | 78 | 64 | 38 |
| | **Percentage Mean (Adj.)** | 45.1 | 37.1 | 17.8 |
| | **Standard Deviation** | 5.4 | 5.5 | 5.1 |

# 4 FUNCTIONAL STUDIES OF MOLECULAR MECHANISMS IN VERTEBRATE FUSION

## 4.1 Introduction

An important feature found in various membrane fusion mechanisms, including those described during *Drosophila* myoblast fusion, is an asymmetry of the molecules present at the surface of cells about to fuse. As was suggested by the *tmem8c* fibroblast-myofibre *in vitro* experiments (Figure 1.13) (Millay et al 2013), this asymmetry is likely present during vertebrate muscle fusion as well. Consistent with this, any fusion asymmetry described so far has been explained by the requirement of different anchoring proteins on the surface of each cell partner. However, the results presented in chapter 3 suggest a much more complex picture, where fusion-competent myoblasts are not only limited to who they fuse by the adhesion proteins present of their cell surface, but by highly regulated molecular networks, therefore allowing cells to "choose" with who they fuse out of a wide selection of cells all present within the same physical space (i.e. the myotome).

The suggested but not proven asymmetry likely present in vertebrate muscle fusion mechanisms serves to illustrate how little is still known about this crucial myogenic process. As shown in chapter 1.3, most of the genes found to be necessary during vertebrate myoblast fusion are related to actin remodelling, and it is likely that these mechanisms are not fusion specific; instead, they are housekeeping protocols likely borrowed during the fusion process. This lack of knowledge could in part be attributed to the constraints presented by current vertebrate models. While zebrafish embryos are excellent tools for the imaging of single fibres in a native environment, teleost myogenesis occurs very different from amniotes. In contrast, mice models undergo myogenesis almost identical to humans; however, their *in utero* development restricts the experimental access to nascent muscles, limiting the observation of phenotypes to newborn mice, where fusion can only be measured by indirect means.

As shown in chapter 3, the chick embryo presents a balance between human-like development and an ease of manipulation, imaging and quantification that enables the detailed characterisation of fusion processes. Furthermore, electroporation

techniques allow us to perform gain and loss of function experiments on multiple genes in a relatively short period when compared to other models.

Here, I present preliminary data obtained from gain of function experiments on fusion candidate genes. Interestingly, over-activation of putative inhibitors of fusion led to lower fusion rates, suggesting regulatory mechanisms are in play. Furthermore, I have developed a doxycycline-dependent inducible system that allows the targeting of fusion processes without affecting other myogenic steps (i.e. proliferation or differentiation) while enabling the visualisation of full length fibres and their nuclei within.

### 4.1.1 Prior work: shRNA screen

In order to gain further insight into the fusion process in vertebrates and decipher the underlying complex molecular mechanisms at work during this process, it was crucial to develop a global and unbiased approach, based on a genome-wide strategy. Prior to my involvement in this project, a genome-wide screen using vector-expressed short hairpin RNAs (shRNAs) on murine myogenic cells C2C12 was performed by CENIX (Dresden, Germany) and aimed to identify novel genes involved in myoblast fusion. Following transfection of a siRNA library representing 9000 independent genes (i.e. about one third of the mouse genome), $EGFP^+$ C2C12 cells were placed in differentiation medium to induce fusion. Three days later, automated cell-recognition software detected fusion by measuring the number of nuclei (stained with Hoechst) per fibre (marked by the EGFP green fluorescence). Since a lack of C2C12 fusion upon shRNA transfection could be due to either a failure to proliferate or differentiate instead of a true effect on cell fusion, cells were also stained with a monoclonal antibody directed against MyHC to evaluate the myogenic differentiation of transfected C2C12-$EGFP^+$ cells at the end of the experiment. The total number of nuclei per well also gave an indication of whether the shRNAs had interfered with cell cycle and survival. As a further control, cells were stained against the MRF myogenin to ensure that not only were cells expressing differentiation markers (MyHC), they did so by following the correct myogenic program. Two rounds of screening were performed to control for

unexpected variables. After obtaining the initial data, bioinformatician Dr. David Salgado normalised the data and performed an initial analysis using clustering tools to determine biological processes or pathways that were over-represented in the gene sets that either activate or inhibit myoblast fusion. These included GO-based clustering, text-mining approaches and extraction of transcriptional signatures from large microarray databases (i.e. Gene Expression Omnibus) to search for the biological contexts in which several genes were regulated.

## 4.2 Results

### 4.2.1 Analysis of candidate genes

The shRNA screen revealed 674 candidate genes that either activate (232) or inhibit (442) muscle fusion in C2C12 cells in a statistically significant way (examples on Table 3.1), with no effect on their differentiation or proliferation. Many actin-interacting genes as well as molecules already known to modulate muscle fusion in vertebrates were identified (see Table 3.1), validating the model used. Due to the high number of genes described in the screen, the expression patterns of a subset of genes were then examined by *in situ* hybridisation in order to determine which of the positive candidates are expressed within the embryonic muscles at the time and place where fusion takes place, as based on our previous findings (seen in Chapter 3). Following a series of criteria based on the aforementioned bioinformatic analyses, genes known to be involved: i) in muscle development or muscular diseases, ii) in knockout models showing skeletal muscle defects, iii) where entire pathways were overrepresented, were given priority. Results show that 34% of the genes tested are expressed within muscle masses, 33% display a mixed expression pattern (that included muscles), 9% are ubiquitous and 24% are not detected at these stages of embryonic development. Out of the 34% present within muscle areas, those most strongly expressed within muscle fibres at the time fusion occurs were picked for further functional experiments within trunk and limb muscles, as will be explained below.

| Gene | Fusion Value |
|---|---|
| Cdc42 | 45.60438309 |
| Rac1 | 61.1215319 |
| Bag3 | 67.26422255 |
| Rab39 | 68.94427231 |
| Tmem47 | 142.4918849 |
| Reep1 | 175.147005 |
| Sgcd | 302.5559686 |

**Table 3.1 Gene samples from shRNA C2C12 screen.**

Shown here are examples of genes and their fusion values as obtained from the shRNA screen. In red are the values for the two controls used in this study (Rac1 and Cdc42). In black are the values for the candidate genes reported below. "Fusion Value" is expressed as a percentage of wild-type fusion, with control (untreated) cells normalised to 100. Values <100 indicate lack of fusion (putative activators). Values >100 indicate excessive fusion (putative inhibitors). The formula for the Fusion Value also takes into account rates of proliferation as well as myogenic progress (myogenin and MyHC).

### 4.2.2 Construction of inducible vectors to assay the function of candidate genes during fusion.

In order to test the function of candidate genes on muscle fusion regardless of their possible function on morphogenetic steps upstream of fusion (e.g. delamination from somites, migration into the limb bud, early myogenic differentiation, etc.), purpose-built molecular tools were designed. Inducible vector strategies were chosen as they can be activated once progenitors have begun differentiation and reached either the myotome or the limb bud mesenchyme but before they initiate fusion. Two vectors, based on the Tet-on Advanced activation system (Clontech, Figure 3.1) that we have previously utilised in the chick embryo (Serralbo et al 2013; Rios et al 2011), were constructed. The first contains the Tet-On transactivator (rtTA) downstream of the ubiquitous CAGGS promoter, while an Internal Ribosome Entry Site (IRES) allows its expression simultaneously with a nuclear RFP variant (NLS-mCherry). The nuclear RFP enables testing for both the efficiency of the electroporation and evaluation of the number of nuclei. The second vector is a response plasmid in which HA-tagged versions of mouse full-length cDNA (obtained from IMAGE consortium, Iowa University) specific for the

candidate genes were inserted (Figure 3.1). Upon addition of doxycycline, the bidirectional tetracycline-response element (TRE) drives the simultaneous expression of a membranal form of EGFP (EGFP-caax) and the full-length gene. In both vectors, the entire constructs are flanked by cis-sequences from the Tol2 transposable element (Kawakami 2004) to allow integration into the genome of transfected cells, and thereby avoiding the gradual dilution of the plasmids upon cell divisions. The integration into the genome is mediated by the co-electroporation of a third vector encoding for the Tol2 transposase.

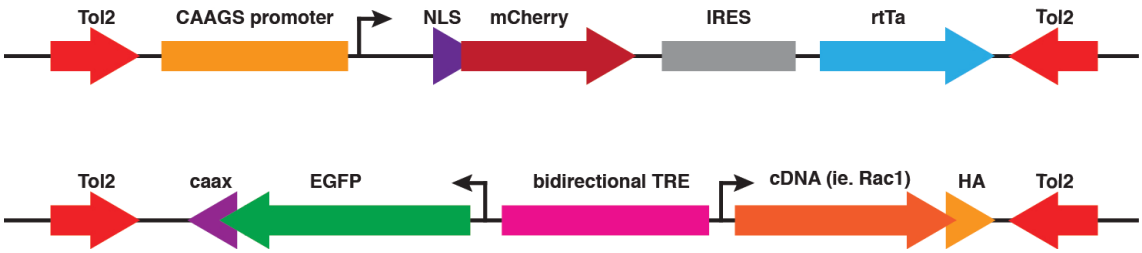


**Figure 3.1 Schematic of the inducible expression system used throughout experiments reported in chapter 3.**

Two plasmids are co-electroporated at E2.5 chick embryos. The first is composed of a CAGGS ubiquitous promoter driving a mCherry red fluorescent protein fused to a nuclear localisation signal (NLS), followed by an IRES and a rtTa protein. The second construct is a bi-directional Tet-responsive element, flanked to one side by a green EGFP tagged with a CAAX box membranal signal. On the other side, a cDNA sequence (for each gene described ahead) is fused to an HA tag. Both constructs are flanked by Tol2 sequences and electroporated along with a transposase to ensure permanent genomic integration. Construct two remains inactive until the addition of doxycycline, at which point the rtTa protein binds the antibiotic present and activates the Tet-responsive element and its downstream targets.

### 4.2.3 Rac1 and CDC42 as modulators of fusion

Prior to performing functional analyses on new potential regulators of fusion, experiments were conducted on known pan-species activators of fusion to ensure the inducible system could indeed affect fusion events. The Rho GTPases Rac1 and Cdc42 are important regulators of the actin cytoskeleton and, as has been mentioned throughout this thesis, there is ample experimental evidence that they play essential roles during muscle fusion both in invertebrates and vertebrates

(Srinivas et al 2007; Vasyutina et al 2009; Hakeda-Suzuki et al 2002; Luo et al 1994). Dominant-negative mutants of Rac1 and Cdc42 were used. These molecules result from the substitution of the highly conserved threonine at position 17 to an asparagine ($Rac1^{T17N}$ and $Cdc42^{T17N}$) and the act by specifically and strongly competing with their normal counterparts for binding to their respective GEFs (Feig 1999). Thus, a lack of correct fusion in fibres transfected with either variant was expected.

#### 4.2.3.1 Inhibition of early trunk muscle fusion

In order to test if the dominant-negative variants of Rac1 and Cdc42 could inhibit fusion in the trunk musculature, the dorso-medial lip (DML) of the inter-limb somites of E2.5 embryos was electroporated. Doxycycline was added to the embryos 24 hours later, shortly after initial fibre formation but prior to fusion occurring, as described before (Chapter 3) (Sieiro-Mosti et al 2014). Embryos were collected at E5.5. Control embryos were electroporated with a response plasmid that contained all other elements described except for either Rho GTPase cDNA sequence. Immunostaining for RFP and GFP was performed together with the terminal differentiation marker Myosin Heavy Chain (MyHC) to test that the effect of inhibiting Rac1 and Cdc42 during fusion was not due to an arrest of differentiation. Indeed, MyHC expression remained unchanged when compared to control or non-electroporated fibres (not shown). HA-specific antibody showed that the mouse DN-Rac1 and DN-Cdc42 were highly expressed, indicating the efficiency of the doxycycline-inducible system (Figure 3.2E,H). Results showed that inducible expression of dominant-negative Rac1 at E3.5 almost completely blocked fusion in E5.5 differentiated trunk muscle fibres with a mean number of 1.3 nuclei per fibre ($P< 0.0001$; Control: 2.4 mean nuclei per fibre; Figure 3.2A-D,L). Overexpression of DN-Cdc42 also resulted in a very similar dramatic reduction in

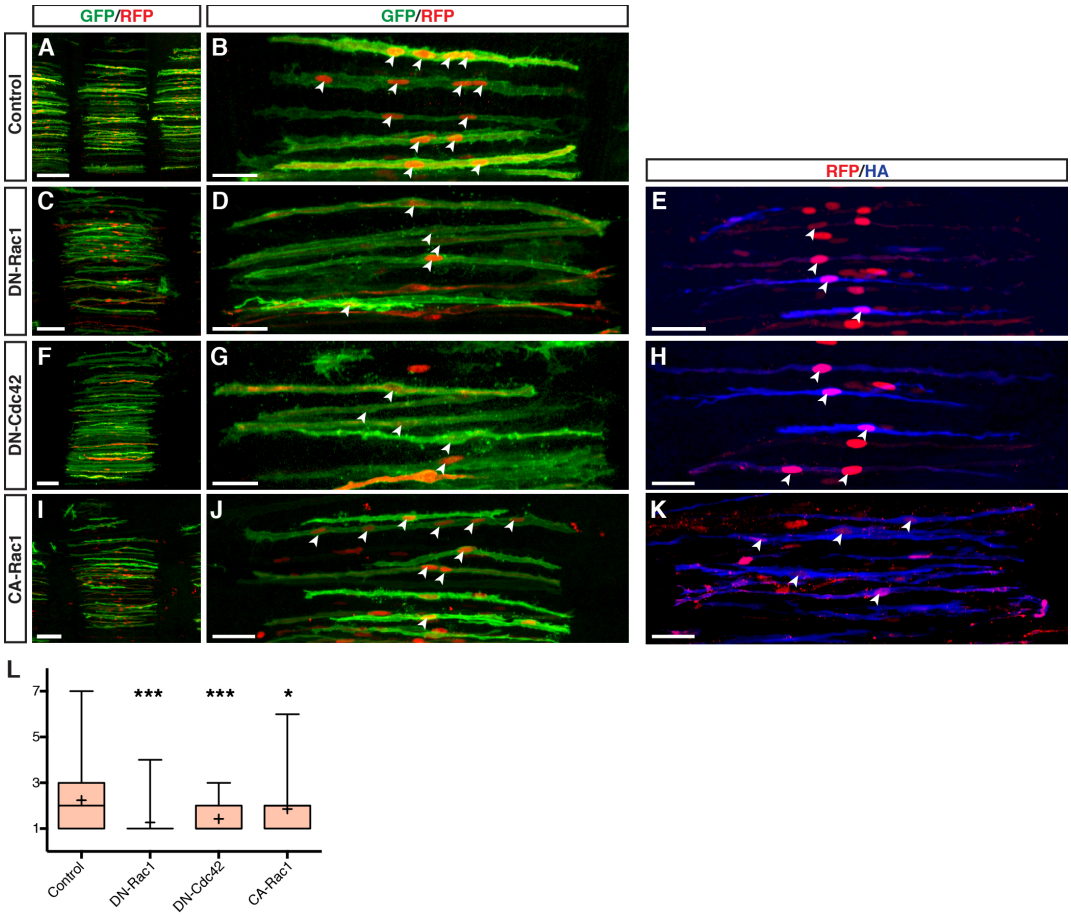


**Figure 3.2 Rac1 and Cdc42 are required in early chick trunk fusion.**

**A-K.** Cells from the DML were electroporated at E2.5 and doxycycline-expression of constructs performed at E3.5. Nuclei number per fibre was counted at E5.5 **E,H,K.** Constructs were tagged with HA and immuno-stained to ensure correct cDNA expression. All images are whole-mount confocal stacks of fixed embryos, immuno-stained for EGFP (green) and RFP (red). Arrowheads (B,D,E,G,H,J,K) indicate cell nuclei within selected fibres. **L.** Quantification of nuclei number per fibre at E5.5. Whiskers indicate minimal and maximal values; the bottom and top of the box indicate the first and third quartile; the horizontal line indicates the median; and '+' indicates the mean for each set of values. *P<0.05; ***P<0.0001. Scale bars: 100 μm in A,C,F,I; 50 μm in B,D,E,G,H,J,K.

fusion (mean number of nuclei: 1.4; P< 0.0001; Figure 3.2F,G,L). Interestingly, despite DN-Rac1 and DN-Cdc42 fibres containing significantly fewer nuclei than controls, the length of the fibres remained constant. All MyHC+ fibres spanned the width of the somite regardless of their genotype, suggesting lack of fusion does not have an effect on fibre length. This is consistent with previous findings

demonstrating that in the trunk somites, length of fibres and nuclei fusion are not correlated (Sieiro-Mosti et al 2014).

While these results demonstrate that a loss of function of genes required for myoblast fusion leads to a lack of fusion, it was important to determine if gain of function of known fusion genes could conversely confer a greater fusing ability. For that purpose, electroporation of a constitutively active form of Rac1 ($Rac1^{V12}$) within the same inducible system was performed. Contrary to the hypothesis that greater gene activity would induce an increased fusion effect, fibres from E5.5 embryos electroporated with CA-Rac1 had significantly less nuclei than controls (mean number of nuclei: 1.9; $P< 0.01$; Figure 3.2I,J,L). While this was unexpected, it is consistent with reports from *Drosophila* where excessive Rac1 (by the use of the same active form V12) leads to impaired fusion (Luo et al 1994; Geisbrecht et al 2008).

#### 4.2.3.2 Inhibition of limb muscle fusion

As it was previously shown that in the chicken limb muscles undergo a different fusion dynamics to those of the trunk, it was necessary to demonstrate that the efficacy of the inducible system could also be applied to limb myogenesis. Furthermore, as fusion begins later in the limb, happens at a faster rate and involves a larger number of events per fibre, it was hypothesised that electroporation of limb muscle progenitors in the early embryo may serve as a fast and reliable paradigm to test the function of candidate fusion genes *in vivo*.

Electroporation of the three vectors previously described in the lateral portion of somites 16-21 of E2.5 embryos (i.e. the somites from which limb muscle progenitors originate in chicken) was performed. Doxycycline was added twice to the developing embryos, once at E4 (just before fusion is initiated in limb muscles), and a second time at E4.5. They were then collected at E5. Results showed that similar to the trunk, the inhibition of Rac1 results in a near arrest of fusion in electroporated MyHC+ cells (mean number of nuclei: 1.7; $P< 0.0001$, Figure 3.3D-F,M), when compared to controls (mean: 4.1, Figure 3.3A-C,M). In contrast, the

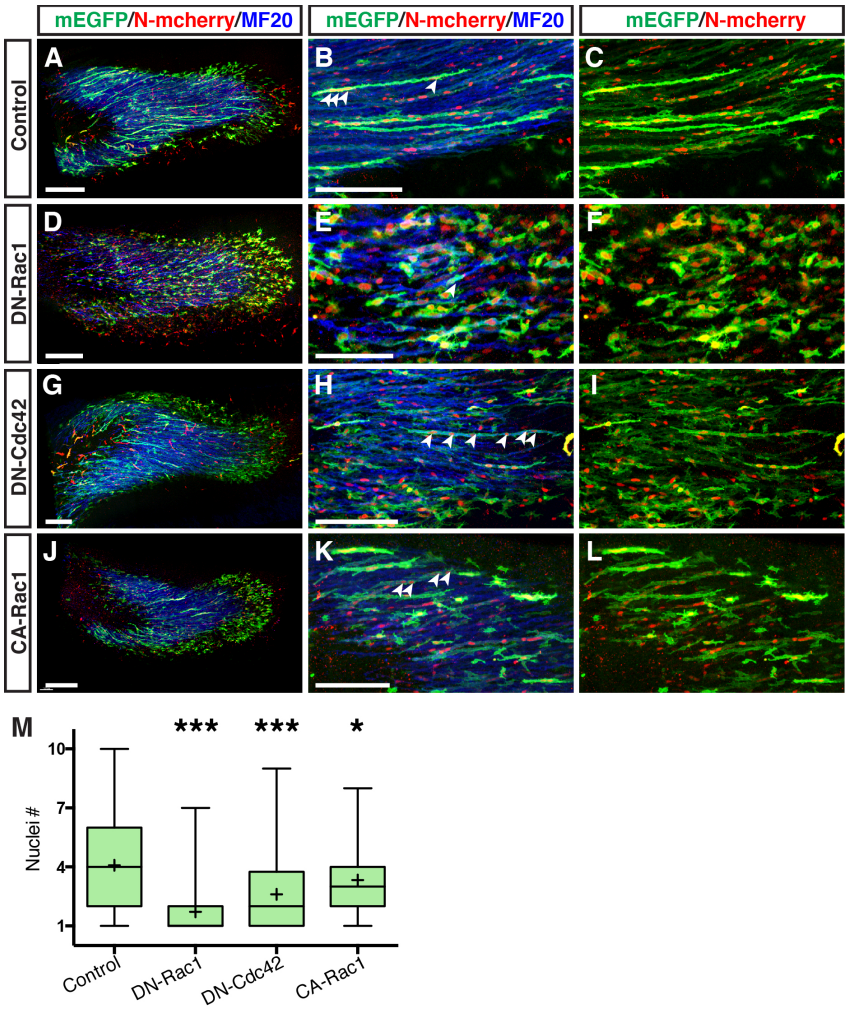


**Figure 3.3 Rac1 and Cdc42 are required in early chick forelimb fusion.**

**A-L.** Cells from the VLL at forelimb level (somites 16-21) were electroporated at E2.5 and doxycycline-expression of constructs performed at E3.5. The nuclei count per fibre was performed at E5. **A,D,G,J.** Confocal images of whole forelimb muscle masses. **B,C,E,F,H,I,K,L.** Close up of fibres within forelimb muscle masses. All images are whole-mount confocal stacks of fixed embryos. In all images blue is MyHC, green is EGFP and red is mCherry. Arrowheads (B,E,H,K) indicate cell nuclei within selected fibres. **M.** Quantification of nuclei number per fibre at the time points in A-O (see Fig. 3.2 legend). *P<0.05; ***P<0.0001. Scale bars: 200 μm in A,D,G,J; 50 μm in B,C,E,F,H,I,K,L.

inhibition of Cdc42 function by DN-Cdc42 led to a less strong phenotype (mean number of nuclei: 2.6; P< 0.0001), compared to controls and Rac1 (Figure 3.3G-I,M). Although this difference was not observed in trunk muscles, it has been reported that a differential activity of Rac1 and Cdc42 during muscle fusion occurs in $Rac1^{-/-}$ and $Cdc42^{-/-}$ mouse limb myoblasts (Vasyutina et al 2009), where the

reduction of the fusion index is more pronounced in $Rac1^{-/-}$ myoblasts than in $Cdc42^{-/-}$ myoblasts. Similar to the trunk, electroporation of CA-Rac1 lead to an opposite effect where greater protein activity resulted in slightly but significantly reduced fusion (mean nuclei number of 3.3; P=0.03; Figure 3.3J-M).

The results shown above demonstrate the inducible system devised here allows for the correct quantification of fusion parameters (mainly nuclei number per fibre) while efficiently expressing genes that are involved in fusion events, leading to an observable phenotype. Therefore, the next aim was to use this system to unveil novel players of early muscle fusion based on the preliminary results obtained from the shRNA and ISH screens.

### 4.2.4 New players in vertebrate myoblast fusion

As mentioned before, 34% of genes tested for expression by ISH showed activation within muscle masses. As expected, expression levels and localisation varied amongst them. Of these, five were selected for gain of function analyses. The criteria used was that amongst all genes tested, these five produced very strong activation or inhibition of fusion when knocked down by shRNA and had the highest levels of expression restricted exclusively at the muscle masses. Furthermore, some of these genes have been previously related to known muscle diseases. Full-length wild-type cDNA for these genes was cloned into the inducible system described above. Electroporation was performed exclusively in limb progenitors. As shown above, while fusion phenotypes are observable in trunk and limb muscles, the greater number of fusion events occurring at the limb likely confers this system a greater spread of data and sensitivity when compared to the trunk. Following this reasoning, doxycycline was added twice at E4 and E5 and embryos were collected and analysed at E5.5 instead of the previous E5 to allow for more rounds of fusion.

The first gene to be tested, *Tmem47* (transmembrane protein 47), encodes a claudin protein family member mainly localised at the ER and plasma membrane. Nothing is known of its function and has only been described as highly expressed

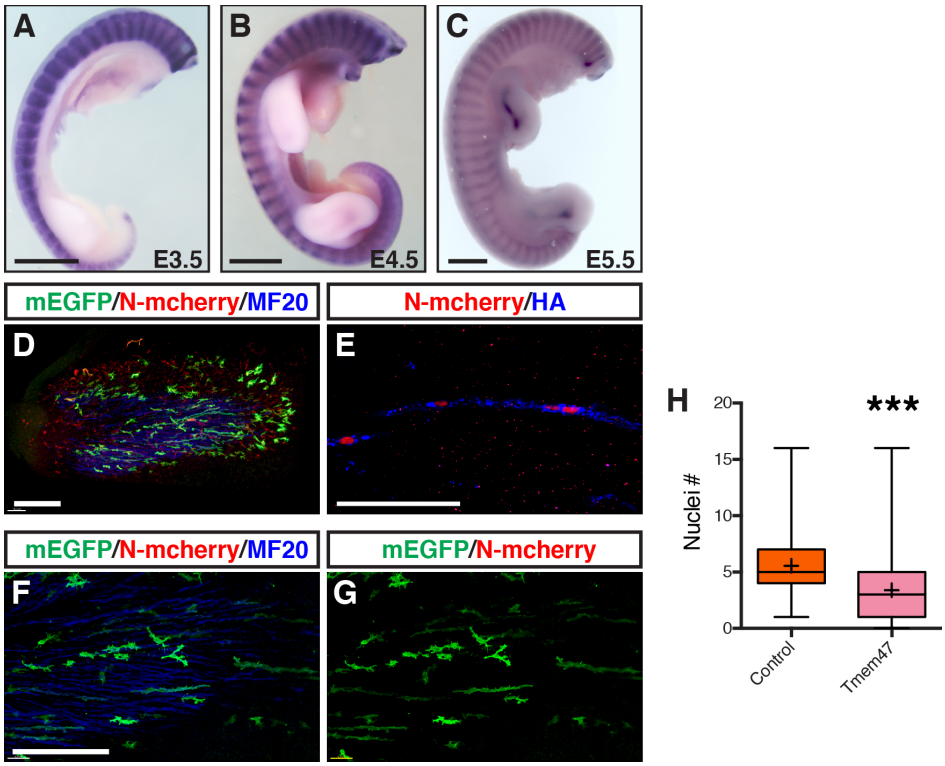


**Figure 3.4 Tmem47 over-expression inhibits myoblast fusion in the chick forelimb.**

**A-C.** *In situ* hybridisation was performed on chick embryos at E3.5 (A), E4.5 (B) and E5.5 (C). Expression was observed exclusively within trunk and limb muscles. **D-G.** Cells from the VLL at forelimb level (somites 16-21) were electroporated at E2.5 and doxycycline-expression of constructs performed at E3.5. The nuclei count per fibre was performed at E5.5. **D.** Confocal images of whole forelimb muscle masses. **E-G.** Close up of fibres within forelimb muscle masses. All images are whole-mount confocal stacks of fixed embryos. **E.** HA staining reveals protein localisation within muscle fibres. **H.** Quantification of nuclei number per fibre. ***P<0.0001. Scale bars: 500 µm in A-D; 200 µm in D; 50 µm in E-G.

in brain tissue (Christophe-Hobertus et al 2001). However, down-regulation of this gene during the screen resulted in massive fusion in C2C12 cells and *in situ* staining revealed very high expression levels in chick myotome and limb muscle masses during embryonic fusion events (Figure 3.4A-C). HA-specific antibody revealed TMEM47 localisation at the membrane and ER structures as expected, with a punctate pattern (Figure 3.4E). An average nuclei number of 3.4 were significantly lower than controls (P< 0.0001, Figure 3.4F-H), although fibres with up to 15 nuclei were observed. MyHC staining revealed no changes to the myogenic program (Figure 3.4D).

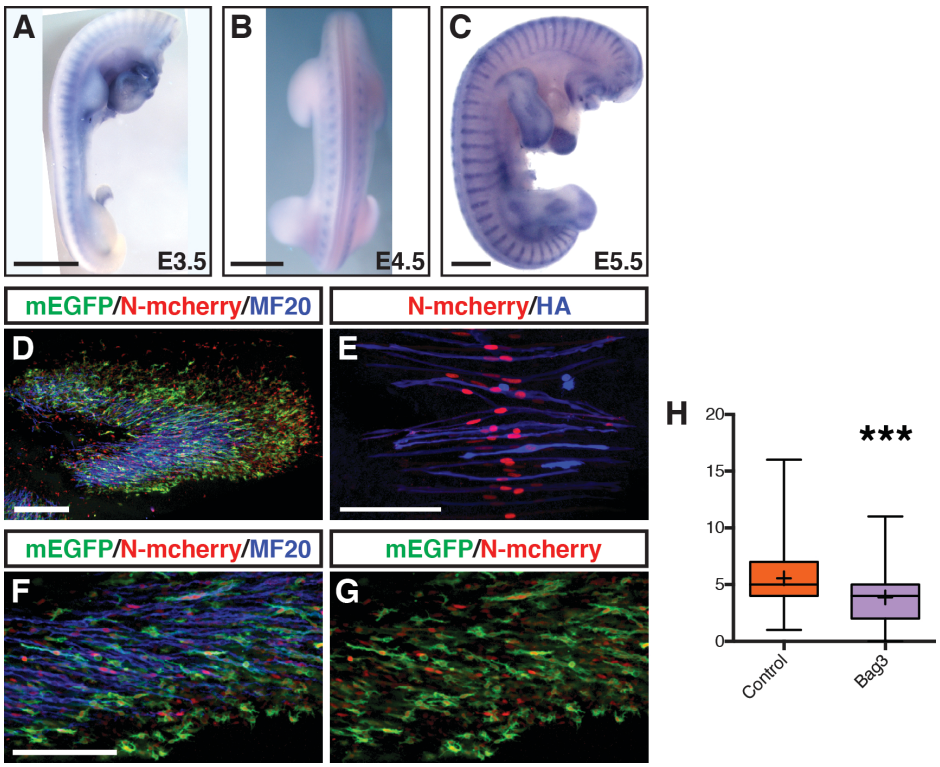


**Figure 3.5 Bag3 over-expression inhibits myoblast fusion in the chick forelimb.**

**A-C.** *In situ* hybridisation was performed on chick embryos at E3.5 (A), E4.5 (B) and E5.5 (C). Expression was observed exclusively within trunk and limb muscles. **D-G.** Cells from the VLL at forelimb level (somites 16-21) were electroporated at E2.5 and doxycycline-expression of constructs performed at E3.5. The nuclei count per fibre was performed at E5.5. **D.** Confocal images of whole forelimb muscle masses. **E-G.** Close up of fibres within forelimb muscle masses. All images are whole-mount confocal stacks of fixed embryos. **E.** HA staining reveals protein localisation within muscle fibres. **H.** Quantification of nuclei number per fibre. ***P<0.0001. Scale bars: 500 µm in A-D; 200 µm in D; 50 µm in E-G.

*Bag3* (Bcl-2 associated athanogene 3) is a member of a conserved family of proteins that bind to and regulate molecular chaperones. It is mutated in human rapidly progressing myofibrillar myopathy, while *Bag3*-null mice develop fulminant myopathy characterised by non-inflammatory myofibrillar degeneration (Homma et al 2006). Results from the shRNA screen exposed it as a likely activator of fusion, while expression in chick embryos was observed in a striped pattern across growing myotomes (Figure 3.5A-C). Average nuclei number per fibre significantly decreased when compared to age-matched controls (3.9 vs 5.7,

P<0.0001, Figure 3.5F-H), but in contrast to *Tmem47*, no fibres with more than 11 nuclei were observed. The inhibition observed here contrasts with the hypothesis suggesting this gene acts an activator of fusion, but is consistent with CA-Rac1 results shown above that reveal a fusion-negative effect when overexpressing activators.

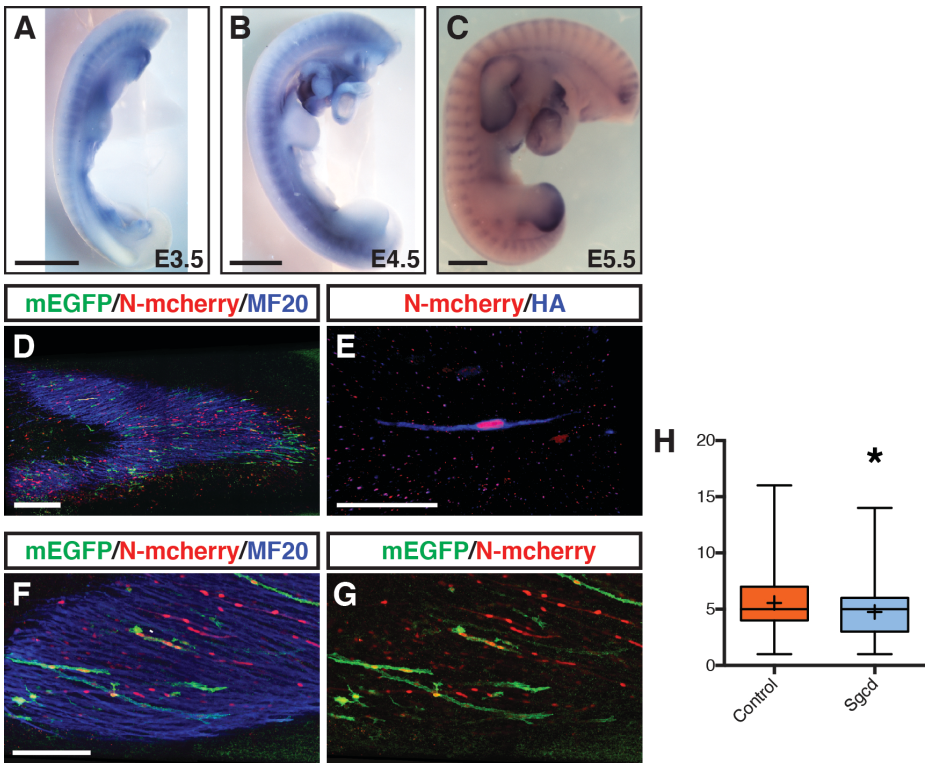


**Figure 3.6 Sgcd over-expression inhibits myoblast fusion in the chick forelimb.**

**A-C.** *In situ* hybridisation was performed on chick embryos at E3.5 (A), E4.5 (B) and E5.5 (C). Expression was observed exclusively within muscles areas. **D-G.** Cells from the VLL at forelimb level (somites 16-21) were electroporated at E2.5 and doxycycline-expression of constructs performed at E3.5. The nuclei count per fibre was performed at E5.5. **D.** Confocal images of whole forelimb muscle masses. **E-G.** Close up of fibres within forelimb muscle masses. All images are whole-mount confocal stacks of fixed embryos. **E.** HA staining reveals protein localisation within muscle fibres. **H.** Quantification of nuclei number per fibre. *P<0.05. Scale bars: 500 µm in A-D; 200 µm in D; 50 µm in E-G.

*Sgcd* (Delta-sarcoglycan) is a known component of the dystrophin-glycoprotein complex (DGC) required for the anchoring of contractile proteins to the plasma membrane of mature myofibres. Interestingly, inhibition of this gene resulted in massive fusion of myotubes *in vitro*. As expected, expression was restricted to

elongated muscle cells (Figure 3.6A-C). Indeed, overexpression of the protein lead to significantly reduced fusion (mean nuclei number of 4.8; P<0.001; Figure 3.5F-H) suggesting it acts as an inhibitor of fusion. However, fusion was still widely observed, with many fibres containing more than five and up to 14 nuclei.

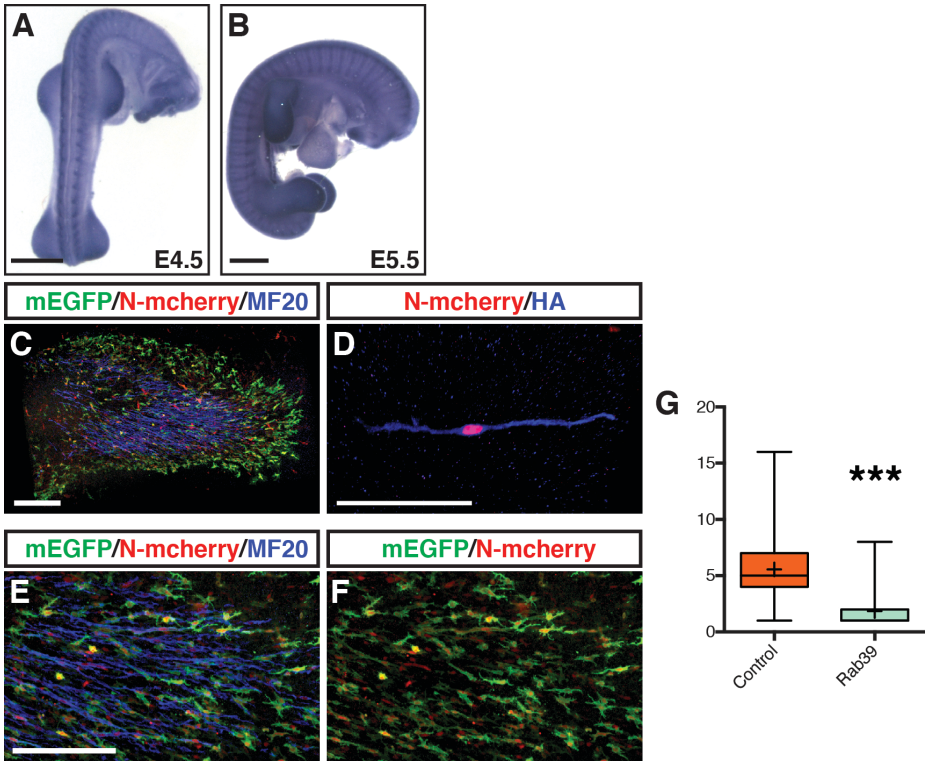


**Figure 3.7 Rab39 over-expression inhibits myoblast fusion in the chick forelimb.**

**A-B.** *In situ* hybridisation was performed on chick embryos at E4.5 (A) and E5.5 (B). E3.5 had no detectable expression levels, expression at E4.5 and E5.5 was observed within forming muscles. **C-F.** Cells from the VLL at forelimb level (somites 16-21) were electroporated at E2.5 and doxycycline-expression of constructs performed at E3.5. The nuclei count per fibre was performed at E5.5. **C.** Confocal images of whole forelimb muscle masses. **D-F.** Close up of fibres within forelimb muscle masses. All images are whole-mount confocal stacks of fixed embryos. **D.** HA staining reveals protein localisation within muscle fibres. **G.** Quantification of nuclei number per fibre. ***P<0.0001. Scale bars: 500 µm in C-F; 200 µm in C; 50 µm in D-F.

*Rab39* (Ras-related protein 39) is a member of the Rab family of small GTPases involved in vesicular trafficking and importantly, membrane fusion (Hutagalung & Novick 2011) (Charrasse et al 2013) and results from the shRNA screen revealed Rab39 to be also acting as a potential activator of the process. Inducible expression

of mouse *Rab39* cDNA construct in limb myoblasts revealed the opposite effect, with a widespread arrest in fusion observed. While few fibres contained up to a maximum of 8 nuclei, the large majority (>90%) of fibres observed did not contain more than 3 nuclei (figure 3.7E,F). Indeed, *Rab39*-overexpressing limb fibres at E5.5 averaged 1.9 nuclei, greatly below the mean of 5.7 nuclei for controls ($P<0.0001$, Figure 3.7G).

Lastly, a potential mediator of the fusion process is the receptor expression-enhancing protein 1 (*Reep1*). Little is known about this gene, but it may be involved in enhancing the cell surface expression of odorant receptors, which in turn could be required for adhesion and anchoring of cell membranes prior to fusion. Interestingly, *Reep1* is likely a strong inhibitor of muscle fusion according to data from C2C12 cells. When overexpressed in chick limb myoblasts, there was significantly less fusion when compared to controls (mean nuclei number of 3.1; $P<0.0001$; Figure 3.8F-H). More than 75% of cells contained two or less nuclei, and a maximum of 11 nuclei in a single fibre was observed, suggesting fusion could still occur, albeit at much lower levels.

## 4.3 Discussion

The results described above represent a first step towards a fast and efficient way of testing and quantifying the effect of candidate genes on muscle fusion. While the fusion-related phenotypes observed in a large number of genes obtained from the screen (some tested genes did not induce fusion phenotypes, not shown) suggest the current list of candidates likely contains many true players of fusion, it is necessary to optimise the protocols in order to guarantee the authenticity of the results. For example, the observed loss of fusion for both the putative activators and inhibitors of fusion likely indicates a delicate balance where over-expression

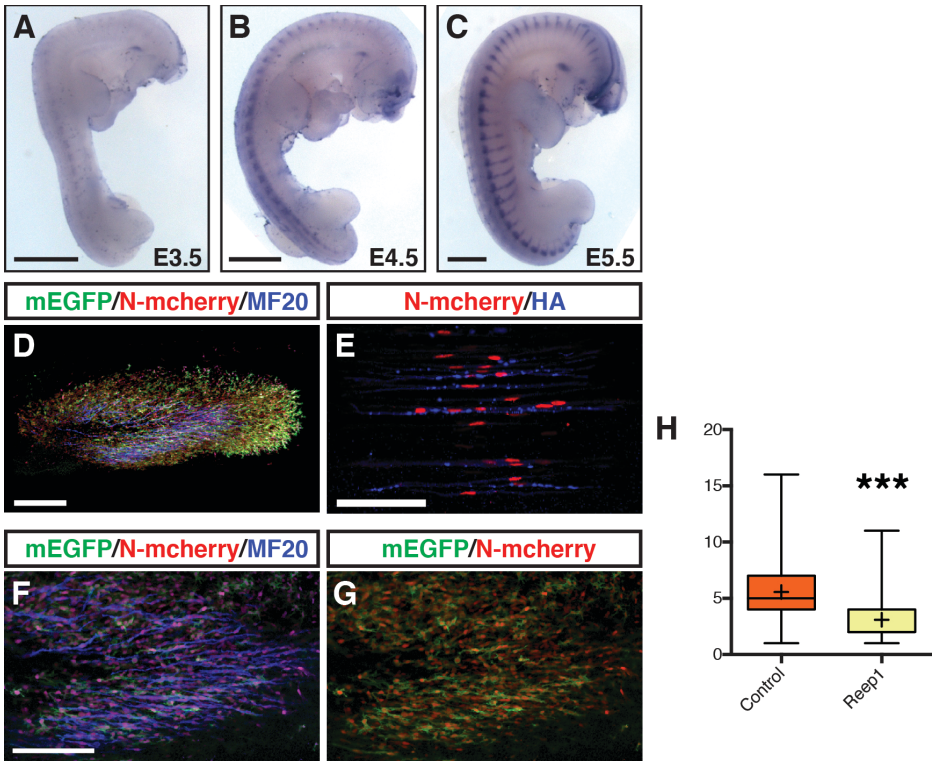


**Figure 3.8 Reep1 over-expression inhibits myoblast fusion in the chick forelimb.**

**A-C.** *In situ* hybridisation was performed on chick embryos at E3.5 (A), E4.5 (B) and E5.5 (C). Expression was observed within muscle areas and dorsal root ganglia (DRG). **D-G.** Cells from the VLL at forelimb level (somites 16-21) were electroporated at E2.5 and doxycycline-expression of constructs performed at E3.5. The nuclei count per fibre was performed at E5.5. **D.** Confocal images of whole forelimb muscle masses. **E-G.** Close up of fibres within forelimb muscle masses. All images are whole-mount confocal stacks of fixed embryos. **E.** HA staining reveals protein localisation within muscle fibres. **H.** Quantification of nuclei number per fibre. ***P<0.0001. Scale bars: 500 µm in A-D; 200 µm in D; 50 µm in E-G.

of activators still perturbs the system, and this is consistent with literature describing a similar effect for the activator *Rac1* (Geisbrecht et al 2008). However, reports from zebrafish where gain of function of fusion activators can lead to over-fusion (Landemaine et al 2014; Srinivas et al 2007) suggest there is a variable not accounted for in our system. Future experiments will focus on gain of function for potential inhibitors while instead performing loss of function (by the use of dominant negative forms, siRNAs or CRISPR-mediated knockdown, all performed in our lab) on candidate activators of fusion.

While the inducible system presented here allows for a very precise targeting of fusion events, it does not account for the heterogeneity present within cell populations. For example, when candidate genes are expressed at E3.5 by the addition of doxycycline, a large number of targeted cells are about to initiate fusion. However, within that population there is also a significant amount of progenitor cells that have not yet reached that stage of differentiation. Therefore, any effect the genes could have on progenitors prior to fusion will still produce a phenotype. In order to solve this, the inducible-system presented here must be combined with specific-promoters that target myogenic cells after cell-cycle arrest but prior to fusion (see figure 1.11). This combination would allow for the highly precise spatial and temporal targeting of fusing populations provided by specific promoters, while still allowing the experimental plasticity conveyed by the inducible system. To date, candidate promoters include myogenin, tmem8c (as described in Millay et al 2014) and 503unc, a very strong zebrafish minimal promoter (Berger & Currie 2013) that is first detected in differentiated fibres prior to fusion.

Even considering the current limitations presented above, the preliminary results shown here pose some interesting points, especially when considering virtually unknown genes like *Tmem47* or *Reep1*. TMEM47 is a member of the Claudin family, and it likely works as an adhesion molecule more similar to TMEM8c and known *Drosophila* fusion anchor-proteins like *Sns* or *Kirre*. In contrast, the known function of REEP1 is to act as a transporter of olfactory receptors to the membrane, therefore enhancing their function (Behrens et al 2006), and this may be a crucial behaviour. Given the nature of the fusion process, it is likely that receptors are needed not only for the anchoring of cells to each other, but also to communicate and find each other. Olfactory receptors are likely candidates for this process; indeed one (MOR23) has been linked to muscle regeneration by mediating migration and anchoring (Griffin et al 2009). This theory also fits the data presented in chapter 3, as cells from the different borders could be "talking" to each other when deciding with which partner to fuse.

# 5 Conclusion

During the course of my PhD studies, I aimed to investigate cellular processes occurring during early vertebrate muscle formation. While studying the cell-fate decision that cells go through to either proliferate or differentiate, I uncovered a novel molecular module that requires pathways to interact in non-canonical ways. Furthermore, this module could potentially be present not only in muscle cells, but in various tissues and cell types active during growth and disease. These are exciting results that go beyond the narrow approach that experimental hypotheses tend to focus on. In the process, I learned to follow the data and trust the results even when they do not conform to what "textbook " knowledge indicates.

At the same time, I investigated cellular interactions occurring during myoblast fusion and again, found that, contrary to my initial hypotheses, cells behave and fuse differently depending on which partners they interact with. The use of the chick as a model allowed me to investigate these and other questions throughout my studies, and it proved to be a very flexible but solid model to work on. As demonstrated by the research on the NOTCH/Wnt signalling module, dozens of different constructs were used, each tailored to a specific purpose, within a reasonable timeframe, because of the speed this model allows us to work in. Similarly, investigating the fusing behaviour of each of the dermomyotome lips was possible only because of the physical properties of electroporation and the directed targeting that it allows, as there are currently no promoters specific for each of the regions. The functional testing of potential candidate fusion genes should also benefit form this model, as again the speed at which experiments can go from planning to result allows for a great deal of testing, and importantly, troubleshooting.

The skills I learned during my studies are invaluable and will prove crucial to me throughout my scientific career. As I learned by the use of the chick embryo, it is important to use the strengths of each model to extract the most out of its potential and importantly, have the right answers by asking the right questions. I have attempted to do so during the course of this thesis, and will continue doing so in projects to come.

# 6 METHODS

## 6.1 Animal Model

Fertilised eggs from 35-36 week-old Hy-line Brown domestic hens (*Gallus gallus*) were obtained from Hy-line Australia Pty Ltd (Huntly, Victoria) and stored at 18˚C, to maintain embryos at stage 0 of development. Eggs were placed within fan-forced incubators at high humidity (95%) at 38.5˚C to induce development and removed at specific time-points for experimental purposes. Embryos were staged according to Hamburger and Hamilton embryonic chicken growth table (Hamburger & Hamilton 1992). For electroporation of neural tube and neural crest cells, embryos at stage 11-12 were used (48 hours of incubation). For electroporation of somite structures, embryos at stages 15-16 were used (60 hours of incubation).

## 6.2 *In ovo* Electroporation technique

### 6.2.1 Preparation of Eggs

Eggs were handled according to routine protocols (Stern & Holland 1993). 4-5 ml of albumin was removed from the incubated eggs and the eggshell windowed. India Ink (Lefranc & Bourgeois, diluted 1/10 in Ringer's solution+antibiotics, see Reagents) was injected underneath the embryo to allow visualisation. The vitelline membrane above the embryo was removed with a 31G needle (BD Medical) pressed into a hook shape.

### 6.2.2 DNA injection

Borosilicate glass capillaries (GC120T-10, Harvard Apparatus) were drawn on a P-2000 laser puller (Sutter Instrument). The tip was removed to create an opening and the capillary's blunt end was then attached to a rubber tube. DNA solution (see Reagents) was aspired into the capillary by mouth. To perform the injection, the capillary was inserted into either the neural tube or somites (depending on the experiment) at the level of anterior segmental plate and pushed towards the anterior end end of the embryo. DNA was injected into the entire neural cavity (for neural tube) or somitocoele (for somite) by mouth pressure while the needle was

removed. For somite injection, the 4 most recently formed somites were targeted. To target forelimb-level structures, somites 16-21 were injected. DNA solution was injected until each cavity was completely filled.

### 6.2.3 Electroporation

Approximately 300 ml of Ringer's solution+antibiotic was added to the embryo surface. Positive (Platinum) and negative (Tunsgsten) electrodes were placed on either side of the embryo (for detailed description of the positioning of the electrodes see (Scaal et al 2004)). The location of the electrodes varied depending on the area to be targeted (DNA will move towards the positive pole). 2-3 electric pulses were delivered with a TSS20 Ovodyne electroporator and an EP21 current amplifier (Intracel). Pulses were 10 msec wide and voltage varied depending on stage and experimental procedure: 25-35 volts were used for neural tube structures, 35-45 volts for the dorsal dermomyotome and 55-65 volts for the somite borders. Voltage was lowered by 5-10 volts when performing two electroporations on the same embryo. Following electroporation, eggshell windows were re-sealed with standard packaging tape (Staples) and returned to incubators for the specified time.

## 6.3 Doxycycline injections

In order to activate doxycycline-mediated expression of electroporated plasmids, a 3 μg/ml doxycycline/PBS (or Ringer) solution was used. Electroporated eggs were windowed and 200-500 ml of doxycycline solution was delivered onto the embryo. If doxycycline pulses were performed for longer than 1 day, an extra dosage of the antibiotic was added every 24 hours until embryo collection.

## 6.4 Whole-mount In Situ Hybridisation (ISH)

Probes for ISH were obtained from BBSRC ChickEST database (Boardman et al 2002). Plasmid DNA containing the EST sequence was digested with NotI (NEB) using standard protocols, electrophoresed and purified from 1% agarose/TBE gel using the Nucleospin PCR and Gel extraction kit (Macherey-Nagel). Probe synthesis

was performed through standard protocols using T3 RNA polymerase (NEB) and stored at -20˚C before use.

ISH protocols were performed essentially as previously described (Henrique et al 1995). Embryos were fixed in 4% formaldehyde (Sigma) then passed through a series of dehydration steps of 25%, 50% and then 75% methanol/PBT solutions. Embryos were then treated with Proteinase K (20 µg/ml, Promega) for 20 mins followed by fixation in 4% formaldehyde+0.1% glutaraldehyde (Sigma) for 20mins. Embryos were washed in PBT and then placed in 1:1 PBT/Hybridisation mix (see Reagents). Three washes in 100% Hybridisation mix were performed before the embryos were incubated at 65˚C overnight in hybridisation mix containing the DIG-tagged RNA probe (10 µl/ml).

After overnight incubation, embryos were washed 2-3 times at 65˚C in hybridisation mix. Then placed in a 1:1 hybridisation mix/MABT solution (see Reagents) at the same temperature. Washes at RT (3-4X) in 100% MABT were followed by a 1 hour incubation in MABT+2% BBR+20% heat-treated serum. Embryos were then transferred to the same solution containing a 1/2000 dilution of anti-DIG-AP antibody (Roche) and incubated overnight at 4˚C or 6 hours at RT.

Embryos were then rinsed at least 3 times in MABT, transferred to 12-well plates covered with aluminium foil and washed 2 times in NTMT solution (see Reagents). After washes the embryos were placed in 1.5 ml NTMT+6.6 µl/ml NBT (Roche)+3.3 µl/ml BCIP (Roche) at RT for at least 30 mins or up to 2 days, until the signal developed. When the desired colour was apparent, embryos were rinsed and washed in PBT. Pictures of whole-mount ISH-stained embryos were obtained on a Zeiss Discovery.V20 microscope equipped with an AxioCam camera and AxioVision software (Zeiss).

## 6.5 Whole-mount Immunohistochemistry

Embryos were dissected in PBS and fixed at 4˚C for 1-2 hours in 4% formaldehyde/PBT (timing varied depending on the antibody used). Then washed in PBT and placed at RT in blocking solution (see Reagents) for at least an hour.

Embryos were then placed in blocking solution containing primary antibodies at 4˚C overnight. The following day embryos were washed at least 4 times in blocking solution and then placed in blocking solution containing secondary antibodies at 4˚C overnight. The following day, embryos were transferred to PBT and washed more than 4 times for at least one day until background signal has disappeared.

## 6.6 Imaging and analysis

Stained embryos were placed in 80% glycerol/PBT solution until tissues were clear and the embryos sank. For mounting, layers of scotch tape were added to a glass slide (Menzel-Gläser) until the desired thickness was achieved. A window was cut and the embryo along with some glycerol solution was placed within the window. A #1.5 coverslip (Menzel-Gläser) was then placed on top and sealed with further tape.

Confocal microscopy was performed at Monash Micro Imaging (MMI, Clayton, Victoria) on an inverted Leica SP5 5-channel confocal microscope with LAS software (Leica). Scanning resonance was used with a scanning speed of 8000 Hertz, laser power at approximately 20% and frame averaging set at 8-16. For tissues larger than the field of view tile scanning and digital stitching were used. Objectives used were: 20 X multi-immersion NA 0.7, 40 X oil NA 1.25 and 63 X glycerol NA 1.3.

Confocal stack images were analysed using Imaris (Bitplane). For quantifications, the cell-counter plugin (Kurt De Vos) on ImageJ (NIH) was used. Images were adjusted for contrast and cropped using Adobe Photoshop CS5.1. Statistical analyses were performed using Prism software (GraphPad), with a p-value of $<0.5$ regarded as significant. Figures, diagrams and graphs were created using Adobe Illustrator CS5.1.

## 6.7 Molecular Biology

### 6.7.1 Cloning

The expression vectors created during the course of these studies, along with previously described vectors, are detailed in the methods sections of chapters 2 and 3. In chapter 4, the following vectors were created:

-pTol2 CAGGS NLSmCherry IRES rtTa

-pTol2 pBI GFPcaax DN-Rac1-HA

-pTol2 pBI GFPcaax CA-Rac1-HA

-pTol2 pBI GFPcaax DN-Cdc42-HA

-pTol2 pBI GFPcaax mTmem47-HA

-pTol2 pBI GFPcaax mSgcd-HA

-pTol2 pBI GFPcaax mRab39-HA

-pTol2 pBI GFPcaax mBag3-HA

-pTol2 pBI GFPcaax mReep1-HA

The vector pTol2 CAGGS NLSmCherry IRES rtTa was created by replacing the GFPcaax from pTol2 CAGGS NLSmCherry IRES GFPcaax (as described in chapter 3) with an rtTA Advanced (Clontech) coding sequence. pTol2 pBI GFPcaax XXX-HA were created by replacing the pTol2 pBI GFPcaax NICD-HA (as described in chapter 2) with the mouse full coding sequences obtained from I.M.A.G.E consortium (University of Iowa).

Vectors were either created using standard cloning techniques or the Gibson cloning protocols (NEB), which works by joining multiple overlapping DNA fragments in a single reaction (Gibson et al 2009, 2010).

Successfully assembled vectors were analysed by colony PCR and verified by sequencing (Monash Micromon DNA Sequencing Facility, Clayton, Victoria) following purification of DNA using the Nucleobond MaxiPrep DNA purification Kit

(Macherey-Nagel). DNA for electroporations was dissolved in MQ sterile water at approximately 7.5 μg/μl.

## 6.8 Reagents

1X Ringer's solution (5000 ml)

-36 g NaCl
-1.2 g $CaCl_2.2H_2O$
-18 g KCl
-rest sterile water

Add 1/25 Penicillin/Streptomycin stock for antibiotic

1X DNA solution (15 µl)

-15 µg DNA plasmid
-2.5 µl 1% high viscosity carboxylmethylcellulose
-0.75 µl 20% fast green dye
-0.3 µl 50 mM $MgCl_2$
-1.5 µl 10X PBS
-rest sterile water

1X Hybridisation mix (500 ml)

-250 ml formamide ultrapure
-32.5 ml 20x SSC pH 5
-5 ml 0.5 M EDTA pH 8
-1.25 ml sterile water + 1 g Yeast RNA
-1 ml Tween-20
-2.5 g CHAPS
-50 mg heparin sodium
-rest sterile water
pH to 7.5 (using Tris in powder form)

1X MABT (1000 ml)

-11.6 g Maleic acid
-8.7 g NaCl
-10 ml Tween-20
-rest sterile water

1X NTMT (50 ml)

| | |
|---|---|
| -1 ml | 1M NaCl |
| -5 ml | 1M TrisHCl pH 9.5 |
| -2.5 ml | 1M $MgCl_2$ |
| -500 µl | tween-20 |
| -rest | sterile water |

1X Blocking solution

| | |
|---|---|
| -1 g | BSA |
| -500 µl | Triton |
| -500 µl | SDS 20% |
| -50 ml | 10X PBS |
| -rest | sterile water |

# 7 REFERENCES

Abramovici, H & Gee, SH 2007, "Morphological changes and spatial regulation of diacylglycerol kinase-zeta, syntrophins, and rac1 during myoblast fusion.," *Cell motility and the cytoskeleton*, vol. 64, no. 7, pp. 549–67.

Adamo, S, Zani, B, Siracusa, G & Molinaro, M 1976, "Expression of differentiative traits in the absence of cell fusion during myogenesis in culture.," *Cell differentiation*, vol. 5, no. 1, pp. 53–67.

Akizawa, Y, Kanno, H, Kawamichi, Y, Matsuda, Y, et al 2013, "Enhanced expression of myogenic differentiation factors and skeletal muscle proteins in human amnion-derived cells via the forced expression of myod1.," *Brain & development*, vol. 35, no. 4, pp. 349–55.

Andrés, V & Walsh, K 1996, "Myogenin expression, cell cycle withdrawal, and phenotypic differentiation are temporally separable events that precede cell fusion upon myogenesis.," *The Journal of cell biology*, vol. 132, no. 4, pp. 657–66.

Angerer, LM & Angerer, RC 2003, "Patterning the sea urchin embryo: gene regulatory networks, signaling pathways, and cellular interactions.," *Current topics in developmental biology*, vol. 53, pp. 159–98.

Aoyama, H & Asamoto, K 1988, "Determination of somite cells: independence of cell differentiation and morphogenesis.," *Development (Cambridge, England)*, vol. 104, no. 1, pp. 15–28.

Artero, RD, Castanon, I & Baylies, MK 2001, "The immunoglobulin-like protein hibris functions as a dose-dependent regulator of myoblast fusion and is differentially controlled by ras and notch signaling.," *Development (Cambridge, England)*, vol. 128, no. 21, pp. 4251–64.

Baas, D, Caussanel-Boude, S, Guiraud, A, Calhabeu, F, et al 2012, "Ckip-1 regulates mammalian and zebrafish myoblast fusion.," *Journal of cell science*, vol. 125, no. Pt 16, pp. 3790–800.

Bach, A-SS, Enjalbert, S, Comunale, F, Bodin, S, et al 2010, "Adp-ribosylation factor 6 regulates mammalian myoblast fusion through phospholipase d1 and phosphatidylinositol 4,5-bisphosphate signaling pathways.," *Molecular biology of the cell*, vol. 21, no. 14, pp. 2412–24.

Bajard, L, Relaix, F, Lagha, M, Rocancourt, D, et al 2006, "A novel genetic hierarchy functions during hypaxial myogenesis: pax3 directly activates myf5 in muscle progenitor cells in the limb.," *Genes & development*, vol. 20, no. 17, pp. 2450–64.

Bardeen, CR 1900, "The development of the musculature of the body wall in the pig," *Johns Hopkins Hosp. Rep*, vol. 9, pp. 367–399.

Barrallo-Gimeno, A & Nieto, MA 2005, "The snail genes as inducers of cell movement and survival: implications in development and cancer.," *Development (Cambridge, England)*, vol. 132, no. 14, pp. 3151–61.

Bate, M 1990, "The embryonic development of larval muscles in drosophila.," *Development (Cambridge, England)*, vol. 110, no. 3, pp. 791–804.

Batlle, E, Sancho, E, Francí, C & Domínguez, D 2000, "The transcription factor snail is a repressor of e-cadherin gene expression in epithelial tumour cells,".

Baylies, M & Bate, M 1996, "Twist: a myogenic switch in drosophila," *Science*.

Bayne, EK & Simpson, SB 1977, "Detection of myosin in prefusion g0 lizard myoblasts in vitro.," *Developmental biology*, vol. 55, no. 2, pp. 306–19.

Beauchamp, JR, Heslop, L, Yu, DS, Tajbakhsh, S, et al 2000, "Expression of cd34 and myf5 defines the majority of quiescent adult skeletal muscle satellite cells.," *The Journal of cell biology*, vol. 151, no. 6, pp. 1221–34.

Beco, S, Gueudry, C, Amblard, F & Coscoy, S 2009, "Endocytosis is required for e-cadherin redistribution at mature adherens junctions," *Proceedings of the National Academy of Sciences*, vol. 106, no. 17, pp. 7010–7015.

Behrens, J, von Kries, JP, Kühl, M, Bruhn, L, et al 1996, "Functional interaction of beta-catenin with the transcription factor lef-1.," *Nature*, vol. 382, no. 6592, pp. 638–42.

Behrens, M, Bartelt, J, Reichling, C, Winnig, M, et al 2006, "Members of rtp and reep gene families influence functional bitter taste receptor expression.," *The Journal of biological chemistry*, vol. 281, no. 29, pp. 20650–9.

Berger, J & Currie, PD 2013, "503unc, a small and muscle-specific zebrafish promoter.," *Genesis (New York, N.Y. : 2000)*, vol. 51, no. 6, pp. 443–7.

Bianchi, E, Doe, B, Goulding, D & Wright, GJ 2014, "Juno is the egg izumo receptor and is essential for mammalian fertilization.," *Nature*, vol. 508, no. 7497, pp. 483–7.

Bischoff, R & Heintz, C 1994, "Enhancement of skeletal muscle regeneration.," *Developmental dynamics : an official publication of the American Association of Anatomists*, vol. 201, no. 1, pp. 41–54.

Bjornson, CRR, Cheung, TH, Liu, L, Tripathi, PV, et al 2012, "Notch signaling is necessary to maintain quiescence in adult muscle stem cells.," *Stem cells (Dayton, Ohio)*, vol. 30, no. 2, pp. 232–42.

Bladt, F, Riethmacher, D, Isenmann, S, Aguzzi, A & Birchmeier, C 1995, "Essential role for the c-met receptor in the migration of myogenic precursor cells into the limb bud.," *Nature*, vol. 376, no. 6543, pp. 768–71.

Blais, A, Tsikitis, M, Acosta-Alvear, D, Sharan, R, et al 2005, "An initial blueprint for myogenic differentiation.," *Genes & development*, vol. 19, no. 5, pp. 553–69.

Blond, JL, Lavillette, D, Cheynet, V & Bouton, O 2000, "An envelope glycoprotein of the human endogenous retrovirus herv-w is expressed in the human placenta and fuses cells expressing the type d mammalian …," *Journal of …*, accessed from <http://jvi.asm.org/content/74/7/3321.short>.

Boardman, PE, Sanz-Ezquerro, J, Overton, IM, Burt, DW, et al 2002, "A comprehensive collection of chicken cdnas.," *Current biology : CB*, vol. 12, no. 22, pp. 1965–9.

Bober, E, Lyons, GE, Braun, T, Cossu, G, et al 1991, "The muscle regulatory gene, myf-6, has a biphasic pattern of expression during early mouse development.," *The Journal of cell biology*, vol. 113, no. 6, pp. 1255–65.

Bois, PR, Brochard, VF, Salin-Cantegrel, AV, Cleveland, JL & Grosveld, GC 2005, "Foxo1a-cyclic gmp-dependent kinase i interactions orchestrate myoblast fusion.," *Molecular and cellular biology*, vol. 25, no. 17, pp. 7645–56.

Bois, PR & Grosveld, GC 2003, "Fkhr (foxo1a) is required for myotube fusion of primary mouse myoblasts.," *The EMBO journal*, vol. 22, no. 5, pp. 1147–57.

Borello, U, Berarducci, B, Murphy, P, Bajard, L, et al 2006, "The wnt/beta-catenin pathway regulates gli-mediated myf5 expression during somitogenesis.," *Development (Cambridge, England)*, vol. 133, no. 18, pp. 3723–32.

Bothe, I, Deng, S & Baylies, M 2014, "Pi(4,5)p2 regulates myoblast fusion through arp2/3 regulator localization at the fusion site.," *Development (Cambridge, England)*, vol. 141, no. 11, pp. 2289–301.

Bour, BA, Chakravarti, M & West…, JM 2000, "Drosophila sns, a member of the immunoglobulin superfamily that is essential for myoblast fusion," *Genes & …*, accessed from <http://genesdev.cshlp.org/content/14/12/1498.short>.

Bovolenta, P, Esteve, P, Ruiz, JM, Cisneros, E & Lopez-Rios, J 2008, "Beyond wnt inhibition: new functions of secreted frizzled-related proteins in development and disease.," *Journal of cell science*, vol. 121, no. Pt 6, pp. 737–46.

Boyd, JD 1960, "Development of striated muscle," in New York: Academic Press, Inc, p. 72.

Brack, AS, Conboy, IM, Conboy, MJ, Shen, J & Rando, TA 2008, "A temporal switch from notch to wnt signaling in muscle stem cells is necessary for normal adult myogenesis.," *Cell stem cell*, vol. 2, no. 1, pp. 50–9.

Braun, T & Arnold, HH 1995, "Inactivation of myf-6 and myf-5 genes in mice leads to alterations in skeletal muscle development.," *The EMBO journal*, vol. 14, no. 6, pp. 1176–86.

Braun, T, Bober, E, Winter, B, Rosenthal, N & Arnold, HH 1990, "Myf-6, a new member of the human gene family of myogenic determination factors: evidence for a gene cluster on chromosome 12.," *The EMBO journal*, vol. 9, no. 3, pp. 821–31.

Braun, T, Buschhausen-Denker, G, Bober, E, Tannich, E & Arnold, HH 1989, "A novel human muscle factor related to but distinct from myod1 induces myogenic conversion in 10t1/2 fibroblasts.," *The EMBO journal*, vol. 8, no. 3, pp. 701–9.

Braun, T, Rudnicki, MA, Arnold, HH & Jaenisch, R 1992, "Targeted inactivation of the muscle regulatory gene myf-5 results in abnormal rib development and perinatal death.," *Cell*, vol. 71, no. 3, pp. 369–82.

Brennan, K, Sanders, P, Balayo, T & DasGupta, R 2005, "Notch modulates wnt signalling by associating with armadillo/β-catenin and regulating its transcriptional activity," …, accessed from <http://dev.biologists.org/content/132/8/1819.short>.

Brohmann, H, Jagla, K & Birchmeier, C 2000, "The role of lbx1 in migration of muscle precursor cells.," *Development (Cambridge, England)*, vol. 127, no. 2, pp. 437–45.

Bryson-Richardson, RJ & Currie, PD 2008, "The genetics of vertebrate myogenesis.," *Nature reviews. Genetics*, vol. 9, no. 8, pp. 632–46.

Buckingham, M 2006, "Myogenic progenitor cells and skeletal myogenesis in vertebrates.," *Current opinion in genetics & development*, vol. 16, no. 5, pp. 525–32.

Buckingham, M 1996, "Skeletal muscle development and the role of the myogenic regulatory factors.," *Biochemical Society transactions*, vol. 24, no. 2, pp. 506–9.

Buckingham, M, Bajard, L & Chang…, T 2003, "The formation of skeletal muscle: from somite to limb," *Journal of …*, accessed from <http://onlinelibrary.wiley.com/doi/10.1046/j.1469-7580.2003.00139.x/full>.

Bulchand, S, Menon, SD, George, SE & Chia, W 2010, "The intracellular domain of dumbfounded affects myoblast fusion efficiency and interacts with rolling pebbles and loner.," *PloS one*, vol. 5, no. 2, p. e9374.

Bullough, PA, Hughson, FM, Skehel, JJ & Wiley, DC 1994, "Structure of influenza haemagglutinin at the ph of membrane fusion.," *Nature*, vol. 371, no. 6492, pp. 37–43.

Cabrera, CV, Alonso, MC, Johnston, P, Phillips, RG & Lawrence, PA 1987, "Phenocopies induced with antisense rna identify the wingless gene.," *Cell*, vol. 50, no. 4, pp. 659–63.

Carmon, KS, Gong, X & Lin, Q 2011, "R-spondins function as ligands of the orphan receptors lgr4 and lgr5 to regulate wnt/β-catenin signaling,".

Carr, CM, Chaudhry, C & Kim, PS 1997, "Influenza hemagglutinin is spring-loaded by a metastable native conformation.," *Proceedings of the National Academy of Sciences of the United States of America*, vol. 94, no. 26, pp. 14306–13.

Chargé, SB & Rudnicki, MA 2004, "Cellular and molecular regulation of muscle regeneration.," *Physiological reviews*, vol. 84, no. 1, pp. 209–38.

Charlton, CA, Mohler, WA & Blau, HM 2000, "Neural cell adhesion molecule (ncam) and myoblast fusion.," *Developmental biology*, vol. 221, no. 1, pp. 112–9.

Charrasse, S, Comunale, F, Fortier, M, Portales-Casamar, E, et al 2007, "M-cadherin activates rac1 gtpase through the rho-gef trio during myoblast fusion.," *Molecular biology of the cell*, vol. 18, no. 5, pp. 1734–43.

Charrasse, S, Comunale, F, Grumbach, Y, Poulat, F, et al 2006, "Rhoa gtpase regulates m-cadherin activity and myoblast fusion.," *Molecular biology of the cell*, vol. 17, no. 2, pp. 749–59.

Charrasse, S, Comunale, F, De Rossi, S, Echard, A & Gauthier-Rouvière, C 2013, "Rab35 regulates cadherin-mediated adherens junction formation and myoblast fusion.," *Molecular biology of the cell*, vol. 24, no. 3, pp. 234–45.

Charrasse, S, Meriane, M, Comunale, F, Blangy, A & Gauthier-Rouvière, C 2002, "N-cadherin-dependent cell-cell contact regulates rho gtpases and beta-catenin localization in mouse c2c12 myoblasts.," *The Journal of cell biology*, vol. 158, no. 5, pp. 953–65.

Charrier-Savournin, FB, Château, M-TT, Gire, V, Sedivy, J, et al 2004, "P21-mediated nuclear retention of cyclin b1-cdk1 in response to genotoxic stress.," *Molecular biology of the cell*, vol. 15, no. 9, pp. 3965–76.

Chen, EH & Olson, EN 2001, "Antisocial, an intracellular adaptor protein, is required for myoblast fusion in drosophila.," *Developmental cell*, vol. 1, no. 5, pp. 705–15, accessed from <http://linkinghub.elsevier.com/retrieve/pii/S1534-5807(01)00084-3>.

Chen, EH, Pryce, BA, Tzeng, JA, Gonzalez, GA & Olson, EN 2003, "Control of myoblast fusion by a guanine nucleotide exchange factor, loner, and its effector arf6.," *Cell*, vol. 114, no. 6, pp. 751–62, accessed from <http://linkinghub.elsevier.com/retrieve/pii/S0092867403007207>.

Chen, W, ten Berge, D, Brown, J, Ahn, S, et al 2003, "Dishevelled 2 recruits beta-arrestin 2 to mediate wnt5a-stimulated endocytosis of frizzled 4.," *Science (New York, N.Y.)*, vol. 301, no. 5638, pp. 1391–4.

Chernomordik, L, Zimmerberg, J & Kozlov, M 2006, "Membranes of the world unite!," *The Journal of Cell Biology*, vol. 175, no. 2, pp. 201–207.

Chernomordik, LV, Vogel, SS, Sokoloff, A, Onaran, HO, et al 1993, "Lysolipids reversibly inhibit ca(2+)-, gtp- and ph-dependent fusion of biological membranes.," *FEBS letters*, vol. 318, no. 1, pp. 71–6.

Chevallier, A, Kieny, M & Mauger, A 1977, "Limb-somite relationship: origin of the limb musculature.," *Journal of embryology and experimental morphology*, vol. 41, pp. 245–58.

Choi, S-CC & Han, J-KK 2002, "Xenopus cdc42 regulates convergent extension movements during gastrulation through wnt/ca2+ signaling pathway.," *Developmental biology*, vol. 244, no. 2, pp. 342–57.

Christ, B, Jacob, HJ & Jacob, M 1977, "Experimental analysis of the origin of the wing musculature in avian embryos.," *Anatomy and embryology*, vol. 150, no. 2, pp. 171–86.

Christ, B, Jacob, M & Jacob, HJ 1983, "On the origin and development of the ventrolateral abdominal muscles in the avian embryo. an experimental and ultrastructural study.," *Anatomy and embryology*, vol. 166, no. 1, pp. 87–101.

Christ, B & Ordahl, CP 1995, "Early stages of chick somite development.," *Anatomy and embryology*, vol. 191, no. 5, pp. 381–96.

Christophe-Hobertus, C, Szpirer, C, Guyon, R & Christophe, D 2001, "Identification of the gene encoding brain cell membrane protein 1 (bcmp1), a putative four-transmembrane protein distantly related to the peripheral myelin protein 22 / epithelial membrane proteins and the claudins.," *BMC genomics*, vol. 2, p. 3.

Cifuentes-Diaz, C, Nicolet, M, Alameddine, H, Goudou, D, et al 1995, "M-cadherin localization in developing adult and regenerating mouse skeletal muscle: possible involvement in secondary myogenesis.," *Mechanisms of development*, vol. 50, no. 1, pp. 85–97.

Cinnamon, Y, Kahane, N, Bachelet, I & Kalcheim, C 2001, "The sub-lip domain--a distinct pathway for myotome precursors that demonstrate rostral-caudal migration.," *Development (Cambridge, England)*, vol. 128, no. 3, pp. 341–51.

Coleman, ME, DeMayo, F, Yin, KC, Lee, HM, et al 1995, "Myogenic vector expression of insulin-like growth factor i stimulates muscle cell differentiation and myofiber hypertrophy in transgenic mice.," *The Journal of biological chemistry*, vol. 270, no. 20, pp. 12109–16.

Collu, GM, Hidalgo-Sastre, A, Acar, A, Bayston, L, et al 2013, "Dishevelled limits notch signalling through inhibition of csl.," *Development (Cambridge, England)*, vol. 139, no. 23, pp. 4405–15.

Conboy, IM, Conboy, MJ, Smythe, GM & Rando, TA 2003, "Notch-mediated restoration of regenerative potential to aged muscle.," *Science (New York, N.Y.)*, vol. 302, no. 5650, pp. 1575–7.

Conboy, IM & Rando, TA 2002, "The regulation of notch signaling controls satellite cell activation and cell fate determination in postnatal myogenesis.," *Developmental cell*, vol. 3, no. 3, pp. 397–409.

Cooke, J 1975, "Control of somite number during morphogenesis of a vertebrate, xenopus laevis.," *Nature*, vol. 254, no. 5497, pp. 196–9.

Cooke, J & Zeeman, EC 1976, "A clock and wavefront model for control of the number of repeated structures during animal morphogenesis.," *Journal of theoretical biology*, vol. 58, no. 2, pp. 455–76.

Cordle, J, Johnson, S, Tay, JZ, Roversi, P, et al 2008, "A conserved face of the jagged/serrate dsl domain is involved in notch trans-activation and cis-inhibition.," *Nature structural & molecular biology*, vol. 15, no. 8, pp. 849–57.

Cordle, J, Redfieldz, C, Stacey, M, van der Merwe, PA, et al 2008, "Localization of the delta-like-1-binding site in human notch-1 and its modulation by calcium affinity.," *The Journal of biological chemistry*, vol. 283, no. 17, pp. 11785–93.

Cui, W, Cuartas, E, Ke, J, Zhang, Q, et al 2007, "Cd200 and its receptor, cd200r, modulate bone mass via the differentiation of osteoclasts.," *Proceedings of the National Academy of Sciences of the United States of America*, vol. 104, no. 36, pp. 14436–41.

Dahl, E, Koseki, H & Balling, R 1997, "Pax genes and organogenesis.," *BioEssays : news and reviews in molecular, cellular and developmental biology*, vol. 19, no. 9, pp. 755–65.

Dale, JK, Malapert, P, Chal, J, Vilhais-Neto, G, et al 2006, "Oscillations of the snail genes in the presomitic mesoderm coordinate segmental patterning and morphogenesis in vertebrate somitogenesis.," *Developmental cell*, vol. 10, no. 3, pp. 355–66.

Daniels, DL & Weis, WI 2005, "Beta-catenin directly displaces groucho/tle repressors from tcf/lef in wnt-mediated transcription activation.," *Nature structural & molecular biology*, vol. 12, no. 4, pp. 364–71.

David, JD, See, WM & Higginbotham, CA 1981, "Fusion of chick embryo skeletal myoblasts: role of calcium influx preceding membrane union.," *Developmental biology*, vol. 82, no. 2, pp. 297–307.

Davis, RL, Weintraub, H & Lassar, AB 1987, "Expression of a single transfected cdna converts fibroblasts to myoblasts.," *Cell*, vol. 51, no. 6, pp. 987–1000.

Denetclaw, WF, Christ, B & Ordahl, CP 1997, "Location and growth of epaxial myotome precursor cells.," *Development (Cambridge, England)*, vol. 124, no. 8, pp. 1601–10.

Denetclaw, WF & Ordahl, CP 2000, "The growth of the dermomyotome and formation of early myotome lineages in thoracolumbar somites of chicken embryos.," *Development (Cambridge, England)*, vol. 127, no. 4, pp. 893–905.

Dennis, CL, Tinsley, JM, Deconinck, AE & Davies, KE 1996, "Molecular and functional analysis of the utrophin promoter.," *Nucleic acids research*, vol. 24, no. 9, pp. 1646–52.

Dequéant, M-LL & Pourquié, O 2008, "Segmental patterning of the vertebrate embryonic axis.," *Nature reviews. Genetics*, vol. 9, no. 5, pp. 370–82.

Derivery, E & Gautreau, A 2010, "Assaying wave and wash complex constitutive activities toward the arp2/3 complex.," *Methods in enzymology*, vol. 484, pp. 677–95.

Dietrich, S, Abou-Rebyeh, F, Brohmann, H, Bladt, F, et al 1999, "The role of sf/hgf and c-met in the development of skeletal muscle.," *Development (Cambridge, England)*, vol. 126, no. 8, pp. 1621–9.

Dietrich, S, Schubert, FR & Lumsden, A 1997, "Control of dorsoventral pattern in the chick paraxial mesoderm.," *Development (Cambridge, England)*, vol. 124, no. 19, pp. 3895–908.

Dockter, J & Ordahl, CP 2000, "Dorsoventral axis determination in the somite: a re-examination.," *Development (Cambridge, England)*, vol. 127, no. 10, pp. 2201–6.

Doherty, KR, Cave, A, Davis, DB, Delmonte, AJ, et al 2005, "Normal myoblast fusion requires myoferlin.," *Development (Cambridge, England)*, vol. 132, no. 24, pp. 5565–75.

Dottermusch-Heidel, C, Groth, V, Beck, L & Önel, S-FF 2012, "The arf-gef schizo/loner regulates n-cadherin to induce fusion competence of drosophila myoblasts.," *Developmental biology*, vol. 368, no. 1, pp. 18–27, accessed from <http://www.ncbi.nlm.nih.gov/pubmed/22595515>.

Dupressoir, A & Marceau, G 2005, "Syncytin-a and syncytin-b, two fusogenic placenta-specific murine envelope genes of retroviral origin conserved in muridae," *Proceedings of the …*, accessed from <http://www.pnas.org/content/102/3/725.short>.

Duprez, D 2002, "Signals regulating muscle formation in the limb during embryonic development.," *The International journal of developmental biology*, vol. 46, no. 7, pp. 915–25.

Duquette, PM & Lamarche-Vane, N 2014, "Rho gtpases in embryonic development.," *Small GTPases*, vol. 5, no. 2, pp. 1–9.

Earp, LJ, Delos, SE, Park, HE & White, JM 2005, "The many mechanisms of viral membrane fusion proteins," *Membrane trafficking in viral …*, accessed from <http://link.springer.com/chapter/10.1007/3-540-26764-6_2>.

Eden, S, Rohatgi, R, Podtelejnikov, AV, Mann, M & Kirschner, MW 2002, "Mechanism of regulation of wave1-induced actin nucleation by rac1 and nck.," *Nature*, vol. 418, no. 6899, pp. 790–3.

Edmondson, DG & Olson, EN 1989, "A gene with homology to the myc similarity region of myod1 is expressed during myogenesis and is sufficient to activate the muscle differentiation program.," *Genes & development*, vol. 3, no. 5, pp. 628–40.

Van den Eijnde, SM, van den Hoff, MJ, Reutelingsperger, CP, van Heerde, WL, et al 2001, "Transient expression of phosphatidylserine at cell-cell contact areas is required for myotube formation.," *Journal of cell science*, vol. 114, no. Pt 20, pp. 3631–42.

Emerson, CP 1990, "Myogenesis and developmental control genes.," *Current opinion in cell biology*, vol. 2, no. 6, pp. 1065–75.

Enwere, EK, Holbrook, J, Lejmi-Mrad, R, Vineham, J, et al 2012, "Tweak and ciap1 regulate myoblast fusion through the noncanonical nf-κb signaling

pathway.," *Science signaling*, vol. 5, no. 246, p. ra75, accessed from <http://www.ncbi.nlm.nih.gov/pubmed/23074266>.

Epstein, JA, Shapiro, DN, Cheng, J, Lam, PY & Maas, RL 1996, "Pax3 modulates expression of the c-met receptor during limb muscle development.," *Proceedings of the National Academy of Sciences of the United States of America*, vol. 93, no. 9, pp. 4213–8.

Erickson, MR, Galletta, BJ & Abmayr, SM 1997, "Drosophila myoblast city encodes a conserved protein that is essential for myoblast fusion, dorsal closure, and cytoskeletal organization.," *The Journal of cell biology*, vol. 138, no. 3, pp. 589–603.

Espinosa, L, Inglés-Esteve, J, Aguilera, C & Bigas, A 2003, "Phosphorylation by glycogen synthase kinase-3 beta down-regulates notch activity, a link for notch and wnt pathways.," *The Journal of biological chemistry*, vol. 278, no. 34, pp. 32227–35.

Estrach, S, Ambler, CA, Lo Celso, C, Hozumi, K & Watt, FM 2006, "Jagged 1 is a beta-catenin target gene required for ectopic hair follicle formation in adult epidermis.," *Development (Cambridge, England)*, vol. 133, no. 22, pp. 4427–38.

Estrada, B, Maeland, AD, Gisselbrecht, SS, Bloor, JW, et al 2007, "The marvel domain protein, singles bar, is required for progression past the pre-fusion complex stage of myoblast fusion.," *Developmental biology*, vol. 307, no. 2, pp. 328–39.

Fadok, VA, Voelker, DR, Campbell, PA, Cohen, JJ, et al 1992, "Exposure of phosphatidylserine on the surface of apoptotic lymphocytes triggers specific recognition and removal by macrophages.," *Journal of immunology (Baltimore, Md. : 1950)*, vol. 148, no. 7, pp. 2207–16.

Fan, CM, Lee, CS & Tessier-Lavigne, M 1997, "A role for wnt proteins in induction of dermomyotome.," *Developmental biology*, vol. 191, no. 1, pp. 160–5.

Fasshauer, D 2003, "Structural insights into the snare mechanism.," *Biochimica et biophysica acta*, vol. 1641, no. 2-3, pp. 87–97.

Feig, LA 1999, "Tools of the trade: use of dominant-inhibitory mutants of ras-family gtpases.," *Nature cell biology*, vol. 1, no. 2, pp. E25–7.

Feng, Y, Broder, CC, Kennedy, PE & Berger, EA 1996, "Hiv-1 entry cofactor: functional cdna cloning of a seven-transmembrane, g protein-coupled receptor.," *Science (New York, N.Y.)*, vol. 272, no. 5263, pp. 872–7.

Foltz, DR, Santiago, MC, Berechid, BE & Nye, JS 2002, "Glycogen synthase kinase-3beta modulates notch signaling and stability.," *Current biology : CB*, vol. 12, no. 12, pp. 1006–11.

Franz, T, Kothary, R, Surani, MA, Halata, Z & Grim, M 1993, "The splotch mutation interferes with muscle development in the limbs.," *Anatomy and embryology*, vol. 187, no. 2, pp. 153–60.

Füchtbauer, EM 1995, "Expression of m-twist during postimplantation development of the mouse.," *Developmental dynamics : an official publication of the American Association of Anatomists*, vol. 204, no. 3, pp. 316–22.

De la Fuente, MA, Sasahara, Y, Calamito, M, Antón, IM, et al 2007, "Wip is a chaperone for wiskott-aldrich syndrome protein (wasp).," *Proceedings of the National Academy of Sciences of the United States of America*, vol. 104, no. 3, pp. 926–31.

Gallagher, TL, Arribere, JA, Geurts, PA & Exner, C 2011, "Rbfox-regulated alternative splicing is critical for zebrafish cardiac and skeletal muscle functions," *Developmental …*, accessed from <http://www.sciencedirect.com/science/article/pii/S0012160611012255>.

Galli, LM, Knight, SR, Barnes, TL, Doak, AK, et al 2008, "Identification and characterization of subpopulations of pax3 and pax7 expressing cells in developing chick somites and limb buds.," *Developmental dynamics : an official publication of the American Association of Anatomists*, vol. 237, no. 7, pp. 1862–74.

Geisbrecht, ER, Haralalka, S, Swanson, SK, Florens, L, et al 2008, "Drosophila elmo/ced-12 interacts with myoblast city to direct myoblast fusion and ommatidial organization.," *Developmental biology*, vol. 314, no. 1, pp. 137–49.

Gibbons, DL, Erk, I, Reilly, B, Navaza, J & Kielian, M 2003, "Visualization of the target-membrane-inserted fusion protein of semliki forest virus by combined electron microscopy and crystallography," *Cell*, accessed from <http://www.sciencedirect.com/science/article/pii/S0092867403006834>.

Gibralter, D & Turner, DC 1985, "Dual adhesion systems of chick myoblasts.," *Developmental biology*, vol. 112, no. 2, pp. 292–307.

Gibson, DG, Smith, HO, Hutchison, CA, Venter, JC & Merryman, C 2010, "Chemical synthesis of the mouse mitochondrial genome.," *Nature methods*, vol. 7, no. 11, pp. 901–3.

Gibson, DG, Young, L, Chuang, R-YY, Venter, JC, et al 2009, "Enzymatic assembly of dna molecules up to several hundred kilobases.," *Nature methods*, vol. 6, no. 5, pp. 343–5.

Gildor, B, Massarwa, R, Shilo, B-ZZ & Schejter, ED 2009, "The scar and wasp nucleation-promoting factors act sequentially to mediate drosophila myoblast fusion.," *EMBO reports*, vol. 10, no. 9, pp. 1043–50.

Glinka, A, Wu, W, Delius, H, Monaghan, AP, et al 1998, "Dickkopf-1 is a member of a new family of secreted proteins and functions in head induction.," *Nature*, vol. 391, no. 6665, pp. 357–62.

Gordon, WR, Roy, M, Vardar-Ulu, D, Garfinkel, M, et al 2009, "Structure of the notch1-negative regulatory region: implications for normal activation and pathogenic signaling in t-all.," *Blood*, vol. 113, no. 18, pp. 4381–90.

Goulding, MD, Chalepakis, G, Deutsch, U, Erselius, JR & Gruss, P 1991, "Pax-3, a novel murine dna binding protein expressed during early neurogenesis.," *The EMBO journal*, vol. 10, no. 5, pp. 1135–47.

Griffin, CA, Kafadar, KA & Pavlath, GK 2009, "Mor23 promotes muscle regeneration and regulates cell adhesion and migration.," *Developmental cell*, vol. 17, no. 5, pp. 649–61.

Grobet, L, Martin, LJ, Poncelet, D, Pirottin, D, et al 1997, "A deletion in the bovine myostatin gene causes the double-muscled phenotype in cattle.," *Nature genetics*, vol. 17, no. 1, pp. 71–4.

Gros, J, Manceau, M, Thomé, V & Marcelle, C 2005, "A common somitic origin for embryonic muscle progenitors and satellite cells.," *Nature*, vol. 435, no. 7044, pp. 954–8.

Gros, J, Scaal, M & Marcelle, C 2004, "A two-step mechanism for myotome formation in chick.," *Developmental cell*, vol. 6, no. 6, pp. 875–82.

Gros, J, Serralbo, O & Marcelle, C 2009, "Wnt11 acts as a directional cue to organize the elongation of early muscle fibres.," *Nature*, vol. 457, no. 7229, pp. 589–93.

Gross, MK, Moran-Rivard, L, Velasquez, T, Nakatsu, MN, et al 2000, "Lbx1 is required for muscle precursor migration along a lateral pathway into the limb.," *Development (Cambridge, England)*, vol. 127, no. 2, pp. 413–24.

Gruenbaum-Cohen, Y, Harel, I, Umansky, K-BB, Tzahor, E, et al 2012, "The actin regulator n-wasp is required for muscle-cell fusion in mice.," *Proceedings of the National Academy of Sciences of the United States of America*, vol. 109, no. 28, pp. 11211–6, accessed from <http://www.ncbi.nlm.nih.gov/pubmed/22736793>.

Gubb, D & García-Bellido, A 1982, "A genetic analysis of the determination of cuticular polarity during development in drosophila melanogaster.," *Journal of embryology and experimental morphology*, vol. 68, pp. 37–57.

Hacker, A & Guthrie, S 1998, "A distinct developmental programme for the cranial paraxial mesoderm in the chick embryo.," *Development (Cambridge, England)*, vol. 125, no. 17, pp. 3461–72.

Hakeda-Suzuki, S, Ng, J, Tzu, J, Dietzl, G, et al 2002, "Rac function and regulation during drosophila development.," *Nature*, vol. 416, no. 6879, pp. 438–42.

Hamburger, V & Hamilton, HL 1992, "A series of normal stages in the development of the chick embryo. 1951.," *Developmental dynamics : an official publication of the American Association of Anatomists*, vol. 195, no. 4, pp. 231–72.

Hamilton, HL 1952, Lillie's development of the chick, an introduction to embryology., Holt, Rinehart and Winston, New York.

Hammond, CL, Hinits, Y, Osborn, DP, Minchin, JE, et al 2007, "Signals and myogenic regulatory factors restrict pax3 and pax7 expression to dermomyotome-like tissue in zebrafish.," *Developmental biology*, vol. 302, no. 2, pp. 504–21.

Hamoud, N, Tran, V, Croteau, L-PP, Kania, A & Côté, J-FF 2014, "G-protein coupled receptor bai3 promotes myoblast fusion in vertebrates.," *Proceedings of the National Academy of Sciences of the United States of America*, vol. 111, no. 10, pp. 3745–50.

Han, X, Sterling, H, Chen, Y, Saginario, C, et al 2000, "Cd47, a ligand for the macrophage fusion receptor, participates in macrophage multinucleation.," *The Journal of biological chemistry*, vol. 275, no. 48, pp. 37984–92.

Hanson, PI, Otto, H, Barton, N & Jahn, R 1995, "The n-ethylmaleimide-sensitive fusion protein and alpha-snap induce a conformational change in syntaxin.," *The Journal of biological chemistry*, vol. 270, no. 28, pp. 16955–61.

Haralalka, S & Abmayr, SM 2010, "Myoblast fusion in drosophila.," *Experimental cell research*, vol. 316, no. 18, pp. 3007–13.

Haralalka, S, Shelton, C, Cartwright, HN, Katzfey, E, et al 2011, "Asymmetric mbc, active rac1 and f-actin foci in the fusion-competent myoblasts during myoblast fusion in drosophila.," *Development (Cambridge, England)*, vol. 138, no. 8, pp. 1551–62.

Hartmann, D, de Strooper, B, Serneels, L, Craessaerts, K, et al 2002, "The disintegrin/metalloprotease adam 10 is essential for notch signalling but

not for alpha-secretase activity in fibroblasts.," *Human molecular genetics*, vol. 11, no. 21, pp. 2615–24.

Hasty, P, Bradley, A, Morris, JH, Edmondson, DG, et al 1993, "Muscle deficiency and neonatal death in mice with a targeted mutation in the myogenin gene.," *Nature*, vol. 364, no. 6437, pp. 501–6.

Hayashi, K & Ozawa, E 1995, "Myogenic cell migration from somites is induced by tissue contact with medial region of the presumptive limb mesoderm in chick embryos.," *Development (Cambridge, England)*, vol. 121, no. 3, pp. 661–9.

He, X, Semenov, M, Tamai, K & Zeng, X 2004, "Ldl receptor-related proteins 5 and 6 in wnt/β-catenin signaling: arrows point the way,".

Heisenberg, CP, Tada, M, Rauch, GJ, Saúde, L, et al 2000, "Silberblick/wnt11 mediates convergent extension movements during zebrafish gastrulation.," *Nature*, vol. 405, no. 6782, pp. 76–81.

Helenius, A, Kartenbeck, J, Simons, K & Fries, E 1980, "On the entry of semliki forest virus into bhk-21 cells.," *The Journal of cell biology*, vol. 84, no. 2, pp. 404–20.

Helming, L & Gordon, S 2007, "Macrophage fusion induced by il-4 alternative activation is a multistage process involving multiple target molecules," *European journal of immunology*, accessed from <http://onlinelibrary.wiley.com/doi/10.1002/eji.200636788/full>.

Helming, L, Winter, J & Gordon, S 2009, "The scavenger receptor cd36 plays a role in cytokine-induced macrophage fusion," *Journal of cell science*, accessed from <http://jcs.biologists.org/content/122/4/453.short>.

Henrique, D, Adam, J, Myat, A, Chitnis, A, et al 1995, "Expression of a delta homologue in prospective neurons in the chick.," *Nature*, vol. 375, no. 6534, pp. 787–90.

Heymann, S, Koudrova, M, Arnold, H, Köster, M & Braun, T 1996, "Regulation and function of sf/hgf during migration of limb muscle precursor cells in chicken.," *Developmental biology*, vol. 180, no. 2, pp. 566–78.

Hinshaw, JE & Schmid, SL 1995, "Dynamin self-assembles into rings suggesting a mechanism for coated vesicle budding.," *Nature*, vol. 374, no. 6518, pp. 190–2.

Hoang, B, Moos, M, Vukicevic, S & Luyten, FP 1996, "Primary structure and tissue distribution of frzb, a novel protein related to drosophila frizzled, suggest a role in skeletal morphogenesis.," *The Journal of biological chemistry*, vol. 271, no. 42, pp. 26131–7.

Hollnagel, A, Grund, C, Franke, WW & Arnold, H-HH 2002, "The cell adhesion molecule m-cadherin is not essential for muscle development and regeneration.," *Molecular and cellular biology*, vol. 22, no. 13, pp. 4760–70.

Homma, S, Iwasaki, M, Shelton, GD, Engvall, E, et al 2006, "Bag3 deficiency results in fulminant myopathy and early lethality.," *The American journal of pathology*, vol. 169, no. 3, pp. 761–73.

Hoppler, S, Brown, JD & Moon, RT 1996, "Expression of a dominant-negative wnt blocks induction of myod in xenopus embryos.,".

Horsley, V, Friday, BB, Matteson, S, Kegley, KM, et al 2001, "Regulation of the growth of multinucleated muscle cells by an nfatc2-dependent pathway.," *The Journal of cell biology*, vol. 153, no. 2, pp. 329–38.

Horsley, V, Jansen, KM, Mills, ST & Pavlath, GK 2003, "Il-4 acts as a myoblast recruitment factor during mammalian muscle growth.," *Cell*, vol. 113, no. 4, pp. 483–94.

Horsley, V & Pavlath, GK 2004, "Forming a multinucleated cell: molecules that regulate myoblast fusion.," *Cells, tissues, organs*, vol. 176, no. 1-3, pp. 67–78.

Hsieh, JC, Kodjabachian, L, Rebbert, ML, Rattner, A, et al 1999, "A new secreted protein that binds to wnt proteins and inhibits their activities.," *Nature*, vol. 398, no. 6726, pp. 431–6.

Hu, C, Ahmed, M, Melia, TJ, Söllner, TH & Mayer, T 2003, "Fusion of cells by flipped snares," *Science*, accessed from <http://www.sciencemag.org/content/300/5626/1745.short>.

Huang, RY, Guilford, P & Thiery, JP 2012, "Early events in cell adhesion and polarity during epithelial-mesenchymal transition.," *Journal of cell science*, vol. 125, no. Pt 19, pp. 4417–22.

Huppertz, B, Bartz, C & Kokozidou, M 2006, "Trophoblast fusion: fusogenic proteins, syncytins and adams, and other prerequisites for syncytial fusion," *Micron*, accessed from <http://www.sciencedirect.com/science/article/pii/S0968432806000035>.

Hutagalung, AH & Novick, PJ 2011, "Role of rab gtpases in membrane traffic and cell physiology," *Physiological reviews*, vol. 91, no. 1, pp. 119–149, accessed from <http://physrev.physiology.org/content/91/1/119.short>.

Imhof, B, Zimmerli, C, Gliki, G, Ducrest-Gay, D, et al 2007, "Pulmonary dysfunction and impaired granulocyte homeostasis result in poor survival of jam-c-deficient mice," *The Journal of Pathology*, vol. 212.

Inoue, N, Hamada, D, Kamikubo, H, Hirata, K, et al 2013, "Molecular dissection of izumo1, a sperm protein essential for sperm-egg fusion.," *Development (Cambridge, England)*, vol. 140, no. 15, pp. 3221–9.

Inoue, N, Ikawa, M, Isotani, A & Okabe, M 2005, "The immunoglobulin superfamily protein izumo is required for sperm to fuse with eggs.," *Nature*, vol. 434, no. 7030, pp. 234–8.

Ivanov, AI, Nusrat, A & Parkos, CA 2004, "Endocytosis of epithelial apical junctional proteins by a clathrin-mediated pathway into a unique storage compartment.," *Molecular biology of the cell*, vol. 15, no. 1, pp. 176–88.

Jagla, K, Dollé, P, Mattei, MG, Jagla, T, et al 1995, "Mouse lbx1 and human lbx1 define a novel mammalian homeobox gene family related to the drosophila lady bird genes.," *Mechanisms of development*, vol. 53, no. 3, pp. 345–56.

Jahn, R & Scheller, RH 2006, "Snares--engines for membrane fusion.," *Nature reviews. Molecular cell biology*, vol. 7, no. 9, pp. 631–43.

Jansen, KM & Pavlath, GK 2006, "Mannose receptor regulates myoblast motility and muscle growth.," *The Journal of cell biology*, vol. 174, no. 3, pp. 403–13.

Jarriault, S, Brou, C, Logeat, F, Schroeter, EH, et al 1995, "Signalling downstream of activated mammalian notch.," *Nature*, vol. 377, no. 6547, pp. 355–8.

Jin, P, Duan, R, Luo, F, Zhang, G, et al 2011, "Competition between blown fuse and wasp for wip binding regulates the dynamics of wasp-dependent actin polymerization in vivo.," *Developmental cell*, vol. 20, no. 5, pp. 623–38.

Jostes, B, Walther, C & Gruss, P 1990, "The murine paired box gene, pax7, is expressed specifically during the development of the nervous and muscular system.," *Mechanisms of development*, vol. 33, no. 1, pp. 27–37.

Kablar, B, Krastel, K, Ying, C, Asakura, A, et al 1997, "Myod and myf-5 differentially regulate the development of limb versus trunk skeletal muscle.," *Development (Cambridge, England)*, vol. 124, no. 23, pp. 4729–38.

Kahane, N, Cinnamon, Y, Bachelet, I & Kalcheim, C 2001, "The third wave of myotome colonization by mitotically competent progenitors: regulating the balance between differentiation and proliferation during muscle development.," *Development (Cambridge, England)*, vol. 128, no. 12, pp. 2187–98.

Kahane, N, Cinnamon, Y & Kalcheim, C 1998, "The origin and fate of pioneer myotomal cells in the avian embryo.," *Mechanisms of development*, vol. 74, no. 1-2, pp. 59–73.

Kahane, N, Ben-Yair, R & Kalcheim, C 2007, "Medial pioneer fibers pattern the morphogenesis of early myoblasts derived from the lateral somite.," *Developmental biology*, vol. 305, no. 2, pp. 439–50.

Kaji, K, Oda, S, Shikano, T, Ohnuki, T & Uematsu, Y 2000, "The gamete fusion process is defective in eggs of cd9-deficient mice," *Nature …*, accessed from <http://www.nature.com/ng/journal/v24/n3/abs/ng0300_279.html>.

Kalcheim, C & Burstyn-Cohen, T 2005, "Early stages of neural crest ontogeny: formation and regulation of cell delamination.," *The International journal of developmental biology*, vol. 49, no. 2-3, pp. 105–16.

Kamei, Y, Miura, S, Suzuki, M, Kai, Y, et al 2004, "Skeletal muscle foxo1 (fkhr) transgenic mice have less skeletal muscle mass, down-regulated type i (slow twitch/red muscle) fiber genes, and impaired glycemic control.," *The Journal of biological chemistry*, vol. 279, no. 39, pp. 41114–23.

Kassar-Duchossoy, L, Gayraud-Morel, B, Gomès, D, Rocancourt, D, et al 2004, "Mrf4 determines skeletal muscle identity in myf5:myod double-mutant mice.," *Nature*, vol. 431, no. 7007, pp. 466–71.

Kassar-Duchossoy, L, Giacone, E, Gayraud-Morel, B, Jory, A, et al 2005, "Pax3/pax7 mark a novel population of primitive myogenic cells during development.," *Genes & development*, vol. 19, no. 12, pp. 1426–31.

Kawakami, K 2004, "Transgenesis and gene trap methods in zebrafish by using the tol2 transposable element," *Methods Cell Biol*, accessed from <http://books.google.com/books?hl=en&lr=&id=72FThfvXgkQC&oi=fnd&pg=PA201&dq=tol2+transposon+system&ots=O-N4letcHi&sig=JzfDqGXEXSdUiOiLgqnMKGXMdK8>.

Kazanskaya, O, Glinka, A, del Barco Barrantes, I, Stannek, P, et al 2004, "R-spondin2 is a secreted activator of wnt/beta-catenin signaling and is required for xenopus myogenesis.," *Developmental cell*, vol. 7, no. 4, pp. 525–34.

Kesper, DA, Stute, C, Buttgereit, D, Kreisköther, N, et al 2007, "Myoblast fusion in drosophila melanogaster is mediated through a fusion-restricted myogenic-adhesive structure (furmas).," *Developmental dynamics : an official publication of the American Association of Anatomists*, vol. 236, no. 2, pp. 404–15.

Kiefer, JC & Hauschka, SD 2001, "Myf-5 is transiently expressed in nonmuscle mesoderm and exhibits dynamic regional changes within the presegmented mesoderm and somites i-iv.," *Developmental biology*, vol. 232, no. 1, pp. 77–90.

Kielian, M & Rey, FA 2006, "Virus membrane-fusion proteins: more than one way to make a hairpin," *Nature Reviews Microbiology*, accessed from <http://www.nature.com/nrmicro/journal/v4/n1/abs/nrmicro1326.html>.

Kim, S, Shilagardi, K, Zhang, S, Hong, SN, et al 2007, "A critical function for the actin cytoskeleton in targeted exocytosis of prefusion vesicles during myoblast fusion.," *Developmental cell*, vol. 12, no. 4, pp. 571–86.

Kimelman, D & Xu, W 2006, "Beta-catenin destruction complex: insights and questions from a structural perspective.," *Oncogene*, vol. 25, no. 57, pp. 7482–91.

Kitzmann, M, Carnac, G, Vandromme, M, Primig, M, et al 1998, "The muscle regulatory factors myod and myf-5 undergo distinct cell cycle-specific expression in muscle cells.," *The Journal of cell biology*, vol. 142, no. 6, pp. 1447–59.

Knudsen, KA & Horwitz, AF 1977, "Tandem events in myoblast fusion.," *Developmental biology*, vol. 58, no. 2, pp. 328–38.

Knudsen, KA, McElwee, SA & Myers, L 1990, "A role for the neural cell adhesion molecule, ncam, in myoblast interaction during myogenesis.," *Developmental biology*, vol. 138, no. 1, pp. 159–68.

Knudsen, KA, Myers, L & McElwee, SA 1990, "A role for the ca2(+)-dependent adhesion molecule, n-cadherin, in myoblast interaction during myogenesis.," *Experimental cell research*, vol. 188, no. 2, pp. 175–84.

Kobayashi, T, Mizuno, H, Imayoshi, I, Furusawa, C, et al 2009, "The cyclic gene hes1 contributes to diverse differentiation responses of embryonic stem cells.," *Genes & development*, vol. 23, no. 16, pp. 1870–5.

Komatsu, H, Chao, MY, Larkins-Ford, J, Corkins, ME, et al 2008, "Osm-11 facilitates lin-12 notch signaling during caenorhabditis elegans vulval development.," *PLoS biology*, vol. 6, no. 8, p. e196.

Kopan, R & Ilagan, MX 2009, "The canonical notch signaling pathway: unfolding the activation mechanism.," *Cell*, vol. 137, no. 2, pp. 216–33.

Krebs, LT, Xue, Y, Norton, CR, Sundberg, JP, et al 2003, "Characterization of notch3-deficient mice: normal embryonic development and absence of genetic interactions with a notch1 mutation.," *Genesis (New York, N.Y. : 2000)*, vol. 37, no. 3, pp. 139–43.

Kurisu, S & Takenawa, T 2010, "Wasp and wave family proteins: friends or foes in cancer invasion?," *Cancer science*, vol. 101, no. 10, pp. 2093–104.

Kuroyanagi, H, Ohno, G & Mitani, S 2007, "The fox-1 family and sup-12 coordinately regulate tissue-specific alternative splicing in vivo," *Molecular and cellular …*, accessed from <http://mcb.asm.org/content/27/24/8612.short>.

Lafuste, P, Sonnet, C, Chazaud, B, Dreyfus, PA, et al 2005, "Adam12 and alpha9beta1 integrin are instrumental in human myogenic cell differentiation.," *Molecular biology of the cell*, vol. 16, no. 2, pp. 861–70.

Lagha, M, Kormish, JD, Rocancourt, D, Manceau, M, et al 2008, "Pax3 regulation of fgf signaling affects the progression of embryonic progenitor cells into the myogenic program.," *Genes & development*, vol. 22, no. 13, pp. 1828–37.

Lamouille, S, Xu, J & Derynck, R 2014, "Molecular mechanisms of epithelial-mesenchymal transition.," *Nature reviews. Molecular cell biology*, vol. 15, no. 3, pp. 178–96.

Landemaine, A, Rescan, P-YY & Gabillard, J-CC 2014, "Myomaker mediates fusion of fast myocytes in zebrafish embryos.," *Biochemical and biophysical research communications*.

Le, TL, Yap, AS & Stow, JL 1999, "Recycling of e-cadherin: a potential mechanism for regulating cadherin dynamics.," *The Journal of cell biology*, vol. 146, no. 1, pp. 219–32.

Lebensohn, AM & Kirschner, MW 2009, "Activation of the wave complex by coincident signals controls actin assembly.," *Molecular cell*, vol. 36, no. 3, pp. 512–24.

Lee, S-H, Rho, J, Jeong, D, Sul, J-Y, et al 2006, "V-atpase v0 subunit d2–deficient mice exhibit impaired osteoclast fusion and increased bone formation," *Nature medicine*, vol. 12, no. 12, pp. 1403–1409, accessed from <http://www.nature.com/nm/journal/v12/n12/abs/nm1514.html>.

Li, T, Wu, R, Zhang, Y & Zhu, D 2011, "A systematic analysis of the skeletal muscle mirna transcriptome of chicken varieties with divergent skeletal muscle growth identifies novel mirnas and …," *BMC genomics*, accessed from <http://www.biomedcentral.com/1471-2164/12/186/>.

Li, L, Hutchins, BI & Kalil, K 2009, "Wnt5a induces simultaneous cortical axon outgrowth and repulsive axon guidance through distinct signaling mechanisms.," *The Journal of neuroscience : the official journal of the Society for Neuroscience*, vol. 29, no. 18, pp. 5873–83.

Lin, T, Ponn, A, Hu, X, Law, BK & Lu, J 2010, "Requirement of the histone demethylase lsd1 in snai1-mediated transcriptional repression during epithelial-mesenchymal transition.," *Oncogene*, vol. 29, no. 35, pp. 4896–904.

Lin, X & Perrimon, N 1999, "Dally cooperates with drosophila frizzled 2 to transduce wingless signalling.," *Nature*, vol. 400, no. 6741, pp. 281–4.

Lindon, C, Montarras, D & Pinset, C 1998, "Cell cycle-regulated expression of the muscle determination factor myf5 in proliferating myoblasts.," *The Journal of cell biology*, vol. 140, no. 1, pp. 111–8.

Logan, CY & Nusse, R 2004, "The wnt signaling pathway in development and disease.," *Annual review of cell and developmental biology*, vol. 20, pp. 781–810.

Lu, Z, Ghosh, S, Wang, Z & Hunter, T 2003, "Downregulation of caveolin-1 function by egf leads to the loss of e-cadherin, increased transcriptional activity of beta-catenin, and enhanced tumor cell invasion.," *Cancer cell*, vol. 4, no. 6, pp. 499–515.

Lubman, OY, Ilagan, MX, Kopan, R & Barrick, D 2007, "Quantitative dissection of the notch:csl interaction: insights into the notch-mediated transcriptional switch.," *Journal of molecular biology*, vol. 365, no. 3, pp. 577–89.

Lubman, OY, Korolev, SV & Kopan, R 2004, "Anchoring notch genetics and biochemistry; structural analysis of the ankyrin domain sheds light on existing data.," *Molecular cell*, vol. 13, no. 5, pp. 619–26.

Luo, L, Liao, YJ, Jan, LY & Jan, YN 1994, "Distinct morphogenetic functions of similar small gtpases: drosophila drac1 is involved in axonal outgrowth and myoblast fusion.," *Genes & development*, vol. 8, no. 15, pp. 1787–802.

Manceau, M, Gros, J, Savage, K, Thomé, V, et al 2008, "Myostatin promotes the terminal differentiation of embryonic muscle progenitors.," *Genes & development*, vol. 22, no. 5, pp. 668–81.

Mao, B, Wu, W, Li, Y, Hoppe, D, et al 2001, "Ldl-receptor-related protein 6 is a receptor for dickkopf proteins.," *Nature*, vol. 411, no. 6835, pp. 321–5.

Marcelle, C, Stark, MR & Bronner-Fraser, M 1997, "Coordinate actions of bmps, wnts, shh and noggin mediate patterning of the dorsal somite.," *Development (Cambridge, England)*, vol. 124, no. 20, pp. 3955–63.

Marcelle, C, Wolf, J & Bronner-Fraser, M 1995, "The in vivo expression of the fgf receptor frek mrna in avian myoblasts suggests a role in muscle growth and differentiation.," *Developmental biology*, vol. 172, no. 1, pp. 100–14.

Mariano, M & Spector, WG 1974, "The formation and properties of macrophage polykaryons (inflammatory giant cells)," *The Journal of pathology*, accessed from <http://onlinelibrary.wiley.com/doi/10.1002/path.1711130102/full>.

Maroto, M, Reshef, R, Münsterberg, AE, Koester, S, et al 1997, "Ectopic pax-3 activates myod and myf-5 expression in embryonic mesoderm and neural tissue.," *Cell*, vol. 89, no. 1, pp. 139–48.

Martinez-Quiles, N, Rohatgi, R, Antón, IM, Medina, M, et al 2001, "Wip regulates n-wasp-mediated actin polymerization and filopodium formation.," *Nature cell biology*, vol. 3, no. 5, pp. 484–91.

Matsuoka, S, Edwards, MC, Bai, C, Parker, S, et al 1995, "P57kip2, a structurally distinct member of the p21cip1 cdk inhibitor family, is a candidate tumor suppressor gene.," *Genes & development*, vol. 9, no. 6, pp. 650–62.

Mauger, A 1972, "[the role of somitic mesoderm in the development of dorsal plumage in chick embryos. ii. regionalization of the plumage-forming mesoderm].," *Journal of embryology and experimental morphology*, vol. 28, no. 2, pp. 343–66.

MAURO, A & ADAMS, WR 1961, "The structure of the sarcolemma of the frog skeletal muscle fiber.," *The Journal of biophysical and biochemical cytology*, vol. 10(4)Suppl, pp. 177–85.

McPherron, AC & Lee, S-J 1997, "Double muscling in cattle due to mutations in the myostatin gene," *Proceedings of the National Academy of Sciences*, vol. 94, no. 23, pp. 12457–12461.

Meier, S 1981, "Development of the chick embryo mesoblast: morphogenesis of the prechordal plate and cranial segments.," *Developmental biology*, vol. 83, no. 1, pp. 49–61.

Melikyan, GB, Markosyan, RM, Hemmati, H, Delmedico, MK, et al 2000, "Evidence that the transition of hiv-1 gp41 into a six-helix bundle, not the bundle configuration, induces membrane fusion.," *The Journal of cell biology*, vol. 151, no. 2, pp. 413–23.

Menon, SD & Chia, W 2001, "Drosophila rolling pebbles: a multidomain protein required for myoblast fusion that recruits d-titin in response to the myoblast attractant dumbfounded.," *Developmental cell*, vol. 1, no. 5, pp. 691–703.

Mi, S, Lee, X, Li, XP, Veldman, GM, et al 2000, "Syncytin is a captive retroviral envelope protein involved in human placental morphogenesis," *Nature*, accessed from <http://www.nature.com/nature/journal/v403/n6771/abs/403785a0.html>.

Millay, DP, O'Rourke, JR, Sutherland, LB, Bezprozvannaya, S, et al 2013, "Myomaker is a membrane activator of myoblast fusion and muscle formation.," *Nature*, vol. 499, no. 7458, pp. 301–5.

Millay, DP, Sutherland, LB, Bassel-Duby, R & Olson, EN 2014, "Myomaker is essential for muscle regeneration.," *Genes & development*, vol. 28, no. 15, pp. 1641–6.

Miner, JH & Wold, B 1990, "Herculin, a fourth member of the myod family of myogenic regulatory genes.," *Proceedings of the National Academy of Sciences of the United States of America*, vol. 87, no. 3, pp. 1089–93.

Miyado, K, Yamada, G, Yamada, S, Hasuwa, H, et al 2000, "Requirement of cd9 on the egg plasma membrane for fertilization," *Science*, vol. 287, no. 5451, pp. 321–324, accessed from <http://www.sciencemag.org/content/287/5451/321.short>.

Mlodzik, M 2002, "Planar cell polarization: do the same mechanisms regulate drosophila tissue polarity and vertebrate gastrulation?," *Trends in genetics : TIG*, vol. 18, no. 11, pp. 564–71.

Mohler, WA, Shemer, G, del Campo, JJ & Valansi, C 2002, "The type i membrane protein eff-1 is essential for developmental cell fusion," *Developmental cell*, accessed from <http://www.sciencedirect.com/science/article/pii/S1534580702001296>.

Molenaar, M, van de Wetering, M, Oosterwegel, M, Peterson-Maduro, J, et al 1996, "Xtcf-3 transcription factor mediates beta-catenin-induced axis formation in xenopus embryos.," *Cell*, vol. 86, no. 3, pp. 391–9.

Molkentin, JD, Firulli, AB, Black, BL, Martin, JF, et al 1996, "Mef2b is a potent transactivator expressed in early myogenic lineages.," *Molecular and cellular biology*, vol. 16, no. 7, pp. 3814–24.

Moore, CA, Parkin, CA, Bidet, Y & Ingham, PW 2007, "A role for the myoblast city homologues dock1 and dock5 and the adaptor proteins crk and crk-like in zebrafish myoblast fusion.," *Development (Cambridge, England)*, vol. 134, no. 17, pp. 3145–53.

Morali, OG, Delmas, V, Moore, R, Jeanney, C, et al 2001, "Igf-ii induces rapid beta-catenin relocation to the nucleus during epithelium to mesenchyme transition.," *Oncogene*, vol. 20, no. 36, pp. 4942–50.

Moreno, JL & Mikhailenko, I 2007, "Il-4 promotes the formation of multinucleated giant cells from macrophage precursors by a stat6-dependent, homotypic mechanism: contribution of e-cadherin," *Journal of leukocyte …*, accessed from <http://www.jleukbio.org/content/82/6/1542.short>.

Mosher, DS, Quignon, P, Bustamante, CD, Sutter, NB, et al 2007, "A mutation in the myostatin gene increases muscle mass and enhances racing performance in heterozygote dogs.," *PLoS genetics*, vol. 3, no. 5, p. e79.

Mukai, A & Hashimoto, N 2008, "Localized cyclic amp-dependent protein kinase activity is required for myogenic cell fusion.," *Experimental cell research*, vol. 314, no. 2, pp. 387–97.

Münsterberg, AE, Kitajewski, J, Bumcrot, DA, McMahon, AP & Lassar, AB 1995, "Combinatorial signaling by sonic hedgehog and wnt family members induces myogenic bhlh gene expression in the somite.," *Genes & development*, vol. 9, no. 23, pp. 2911–22.

Nabeshima, Y, Hanaoka, K, Hayasaka, M, Esuml, E & Li, S 1993, "Myogenin gene disruption results in perinatal lethality because of severe muscle defect,", accessed from <http://www.nature.com/nature/journal/v364/n6437/abs/364532a0.html>.

Naour, LF, Rubinstein, E, Jasmin, C & Prenant, M 2000, "Severely reduced female fertility in cd9-deficient mice," *Science*, accessed from <http://www.sciencemag.org/content/287/5451/319.short>.

Nicolas, M, Wolfer, A, Raj, K, Kummer, JA & Mill, P 2003, "Notch1 functions as a tumor suppressor in mouse skin," *Nature …*, accessed from <http://www.nature.com/ng/journal/v33/n3/abs/ng1099.html>.

Nishiyama, T, Kii, I & Kudo, A 2004, "Inactivation of rho/rock signaling is crucial for the nuclear accumulation of fkhr and myoblast fusion.," *The Journal of biological chemistry*, vol. 279, no. 45, pp. 47311–9.

Ochoa, G-C, Slepnev, VI, Neff, L, Ringstad, N, et al 2000, "A functional link between dynamin and the actin cytoskeleton at podosomes," *The Journal of cell biology*, vol. 150, no. 2, pp. 377–390, accessed from <http://jcb.rupress.org/content/150/2/377.abstract>.

Ontell, M & Kozeka, K 1984, "The organogenesis of murine striated muscle: a cytoarchitectural study.," *The American journal of anatomy*, vol. 171, no. 2, pp. 133–48, accessed from <http://dx.doi.org/10.1002/aja.1001710202>.

Ordahl, CP, Berdougo, E, Venters, SJ & Denetclaw, WF 2001, "The dermomyotome dorsomedial lip drives growth and morphogenesis of both the primary myotome and dermomyotome epithelium.," *Development (Cambridge, England)*, vol. 128, no. 10, pp. 1731–44.

Otto, A, Schmidt, C & Patel, K 2006, "Pax3 and pax7 expression and regulation in the avian embryo.," *Anatomy and embryology*, vol. 211, no. 4, pp. 293–310.

Palacios, F, Price, L, Schweitzer, J, Collard, JG & D'Souza-Schorey, C 2001, "An essential role for arf6-regulated membrane traffic in adherens junction turnover and epithelial cell migration.," *The EMBO journal*, vol. 20, no. 17, pp. 4973–86.

Park, D, Tosello-Trampont, A-CC, Elliott, MR, Lu, M, et al 2007, "Bai1 is an engulfment receptor for apoptotic cells upstream of the elmo/dock180/rac module.," *Nature*, vol. 450, no. 7168, pp. 430–4.

De Parseval, N, Lazar, V, Casella, JF & Benit, L 2003, "Survey of human genes of retroviral origin: identification and transcriptome of the genes with coding capacity for complete envelope proteins," *Journal of …*, accessed from <http://jvi.asm.org/content/77/19/10414.short>.

Patapoutian, A, Yoon, JK, Miner, JH, Wang, S, et al 1995, "Disruption of the mouse mrf4 gene identifies multiple waves of myogenesis in the myotome.," *Development (Cambridge, England)*, vol. 121, no. 10, pp. 3347–58.

Patel, K, Christ, B & Stockdale, FE 2002, "Control of muscle size during embryonic, fetal, and adult life.," *Results and problems in cell differentiation*, vol. 38, pp. 163–86.

Pavlath, GK & Horsley, V 2003, "Cell fusion in skeletal muscle--central role of nfatc2 in regulating muscle cell size.," *Cell cycle (Georgetown, Tex.)*, vol. 2, no. 5, pp. 420–3.

Peinado, H, Ballestar, E, Esteller, M & Cano, A 2004, "Snail mediates e-cadherin repression by the recruitment of the sin3a/histone deacetylase 1 (hdac1)/hdac2 complex.," *Molecular and cellular biology*, vol. 24, no. 1, pp. 306–19.

Pérez-Vargas, J, Krey, T, Valansi, C, Avinoam, O, et al 2014, "Structural basis of eukaryotic cell-cell fusion.," *Cell*, vol. 157, no. 2, pp. 407–19.

Podbilewicz, B & White, JG 1994, "Cell fusions in the developing epithelia of< i> c. elegans</i>," *Developmental biology*, accessed from <http://www.sciencedirect.com/science/article/pii/S0012160684710414>.

Podbilewicz, B, Leikina, E, Sapir, A, Valansi, C, et al 2006, "The c. elegans developmental fusogen eff-1 mediates homotypic fusion in heterologous cells and in vivo.," *Developmental cell*, vol. 11, no. 4, pp. 471–81.

Posey, AD, Pytel, P, Gardikiotes, K, Demonbreun, AR, et al 2011, "Endocytic recycling proteins ehd1 and ehd2 interact with fer-1-like-5 (fer1l5) and mediate myoblast fusion.," *The Journal of biological chemistry*, vol. 286, no. 9, pp. 7379–88, accessed from <http://www.ncbi.nlm.nih.gov/pubmed/21177873>.

Pourquié, O 2011, "Vertebrate segmentation: from cyclic gene networks to scoliosis.," *Cell*, vol. 145, no. 5, pp. 650–63.

Powell, GT & Wright, GJ 2011, "Jamb and jamc are essential for vertebrate myocyte fusion.," *PLoS biology*, vol. 9, no. 12, p. e1001216, accessed from <http://www.ncbi.nlm.nih.gov/pubmed/22180726>.

Praetor, A, McBride, J, Chiu, H, Rangell, L, et al 2008, "Genetic deletion of jam-c reveals a role in myeloid progenitor generation," *Blood*, vol. 113.

Quach, NL, Biressi, S, Reichardt, LF, Keller, C & Rando, TA 2009, "Focal adhesion kinase signaling regulates the expression of caveolin 3 and beta1 integrin, genes essential for normal myoblast fusion.," *Molecular biology of the cell*, vol. 20, no. 14, pp. 3422–35.

Rand, R, Fuller, N, Parsegian, V & Rau, D 1988, "Variation in hydration forces between neutral phospholipid bilayers: evidence for hydration attraction," *Biochemistry*, vol. 27, no. 20, p. 77117722.

Rawls, A, Valdez, MR, Zhang, W, Richardson, J, et al 1998, "Overlapping functions of the myogenic bhlh genes mrf4 and myod revealed in double mutant mice.," *Development (Cambridge, England)*, vol. 125, no. 13, pp. 2349–58.

Relaix, F, Rocancourt, D, Mansouri, A & Buckingham, M 2005, "A pax3/pax7-dependent population of skeletal muscle progenitor cells.," *Nature*, vol. 435, no. 7044, pp. 948–53.

Relaix, F, Rocancourt, D, Mansouri, A & Buckingham, M 2004, "Divergent functions of murine pax3 and pax7 in limb muscle development.," *Genes & development*, vol. 18, no. 9, pp. 1088–105.

Remak, R 1855, Untersuchungen uber die entwicking der wibelthiere, G. Reimer, Berlin.

Reporter, M & Raveed, D 1973, "Plasma membranes: isolation from naturally fused and lysolecithin-treated muscle cells," *Science*, vol. 181, no. 4102, pp. 863–865, accessed from <http://www.sciencemag.org/content/181/4102/863.short>.

Richardson, BE, Beckett, K, Nowak, SJ & Baylies, MK 2007, "Scar/wave and arp2/3 are crucial for cytoskeletal remodeling at the site of myoblast fusion.," *Development (Cambridge, England)*, vol. 134, no. 24, pp. 4357–67.

Rickman, C & Davletov, B 2003, "Mechanism of calcium-independent synaptotagmin binding to target snares.," *The Journal of biological chemistry*, vol. 278, no. 8, pp. 5501–4.

Rijsewijk, F, Schuermann, M, Wagenaar, E, Parren, P, et al 1987, "The drosophila homolog of the mouse mammary oncogene int-1 is identical to the segment polarity gene wingless.," *Cell*, vol. 50, no. 4, pp. 649–57.

Rios, AC, Serralbo, O, Salgado, D & Marcelle, C 2011, "Neural crest regulates myogenesis through the transient activation of notch.," *Nature*, vol. 473, no. 7348, pp. 532–5.

Rochlin, K, Yu, S, Roy, S & Baylies, MK 2010, "Myoblast fusion: when it takes more to make one.," *Developmental biology*, vol. 341, no. 1, pp. 66–83.

Rudnicki, MA, Braun, T, Hinuma, S & Jaenisch, R 1992, "Inactivation of myod in mice leads to up-regulation of the myogenic hlh gene myf-5 and results in apparently normal muscle development.," *Cell*, vol. 71, no. 3, pp. 383–90.

Rudnicki, MA, Schnegelsberg, PN, Stead, RH, Braun, T, et al 1993, "Myod or myf-5 is required for the formation of skeletal muscle.," *Cell*, vol. 75, no. 7, pp. 1351–9.

Runge, KE, Evans, JE, He, ZY & Gupta, S 2007, "Oocyte cd9 is enriched on the microvillar membrane and required for normal microvillar shape and distribution," *Developmental …*, accessed from <http://www.sciencedirect.com/science/article/pii/S0012160606015004>.

Saginario, C, Sterling, H & Beckers, C 1998, "Mfr, a putative receptor mediating the fusion of macrophages," *Molecular and …*, accessed from <http://mcb.asm.org/content/18/11/6213.short>.

Saginario, C, Qian, HY & Vignery, A 1995, "Identification of an inducible surface molecule specific to fusing macrophages.," *Proceedings of the National Academy of Sciences of the United States of America*, vol. 92, no. 26, pp. 12210–4.

Sahlgren, C, Gustafsson, MV, Jin, S, Poellinger, L & Lendahl, U 2008, "Notch signaling mediates hypoxia-induced tumor cell migration and invasion.," *Proceedings of the National Academy of Sciences of the United States of America*, vol. 105, no. 17, pp. 6392–7.

Sakaguchi, T, Nishimoto, M, Miyagi, S, Iwama, A, et al 2006, "Putative 'stemness' gene jam-b is not required for maintenance of stem cell state in embryonic, neural, or hematopoietic stem cells," *Molecular and Cellular Biology*, vol. 26.

Sanders, PG, Muñoz-Descalzo, S, Balayo, T, Wirtz-Peitz, F, et al 2009, "Ligand-independent traffic of notch buffers activated armadillo in drosophila," *PLoS biology*, vol. 7, no. 8, p. e1000169, accessed from <http://dx.plos.org/10.1371/journal.pbio.1000169.g011>.

Sapir, A, Choi, J, Leikina, E, Avinoam, O & Valansi, C 2007, "Aff-1, a fos-1-regulated fusogen, mediates fusion of the anchor cell in< i> c. elegans</i>," *Developmental cell*, accessed from

<http://www.sciencedirect.com/science/article/pii/S1534580707001037>.

Sapir, A, Avinoam, O, Podbilewicz, B & Chernomordik, L 2008, "Viral and developmental cell fusion mechanisms: conservation and divergence," *Developmental Cell*, vol. 14, no. 1.

Sassoon, D, Lyons, G, Wright, WE, Lin, V, et al 1989, "Expression of two myogenic regulatory factors myogenin and myod1 during mouse embryogenesis.," *Nature*, vol. 341, no. 6240, pp. 303–7.

Scaal, M, Gros, J, Lesbros, C & Marcelle, C 2004, "In ovo electroporation of avian somites.," *Developmental dynamics : an official publication of the American Association of Anatomists*, vol. 229, no. 3, pp. 643–50.

Von Scheven, G, Alvares, LE, Mootoosamy, RC & Dietrich, S 2006, "Neural tube derived signals and fgf8 act antagonistically to specify eye versus mandibular arch muscles.," *Development (Cambridge, England)*, vol. 133, no. 14, pp. 2731–45.

Schramm, C & Solursh, M 1990, "The formation of premuscle masses during chick wing bud development.," *Anatomy and embryology*, vol. 182, no. 3, pp. 235–47.

Schröter, RH, Lier, S, Holz, A, Bogdan, S, et al 2004, "Kette and blown fuse interact genetically during the second fusion step of myogenesis in drosophila.," *Development (Cambridge, England)*, vol. 131, no. 18, pp. 4501–9.

Schuelke, M, Wagner, KR, Stolz, LE, Hübner, C, et al 2004, "Myostatin mutation associated with gross muscle hypertrophy in a child.," *The New England journal of medicine*, vol. 350, no. 26, pp. 2682–8.

Schultz, E & McCormick, KM 1994, "Skeletal muscle satellite cells.," *Reviews of physiology, biochemistry and pharmacology*, vol. 123, pp. 213–57.

Schuster-Gossler, K, Cordes, R & Gossler, A 2007, "Premature myogenic differentiation and depletion of progenitor cells cause severe muscle hypotrophy in delta1 mutants.," *Proceedings of the National Academy of Sciences of the United States of America*, vol. 104, no. 2, pp. 537–42.

Schwander, M, Leu, M, Stumm, M, Dorchies, OM, et al 2003, "Beta1 integrins regulate myoblast fusion and sarcomere assembly.," *Developmental cell*, vol. 4, no. 5, pp. 673–85, accessed from <http://linkinghub.elsevier.com/retrieve/pii/S1534580703001187>.

Seale, P, Sabourin, LA, Girgis-Gabardo, A, Mansouri, A, et al 2000, "Pax7 is required for the specification of myogenic satellite cells.," *Cell*, vol. 102, no. 6, pp. 777–86.

Semënov, M, Tamai, K & He, X 2005, "Sost is a ligand for lrp5/lrp6 and a wnt signaling inhibitor,".

Semënov, MV, Tamai, K, Brott, BK, Kühl, M, et al 2001, "Head inducer dickkopf-1 is a ligand for wnt coreceptor lrp6.," *Current biology : CB*, vol. 11, no. 12, pp. 951–61.

Sens, KL, Zhang, S, Jin, P, Duan, R, et al 2010, "An invasive podosome-like structure promotes fusion pore formation during myoblast fusion.," *The Journal of cell biology*, vol. 191, no. 5, pp. 1013–27.

Serralbo, O & Marcelle, C 2014, "Migrating cells mediate long-range wnt signaling.," *Development (Cambridge, England)*, vol. 141, no. 10, pp. 2057–63.

Serralbo, O, Picard, CA & Marcelle, C 2013, "Long-term, inducible gene loss-of-function in the chicken embryo.," *Genesis (New York, N.Y. : 2000)*, vol. 51, no. 5, pp. 372–80.

Sessions, A & Horwitz, AF 1983, "Differentiation-related differences in the plasma membrane phospholipid asymmetry of myogenic and fibrogenic cells.," *Biochimica et biophysica acta*, vol. 728, no. 1, pp. 103–11.

Shainberg, A, Yagil, G & Yaffe, D 1969, "Control of myogenesis in vitro by ca 2 + concentration in nutritional medium.," *Experimental cell research*, vol. 58, no. 1, pp. 163–7.

Sharma, RP 1973, "Wingless a new mutant in drosophila melanogaster,".

Shemer, G, Suissa, M, Kolotuev, I, Nguyen, K & Hall, DH 2004, "Eff-1 is sufficient to initiate and execute tissue-specific cell fusion in< i> c. elegans</i>," *Current biology*, accessed from <http://www.sciencedirect.com/science/article/pii/S0960982204005585>.

Shibukawa, Y, Yamazaki, N, Daimon, E & Wada, Y 2013, "Rock-dependent calponin 3 phosphorylation regulates myoblast fusion.," *Experimental cell research*, vol. 319, no. 5, pp. 633–48, accessed from <http://www.ncbi.nlm.nih.gov/pubmed/23276748>.

Shimada, Y 1971, "Electron microscope observations on the fusion of chick myoblasts in vitro," *The Journal of cell biology*, accessed from <http://jcb.rupress.org/content/48/1/128.abstract>.

Sieiro-Mosti, D, De La Celle, M, Pelé, M & Marcelle, C 2014, "A dynamic analysis of muscle fusion in the chick embryo.," *Development (Cambridge, England)*, vol. 141, no. 18, pp. 3605–11.

Singh, RK, Xia, Z, Bland, CS, Kalsotra, A, et al 2014, "Rbfox2-coordinated alternative splicing of mef2d and rock2 controls myoblast fusion during myogenesis.," *Molecular cell*, vol. 55, no. 4, pp. 592–603.

Slusarski, DC, Yang-Snyder, J, Busa, WB & Moon, RT 1997, "Modulation of embryonic intracellular ca2+ signaling by wnt-5a.," *Developmental biology*, vol. 182, no. 1, pp. 114–20.

Smith, AE & Helenius, A 2004, "How viruses enter animal cells.," *Science (New York, N.Y.)*, vol. 304, no. 5668, pp. 237–42.

Sohn, RL, Huang, P, Kawahara, G, Mitchell, M, et al 2009, "A role for nephrin, a renal protein, in vertebrate skeletal muscle cell fusion.," *Proceedings of the National Academy of Sciences of the United States of America*, vol. 106, no. 23, pp. 9274–9.

Söllner, T, Bennett, MK, Whiteheart, SW, Scheller, RH & Rothman, JE 1993, "A protein assembly-disassembly pathway in vitro that may correspond to sequential steps of synaptic vesicle docking, activation, and fusion.," *Cell*, vol. 75, no. 3, pp. 409–18.

Söllner, T, Whiteheart, SW, Brunner, M, Erdjument-Bromage, H, et al 1993, "Snap receptors implicated in vesicle targeting and fusion.," *Nature*, vol. 362, no. 6418, pp. 318–24.

Sotillos, S, Roch, F & Campuzano, S 1997, "The metalloprotease-disintegrin kuzbanian participates in notch activation during growth and patterning of drosophila imaginal discs.," *Development (Cambridge, England)*, vol. 124, no. 23, pp. 4769–79.

Srinivas, BP, Woo, J, Leong, WY & Roy, S 2007, "A conserved molecular pathway mediates myoblast fusion in insects and vertebrates.," *Nature genetics*, vol. 39, no. 6, pp. 781–6, accessed from <http://www.ncbi.nlm.nih.gov/pubmed/17529975>.

Städeli, R, Hoffmans, R & Basler, K 2006, "Transcription under the control of nuclear arm/beta-catenin.," *Current biology : CB*, vol. 16, no. 10, pp. R378–85.

Stemmer, V, de Craene, B, Berx, G & Behrens, J 2008, "Snail promotes wnt target gene expression and interacts with beta-catenin.," *Oncogene*, vol. 27, no. 37, pp. 5075–80.

Stern, CD & Holland, P 1993, "Essential developmental biology: a practical approach.,", accessed from <http://www.cabdirect.org/abstracts/19950109416.html>.

Strünkelnberg, M, Bonengel, B, Moda, LM, Hertenstein, A, et al 2001, "Rst and its paralogue kirre act redundantly during embryonic muscle development in drosophila.," *Development (Cambridge, England)*, vol. 128, no. 21, pp. 4229–39.

Strutt, D 2003, "Frizzled signalling and cell polarisation in drosophila and vertebrates.," *Development (Cambridge, England)*, vol. 130, no. 19, pp. 4501–13.

Sun, TQ, Lu, B, Feng, JJ, Reinhard, C, et al 2001, "Par-1 is a dishevelled-associated kinase and a positive regulator of wnt signalling.," *Nature cell biology*, vol. 3, no. 7, pp. 628–36.

Tachibana, I & Hemler, ME 1999, "Role of transmembrane 4 superfamily (tm4sf) proteins cd9 and cd81 in muscle cell fusion and myotube maintenance.," *The Journal of cell biology*, vol. 146, no. 4, pp. 893–904.

Tajbakhsh, S, Borello, U, Vivarelli, E, Kelly, R, et al 1998, "Differential activation of myf5 and myod by different wnts in explants of mouse paraxial mesoderm and the later activation of myogenesis in the absence of myf5.," *Development (Cambridge, England)*, vol. 125, no. 21, pp. 4155–62.

Tajbakhsh, S, Rocancourt, D, Cossu, G & Buckingham, M 1997, "Redefining the genetic hierarchies controlling skeletal myogenesis: pax-3 and myf-5 act upstream of myod.," *Cell*, vol. 89, no. 1, pp. 127–38.

Tang, J, Maximov, A, Shin, O-HH, Dai, H, et al 2006, "A complexin/synaptotagmin 1 switch controls fast synaptic vesicle exocytosis.," *Cell*, vol. 126, no. 6, pp. 1175–87.

Timmerman, LA, Grego-Bessa, J & Raya, A 2004, "Notch promotes epithelial-mesenchymal transition during cardiac development and oncogenic transformation,".

Tixier, V, Bataillé, L & Jagla, K 2010, "Diversification of muscle types: recent insights from drosophila.," *Experimental cell research*, vol. 316, no. 18, pp. 3019–27.

Top, D, de Antueno, R, Salsman, J & Corcoran, J 2005, "Liposome reconstitution of a minimal protein-mediated membrane fusion machine," *The EMBO …*, accessed from <http://onlinelibrary.wiley.com/doi/10.1038/sj.emboj.7600767/full>.

Tremblay, P, Dietrich, S, Mericskay, M, Schubert, FR, et al 1998, "A crucial role for pax3 in the development of the hypaxial musculature and the long-range migration of muscle precursors.," *Developmental biology*, vol. 203, no. 1, pp. 49–61.

Trimble, WS, Cowan, DM & Scheller, RH 1988, "Vamp-1: a synaptic vesicle-associated integral membrane protein.," *Proceedings of the National Academy of Sciences of the United States of America*, vol. 85, no. 12, pp. 4538–42.

Uyttendaele, H, Soriano, JV, Montesano, R & Kitajewski, J 1998, "Notch4 and wnt-1 proteins function to regulate branching morphogenesis of mammary epithelial cells in an opposing fashion.," *Developmental biology*, vol. 196, no. 2, pp. 204–17.

Valdez, MR, Richardson, JA, Klein, WH & Olson, EN 2000, "Failure of myf5 to support myogenic differentiation without myogenin, myod, and mrf4.," *Developmental biology*, vol. 219, no. 2, pp. 287–98.

Vasyutina, E, Lenhard, DC, Wende, H, Erdmann, B, et al 2007, "Rbp-j (rbpsuh) is essential to maintain muscle progenitor cells and to generate satellite cells.," *Proceedings of the National Academy of Sciences of the United States of America*, vol. 104, no. 11, pp. 4443–8.

Vasyutina, E, Martarelli, B, Brakebusch, C, Wende, H & Birchmeier, C 2009, "The small g-proteins rac1 and cdc42 are essential for myoblast fusion in the mouse.," *Proceedings of the National Academy of Sciences of the United States of America*, vol. 106, no. 22, pp. 8935–40.

Vasyutina, E, Stebler, J, Brand-Saberi, B, Schulz, S, et al 2005, "Cxcr4 and gab1 cooperate to control the development of migrating muscle progenitor cells.," *Genes & development*, vol. 19, no. 18, pp. 2187–98.

Venuti, JM, Morris, JH, Vivian, JL, Olson, EN & Klein, WH 1995, "Myogenin is required for late but not early aspects of myogenesis during mouse development.," *The Journal of cell biology*, vol. 128, no. 4, pp. 563–76.

Vinson, CR, Conover, S & Adler, PN 1989, "A drosophila tissue polarity locus encodes a protein containing seven potential transmembrane domains,".

Vinson, CR & Adler, PN 1987, "Directional non-cell autonomy and the transmission of polarity information by the frizzled gene of drosophila.," *Nature*, vol. 329, no. 6139, pp. 549–51.

Weinstein, M, Xu, X, Ohyama, K & Deng, CX 1998, "Fgfr-3 and fgfr-4 function cooperatively to direct alveogenesis in the murine lung.," *Development (Cambridge, England)*, vol. 125, no. 18, pp. 3615–23.

Van de Wetering, M, Cavallo, R, Dooijes, D, van Beest, M, et al 1997, "Armadillo coactivates transcription driven by the product of the drosophila segment polarity gene dtcf.," *Cell*, vol. 88, no. 6, pp. 789–99.

Wickner, W & Schekman, R 2008, "Membrane fusion," *Nature Structural & Molecular Biology*, vol. 15, no. 7, pp. 658–664.

Willert, K, Brown, JD, Danenberg, E & Duncan, AW 2003, "Wnt proteins are lipid-modified and can act as stem cell growth factors,".

Wilson, DW, Wilcox, CA, Flynn, GC, Chen, E, et al 1989, "A fusion protein required for vesicle-mediated transport in both mammalian cells and yeast.," *Nature*, vol. 339, no. 6223, pp. 355–9.

Wolfe, MS & Kopan, R 2004, "Intramembrane proteolysis: theme and variations.," *Science (New York, N.Y.)*, vol. 305, no. 5687, pp. 1119–23.

Wong, H-CC, Bourdelas, A, Krauss, A, Lee, H-JJ, et al 2003, "Direct binding of the pdz domain of dishevelled to a conserved internal sequence in the c-terminal region of frizzled.," *Molecular cell*, vol. 12, no. 5, pp. 1251–60.

Xu, Q, Wang, Y, Dabdoub, A, Smallwood, PM, et al 2004, "Vascular development in the retina and inner ear: control by norrin and frizzled-4, a high-affinity ligand-receptor pair.," *Cell*, vol. 116, no. 6, pp. 883–95.

Yablonka-Reuveni, Z & Rivera, AJ 1994, "Temporal expression of regulatory and structural muscle proteins during myogenesis of satellite cells on isolated adult rat fibers.," *Developmental biology*, vol. 164, no. 2, pp. 588–603.

Yaffe, D & Saxel, O 1977, "Serial passaging and differentiation of myogenic cells isolated from dystrophic mouse muscle," *Nature*, accessed from <http://www.nature.com/nature/journal/v270/n5639/abs/270725a0.html>.

Yaffe, D 1971, "Developmental changes preceding cell fusion during muscle differentiation in vitro.," *Experimental cell research*, vol. 66, no. 1, pp. 33–48.

Yagi, M, Miyamoto, T, Sawatani, Y & Iwamoto, K 2005, "Dc-stamp is essential for cell–cell fusion in osteoclasts and foreign body giant cells," *The Journal of …*, accessed from <http://jem.rupress.org/content/202/3/345.short>.

Yamashita, J, Itoh, H, Hirashima, M, Ogawa, M, et al 2000, "Flk1-positive cells derived from embryonic stem cells serve as vascular progenitors.," *Nature*, vol. 408, no. 6808, pp. 92–6.

Yan, D & Lin, X 2009, "Shaping morphogen gradients by proteoglycans,".

Yang, L, Ding, L & Huang, HW 2003, "New phases of phospholipids and implications to the membrane fusion problem.," *Biochemistry*, vol. 42, no. 22, pp. 6631–5.

Yook, J, Li, X-Y, Ota, I, Hu, C, et al 2006, "A wnt–axin2–gsk3β cascade regulates snail1 activity in breast cancer cells," *Nature Cell Biology*, vol. 8.

Yutzey, KE, Rhodes, SJ & Konieczny, SF 1990, "Differential trans activation associated with the muscle regulatory factors myod1, myogenin, and mrf4.," *Molecular and cellular biology*, vol. 10, no. 8, pp. 3934–44.

Zabludoff, SD, Csete, M, Wagner, R, Yu, X & Wold, BJ 1998, "P27kip1 is expressed transiently in developing myotomes and enhances myogenesis.," *Cell growth & differentiation : the molecular biology journal of the American Association for Cancer Research*, vol. 9, no. 1, pp. 1–11.

Zacksenhaus, E, Jiang, Z, Chung, D, Marth, JD, et al 1996, "Prb controls proliferation, differentiation, and death of skeletal muscle cells and other lineages during embryogenesis.," *Genes & development*, vol. 10, no. 23, pp. 3051–64.

Zammit, PS, Golding, JP, Nagata, Y, Hudon, V, et al 2004, "Muscle satellite cells adopt divergent fates: a mechanism for self-renewal?," *The Journal of cell biology*, vol. 166, no. 3, pp. 347–57.

Zavadil, J, Cermak, L, Soto-Nieves, N & Böttinger, EP 2004, "Integration of tgf-beta/smad and jagged1/notch signalling in epithelial-to-mesenchymal transition.," *The EMBO journal*, vol. 23, no. 5, pp. 1155–65.

Zeng, Q, Subramaniam, VN, Wong, SH, Tang, BL, et al 1998, "A novel synaptobrevin/vamp homologous protein (vamp5) is increased during in vitro myogenesis and present in the plasma membrane.," *Molecular biology of the cell*, vol. 9, no. 9, pp. 2423–37.

Zhang, M & McLennan, IS 1995, "During secondary myotube formation, primary myotubes preferentially absorb new nuclei at their ends.," *Developmental dynamics : an official publication of the American Association of Anatomists*, vol. 204, no. 2, pp. 168–77, accessed from <http://dx.doi.org/10.1002/aja.1002040207>.

Zhang, P, Wong, C, Liu, D, Finegold, M, et al 1999, "P21(cip1) and p57(kip2) control muscle differentiation at the myogenin step.," *Genes & development*, vol. 13, no. 2, pp. 213–24.

Zhang, W, Behringer, RR & Olson, EN 1995, "Inactivation of the myogenic bhlh gene mrf4 results in up-regulation of myogenin and rib anomalies.," *Genes & development*, vol. 9, no. 11, pp. 1388–99.

Zhou, BP, Deng, J, Xia, W, Xu, J, et al 2004, "Dual regulation of snail by gsk-3beta-mediated phosphorylation in control of epithelial-mesenchymal transition.," *Nature cell biology*, vol. 6, no. 10, pp. 931–40.